

**SCALE-DOWN TECHNOLOGIES FOR
PERFUSION CULTURE FOR RAPID
BIOPHARMACEUTICAL PROCESS
DEVELOPMENT**

Molly Beth Tregidgo

Thesis submitted for the degree of Doctor of Engineering

University College London

Department of Biochemical Engineering

2021

I, Molly Beth Tregidgo, confirm that the work presented in this thesis is my own. Where information has been derived from other sources, I confirm that this has been indicated in the thesis.

Signature

ACKNOWLEDGEMENTS

I cannot thank Martina Micheletti enough for guiding me through the process of completing this thesis from start to finish, from improving my confidence in the lab and beyond, rationalising thoughts at times of panic to showing me how to get the most out of a conference. Additionally, to Suzy Farid and David Pollard, who provided invaluable insight and industry perspectives at crucial decision stages.

To the Mammalian cell group, in particular, Hai-Yuan, Ricardo, Milena and Vincent, and to Mike Sulu, I loved working with you all and can't thank you enough for everything you taught me, and for every favour; from weekend passages and troubleshooting to amateur detective work. To the Mixing Group, for help in characterisation, and to Graeme at the engineering workshop, thanks for turning my designs into a reality!

My friends, those inside the department over my 9 years(!) here; Nick, Jay, Saz, Mek, Becci, Sam, Robbie, Clau and Daryl, and outside; Frangipane, Eliza, Tim, and Jade and so many others. You put up with cancelled plans due to lab emergencies, you were there for spontaneous plans or phone calls at times it was desperately needed and you helped me laugh when I felt overwhelmed, what can I say other than I love and appreciate you all so much. Tay, I listened to our music and smiled whenever I needed a boost, you are always in my heart and thoughts and I miss you so much. Joe, who I met on the first day when we discovered a shared interest in free wine, I cannot express how happy I am that I met you and how much your support and love over these years has meant to me.

Harv, Haz, Simon, Is, Tom, Nan and Hats your love, teasing and ability to help me forget my thesis stress by taking me to jump in the sea is a dream. And the fact you print out my abstracts to put on the fridge even though they don't understand what it means (looking at you, Nan) fills me with happiness. Finally, to my mum, the most amazing and inspirational person I have ever met, there are no words for how grateful I am for everything you have done and sacrificed for me, and I love you so much.

ABSTRACT

Perfusion culture is becoming an increasingly popular choice for the production of therapeutic proteins, however few scale-down devices capable of small scale and/or high throughput optimisation of high cell density perfusion cultures have been published. To address this technology gap, this thesis describes the development, implementation, and engineering characterisation of two scale-down technologies; (i) a quasi-perfusion method at mL-scale in microwell plates (MWP) and (ii) a purposely designed novel bioreactor (BR) at 250mL scale.

Quasi-perfusion in MWP was developed at mL-scale and is capable of achieving many of the specific characteristics of perfusion culture, namely elevated cell density, cell retention and good productivity. The quasi-perfusion methodology was implemented to screen a range of process conditions, exchanging at a constant vessel volume per day (VVD) between 0.5-1.8, or at constant cell specific perfusion rate (CSPR) with a range of media, with cell retention achieved via sedimentation or centrifugation. Viable cell densities (VCDs) of 42×10^6 cells mL⁻¹ and volumetric productivities up to 2 fold greater than fed-batch were achieved.

Design and engineering characterisation of the novel 250mL BR ensured favourable hydrodynamics, with a dual impeller system selected to maximise mass transfer. Cell retention was achieved via a tangential flow filter (TFF) at perfusion rates between 0.5-1.8 VVD, maintaining maximum VCDs of 92×10^6 cells mL⁻¹ at >95% viability. Good scalability was demonstrated for a range of performance metrics, including μ_{max} , q_{Ab} and biomass production, between each system when compared to a bench scale 5L BR, while scaling was based on constant volumetric power input.

The combined use of quasi-perfusion methodologies, shown to be sensitive to changes in perfusion rate and media composition, for high throughput screening studies,

followed by the 250mL BR for in-depth study of a small range of conditions, is shown to be a powerful tool for the development and optimisation of perfusion processes.

IMPACT STATEMENT

The biopharmaceutical industry faces consistent pressure to lower the cost of manufacturing drug products while increasing process knowledge to ensure safety and decrease process development timelines. To address this in the context of development of perfusion culture processes, this thesis presents the development of tools for small scale perfusion culture.

The development of quasi-perfusion methodologies in MWP provides a robust, cost-effective, and high-throughput tool for early phase development of perfusion cultures that can be utilised for a range of investigations in both academic and industrial process development. From an academic perspective, the development of a perfusion culture scale-down tool which does not require the purchase of expensive systems with high capital cost and, on in addition, has low cost of goods (CoGs), is highly beneficial for experimental studies of perfusion culture.

From an industrial perspective, developed methodologies allow the investigation of perfusion-based manufacturing systems with a low upfront cost. The present study outlines the implementation of MWP based techniques for media and perfusion rate screening applications, however the techniques developed have additional applications related to CHO cell perfusion culture, for example in cell clone screening, and metabolite analysis for kinetic modelling. High-throughput systems such as this are especially attractive to early phase development studies, since design of experiments (DoE) can be introduced to speed up development timelines and contributes to quality by design (QbD) initiatives. In addition to providing a tool for CHO cell culture process development, the discontinuous media exchange approach for cell retention presented in this thesis are commonplace in the industrialisation of cell therapy products, which rely on media exchange techniques to convert from lab-based static cultures into suspension based systems for commercial production.

The design, characterisation, and development of a 250mL BR for perfusion studies further benefits the optimisation of manufacturing at small scale. While quasi-perfusion methodologies allow for rapid high throughput screening, the novel 250mL BR allows for the in-depth analysis of a smaller number of parameters, and additionally, investigation of critical and target process parameters, which ensure maintenance of critical quality attributes. Understanding process control and parameters at an early phase of development reduces development timelines and contributes to QbD studies. In addition, the 250mL BR contains removable baffles, has an adjustable H_i and the impeller shaft is compatible with multiple configurations of impellers, including dual or single, Rushton-style, marine or pitched-blade impellers. The flexibility of geometry is beneficial to future scale-down studies, where some adjustments can be made to mimic the geometry of the large scale vessel.

Engineering characterisation studies assist scale up between shaken and stirred perfusion vessels, and support investigations into specific problems associated with perfusion culture, for example the elevated viscosity associated with high cell density cultures and the impact of the recirculation loop on mixing hydrodynamics. An in-depth understanding of the hydrodynamic characteristics alongside developed cell culture methodologies provides a strong basis for the successful development of next generation scale down perfusion systems.

TABLE OF CONTENTS

ACKNOWLEDGEMENTS	3
ABSTRACT	4
IMPACT STATEMENT	6
TABLE OF CONTENTS	8
LIST OF FIGURES	13
LIST OF TABLES	20
NOMENCLATURE	22
<i>Abbreviations</i>	22
<i>Greek Symbols</i>	23
<i>Roman symbols</i>	23
1. CHAPTER 1: INTRODUCTION	25
1.1. <i>The context of the research</i>	25
1.2. <i>Literature Survey</i>	28
1.2.1. Mammalian cell culture.....	29
1.2.2. Perfusion Culture	30
1.2.3. Microscale Bioprocessing.....	39
1.2.4. Engineering characterisation	53
1.3. <i>Concluding remarks</i>	57
1.4. <i>The present contribution</i>	59
1.5. <i>Outline of the thesis</i>	60
2. CHAPTER 2: MATERIALS AND METHODS	62
2.1. <i>Introduction</i>	62
2.2. <i>Cell culture</i>	62

2.2.1.	Cell line used.....	62
2.2.2.	Revival of cells from liquid nitrogen.....	62
2.2.3.	Preparation of working cell bank.....	63
2.3.	<i>Shake flask culture</i>	64
2.4.	<i>Microwell culture</i>	64
2.4.1.	Fed-batch culture in 24-well MWP.....	64
2.4.2.	Determination of evaporation in 24-well MWP.....	65
2.5.	<i>Perfusion microwell culture</i>	65
2.5.1.	Development of quasi-perfusion techniques in 24-well MWP	65
2.5.2.	Determination of sedimentation time and centrifugation conditions for quasi-perfusion cultures.....	66
2.5.3.	Media exchange for consistent VVD	68
2.5.4.	Media exchange to maintain constant cell specific perfusion rate (CSPR)	68
2.6.	<i>Design and fabrication of novel 250mL bioreactor</i>	69
2.7.	<i>Culture in novel 250mL bioreactor</i>	73
2.7.1.	Batch and fed-batch	76
2.7.2.	Bioreactor perfusion operation.....	77
2.8.	<i>Cell culture in commercial 5L bioreactor</i>	78
2.8.1.	Fed-batch	79
2.8.2.	Perfusion	79
2.9.	<i>Cell culture analytical techniques</i>	80
2.9.1.	Determination of cell number and viability	80
2.9.2.	Determination of metabolite concentration	80
2.9.3.	IgG quantification.....	80
2.9.4.	Determination of osmolality	80
2.9.5.	Gel analysis.....	80
2.9.6.	Derived growth parameters for batch and fed-batch cultures	81
2.9.7.	Derived growth parameters for perfusion cultures	82

2.10.	<i>Rheological characterisation</i>	82
2.10.1.	Viscosity measurement.....	82
2.11.	<i>Mixing time determination</i>	84
2.11.1.	DISMT reagent preparation.....	85
2.11.2.	Experimental mixing time measurements.....	86
2.11.3.	Production of mixing maps.....	87
2.12.	<i>Determination of power input and impeller power number</i>	89
2.12.1.	Calculation of power input.....	89
2.12.2.	Determination of impeller power number in 250mL bioreactor.....	89
2.13.	<i>Determination of oxygen mass transfer coefficients</i>	91
2.13.1.	Calculation of k_{La} in MWPs.....	91
2.13.2.	Determination of k_{La} in bioreactors.....	92
3.	CHAPTER 3: ESTABLISHMENT OF QUASI-PERFUSION METHODS IN MICROWELL PLATES	93
3.1.	<i>Introduction</i>	93
3.2.	<i>Results</i>	95
3.2.1.	Determination of evaporation profiles and cell culture variability in 24-well MWP cultures.....	95
3.2.2.	Development of batch and fed-batch cultures in 24 MWP.....	98
3.2.3.	Quasi-perfusion proof of concept studies.....	102
3.2.4.	Media development for quasi-perfusion methodologies at 1VVD.....	105
3.2.5.	Process optimisation using quasi-perfusion methodologies at varying perfusion rates 0.5-1.8 VVD.....	115
3.2.6.	Expansion of quasi-perfusion methodologies to enable maintenance of constant cell-specific perfusion rates.....	126
3.3.	<i>Summary</i>	134
4.	CHAPTER 4: DETERMINATION OF ENGINEERING ENVIRONMENT AND HYDRODYNAMIC ANALYSIS IN MWP, 250ML AND 5L BIOREACTORS	137

4.1.	<i>Introduction</i>	137
4.2.	<i>Results</i>	138
4.2.1.	Design Considerations.....	138
4.2.2.	Oxygen Mass Transfer Coefficient (k_{La}).....	143
4.2.3.	Power Input.....	147
4.2.4.	Evaluation of impact of H_i on mixing time in 250mL BR.....	150
4.2.5.	Viscosity in HCD CHO cell cultures.....	152
4.2.6.	Impact of HCD on mixing dynamics.....	157
4.2.7.	Impact of perfusion recirculation loop on mixing time.....	159
4.2.8.	Selection of scaling criteria.....	164
5.	CHAPTER 5: ESTABLISHMENT AND SCALE COMPARISON OF CELL CULTURE PROTOCOLS IN BATCH, FED-BATCH AND PERFUSION CULTURE MODES.....	166
5.1.	<i>Introduction</i>	166
5.2.	<i>Results</i>	167
5.2.1.	Development and optimisation of cell culture techniques in novel 250mL BR in batch and fed-batch modes.....	167
5.2.2.	Comparison of cell culture performance across scales in batch and fed-batch modes.....	173
5.2.3.	Development of perfusion culture methodologies in novel bioreactor.....	180
5.2.4.	Comparison of culture performance across scales in perfusion mode.....	188
5.2.5.	Validation of scale-down quasi-perfusion MWP mimic against novel BR at varying perfusion rates.....	194
5.3.	<i>Summary</i>	206
6.	CHAPTER 6: CONCLUSIONS.....	209
6.1.	<i>Concluding remarks</i>	209
6.2.	<i>Recommendations for future work</i>	214
7.	CHAPTER 7: RESEARCH IMPLEMENTATION.....	218

7.1.	<i>Validation and commercialisation</i>	218
7.2.	<i>Economic and environmental appraisal</i>	219
REFERENCES.....		221
8.	CHAPTER 8: APPENDIX.....	229
8.1.	<i>VCD in MWP with fill volumes of 0.8 and 1.2mL.....</i>	229
8.2.	<i>Tm in 250mL BR fitted with single Ruston-style turbine $H_i = 2.5\text{cm}$.....</i>	230
8.3.	<i>Rotational speed of centrifugal pump in 250mL BR at 0.5 VVD.....</i>	231
8.4.	<i>Rotational speed of centrifugal pump in 250mL BR at 1.8 VVD.....</i>	232
8.5.	<i>Rotational speed of centrifugal pump in 5L BR.....</i>	233

LIST OF FIGURES

FIGURE 1.1 - OPERATIONAL OVERVIEW OF BIOREACTORS IN (A) FED-BATCH CULTURES (B) PERFUSION CULTURES WITH TFF (C) PERFUSION CULTURES WITH ATF.....	31
FIGURE 2.1 - SEPARATION EFFICIENCY WITH TIME FOR CELL CULTURE SEEDED AT 40×10^6 AND ALLOWED TO SETTLE VIA GRAVITY.....	67
FIGURE 2.2 - REACTOR GEOMETRY AND DESIGN DRAWING. (A) 2-D CROSS-SECTION (B) 2-D HEADPLATE (C) 3-D VIEW WITH X-RAY ALLOWING OBSERVATION OF INTERNAL COMPONENTS.....	70
FIGURE 2.3 - ACRYLIC MIMIC REACTOR DESIGN DRAWING. (A) 2-D CROSS-SECTION (B) 2-D HEADPLATE (C) 3-D VIEW WITH X-RAY ALLOWING OBSERVATION OF INTERNAL COMPONENTS.....	73
FIGURE 2.4 - PHOTOGRAPHS OF 250ML BRs, FABRICATED BY UCL BIOCHEMICAL ENGINEERING WORKSHOP. (A) STAINLESS STEEL CELL CULTURE BIOREACTOR. (B) ACRYLIC MIMIC FOR HYDRODYNAMIC ANALYSIS.....	74
FIGURE 2.5 – BIOREACTOR CONFIGURATION FOR BATCH AND FED-BATCH OPERATION.....	76
FIGURE 2.6 – BIOREACTOR CONFIGURATION FOR PERFUSION MODE OPERATION, WITH CELL RETENTION ACHIEVED BY TFF.....	78
FIGURE 2.7 – EXPERIMENTAL SET UP FOR MIXING TIME EXPERIMENTS.....	85
FIGURE 2.8 – MATLAB PROCESSING OF MIXING TIME IMAGES TO DETERMINE T_M	88
FIGURE 3.1 - CHARACTERISATION OF CELL GROWTH ENVIRONMENT IN 24-WELL MWPs.....	97
FIGURE 3.2 - COMPARISON OF EVAPORATION AND CHO CELL CULTURE PERFORMANCE IN 24-WELL MWP COVERED WITH FILTER OR SILICONE BASED DUETZ SANDWICH LIDS. CELL CULTURES WERE INCUBATED AT 37°C AT AN INITIAL SEEDING DENSITY OF 0.2×10^6 CELLS mL^{-1} , $N=220$ RPM.....	99

FIGURE 3.3 - VCD AND VIABILITY OF FED-BATCH CHO CELL CULTURE IN 24-WELL MWP, SEEDED AT A RANGE OF DENSITIES BETWEEN $0.2-2 \times 10^6$ CELLS mL^{-1} . CULTURES WERE COVERED WITH A DUETZ SANDWICH LID, INCUBATED AT 37°C , $N=220$ RPM.....100

FIGURE 3.4 - FED-BATCH, SEDIMENTATION QUASI-PERFUSION AND CENTRIFUGATION QUASI-PERFUSION CULTURES IN 24-WELL MWPs. CULTURES WERE SEEDED AT 2×10^6 CELLS mL^{-1} INCUBATED AT 37°C , $N=220$ RPM AND COVERED WITH DUETZ SANDWICH LIDS. QUASI-PERFUSION CULTURES WERE EXCHANGED WITH CD-CHO MEDIA FROM DAY 3 AT A RATE OF 1 VVD.....104

FIGURE 3.5 - FED-BATCH AND CENTRIFUGATION QUASI-PERFUSION CULTURES EXCHANGED WITH 1, 1.5 AND 2 TIMES CONCENTRATED CD-CHO MEDIUM AT A RATE OF 1 VVD. CULTURES WERE SEEDED AT 2×10^6 CELLS mL^{-1} INCUBATED AT 37°C , $N= 220$ RPM AND COVERED WITH DUETZ SANDWICH LIDS.....106

FIGURE 3.6 - FED-BATCH, SEDIMENTATION QUASI-PERFUSION AND CENTRIFUGATION QUASI-PERFUSION CULTURES IN 24-WELL MWPs. CULTURES WERE SEEDED AT 2×10^6 CELLS mL^{-1} INCUBATED AT 37°C , $N=220$ RPM AND COVERED WITH DUETZ SANDWICH LIDS. QUASI-PERFUSION CULTURES WERE EXCHANGED FROM DAY 3 AT 1 VVD WITH CD-CHO AND GLUCOSE-SUPPLEMENTED CD-CHO MEDIA AT 9 AND 12 g L^{-1}108

FIGURE 3.7 - FED-BATCH, SEDIMENTATION QUASI-PERFUSION AND CENTRIFUGATION QUASI-PERFUSION CULTURES. CULTURES WERE SEEDED AT 2×10^6 CELLS mL^{-1} INCUBATED AT 37°C , $N= 220$ RPM AND COVERED WITH DUETZ SANDWICH LIDS. QUASI-PERFUSION CULTURES WERE EXCHANGED FROM DAY 3 AT A RATE OF 1 VVD WITH CD-CHO MEDIA BLENDED WITH EFFICIENT FEED B AT 5, 15, 30 AND 45% VOLUME/VOLUME.....110

FIGURE 3.8 - PRODUCTIVITY OF FED-BATCH, SEDIMENTATION QUASI-PERFUSION AND CENTRIFUGATION QUASI-PERFUSION CULTURES. CULTURES WERE SEEDED AT 2×10^6 CELLS mL^{-1} INCUBATED AT 37°C , $N= 220$ RPM AND COVERED WITH DUETZ SANDWICH LIDS. QUASI-PERFUSION

CULTURES WERE EXCHANGED FROM DAY 3 AT A RATE OF 1 VVD WITH CD-CHO MEDIA BLENDED WITH EFFICIENT FEED B AT 5, 15, 30 AND 45% VOLUME/VOLUME.....	113
FIGURE 3.9 - SEDIMENTATION QUASI-PERFUSION AND CENTRIFUGATION QUASI-PERFUSION CULTURES EXCHANGED AT RATES BETWEEN 0.5-1.8 VVD. CULTURES WERE SEEDED AT 2×10^6 CELLS mL^{-1} INCUBATED AT 37°C , $N= 220$ RPM AND COVERED WITH DUETZ SANDWICH LIDS. QUASI-PERFUSION CULTURES WERE EXCHANGED FROM DAY 3 WITH CD-CHO MEDIA BLENDED WITH 15% EFFICIENT FEED B AT EXCHANGE RATES BETWEEN 0.5-1.8 VVD.	119
FIGURE 3.10 - SEDIMENTATION QUASI-PERFUSION AND CENTRIFUGATION QUASI-PERFUSION CULTURES EXCHANGED AT RATES BETWEEN 0.5-1.8 VVD. CULTURES WERE SEEDED AT 2×10^6 CELLS mL^{-1} INCUBATED AT 37°C , $N= 220$ RPM AND COVERED WITH DUETZ SANDWICH LIDS. QUASI-PERFUSION CULTURES WERE EXCHANGED FROM DAY 3 WITH CD-CHO MEDIA BLENDED WITH 30% EFFICIENT FEED B AT AN EXCHANGE RATE OF 1.5 AND 1.8 VVD, OR CD-CHO MEDIA BLENDED WITH 5% EFFICIENT FEED B AT AN EXCHANGE RATE OF 0.5 AND 0.75 VVD.....	121
FIGURE 3.11- VOLUMETRIC PRODUCTIVITY (BARS) AND MAXIMUM TITRE (SCATTER) FOR FED-BATCH, SEDIMENTATION QUASI-PERFUSION AND CENTRIFUGATION QUASI-PERFUSION CULTURES EXCHANGED AT PERFUSION RATES BETWEEN 0.5-1.8 VVD WITH CD-CHO MEDIUM BLENDS WITH EFFICIENT FEED B AT 5, 15 AND 30%.....	123
FIGURE 3.12 - SEDIMENTATION QUASI-PERFUSION AND CENTRIFUGATION QUASI-PERFUSION CULTURES EXCHANGED AT CONSTANT CSPRS. CULTURES WERE SEEDED AT 2×10^6 CELLS mL^{-1} INCUBATED AT 37°C , $N= 220$ RPM AND COVERED WITH DUETZ SANDWICH LIDS. QUASI-PERFUSION CULTURES WERE EXCHANGED FROM DAY 3 WITH CD-CHO MEDIA BLENDED WITH 15% EFFICIENT FEED B AT RATES CALCULATED TO MAINTAIN CSPR BETWEEN $0.02 - 0.06 \text{ nL CELL}^{-1} \text{ DAY}^{-1}$	129
FIGURE 3.13 - VOLUMETRIC PRODUCTIVITY (BARS) AND MAXIMUM TITRE (SCATTER) FOR FED-BATCH, SEDIMENTATION QUASI-PERFUSION AND CENTRIFUGATION QUASI-PERFUSION CULTURES EXCHANGED AT CSPRS BETWEEN 0.02 AND $0.06 \text{ nL CELL}^{-1} \text{ DAY}^{-1}$	130

FIGURE 3.14 - MAXIMUM VCD ACHIEVED ON DAY 7 FOR SEDIMENTATION QUASI-PERFUSION AND CENTRIFUGATION QUASI-PERFUSION CULTURES EXCHANGED WITH CD-CHO WITH 15% EFFICIENT FEED B AT CONSTANT CSPR BETWEEN 0.02-0.06 NL CELL ⁻¹ DAY ⁻¹ OR A CONSTANT EXCHANGE RATE BETWEEN 0.5-1.8 VVD.....	132
FIGURE 4.1 – SCHEMATIC DIAGRAM 250ML NOVEL BIOREACTOR (A) 2-D CROSS-SECTION (B) HEADPLATE AND ACRYLIC MIMIC (A) 2-D CROSS-SECTION AND (B) HEADPLATE.....	139
FIGURE 4.2 - DETERMINATION OF OXYGEN MASS TRANSFER COEFFICIENT (K _{LA}) IN NOVEL 250ML BR. K _{LA} WAS DETERMINED USING THE STATIC GASSING OUT METHOD, AS DESCRIBED IN SECTION 2.13, AT GAS FLOWRATES OF 25, 50, 75 AND 100 ML MIN ⁻¹ , N=100-600 RPM.....	145
FIGURE 4.3 - COMPARISON OF K _{LA} ACROSS SCALES. K _{LA} IN 250ML BR WAS EXPERIMENTALLY DETERMINED AT Q = 50 ML MIN ⁻¹ , T = 37°C. K _{LA} IN 5L BR WAS CALCULATED FOLLOWING K _{LA} = K(P/V) ^A W _{sc} ^B ASSUMING; K = 1.64, A = 0.55, B = 0.81. K _{LA} IN MWP WAS CALCULATED FOLLOWING DOIG ET AL. (2006), OUTLINED IN EQUATIONS 2.25-2.27.....	146
FIGURE 4.4 - POWER INPUT MEASURED IN THE 250ML BR, DETERMINED EXPERIMENTALLY BY ROTATING THE BR ON AN AIR BEARING AND MEASURING THE FORCE APPLIED AT N = 50-700 RPM. BR WAS FILLED WITH GLYCEROL, WATER, AND WATER AND GLYCEROL MIXTURES TO ENABLE ADEQUATE FORCE APPLIED AT LOW RE WITH IMPELLERS ROTATED IN DOWN-PUMPING OR UP-PUMPING CONFIGURATIONS.....	149
FIGURE 4.5 - COMPARISON OF GASSED POWER INPUT PER UNIT VOLUME (P _G /V) ACROSS SCALES. P _G /V IN 250ML AND 5L BRs WERE CALCULATED FOLLOWING EQUATIONS 2.18-2.19; N _p = 4.9, 250ML; N _p = 0.75, 5L. P/V IN MWP WAS CALCULATED FOLLOWING EQUATION 2.17.....	150
FIGURE 4.6 - MIXING IN 250ML BR FITTED WITH DUAL PITCHED-BLADE AND RUSHTON-TYPE IMPELLERS AT H _i = 1 AND 2.5 CM, MEASURED USING DISMT METHOD.....	152
FIGURE 4.7 - VISCOSITY OF CHO CELL SUSPENSIONS AT DENSITIES 20-100 × 10 ⁶ CELLS ML ⁻¹	154

FIGURE 4.8 - DEVELOPMENT OF MODEL FLUID TO MIMIC CHO CELL SUSPENSIONS AT DENSITIES OF 100×10^6 CELLS mL^{-1} .	156
FIGURE 4.9 - INFLUENCE OF ELEVATED VISCOSITY HCD ON MIXING DYNAMICS. $H_i = 2\text{CM}$.	158
FIGURE 4.10 - INFLUENCE OF PERFUSION RECIRCULATION WITH RETURN FROM SIDE OR TOP PORTS AT 80 mL MIN^{-1} ON MIXING DYNAMICS. $N = 50 - 600 \text{ RPM}$, $H_i = 2 \text{ CM}$, MIXED WITH DISMT HCD MIMIC SOLUTION.	162
FIGURE 4.11 - INFLUENCE OF PERFUSION RECIRCULATION WITH RETURN FROM SIDE PORT AT $40 - 140 \text{ mL MIN}^{-1}$ AND FROM THE TOP PORT AT 80 mL MIN^{-1} , $N = 0 \text{ RPM}$.	163
FIGURE 5.1 - BATCH CHO CELL CULTURE IN 250ML BR. CULTURES WERE SEEDED AT 2×10^6 CELLS mL^{-1} AND MAINTAINED AT 37°C , $\text{pH } 7.2$, $\text{DO } 30\%$, $N = 250 \text{ RPM}$.	169
FIGURE 5.2 - FED-BATCH CHO CELL CULTURE IN 250ML BR WITH STEP-WISE IMPROVEMENTS TO PID CONTROL. CULTURES WERE SEEDED AT 2×10^6 CELLS mL^{-1} AND MAINTAINED AT 37°C , $\text{pH } 7.2$, $\text{DO } 30\%$, $N = 250 \text{ RPM}$. FEEDING COMMENCED ON DAY 3 AND INVOLVED A 5% DAILY ADDITION OF EFFICIENT FEED B.	170
FIGURE 5.3 - CONTROL TRACERS FOR FED-BATCH CHO CELL CULTURE IN THE 250ML BR. DO CONCENTRATION (BLUE), PH (RED), TEMPERATURE (BLACK).	172
FIGURE 5.4 - COMPARISON OF BATCH CHO CELL CULTURE PERFORMANCE IN MWPs AND 250ML BR. CULTURES WERE SEEDED AT 2×10^6 CELLS mL^{-1} AND MAINTAINED AT 37°C , $\text{pH } 7.2$, $\text{DO } 30\%$. $N = 220 \text{ RPM}$ IN MWP, $N = 250 \text{ RPM}$ IN 250ML BR.	175
FIGURE 5.5 - COMPARISON OF FED-BATCH CHO CELL CULTURE PERFORMANCE IN; MWPs AND 250ML AND 5L BRs. CULTURES IN MWP AND 250ML BRs WERE SEEDED AT 2×10^6 CELLS mL^{-1} AND IN 5L BR WERE SEEDED AT 0.3×10^6 CELLS mL^{-1} . CULTURES ACROSS SCALES WERE MAINTAINED AT 37°C , $\text{pH } 7.2$, $\text{DO } 30\%$. FEEDING COMMENCED ON DAY 3 AND INVOLVED A 5% ADDITION OF EFFICIENT FEED B. $N = 220, 250$ AND 260 RPM IN MWPs, 250ML BR AND 5L BR RESPECTIVELY.	176

FIGURE 5.6 - COMPARISON OF FED-BATCH AND PERFUSION CHO CELL CULTURE IN 250ML BR. CULTURES WERE SEEDED AT 2×10^6 CELLS mL^{-1} AND MAINTAINED AT 37°C , pH 7.2, DO 30%, N = 250 RPM. FOR FED-BATCH CULTURES, FEEDING COMMENCED ON DAY 3 AND INVOLVED A 5% DAILY ADDITION OF EFFICIENT FEED B. FOR PERFUSION CULTURES, PERFUSION WAS INITIATED ON DAY 3 AT A RATE OF 1 VVD, EXCHANGING WITH CD-CHO MEDIA BLENDED WITH 15% EFFICIENT FEED B. CELL RETENTION WAS ACHIEVED WITH TFF AND A RECIRCULATION FLOW RATE OF 80 mL MIN^{-1}181

FIGURE 5.7 - CONTROL PROFILES OF PERFUSION CHO CELL CULTURE IN THE 250ML BR.....184

FIGURE 5.8 - PERFUSION CHO CELL CULTURE IN 250ML BR. CULTURES WERE SEEDED AT 2×10^6 CELLS mL^{-1} AND MAINTAINED AT 37°C , pH 7.2, DO 30%, N = 250 RPM. PERFUSION WAS INITIATED ON DAY 3, EXCHANGING WITH CD-CHO MEDIA BLENDED WITH 15% EFFICIENT FEED B AT AN EXCHANGE RATE OF 0.5, 1 OR 1.8 VVD. CELL RETENTION WAS ACHIEVED WITH TFF AND A RECIRCULATION FLOW RATE OF 80 mL MIN^{-1}186

FIGURE 5.9 - COMPARISON OF PERFUSION CHO CELL CULTURE PERFORMANCE IN MWP, 250ML BR AND 5L BR. CULTURES WERE SEEDED AT 2×10^6 CELLS mL^{-1} AND MAINTAINED AT 37°C , pH 7.2, DO 30%, PERFUSION WAS INITIATED ON DAY 3 AT A RATE OF 1 VVD, EXCHANGED WITH CD-CHO MEDIA BLENDED WITH 15% EFFICIENT FEED B. CELL RETENTION IN 250ML AND 5L BRs WERE ACHIEVED WITH TFF, AND IN MWP WAS ACHIEVED VIA DISCONTINUOUS MEDIA EXCHANGES FOLLOWING CENTRIFUGATION191

FIGURE 5.10 - CONTROL PROFILE IN 5L BR DURING PERFUSION CHO CELL CULTURE AT AN EXCHANGE RATE OF 1 VVD. DO (BLUE), pH (RED) AND TEMPERATURE (BLACK).....192

FIGURE 5.11 - COMPARISON OF PERFUSION CHO CELL CULTURE PERFORMANCE IN MWP, IN QUASI-PERFUSION SEDIMENTATION AND QUASI-PERFUSION CENTRIFUGATION MODES, AND IN 250ML BR AT EXCHANGE RATES OF 0.5, 1 OR 1.8 VVD. CULTURES WERE SEEDED AT 2×10^6 CELLS mL^{-1} AND MAINTAINED AT 37°C , pH 7.2, DO 30%. N = 220 RPM IN MWP, N = 250 RPM IN 250ML BR.....197

FIGURE 5.12 - COMPARISON OF CELL GROWTH, VIABILITY AND BIOMASS PRODUCTION OF PERFUSION CHO CELL CULTURES IN MWP, IN QUASI-PERFUSION SEDIMENTATION AND QUASI-PERFUSION CENTRIFUGATION MODES, AND IN 250ML BR AT EXCHANGE RATES OF 0.5, 1 OR 1.8 VVD. CULTURES WERE SEEDED AT 2×10^6 CELLS mL^{-1} AND MAINTAINED AT 37°C, PH 7.2, DO 30%. N = 220 RPM IN MWP, N = 250 RPM IN 250ML BR.....199

FIGURE 5.13 - COMPARISON OF METABOLITE CONCENTRATION AND SPECIFIC PRODUCTION OR CONSUMPTION OF PERFUSION CHO CELL CULTURES IN MWP, IN QUASI-PERFUSION SEDIMENTATION AND QUASI-PERFUSION CENTRIFUGATION MODES, AND IN 250ML BR AT EXCHANGE RATES OF 0.5, 1 OR 1.8 VVD. CULTURES WERE SEEDED AT 2×10^6 CELLS mL^{-1} AND MAINTAINED AT 37°C, PH 7.2, DO 30%. N = 220 RPM IN MWP, N = 250 RPM IN 250ML BR.....201

FIGURE 5.14 - COMPARISON OF mAb PRODUCTION AND PRODUCTIVITY OF PERFUSION CHO CELL CULTURES IN MWP, IN QUASI-PERFUSION SEDIMENTATION AND QUASI-PERFUSION CENTRIFUGATION MODES, AND IN 250ML BR AT EXCHANGE RATES OF 0.5, 1 AND 1.8 VVD. CULTURES WERE SEEDED AT 2×10^6 CELLS mL^{-1} AND MAINTAINED AT 37°C, PH 7.2, DO 30%. N = 220 RPM IN MWP, N = 250 RPM IN 250ML BR.....203

LIST OF TABLES

TABLE 1.1 - IMPACT OF SCALE-DOWN CRITERIA SELECTION ON OPERATIONAL PARAMETERS; POWER INPUT PER UNIT VOLUME, MIXING TIME AND IMPELLER TIP SPEED. ADAPTED FROM OOSTERHUIS AND KOSSEN (1985).....	41
TABLE 1.2 - COMPARISON OF SCALE, THROUGHPUT, COST AND MONITORING AND CONTROL CAPABILITIES OF EQUIPMENT COMMONLY UTILISED FOR PROCESS DEVELOPMENT	44
TABLE 1.3 – SUMMARY OF PUBLISHED SCALE-DOWN MODELS FOR PERFUSION CULTURE PROCESSES	49
TABLE 2.1 - REACTOR GEOMETRY AND DESIGN SPECIFICATION	69
TABLE 3.1 - MAXIMUM SPECIFIC GROWTH RATE (μ_{MAX}) FOR FED-BATCH CHO CULTURES IN MWP WITH SEEDING DENSITIES BETWEEN $0.2-2 \times 10^6$ CELLS ML^{-1}	101
TABLE 3.2 - SPECIFIC GLUCOSE CONSUMPTION (Q_{GLUC}), AND LACTATE (Q_{LAC}) AND ANTIBODY (Q_{AB}) PRODUCTION RATES FOR FED-BATCH CULTURES.....	124
TABLE 3.3 - SPECIFIC GLUCOSE CONSUMPTION (Q_{GLUC}), AND LACTATE (Q_{LAC}) AND ANTIBODY (Q_{AB}) PRODUCTION RATES FOR (A) SEDIMENTATION QUASI-PERFUSION AND CENTRIFUGATION QUASI-PERFUSION CULTURES EXCHANGED AT PERFUSION RATES BETWEEN 0.5-1.8 VVD WITH MEDIA BLENDED WITH 15% EFFICIENT FEED B AND (B) SEDIMENTATION QUASI-PERFUSION AND CENTRIFUGATION QUASI-PERFUSION CULTURES EXCHANGED AT PERFUSION RATES OF 0.5 AND 0.75 VVD EXCHANGED WITH MEDIA BLENDED WITH 5% EFFICIENT FEED B AND AT PERFUSION RATES OF 1.5 AND 1.8 VVD EXCHANGED WITH MEDIA BLENDED WITH 30% EFFICIENT FEED B.....	124
TABLE 3.4 - SPECIFIC GLUCOSE CONSUMPTION (Q_{GLUC}), AND LACTATE (Q_{LAC}) AND ANTIBODY (Q_{AB}) PRODUCTION RATES FOR SEDIMENTATION QUASI-PERFUSION AND CENTRIFUGATION QUASI-PERFUSION CULTURES EXCHANGED AT CONSTANT CSPR, BETWEEN 0.02 AND 0.06 $NL CELL^{-1} DAY^{-1}$	140

TABLE 4.1- KEY GEOMETRIES OF MWP, 250ML BR AND 5L BR.....	157
TABLE 4.2- SUMMARY OF PUBLISHED COEFFICIENTS CORRELATING EXPERIMENTALLY DETERMINED K_{LA} TO THE EQUATION: $K_{LA} = K(P/V)^A W_{SG}^B$ COMPARED TO EXPERIMENTALLY DETERMINED COEFFICIENTS IN 250ML BR.....	144
TABLE 4.3 -(A) SUMMARY OF POWER INPUT, IMPELLER TIP SPEED, K_{LA}, MIXING TIME, IMPELLER SPEED AND REYNOLDS NUMBER IN THE 250ML BR AT OPERATING CONDITIONS. (B) SUMMARY OF THE IMPACT OF SELECTION OF SCALING PARAMETERS ON KEY PROCESS VARIABLES WHEN SCALING FROM 250ML BR INTO 5L BR AND MWPs.....	163
TABLE 5.1 – REYNOLDS NUMBER, K_{LA}, POWER INPUT AND U_{TIP} AT OPERATIONAL CONDITIONS IN MWP AND 250 ML AND 5L BRs	174
TABLE 5.2- MAXIMUM SPECIFIC GROWTH RATE (μ_{MAX}), VOLUMETRIC PRODUCTIVITY (VOL PROD) AND SPECIFIC ANTIBODY PRODUCTION (Q_{AB}) FOR FED-BATCH CELL CULTURES IN MWP, 250ML BR AND 5L BR.....	177
TABLE 5.3 – K_{LA} IN THE 250ML BR AT STEP-WISE RPM INCREASES DURING PERFUSION CULTURE. K_{LA} WAS CALCULATED FOLLOWING THE VAN'T RIET EQUATION, UTILISING COEFFICIENTS THAT WERE EXPERIMENTALLY DETERMINED; $K = 3.8$, $A = 1.067$, $B = 1.371$	183
TABLE 5.4- SPECIFIC GLUCOSE CONSUMPTION (Q_{GLUC}), AND LACTATE (Q_{LAC}) AND ANTIBODY (Q_{AB}) PRODUCTION RATES AND VOLUMETRIC PRODUCTIVITY FOR PERFUSION CULTURES IN 250ML BR AT PERFUSION RATES OF 0.5, 1 AND 1.8 VVD WITH MEDIA BLENDED WITH 15% EFFICIENT FEED B...186	186

NOMENCLATURE

Abbreviations

2-D	Two-Dimensional
3-D	Three-Dimensional
ATF	Alternating tangential flow
BR	Bioreactor
CHO	Chinese hamster ovary
CIP	Clean in place
CoGs	Cost of goods
CoG/g	Cost of goods per gram
CQAs	Critical quality attributes
CSPR	Cell specific perfusion rate
CSPR _{min}	Minimum cell specific perfusion rate
DISMT	Dual indicator system for mixing time
DoE	Design of experiments
DWP	Deep well plates
HCD	High cell density
HPLC	High performance liquid chromatography
LiHa	Liquid handling arm
mAbs	Monoclonal antibodies
MSX	Methyl sulphoximine
MWP	Microwell plate
NPV	Net present value
OTR	Oxygen transfer rate
PBS	Phosphate buffered saline
PID	Proportional integral derivative
PLIF	Planar laser induced fluorescence
RGB	Red green and blue

RoMa	Robotic manipulator arm
RTP	Relative temperature pressure
SF	Shake Flask
TFF	Tangential flow filter
TMP	Transmembrane pressure
VCD	Viable cell density
VVD	Vessel volumes per day

Greek Symbols

ρ	Density	[kg m ⁻³]
μ	Viscosity	[Pa s]
γ	Shear rate	[s ⁻¹]
τ	Shear stress	[dyn cm ⁻²]
τ_p	Probe response time	[s ⁻¹]

Roman symbols

A_{630}	Absorbance at 630nm	[-]
Bo	Bond number	[-]
d	Microwell diameter	[cm]
D_B	Baffle diameter	[cm]
D_i	Impeller outer diameter	[cm]
DO	Dissolved oxygen concentration	[%]
do	Orbital shaking diameter	[mm]
D_T	Tank diameter	[cm]
F	Force	[N]
Fr	Froude number	[-]
g	Acceleration due to gravity	[ms]
H_B	Baffle height	[cm]
H_i	Impeller height, clearance from base	[cm]
H_L	Liquid height	[cm]

IVCD	Cumulative cell time	[hrs ⁻¹]
k _{La}	Volumetric oxygen mass transfer coefficient	[hrs ⁻¹]
N	Rotational speed	[RPM]
N _p	Impeller power number	[-]
N _{tm}	Mixing number	[-]
P/V	Power input per unit volume	[W m ⁻³]
P _g	Gassed power number	[W]
P _{ug}	Ungassed power number	[W]
Q	Volumetric gas velocity	[m ³ s ⁻¹]
q _{Ab}	Specific productivity	[g cell ⁻¹ day ⁻¹]
q _{Gluc}	Specific glucose consumption	[g cell ⁻¹ day ⁻¹]
q _{Lac}	Specific lactate consumption	[g cell ⁻¹ day ⁻¹]
r	Lever arm length	[cm]
Re	Reynolds number	[-]
Sc	Schmidt number	[-]
T	Torque	[N m]
T _{in}	Internal bioreactor temperature	[°C]
t _m	Mixing Time	[s]
T _{out}	External bioreactor temperature	[°C]
t _n	Time	[s]
t _s	Settling time	[s]
μ _{max}	Maximum specific growth rate	[hr ⁻¹]
u _{tip}	Impeller tip speed	[ms ⁻¹]
V _L	Volume of liquid	[mL]
V _s	Volume of supernatant	[mL]
V _t	Settling velocity	[N]
W	Wetting number	[N m ⁻¹]
W _{sg}	Superficial gas velocity	[ms]

1. CHAPTER 1: INTRODUCTION

1.1. The context of the research

Over the last few decades, animal cell culture technology has matured significantly. Notable advancements have been made towards improving the reliability and robustness of the technologies (Liu, 2014). Manufacture in cell culture systems is typically based on a suspension system, where cells are freely suspended in culture and agitated to ensure efficient transport processes. Suspension cultures are well characterised, easily scaled, and have well-established automated processes for start-up, operation and cleaning in place (Birch and Arathoon, 1990). Bioreactors for suspension cell culture have been developed over the last 60 years and are available at scales from mL to 20,000 L (Eibl et al., 2008). The scale selected for manufacture is determined by the annual throughput required, the culture mode selected and the number of reactors. The scope for production in cell culture is incredibly broad, from viral vaccines and interferons to recombinant therapeutic proteins and monoclonal antibodies (mAbs) (Eibl et al., 2008).

mAbs were first developed for therapeutic use in 1975, but did not achieve clinical or commercial success until advancements in the technology led to Humira® to become the first human mAb to be approved by the FDA in 2002 (Nelson et al., 2010). Following the success of Humira®, mAbs are now commonly utilised to treat numerous diseases, ranging from Alzheimer's to rheumatoid arthritis. Currently, mAbs are produced almost exclusively in mammalian cells because alternative host cells, such as *E.coli*, lack the required capacity to secrete antibodies and perform post-translational modifications such as glycosylation. The glycosylation of mAbs is vital for biological function and pharmacokinetics and, while genetic engineering is being employed to allow microbes to perform such modifications (Zhang, 2010), mammalian cells remain the predominant production hosts. While such engineering has enabled yeast (Zha, 2012, Spadiut, 2014)

and insect (Korn, 2020, Palmberger, 2011) cell lines to produce antibodies with human-like post translational modifications, production in mammalian cell lines reduces the risk of immunogenicity due to altered, non-human glycosylation patterns (Frenzel, 2013). Three cell types are currently adopted in the manufacture of mAbs; murine monoclonal antibodies are produced in hybridoma cells, while genetically engineered antibodies are produced either in Chinese hamster ovary (CHO) cells or in mouse myeloma cells (Farid, 2006). CHO cells are the dominant manufacturing choice having demonstrated beneficial process performance attributes such as high expression, rapid growth and the ability to grow in chemically defined media (Kelley, 2009). Over 84% of approved mAb products from 2015-2018 were produced in CHO cell lines, suggesting there is little industry interest in exploring new expression systems (Walsh, 2018). Murine antibodies represented 30% of mAbs in clinical development from 1990-1999, however this figure decreased to 7% between 2000 and 2008 (Nelson et al., 2010). The majority of mAbs in clinical development from 2000 to 2008 were genetically engineered humanised or human mAbs, representing 39 and 45% of total mAbs respectively (Nelson et al., 2010). The humanisation of mAbs is believed to improve clinical efficacy and safety, particularly in terms of reducing incidents of cytokine release syndrome, which is a common human immunological response following the administration of foreign proteins (Getts et al., 2010).

mAbs represent both the dominant and the most rapidly expanding class of biopharmaceuticals. mAbs represented between 20-27% of all first-time biologics approvals in 4 year time periods between 1995 and 2014, and have shown continued growth to 53% of first time approvals from 2015 to 2018 (Walsh, 2018). Reflecting high approval rates, mAbs represented upwards of 50% of total biopharmaceutical sales each year, from 2012 to 2017, with sales in 2017 generating almost two thirds of total sales (Walsh, 2018). The single most lucrative mAb up to the 2018 survey period was Humira®, a mAb treatment for various indications including rheumatoid arthritis,

manufactured by Abbot, generating global sales of \$19 billion in 2017 and \$62.6 billion cumulatively from 2014 to 2017. Eight of the top ten products by sales in 2017 were mAbs, with total sales reaching \$123 billion, with cancer treatment a common target, however recently more noncommon target indications have been approved including; migraine, asthma, psoriasis and HIV infection (Walsh, 2018).

Despite the high earning potential of mAbs, the cost of treatment per patient per year is among the highest of all pharmaceuticals. In 2008, the media US wholesale price of mAbs was \$8,000 g⁻¹, with some products marketed at values up to \$20,000 g⁻¹ (Kelley, 2009), relating to a typical cost of treatment per patient per year of between \$10,000 - \$15,000 (Farid, 2006). Pressure from healthcare providers means that the manufacturing costs are continually being driven down, from \$1,000's per gram to \$100's per gram (Farid, 2006). One of the key factors influencing the high cost of goods per patient for mAbs is the high dosage required, typically in the order of 1000-3000 mg cumulative dose per patient per year, up to 1000 fold greater than typical small molecule and protein dosage. Voisard et al. (2003) predicted that, due to the high required dosage compared to small molecules and simple proteins, worldwide production capacity would not satisfy the production demands of mAbs. Several methods to increase available capacity have been considered, including the utilisation of high producer host cell clones, improvement of the overall yield of the purification train and the implementation of continuous technologies. A continuous culture approach can achieve a reduction in cost of goods per gram and increase production capacity by operating at elongated production times at elevated cell densities (Farid, 2006). This in turn reduces required bioreactor volume from up to 12,000 L required in fed-batch culture approaches to 500-1000 L (Konstantinov, 2015). A smaller bioreactor reduces the facility footprint considerably, which not only reduces initial capital cost but can also significantly affect operational costs in high throughput facilities. There are a number of mAbs currently on the market using continuous cultures and/or purification trains,

including Simulect® manufactured by Novartis and ReoPro® and Remicade® manufactured by Centocor. Recently, BiosanaPharma received approval for Phase I clinical trial for a biosimilar of omalizumab to become the first mAb produced with a fully continuous biomanufacturing process (BiosanaPharma, 2019). The upstream process is based on high cell density perfusion, with downstream processing based on simulated moving bed chromatography and flow-through adsorption (BiosanaPharma, 2019). End-to-end continuous manufacturing is particularly attractive in the production of biosimilars, due to the flexibility afforded by high productivity continuous processing.

The pressure to drive down the cost of manufacture has caused research efforts to focus on increasing process efficiencies and productivities whilst reducing development time. This need has driven great advances in the field of scale-down and microscale bioprocessing techniques. Small scale mimics of production scale operations mean that processes are able to be optimised cheaply, by using small process volumes and rapidly, by using several systems in parallel for high throughput optimisation. The application and use of these scale-down systems has been further improved with the development and implementation of automated systems. Automated systems capable of liquid handling, analysis and sampling and vessel manipulation increase the available throughput of scale-down devices far beyond what is feasible in manual systems.

1.2. Literature Survey

A literature survey has been conducted, primarily focused on history and modes of cell culture operation at production scales, and the subsequent development of scale down tools for fed-batch and perfusion CHO cell culture. The current contribution of scale-down tools for fed-batch and perfusion cultures has been summarised and critically reviewed. Finally, engineering characterisations and rules of thumb for use in designing scale-down methodologies have been examined.

1.2.1. Mammalian cell culture

Mammalian cell culture is the historical cell culture technique of choice in the bioprocessing of recombinant proteins, including mAbs. Several mammalian cell types are adapted for bioprocessing, however CHO cells represent the predominant cell line, becoming the workhorse of recombinant protein bioprocessing since inception in 1957. Manufacture is typically based on a suspension system, where cells are freely suspended in culture and agitated to provide efficient transport of metabolites and O₂. Suspension cultures are well characterised, easily scaled and have well established automated processes for start-up, operation and cleaning in place (CIP) (Birch and Arathoon, 1990). Bioreactors for suspension cell cultures are available at a wide range of scales, from mL to 20,000 L (Eibl et al., 2008). Scale selection for manufacture is determined by the annual throughput required, culture mode selected and productivity of the particular process. Fed-batch culture is the predominant cell culture technique utilised in the bioprocessing of mAb from CHO cells. Fed-batch culture involves the gradual addition of fresh media and substrates into the bioreactor, either at a continuous flowrate or bolus additions at specific timepoints during the culture (Choo et al., 2007). Continued improvement of fed-batch cultures including the optimisation of culture media and increased availability of high throughput scale-down systems for optimisation, have led to a 20-fold (Wuest et al., 2012) increase in productivity of fed-batch cultures since the first processes in the 1980's, with titres of > 5g L⁻¹ routinely reported (Shukla et al., 2017). Despite the capability of fed-batch cultures to generate high titres, throughput per reactor is limited by the feasibility of increasing bioreactor scale beyond 2000 L and capacity to increase bioreactor numbers. Increases in throughput can be alternately achieved by selection of alternative culture modes, for example the implementation of perfusion culture methodologies.

1.2.2. Perfusion Culture

Perfusion culture has historically been a popular production methodology for the production of unstable proteins, compared to fed-batch cultures which more commonly represent the manufacturing method of choice for stable therapeutic proteins such as mAbs. While the implementation of perfusion methodologies offer greater productivity, a smaller facility footprint and reduced cost of goods (CoGs) (Pollock et al., 2013) compared to fed-batch, widespread uptake of the technologies has previously been hindered by elevated batch failure rates and increase complexity of set-up. Technological improvements have decreased perfusion culture failure rates and have allowed the advantages of perfusion culture to be recognised. Additionally, regulatory bodies, such as the FDA, have outlined desire for implementation of continuous biomanufacturing (Bonham-Carter and Shevitz, 2011, Konstantinov, 2015), which in turn has further increased industry interest in perfusion cell culture.

Figure 1.1 demonstrates operational set-up for fed-batch and perfusion culture processes, utilising either tangential flow filtration (TFF) or alternating flow filtration (ATF) for cell retention. Fed-batch cultures involve the addition of media and nutrients at defined time points throughout the culture, leading to an increasing working volume with time. Perfusion culture is a constant volume cell culture process; incorporating continuous addition of substrate and removal of product, alongside by-products and metabolites, while retaining cells in culture with the utilisation of a cell retention device. Steady-state processing creates a stable environment for the promotion of cell growth and product expression for extended culture times, up to several months. In addition to promoting cell proliferation, product quality can be improved with the implementation of perfusion cultures, with continuous removal of cell waste and by-products which can cause product degradation, and by reducing residence time. While fed-batch processes have typical operation times of 14-28 days, with set up and cleaning required between each batch, a single perfusion operation can run for a matter of months uninterrupted.

Since perfusion culture provides a steady state, nutrient rich environment for cell culture, cell densities attained in perfusion cultures are often 1-2 orders of magnitude higher than those reported in fed-batch, and there have been reports of a 10-fold improvement in volumetric efficiencies (Lim et al., 2006, Konstantinov, 2015). Increased volumetric productivity and less bioreactor downtime contributes to perfusion reactors typically being 5 times smaller than fed-batch counterparts whilst achieving the same

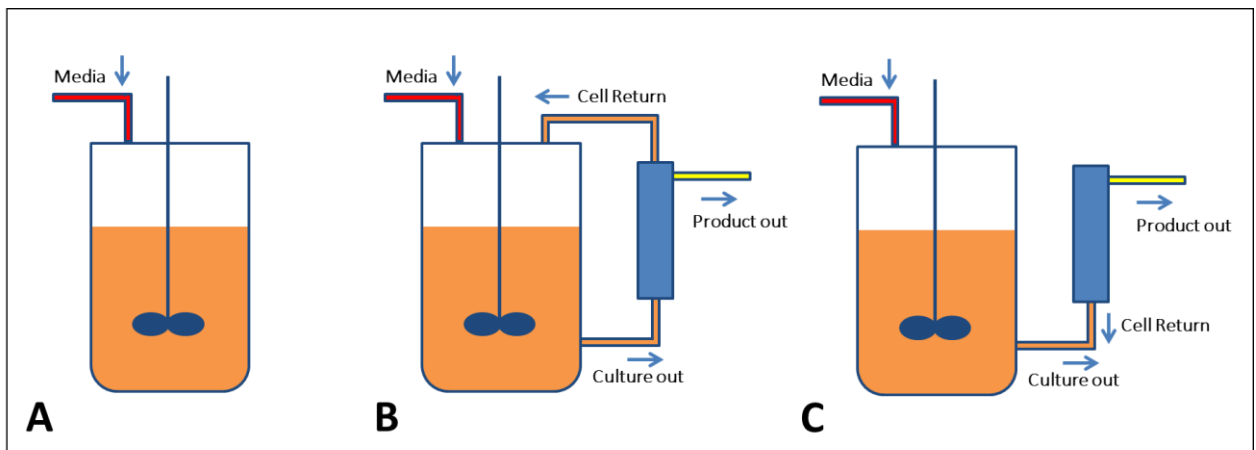


Figure 1.1 - Operational overview of bioreactors in (A) Fed-batch cultures (B) Perfusion cultures with TFF (C) Perfusion cultures with ATF

annual production. Smaller bioreactor volume reduce facility footprint and has the additional advantage of reducing the scale seed train and cell expansion steps, and therefore associated costs. A further advantage of smaller scale systems is the potential implementation of single use technologies. Single-use technologies create a more flexible process, driving manufacturing towards the multiproduct facility concept expected in the near future (Konstantinov, 2015). Further flexibility is offered with the possibility to vary production rate, running at low or intensified capacities, meaning that capacity response to clinical needs are overcome without requiring volumetric expansion of the system (Croughan et al., 2015). The advantages discussed, combined with increasingly sophisticated cell retention devices, media, filtration systems and pumps, mean that perfusion is rapidly set to become the manufacturing method of choice for mAbs.

Despite many advantages, the implementation of a perfusion culture system in place of fed-batch does not come without challenges. Firstly, additional components such as the cell retention device introduce greater process complexity, meaning that perfusion cultures are often associated with elevated failure rates than those incurred in batch and fed-batch cultures. High failure rates are predominantly associated with internal cell retention devices, such as spin filters, which are prone to fouling. Internal cell retention devices, however, are not commonplace, and external cell retention systems such as ATF and TFF filters are preferred (Pollock et al., 2013). Additional complexities in perfusion cultures include the selection of perfusion rates. Low perfusion rates promote higher titres and reduce medium utilisation, which significantly reduces costs associated with maintenance of culture throughout the duration. However, the implementation of reduced perfusion rates often reduces productivity by limiting maximum cell density. Common media formulations are capable of supporting cell densities of up to 10^6 cell mL^{-1} (Kompala and Ozturk, 2006) meaning that a perfusion rate of 10 reactor volumes per day would be necessary to maintain productivity of a perfusion culture maintained at 10^8 cells mL^{-1} . To address this, concentrated and perfusion-specific feeds and media (Sieck, 2017) are being developed, capable of supporting much greater cell densities and facilitating low perfusion rates. This improves productivity, overall yield and reduces costs associated with media utilisation (Xu et al., 2015). Low perfusion rates have the additional advantage of reducing the dilution of the product stream, which causes low titres in perfusion culture compared to fed batch. A perfusion process with a cell density of 60 million cells mL^{-1} has been reported to generate a titre of 0.3 g L^{-1} (Carstens, 2009), whereas in fed-batch processes titres upwards of 5 g L^{-1} are common. Low titres can have a detrimental impact on downstream processing, with a requirement to handle large process volumes causing economic and scheduling difficulties. The difficulties associated with perfusion culture, alongside long timescales associated with process development, have meant that fed batch cultures are currently more widely

implemented in industry (Croughan et al., 2015), however efforts to facilitate ease of implementation and technology advancements are leading perfusion culture to become increasingly attractive.

1.2.2.1. Cell retention devices

The most common cell retention devices for perfusion culture include centrifugation, gravitational settling, spin filters, TFF and, more recently ATF (Castilho and Medronho, 2002). Historically, the most commonly used devices in industrial manufacture have been gravitational settlers and spin filtration. Both of these systems, however, coincide with great validation complexity and have an increased chance of technical failure. New perfusion technologies, such as the ATF system, aim to overcome some of these obstacles (Pollock et al., 2013) to facilitate a wider industry implementation of perfusion culture.

1.2.2.1.1. Centrifugation

Centrifugation achieves separation of cells from supernatant via centrifugal force, achieved in rapidly rotating discs or bowls. A wide variety of centrifuges are available for cell separation, but it is disc stack centrifuges that currently dominate in large scale manufacturing applications. Centrifuges have high separation efficiencies are relatively straightforward to scale. However, mammalian cells can be sensitive to shearing effects in centrifuges, with the potential to detrimentally impact on cell viability and growth as the culture progresses. While shearing effects are not catastrophic for primary recovery processes, in perfusion cultures cells are recycled and cultured for extended time periods, leading to reductions in cell productivity with time and cycle number. Despite this, several manufacturing perfusion processes utilised centrifugation, largely immunoglobulins produced in HeLa, CHO or Hybridoma cell lines (Castilho and Medronho, 2002).

1.2.2.1.2. Gravity settlers

Gravity settlers achieve separation via a terminal settling velocity. The density difference between mammalian cells and supernatant tends to be small, meaning that the terminal settling velocity of the cells is very low, therefore requiring a large settling area to allow the cells to sediment (Castilho and Medronho, 2002). One technique to increase available surface area for settling is to introduce multiple plates, maximising surface area for settling without exponentially increasing the size of the settling unit.

Choo et al. (2007) described a perfusion system for the production of human mAbs in myeloma cells which tend to have low productivity in fed-batch culture. Cell separation was achieved utilising commercially available gravity settlers with multi-plates and a vibrating unit for the perfusion culture process. The gravity settler was found to have a separation efficiency of 98% and perfusion culture utilising gravity settlers was found to be a viable alternative to fed-batch, generating high production efficiencies.

An alternative technique to enhance settling velocity in gravitational settling devices is to apply an acoustic resonance field. Simply, the acoustic resonance field causes cells to aggregate, enabling settling with much higher efficiencies than single cells (Voisard et al., 2003). Commercially available acoustic settlers are beginning to become commercially available for perfusion cultures at a range of scales up, for perfusion rates ranging from 1 to 1000 L day⁻¹ (Applikon., 2014). Separation efficiencies of over 99% are generated by increasing the density differentials between cells and supernatant (Gorenflo et al., 2002), without impacting cell viability. Acoustic settlers are not currently utilised at manufacturing scales, however a new patented design from FloDesign sonics is expected to be marketed for large scale applications in the near future.

Companies such as Genzyme, Janssen Biotech and Eli Lilly all implement gravity settlers for large scale production, with reactor scales between 1500-4000 L. Approved

processes for the production of mAbs involving gravity settlers have been in use early as 1994 (Pollock et al., 2013), meaning the technology is now well characterised and understood.

1.2.2.1.3. Spin filters

Spin filters are cylinders comprised of a porous wall and achieve separation via size differentials. Spin filters can either be mounted internally, driven by the impeller shaft or by an independent motor, or fitted externally. There are many factors which influence the cell retention performance of a spin filter, including but not limited to rotational speed, perfusion rate, cell concentration and filter material (Castilho and Medronho, 2002). The key disadvantage of spin filters is that they are prone to membrane fouling, which in the best case can lead to reduced cell separation efficiencies and in the worst can lead to failures and discarded batches. The risk of fouling can be minimised by utilising low perfusion rates, reducing VCD or increasing pore size of the filter (Deo et al., 1996), however there is a trade-off between optimising these parameters to reduce failure rates without negatively impacting process performance and productivity.

Despite high failure rates, spin filters have been commonplace in perfusion manufacturing for mAbs from as early as 1994. Blockbuster mAbs; Remicade® and ReoPro® by Janssen Biotech both utilise spin filters for production, with Remicade® achieving \$3.6 billion in sales in 2012 in the US alone (Aggarwal, 2014). Spin filters are suitable for the manufacture of large volumes and achieve high throughputs, however the implementation has largely been phased out as new technologies with greater reliability and scale up potential emerge (Bonham-Carter and Shevitz, 2011).

1.2.2.1.4. Alternating tangential (ATF) and tangential flow filtration (TFF)

TFFs are cross flow filtration devices, with supernatant pumped perpendicular to the filter surface, and rate of filtration defined by transmembrane pressure (TMP). Multiple studies have demonstrated the applicability of TFF for perfusion culture of mammalian

cell lines (Clincke et al., 2013, Zhang et al., 2015, Shi et al., 2011). Scale-up parameters have been identified, including maintaining constant shear rate within the filter module and constant flux (van Reis et al., 1997, van Reis et al., 1991, Stressmann and Moresoli, 2008). Membrane fouling is minimised by perpendicular flow, limiting the build up of filter cake, however over the duration of a perfusion cell culture, some fouling is expected. It has been reported that TFF produces lower viability cell cultures with time compared to alternative cell retention devices (Clincke et al., 2013), however recently it has been concluded that the key cause of cell damage in TFF operations is pump type (Karst et al., 2016). Traditional pumping for TFF is achieved with peristaltic pumps, which have poor product sieving and were found to be the single major contributor in TFF systems to shear stress and cell lysis (Wang et al., 2017). Alternative pumps, including a low shear centrifugal pump from Levitronix®, were found to reduce shear and therefore produce improved cell culture performance comparable to alternative cell retention devices (Wang et al., 2017).

ATF is one newly emerging technology that seeks to gain improved process performance and to overcome the limitations of previously discussed technologies. The principle of ATF is a TFF fitted with a diaphragm pump which causes the filter to backflush at periodic intervals, usually every 5 to 10 seconds (Bonham-Carter and Shevitz, 2011). This backflush mechanism allows the filter to operate in high cell density (HCD) cultures for extended periods of time without being subject to fouling, translating to a reduction in failure rates when compared to spin filters. The scale up or down of ATF is also relatively linear and therefore the technology offers simplicity in terms of optimisation and validation.

Clincke et al. (2013) compared the performance of ATF in a HCD perfusion process of antibody producing CHO cells performed in a WAVE bioreactor™ against TFF. They concluded that TFF was able to generate higher cell densities, with performance limited

by the filter capacity. Using ATF, the cell density was limited by pump capacity to pull the increasing viscous broth through the filter. For both ATF and TFF, a working density of below 1.46×10^8 cells mL⁻¹ was recommended, which is greater than typical maximum VCDs in perfusion manufacture of up to 1×10^8 cells mL⁻¹. Karst et al. (2016) compared commercially available ATF system and a TFF system utilising a low shear centrifugal pump. They concluded that while both ATF and TFF were capable of supporting perfusion cell cultures at a range of VCD setpoints, however TFF set ups were found to have high percentage of product retention, whereas no significant retention was observed in the ATF.

It has been previously observed that TFF systems typically result in reduced cell viability and reduced product recovery compared to ATF systems (Voisard et al., 2003, Clincke et al., 2013). This was determined to be a factor of the operating principles of TFF, which requires the generation of liquid shear at the membrane surface to reduce gel layer formation and to minimise fouling (Velez, 1989). Due to the shear-sensitivity of mammalian cells, recirculation flow rate is restricted in order to maintain viability, which causes a degree of membrane fouling which facilitates product retention within the filter (van Reis et al., 1997). Wang et al. (2017) compared performance of TFF and ATF systems, and similarly concluded that TFF systems resulted in increased product retention and reduced cell viability compared to ATF systems when recirculation was achieved with a peristaltic pump. However, the study demonstrated that the peristaltic pump was the major contributing factor to shear stress and cell lysis in the system, and was the primary cause of performance deviation between systems. Further investigations found that TFF systems utilising low-shear centrifugal pumps generated comparable performance to ATF perfusion systems for CHO cell culture, in terms of cell density, viability, and product recovery.

The utilisation of ATF filters in large scale manufacture has been relatively recent, with some of the first validated systems being introduced in 2009. Janssen Biotech utilise ATF systems for the production of mAbs Simponi® and Stelara®, using hybridoma and mice myeloma cells as hosts respectively, at scales between 500 and 1000L (Pollock et al., 2013).

1.2.2.2. Fed batch vs Perfusion economics

Costs associated with cell culture modes vary widely, and several studies have focussed on defining the economic impacts of the implementation of fed batch or perfusion cell culture methodologies for a particular process. The reduction in bioreactor volume for perfusion culture systems reduces capital costs for facility set up. However, additional equipment required for perfusion cultures and the requirement for continual media feeding means the relationship of cost of goods per gram (COG/g) between alternate culture methods is complex, dependant on a large range of factors and is subject to uncertainty.

Pollock et al. (2013) designed a decisional tool model to evaluate the economic implications of employing a perfusion culture, with cell retention achieved utilising either a spin filter or ATF, compared to a fed-batch process with the same required throughput. Comparison of COG/g between the 3 modes at production scales between 100-1000 kg year⁻¹ showed that the implementation of ATF perfusion cultures reduced the COG/g by ~20% across all scales compared to fed batch, whereas the implementation of spin filter perfusion culture provided no economic advantage. A second study conducted by Lim et al. (2006) assessed the economic feasibility of perfusion cultures with spin filters. It was assumed that the bioreactor for perfusion culture was 5 times smaller than the fed batch counterpart at the same production capacity of 50 kg year⁻¹. While the COG/g was comparable between the culture modes, with improved economics from the elevated productivity in perfusion cultures matched

by a requirement for high volumes of media. Despite comparable COGs, capital costs of perfusion culture were 42% lower than fed batch and a facility utilising perfusion can expect a 12% higher net present value (NPV). The study concluded that the implementation of perfusion culture was more economically feasible than fed batch, however the potential of high failure rates associated with perfusion meant that under uncertainty analysis fed batch was found to be more robust.

1.2.3. Microscale Bioprocessing

Increasing pressure to reduce the cost per patient of biologics has driven increasing process efficiency and reducing development times (Betts and Baganz, 2006). The utilisation of scale-down models facilitates high throughput optimisation and process development because of the ability to run multiple experiments in parallel, which reduces timeframes associated with multi-parameter optimisation and process volumes to reduce development costs. Parallel experiments allow a wide range of variables such as cell line, carbon and nitrogen sources, nutrient concentrations, pH and temperature to be simultaneously examined (Doig et al., 2006). Most companies have in-house validated scale-down models of manufacturing and pilot scale bioreactors, commonly at a scale between 0.5-10 L for bioprocess development and optimisation (Betts and Baganz, 2006). Scale-down technologies allow not only for the examination of either standalone unit operations but of whole bioprocess sequences. Microscale bioprocessing techniques are well established for fed batch processes, however, these are less common for perfusion cultures due to increased complexity. In recent years an increasing number of scale-down models for perfusion cultures are in development. Considering that perfusion culture process development and optimisation is associated with high cost and elongated time scales (Croughan et al., 2015), microscale bioprocessing techniques represent an attractive tool for development of perfusion culture processes.

1.2.3.1. Scale-down criteria

The principal aim when designing a successful scale down model is to achieve the same conditions as those established at manufacturing scale. The criterion selected for scale down perfusion bioreactors can be categorised into physical and operational parameters. Physical parameters include maintaining geometric similarities, aspect ratios, type and mode of agitation and location of sensors (Shimoni et al., 2014). Many scale-down devices are based on maintaining physical parameters, however the usefulness of scaling based on physical parameters alone can be limiting for certain unit operations. Mimicking key operational parameters, such as agitation and power input (Titchener-Hooker et al., 2008), can therefore become a powerful tool for scale-down when the ability to maintain physical parameters is limited. The selection of optimal scaling criteria is highly dependent on the particular process and the critical factors that affect performance. Methods of scaling can be broadly categorised into fundamental methods, dimensional analysis, rules of thumb and regime analysis. Rules of thumb involve the selection of operating variables to remain constant throughout scale. Scale translation in biomanufacturing is routinely based upon rules of thumb, including mixing time (t_m), power input per unit volume (P/V), dissolved oxygen concentration (DO), impeller tip speed (u_{tip}), volumetric mass transfer coefficient (k_{La}), or a combination of parameters. Common scaling criteria for aerobic cell cultures are k_{La} and P/V , since oxygen transfer is considered a critical parameter for cell growth. Impeller tip speed and t_m are less commonly implemented because they often do not represent the limiting factor, or maintaining the scaled values are unfeasible (Nienow, 2006). The relationship between the selection of scale-down criteria and output process parameters is complex, with selection of each scaling criteria resulting in vastly different operational conditions across scales. The relationship is described numerically in **Table 1.1**, when scaling based on constant P/V , t_m or u_{tip} . When scaling based on constant k_{La} or DO, the

operational parameters are not defined solely by mathematical relationships and can vary dependant on each process and have therefore been excluded.

Table 1.1- Impact of scale-down criteria selection on operational parameters; power input per unit volume, mixing time and impeller tip speed. Adapted from Oosterhuis and Kossen (1985)

Scale-Down Criteria	P	P/V	Mixing Time	Tip Speed
Constant P/V	10^{-3}	1	0.22	0.47
Constant Mixing time	10^{-5}	10^{-2}	1	10^{-2}
Constant tip speed	10	10^{-5}	0.1	1

Tescione et al. (2015) investigated the impact of scaling criteria on the performance of a scale-down device mimicking a 2000 L CHO cell culture. Three scaling parameters were analysed, namely constant P/V, $k_{L,a}$ and oxygen transfer rate (OTR). Lower viable cell densities (VCD) were reported when utilising P/V as the scaling criterion, attributed to elevated gas flowrates and reduced $k_{L,a}$ in the small scale model. Scaling based on constant $k_{L,a}$ and OTR also failed to produce comparable cell growth performance, demonstrating the complexity of scaling cell culture processes. Mammalian cell processes are most commonly scaled on the basis of any combination of; geometric similarity, $k_{L,a}$, impeller tip speed and impeller speed (Xing et al., 2009).

In addition to scale-down techniques applicable to fed-batch cultures, several scaling parameters specific to perfusion culture have been proposed. Kompala and Ozturk (2006) suggest cell specific perfusion rate (CSPR) as a means to ensure consistent operation throughout scale. When perfusion cell cultures are operated at a constant CSPR, cellular activities do not change with time and cell density. Perfusion rate in constant CSPR processes is variable, dependant on cell density, increasing as the cell density increases through the exponential phase but is relatively consistent through the stationary production phase. The limitation of maintaining CSPR for scale-down is that a high degree of instrumentation and control is required, which is not always feasible in

small scale devices. An alternative to CSPR is maintaining a constant perfusion rate, measured in vessel volumes per day (VVD).

The inherent difference in operation between small and manufacturing scale devices is the mechanism of agitation. Agitation is typically achieved in stirred tank bioreactors with impellers at lab and pilot scale and by shaking in small scale high throughput experimentation. To ensure comparable hydrodynamics and mixing are maintained across vessels utilising varying modes of agitation, several techniques have been proposed. Firstly, dimensionless analysis can be implemented to maintain a constant Reynolds number across scales. Reynolds number in stirred tank systems can be calculated based on impeller speed, type and diameter, and in shaken systems can be calculated on the based on shaking diameter and frequency (Micheletti et al., 2006). An alternative to dimensionless analysis is the maintenance of mixing time. Several methods have been suggested to quantify mixing time in both shaken and stirred vessels, primarily focused identifying colour or concentration changes in a solution with time. Colour based methodologies include iodine (Betts et al., 2014) and the dual indicator system for mixing time (DISMT) (Rodriguez et al., 2013).

1.2.3.2. Scale-down devices

A wide range of devices are commercially available for scale-down studies of cell culture, from simple, low instrumentation devices such as microwell plates to highly controlled miniaturised bioreactors. Scale-down devices are typically mL-scale, however commercially validated scale down models can be at scales up to 10s of L (Doig, 2006). Choice of scale-down model can be dependent on application, for example early phase optimisation requires a high throughput, and microwell plates (MWP) and small scale parallel bioreactor systems are preferable, whereas late stage validation requires systems that are more geometrically similar such as lab scale bioreactors.

1.2.3.2.1. Shake flasks

Shake flasks have been pivotal to process development and optimisation since their adoption for small scale experimentation and cell culture in the 1880s (Duetz, 2007). Shake flasks comprise of simple plastic or glass flasks, with a volume between 10-500 mL, which are agitated via orbital or linear shaking platforms. The extensive use of shake flasks in industry for over 50 years means that they are well characterised and inexpensive (Betts and Baganz, 2006). As the use of shake flasks has developed, instrumentation has been introduced to enable greater process control and analysis. Modern shake flask systems are able to monitor pH and DO sensors in addition to baffles to assist agitation. Despite this, shake flasks have high operating costs and require large lab space (Ngibuini, 2014) when utilised for early process development compared to alternative high throughput systems. Additionally, results obtained in shake flasks are often not directly transferable to manufacturing scale processes, due to geometric and operational differences (Siurkus et al., 2010).

1.2.3.2.2. Microwell plates

Microwell plates (MWP) were initially designed for high throughput analytics. More recently, the use of MWPs in cell culture experimentation has proved a powerful tool for high throughput early phase optimisation. The optimisation of cell culture protocols in MWPs from initial use in the 1980s means that cell culture in MWP is well characterised, and acceptable mixing and O₂ transfer with minimal well-to-well variability is consistently achieved (Duetz et al., 2000). Additional increases in throughput can be achieved with compatibility into automated systems, which provide the potential to increase throughput to allow up to thousands of conditions to be managed per technician, a vast increase compared to shake flasks, which have a feasible limit of up to 50 (Doig et al., 2006). This translates to significantly lower operating costs and elevated throughput in MWP compared to shake flasks. **Table 1.2** compares MWPs to

conventional process development equipment in terms of scale, throughput, control and costs.

Table 1.2- Comparison of scale, throughput, cost and monitoring and control capabilities of equipment commonly utilised for process development

Equipment	Scale	Throughput	Monitoring and Control	Raw Material Cost	Labour Cost	Capital Cost
Stirred Tank Bioreactor	1-100L	1-5 per technician	pH, T, DO, biomass and product	High	High	High
Micro-bioreactor	10-250mL	15-20 per technician	pH, T, DO, biomass and product	Low	Medium	Medium
Shake Flask	25-1000mL	<50 per technician	T, biomass and product	Low	Low	Low
Microwell Plate	0.1-5mL	>1000's per technician	T, biomass and product	Medium	Low	Low

Commercially available plates contain varying numbers of wells between 6 and 196 and are agitated with orbital or linear shaking. Increase in monitoring and control have included the incorporation of pH and DO probes, often in the form of fluorescent dyes immobilised in an adhesive silicone patch on a fibre optic cable. The dye is excited by light at a given wavelength and fluorescence can be quantitatively linked to the given parameter, allowing for accurate online measurements of process parameters (Doig et al., 2006).

Despite recent advances in instrumentation, MWP's often do not have the ability to perform on-line liquid or gas additions, leading to limitations in maintaining required $k_{L,a}$ to support cell growth during cell culture. Oxygen transfer is achieved through the headspace, with shaking speed and surface area to volume ratio determined as the key influencing factors to $k_{L,a}$ (Barrett et al., 2010, Duetz, 2007, Ozturk, 1996). MWP's are commonly sealed with a membrane to reduce evaporation and promote sterility; however the use of these membranes are expected to further reduce $k_{L,a}$, which can limit cell growth and provide misleading results for scale up. Barrett et al. (2010) predicted the $k_{L,a}$ values for shaken MWP's covered with a Breathe-easy membrane at multiple fill

volumes and shaking speeds. The lowest predicted k_{La} value as 1 hr^{-1} , capable of supporting cell densities up to 10^6 - 10^7 cells mL^{-1} . The highest predicted value, obtained at the lowest fill volume and highest rpm, was 29 hr^{-1} , capable of supporting cell densities up to 10^8 cells mL^{-1} (Barrett et al., 2010).

Products such as an EnBase® have sought to overcome the limitations of batch culture without increasing device complexity and requiring additional instrumentation. The EnBase system contains a gel which provides an auto delivery system of nutrients, simulating fed-batch mode without requiring manual media additions. Siurkus et al. (2010) utilised EnBase® technology to enable the use of a 96 microwell plate to evaluate the fed-batch cultivation of an RNase inhibitor in *E.coli*. The small scale process with EnBase produced results comparable to large scale in terms of cell densities and productivity.

Alternatively, fed-batch feeding strategies have been developed for the utilisation in MWP. Silk et al. (2010) described a fed-batch protocol in 24 round well plates, covered with either a Breathe-easy membrane or Duetz sandwich lid to minimise evaporation. The wells were initially filled with 800 μL of medium, and a sacrificial well approach was utilised such that samples could be taken throughout experimentation. Feeding was achieved manually with the addition of fresh media, followed by bicarbonate solution for pH control. This feeding strategy was implemented for 5 consecutive days and was followed by feeding with a diluted feed in line with evaporation rates to ensure a consistent osmolality. This feeding strategy produced comparable results in terms of viable cell concentration, cell viability and antibody titre when compared to results achieved in 250mL shake flasks.

1.2.3.2.3. Automated systems

Automated systems offer the ability to increase throughput far beyond what can feasibly be expected from manual manipulations. Increased throughput from incorporating

automation therefore allows for the investigation of an increased number of parameters at reduced cost and timescales (Lye et al., 2009), thus enhancing the advantages of microscale bioprocessing. Historical application of automated systems is high throughput cell line development, with the ability to screen up to 10,000 clones in a single cycle (Shi et al., 2011), however the use of such systems in process development and optimisation is becoming more common.

The Tecan automated liquid handling platform is one common example of an automated system. It comprises of a liquid handling arm (LiHa) and a robotic manipulator arm (RoMa) within a workstation. In cell culture applications, the workstation is often adjusted to include an incubator as well as microplate readers for analytics, HPLC for product specific analytics and freezers for sample storage. The ability to incorporate a broad range of additional devices into the workstation means that the Tecan has vast experimental potential. Puskeiler et al. (2005) was among the first to describe an *E.coli* fermentation performed within a Tecan platform. Automated capabilities were utilised for media additions in the 48 novel parallel reactors, and for at-line analytics, which were achieved using an integrated plate reader. Physical parameters achieved in the novel bioreactor, such as pH, and DO were comparable to a 3L fed batch fermentation and k_{LA} was capable of adequately supporting cell growth, at 720 hrs^{-1} .

Commercial systems are also becoming available which use automation to gain the throughput of microwell plates whilst achieving the high levels control reported for microbioreactors. Examples of these systems include the $\mu 24$ bioreactor by Pall and ambr™ by TAP Biosystems. These systems are being developed as the industry seeks to overcome the limitations of poor control in microscale systems, shifting towards the ability to more closely maintain the physical characteristics of large scale processes (Nienow et al., 2013).

The μ 24 system is a 3-7mL system based on microwell plate format, agitated via shaking with the capacity for individual well control of temperature, pH and DOT (Pall, 2014). This function expands the range of reaction conditions that can be tested across a single plate. pH and DOT are continually measured by optical monitoring and control is achieved via liquid and gas addition ports. The ability to sparge air into the wells overcomes the oxygen transfer limitations of microwells and promotes greater comparability to the large scale processes. The μ 24 is currently used as an optimisation and evaluation tool, Betts et al. (2014) utilised the μ 24 to evaluate the impact of aeration strategies on fed-bath CHO cell culture kinetics and to perform a full engineering characterisation of the system. The results showed the μ 24 to have good control of environmental parameters and the ability to provide adequate k_La and DO controls.

1.2.3.2.4. Microbioreactors

Microbioreactors seek to overcome the challenges associated with current high throughput scale-down systems, the limited process monitoring and control capabilities and agitation via shaking. Microbioreactors are designed to retain the high throughput, low cost benefits of microscale systems whilst maintaining the high levels of monitoring and control that exist in large scale systems. Currently microbioreactors include miniature stirred tank bioreactors at mL scale, modified MWP's allowing for greater online process control and nutrient feeding and microfluidic devices which operate at volumes in the μ L scale (Bower et al., 2012).

The ambr™ system is an example of a widely utilised, off the shelf microbioreactor system with a wide range of process applications, available at scales of 15 and 250mL. Each reactor is baffled and has compatibility with impellers to provide agitation. There are 4 dedicated feed lines per reactor for alkali, acid, media and antifoam as well as a gas sparger which is able to provide air either in the headspace or at the reactor base. The

feed inlets facilitate feeding regimes meaning the reactors can run in batch or fed-batch mode, and newly developed devices allow capability for parallel perfusion cultures.

There is an ever-growing number of studies using the ambr™ platform, either investigating the performance or for high throughput optimisation of manufacturing scale processes. Nienow et al. (2013) investigated the physical characteristics of the ambr™ platform. They concluded that the ambr™ system produced results consistent with those reported for large scale vessels in terms of operational parameters, such as pH and DOT, as well as cell growth and productivity characteristics. The ambr™ platform is able to collect more consistent results than shake flasks, which are usually subject to wide pH and DOT variations throughout culture, translating to lower cell viabilities. Hsu et al. (2012) evaluated the ambr™ system using a CHO cell line and compared to bench top bioreactors and shake flasks in terms of environmental control and performance. The performance metrics studies included environmental controls; temperature control, DOT and pH and culture performance; growth, viability, substrate concentration, titre and product quality. They observed consistent performance across all replicates in the ambr™ system with close comparability to the bench top vessel in all measured metrics. Both Nienow et al. (2013) and Hsu et al. (2012) successfully utilised for scale-down of fed-batch CHO cell processes, achieving reliable and consistent results to large scale vessels. Other studies have focused on engineering characterisation of the platform, defining k_{La} , power input and mixing time at a range of process conditions. Xu et al. (2017) conducted an engineering characterisation of the ambr™250. The static gassing out method was utilised to define a k_{La} between 1-12 hrs^{-1} at a range of process conditions at $N=150-650$ RPM. Power input was calculated following **Equation 2.21** at 10-50 W m^{-3} at $N=300-550$ RPM, comparable to the range of power input calculated for a 5L Sartorius bioreactor at $N=150-300$ RPM.

There are a board range of alternative microbioreactors available off the shelf, both in single use formats, such the ambr™ system, and in fixed glass and stainless steel configurations. Many publications focus on the utilisation of a wide range of bioreactors for scale down studies for fed-batch cultures, both analysing engineering parameters and demonstrating comparability between scales. The most popular fed-batch devices are at scales of 10s to 100s of mL, with several configurations available at L scale. Examples include but are not limited to; the DASBOX by Eppendorf, Mobius® CellReady by Millipore and WAVE by Pall.

1.2.3.3. Scale-down devices for perfusion culture

While scale-down devices for fed-batch cultures are common, well characterised and have been established for many years, comparable systems for perfusion culture modelling have only recently begun to be described and are being rapidly developed. Recently described mimics for perfusion cultures include a range of scales and operational types, from 96 DWP to 3L fixed bioreactors. Perfusion culture scale-down mimics can include a cell retention device for continuous culture, or alternatively incorporate periodic media exchange following cell separation in semi-continuous perfusion culture. **Table 1.3** summarises several published scale-down devices for perfusion cell culture.

Table 1.3 – Summary of published scale-down models for perfusion culture processes

Company / Device	Scale	Type of perfusion	Process Controls	Reference(s)
96 DWP	0.45mL	Discontinuous - Sedimentation	Temperature	Bielser et al. (2019)
Shake Tubes	10-30mL	Discontinuous - Centrifugation	Temperature	Wolf et al. (2018) Bielser et al. (2019) Gomez et al. (2017) Sieck et al. (2018) Villiger-Oberbek et al. (2015)
Sartorius / Ambr15™	10-15mL	Discontinuous - Sedimentation	pH, DO, Temperature	Kreye and Zoro (2016) Kreye et al. (2019)
Sartorius / Ambr15™	10-15mL	Discontinuous - Centrifugation	pH, DO, Temperature	Janoschek et al. (2018)
Sartorius / Ambr250	150-250mL	Continuous - TFF	pH, DO, Temperature	Zoro and Tait (2017)
Eppendorf / DASBOX	150-250mL	Continuous - ATF/TFF	pH, DO, Temperature	Chotteau (2017)

Spin tubes were among the first perfusion culture mimics to be described (Gomez et al., 2017, Villiger-Oberbek et al., 2015, Wolf et al., 2018, Sieck et al., 2018). Spin tubes have operational volumes between 5-20 mL and are mixed by a speed N between 220 and 320 rpm. Cells are separated via centrifugation prior to periodic media exchanges of 40-100% of the total working volume to achieve desired perfusion rate. Several studies have critically analysed results obtained in spin tubes to those obtained at bench scale in bioreactors, with varying degrees of success. While performance metrics such as peak VCD varied between scales, comparable performance is observed for CSPR_{min}, growth rate, productivity and metabolite consumption rate. Karst et al. (2018) incorporated cell bleeds utilised spin tubes for CHO cell cultures, maintaining a stationary phase culture at 15×10^6 cells mL⁻¹ to perform dynamic metabolic analysis. Wolf et al. (2018) conducted a similar study, utilising shake tubes to investigate peak VCD of clones by daily discontinuous media exchanges at 1 VVD. The best performing clones were then selected for a stationary phase study at a target VCD of 20×10^6 cells mL⁻¹, achieved by incorporating cell bleeds. Villiger-Oberbek et al. (2015) allowed continued cell growth in shake tubes without incorporating cell bleeds and reported peak VCDs up to 50×10^6 cells mL⁻¹.

The utilisation of ambr15® cell culture bioreactors to mimic perfusion has additionally been reported, operated in chemostat mode (Poulsen, 2013, Kelly et al., 2018) or utilising sedimentation (Kreye et al., 2019, Kreye and Zoro, 2016) or, more recently, centrifugation (Janoschek et al., 2018) as cell retention mechanisms. Sedimentation methodologies describe a stirring and control shutdown period of 40-60 minutes to allow for cell separation before supernatant removal and pulse media additions, repeated up to 8 times daily, with separation efficiencies reported >95%. The extended period of control shutdown during sedimentation causes pH and DO spikes that become detrimental to cell health and proliferation as the culture progresses. Despite this, promising results have been obtained, with comparability demonstrated to ATF

perfusion bioreactors up to scales of up to 200 L in terms of VCD and product quality attributes. More recent studies have discussed the development of centrifugation capabilities into the ambr15® for cell separation. To enable centrifugation of ambr15® bioreactors for cell separation, 3D printed baskets were fabricated and fitted to each individual bioreactor. Centrifugation methods vastly reduce manipulation time, and therefore reduce exposure to low pH and DO, improving cell culture performance with maximum VCDs between $20\text{-}40 \times 10^6$ cells mL⁻¹ reported (Janoschek et al., 2018, Kreye and Zoro, 2016). Chemostat mode cultures include pulse media additions, in the absence of a cell retention step, whilst maintaining a constant volume. VCDs of up to 20×10^6 cells mL⁻¹, but whilst periodic media exchange can be considered to be stepping stone towards the mimicking of perfusion methodologies, chemostat methods are limited by the absence of a cell retention step.

Microwell plates have potential to achieve a significant reduction in operational costs and vastly increased experimental throughput. Since MWP are reliant on headspace O₂ transfer only, the capability of MWPs to generate necessary k_La to support HCD cultures has been previously questioned. While k_La can be increased with increasing shaking frequency, maximum k_La is limited by critical shaking frequency at which detrimental impacts to cell culture are observed. It is reported that a k_La between 5-55 hrs⁻¹ can support VCDs up to 10⁸ cells mL⁻¹ (Ozturk, 1996). Published k_La for MWPs at operational conditions; 1mL fill volume, N=225 RPM is 12 hrs⁻¹ in 24 round well plates covered with a gas permeable membrane. Published k_La measurements therefore suggest O₂ should not limit cell growth, even for very HCD perfusion cell cultures. Huang developed a methodology in 24 deep well plates (DWP) with a working volume of 3mL in which cells are seeded at the target density, between $20\text{-}30 \times 10^6$ cells mL⁻¹. Cell retention was achieved via daily centrifugation and media exchange of 100% of the working volume (Huang et al., 2015). The study of stationary phase cultures is a useful tool for metabolic

modelling, however analysis of stationary phase only limits ability to select best-performing cell clones and media.

Recent studies have incorporated the growth phase and compared the use of 96 DWP to previously established spin tube methodologies for scale-down perfusion cultures (Bielser et al., 2019). Bielser et al. (2019) compared performance of both shake tube and 96 DWP scale down mimic to an established 2L BR for clone selection. Scale down in 96 DWP was achieved via incorporating centrifugation as a cell retention step prior to media exchange of 1 VVD. It was concluded that although maximum VCDs and volumetric productivities obtained in DWP were approximately 2 fold lower than those obtained in shake tubes and BRs, the DWP model provided an accurate ranking of cell clone performance.

In addition to semi-continuous perfusion devices, several microbioreactors with connections to cell retention devices have been developed at 100's of mL scale. Additions of TFF filter modules with integrated pump into the ambr™250 have enabled the parallel investigation of perfusion cell culture within the platform. Zoro and Tait (2017) demonstrated design of experiments (DoE) approach to optimise perfusion cell culture processes in the ambr™250 perfusion, with the ability to individually control pH, DO and stirring speed setpoints. Chotteau (2017) developed perfusion culture systems for CHO and HEK293 cells at 250mL in the Eppendorf DASBOX, with cell retention achieved with ATF or TFF. VCDs of up to 100×10^6 cells mL⁻¹ were maintained, with cell retention via ATF maintaining higher viability for elongated periods compared to TFF.

Rapid development of perfusion culture scale-down mimics has begun to provide mimics at a range of scale and operational types, from semi-continuous shake tubes and MWPs to microbioreactors fitted with traditional cell retention devices, such as ATF and TFF. Developments have focused on incorporating cell retention via sedimentation or centrifugation into MWP or shake tube methodologies, previously utilised in fed-batch,

or the retrofitting of cell retention devices onto bioreactors designed initially for fed-batch processes.

1.2.4. Engineering characterisation

As previously mentioned, characterising the environment inside cell culture vessels is vital to understand the hydrodynamic environment, and ensure accurate scaling between vessels of differing geometries and scales. Understanding the hydrodynamics with increasing scale is particularly important in cell culture applications, where heterogeneities can occur due to mixing inefficiencies which, in the case of pH variations can result in cell lysis (Langheinrich and Nienow, 1999). An additional factor influencing cell health in bioreactors is shear stress, which is primarily influenced by impeller configuration, type and rotational speed. Shear stress was historically considered to damage cell health and reduce proliferation, however more recent studies have suggested cell damage is more likely to be a function of the 'bubble bursting effect' due to aeration, rather than shear induced by impeller configurations (Nienow, 2006, Nienow et al., 2013).

1.2.4.1. Mixing dynamics

Mixing time, t_m , can be implemented as a parameter for scaling between vessels. Additionally, mixing time measurements can assist the identification of heterogenous mixing zones, where gradients of O_2 , pH and nutrients can occur. Bioreactor heterogeneities are particularly common in large scale vessels, and can reduce yields and cell proliferation (Lara et al., 2006). Mixing time is influenced by scale, impeller type(s) and speed, fill volume and bioreactor configurations, such as the presence of baffles. Mixing time can additionally be utilised to calculate mixing number (Ntm), a dimensionless parameter defined as the number of revolutions required to achieve a specific degree of homogeneity. Ntm is calculated by multiplying rotational speed by mixing time and is constant in turbulent flow in any given bioreactor configuration.

Several techniques have been suggested for the measurement of t_m , which can be broadly categorised into two groups, utilising either local or global measurement techniques. Local measurements tend to involve a probe within the reactor that monitors the point at which homogeneity is reached for a single point in the bioreactor. To enable measurement throughout the reactor volume, multiple probes can be implemented, however multiple probes impact flow patterns and are unable to identify dead zones (Kasat and Pandit, 2004). Global measurements allow the definition of mixing effectiveness across the entire vessel volume. This allows for non-intrusive measurement of mixing, and identification of dead zones. Historically, this technique has been implemented with visual determination, which is subject to inaccuracy, however more recent methods have improved accuracy with computational image analysis.

Dye visualisation techniques via additions of methylene blue into bulk liquid was one of the first global mixing measurement techniques defined by (Muller, 1985). Manual image analysis was utilised to define the time at which homogeneity was reached at thousands of specified points to obtain t_m . More recently, techniques have expanded on methylene blue measurements (Muller, 1985) by introducing two-phase colour changes with computer-based analytics to allow for increased measurement accuracy and reduced processing times. Melton et al. (2002) described a dual indicator system for mixing time (DISMT), a global measurement technique that incorporates two pH indicators, namely methyl red and thymol blue. Methyl red is red under acidic conditions and thymol blue is blue in basic conditions and yellow at pH 8. Colour changes are induced with the addition of acid and base; HCl and NaCl, at identical molar concentrations and volumes. This technique produces 3 distinct colours during measurements; red in unmixed acidic regions, blue in unmixed basic regions and yellow at pH 5.6-8, defined as the well-mixed region. Since the initial description of DISMT methodologies, several studies have improved the technique, further increasing accuracy and reliability. One recent study by Rodriguez et al. (2013) measured the

standard deviation of the green colour component in orbitally shaken bioreactors. High resolution, fast speed cameras took images throughout mixing which were later analysed using a purposely written code. This technique additionally allowed for the definition of mixing maps, mixing effectiveness in defined regions within the vessel volume.

Mixing time measurements as a tool for cell culture modelling can be limited by the measurement in single phase systems, whereas cell culture conditions often comprise of complex multi-phase conditions, including gas sparging. Several studies have sought to define the effect of multi-phase conditions on mixing efficiency. Grein et al. (2016) examined the impact of aeration on mixing time in the Mobius CellReady bioreactor, finding that aeration had little effect on mixing time at low fill volumes, however at elevated fill volumes and low rotational speeds, mixing time was reduced by up to 50%.

Alternative methods to examine mixing time include planar laser induced fluorescence (PLIF) (Busciglio et al., 2012), where measurements are taken from a number of planes within the working volume. PLIF was compared to local measurements, taken utilising pH probes, and were shown to be more accurate and less sensitive to measurement location (Jardon-Perez et al., 2019).

1.2.4.2. Power consumption

Power consumption relative to volume can be a valuable tool for scaling between vessels with varying geometries and agitation methodologies. Power consumption is defined as the amount of energy necessary to generate the movement of fluid within the vessel, and is commonly calculated as a function of volume for scaling processes. Power consumption in STRs can be calculated following **Equations 2.20** and **2.21**, assuming impeller power number (N_p) from published values based on impeller geometry. Alternatively, power consumption can be measured for specific bioreactor configurations utilising a broad range of methodologies including; electrical or

calorimetric measurements, or the with use of strain gauges, dynamometers or torquemeters (Ascanio et al., 2004).

The first techniques utilised in power consumption measurements were based on electrical measurements, where measurements are taken directly in the motor by wattmeters and ammeters (Brown, 1997). Electrical measurements are simple with little instrumentation required, however power measurements do not take losses due to friction and heat into account. Conversely, calorimetric measurements, involving an energy balance and temperature measurements, are high precision but require complex set up and high degrees of instrumentation (Oosterhuis and Kossen, 1985).

Dynamometers measure force as the agitator applies mechanical force into the liquid contained within the tank. This in turn causes the liquid to exert torque onto the impellers, which causes the vessel to freely rotate within supports on pre-calibrated bearings. Movement of the vessel on the bearings can be measured through mechanical coupling. This technique is a good option for bench and pilot scale vessels, precisely measuring at a wide range of torque, however, requires custom mounting on bearings, and large vessels cannot be supported. Torquemeters allow measurement of torque from strain applied, and can be applied in multiple configurations, measuring torque directly from impeller or in systems comparable to dynamometers, where torque is measured from liquid movement in the vessel when the vessel is fixed to a bearing system (Ascanio et al., 2004). Following power number determination, N_p can be determined for the impeller configuration by re-arranging **Equation 2.20**.

Calculation of power input in MWP's has been defined by Klöckner et al. (2012) A torque and temperature method was utilised to determine power input in shaken cylindrical vessels between 10 – 200 L, and were subsequently correlated with calculated dimensionless numbers to determine influencing factors in power input. Following correlation, dimensionless numbers were replaced by influencing variables to define a

calculation, shown in **Equation 2.19**. Correlations found that well or bioreactor diameter and shaking frequency are the most significant factors influencing power input per unit volume. Considering the impact of vessel hydrodynamics on power input is particularly relevant for perfusion cell cultures, where viscosity and density is expected to increase with time, as HCD is achieved and maintained (Clincke et al., 2013). Viscosity impacts expected in CHO cell cultures have not previously been published, however Blunt (2019) reported that *Pseudomonas putida* cultures experienced near Newtonian behaviours at low cell densities, with increasingly shear-thinning Non-Newtonian behaviour observed at elevated cell densities, This in turn would result in areas where mixing dynamics are slower, meaning viscosity changes expected in HCD cultures influencing heat and mass transfer processes occurring in the vessel (Nienow, 1997, Nienow, 1996). It is therefore important to understand the viscosity changes experienced in HCD CHO cell cultures and subsequent impact on fluid and mixing dynamics in perfusion culture systems,

1.3. Concluding remarks

Continuous bioprocessing, and therefore perfusion culture, is gaining increasing interest in industry. Not only does the technology demonstrate the potential to reduce cost of goods per gram of product, but it is thought that the implementation of perfusion can alleviate the pressures of limited manufacturing capacity when producing high dosage mAbs. The advancements in the field of perfusion, particularly in terms of cell retention devices, have alleviated challenges associated with the technology, such as complexity of set up, operation and associated elevated failure rates compared to fed-batch. These factors, alongside recommendations from regulatory bodies such as the FDA to implement continuous biomanufacturing, have ignited renewed industry interest. With several companies already utilising perfusion cultures in manufacture of mAb products, the number of products on the market manufactured utilising perfusion culture methodologies is set to increase.

Scale-down devices have been commonplace in process development and optimisation stages of a manufacturing facility for many years. Scale-down devices allow for rapid, precise and high throughput experimentation at low cost. While a wide range of scale-down models exist for batch and fed-batch culture processes, including novel and commercially available devices, the same range does not exist for perfusion culture. In recent years, several studies have described the development of scale-down systems for perfusion culture in semi-continuous quasi-perfusion modes in simple MWP or spin tube systems or via the incorporation of cell retention devices into small scale bioreactors. The development of perfusion culture scale-down devices is in its infancy compared to those available for fed-batch processes, with a handful of devices described for specific process applications. Continued design and engineering characterisation for scale-down perfusion culture mimics is required to generate a wide-ranging robust range of scale-down tools for process development of perfusion cultures, ranging from high throughput designs for early phase optimisation of a broad range of process variables, to high functionality models for investigation of a smaller range of parameters.

Herein described is the development of two small scale devices for perfusion culture processes for the production of mAbs. CHO cells were utilised as cell production hosts for the PoC studies, since they represent the most popular cell hosts for production of therapeutic mAbs and therefore represent an industrially relevant expression system. Alternative cell hosts, such as alternative mammalian cell types with similar shear sensitivity and O_2 respiration rates are expected to perform comparably, however confirmation experiments would be required. Hosts with varying shear sensitivity and respiration rates, such as yeast or insect cells, would require further investigation to determine the applicability of developed methods, however since design focused on maximising mass transfer and included built-in flexibility of elements such as sparger design, impeller geometry and utilisation of baffles, developed methods are expected to support a wide range of cell hosts with minor optimisation.

1.4. The present contribution

Recent studies have begun to outline the development of perfusion culture mimics at scales ranging from mL to L. Primarily, these studies involve the incorporation of periodic cell retention and media exchange steps into pre-existing fed-batch methodologies, or the retrofitting of cell retention devices into pre-existing bioreactor systems.

Devices have been shown to be capable of supporting HCD cultures, beyond what has previously been obtained in fed-batch methodologies, generating high volumetric productivities and demonstrating comparability to bench scale perfusion culture systems. Low instrumentation methodologies have been centred around incorporating either sedimentation or centrifugation techniques for cell separation prior to media exchange. These techniques have been demonstrated in spin tubes, ambr15™ and most recently DSW plates. Low instrumentation semi-continuous techniques have been utilised for high throughput clone selection in perfusion culture development, prior to investigation of a small number of parameters at bench scale and to determine operational parameters, such as minimum VCD required to support a desired cell density. Despite the promising number of scale-down devices in development, little comparison has been made between available plate-based methodologies, such as cell retention mechanisms in semi-continuous quasi-perfusion cultures.

Bioreactor systems retrofitted with cell retention devices include the ambr250™ and the DASBOX. Both systems were retrofitted with TFF or ATF cell retention devices and were shown to be capable of generating and maintaining HCD and demonstrate comparability to L-scale perfusion bioreactors. While studies have demonstrated capabilities and, in some cases, compared cell retention devices, little work has focused on the impact of hydrodynamics in small scale cell culture systems specific to perfusion culture. HCD perfusion cultures are expected to have elevated viscosity and therefore differing flow

dynamics compared to fed-batch systems, which could cause problems during scale up, which increasing power demand as scale increases. Additionally, the placement of cell retention loops is expected to have a significant impact on the hydrodynamics of the system, impacting the effectiveness of mixing, introducing shear and potentially introducing excessive foaming into the system.

The aim of this thesis is to provide solutions to bridge this technology gap with the development of scalable, well-characterised, mL-scale methodologies and devices for perfusion culture processes. Quasi-perfusion methodologies in MWP were developed and assessed to increase the availability and throughput while reducing the volume of tools for early process development of perfusion culture. In addition, a novel 250mL BR is designed in order to optimise the hydrodynamic conditions of benchtop BRs specific to HCD, enabling the support of HCD perfusion culture processes. Mass transfer was considered throughout reactor design, incorporating dual impeller configurations, specialised sparger geometry and baffles to facilitate the support and maintenance of HCD cultures by maximising the supply of O₂ and capacity for CO₂ stripping without requirement for utilising elevated RPM or airflow rate, inducing excess shear or foaming.

1.5. Outline of the thesis

The remainder of this thesis comprises 7 chapters. Chapter 2 outlines the experimental set up of quasi-perfusion methodologies, along with corresponding analytical techniques relating to CHO cell culture. Development and design of a novel 250mL BR is described in addition to development of cell culture methodologies in fed-batch and perfusion modes. Techniques of engineering characterisation are outlined, including determination of mixing time, k_La and power input.

Chapter 3 presents the results of development of quasi-perfusion techniques in MWPs. In this chapter, fed-batch methodologies are initially developed in 24 standard round well plates before the introduction of sedimentation and centrifugation methodologies

for quasi-perfusion cultures. The developed quasi-perfusion techniques are subsequently analysed for applicability for use in scale-down studies and implemented in high throughput investigation of perfusion culture parameters, including VVD and media composition.

Chapter 4 outlines the design of the 250mL BR, including design considerations and geometries, compared to the geometries of MWP and 5L BR utilised for scale comparisons. Additionally, characterisation of vessels at each scale is outlined alongside recommendations for scaling criteria between the vessels including k_{La} , mixing time and power input. Finally, the impact of perfusion specific parameters, such as positioning of the cell retention loop and viscosity increases at HCD on the hydrodynamics of the system is discussed.

Chapter 5 draws together quasi-perfusion methodologies developed in MWPs in Chapter 3 and utilises scaling criteria developed in Chapter 4 to design a perfusion culture process in the 250mL BR at a range of VVDs. Perfusion was achieved by the addition of a TFF, recirculated via a low-shear centrifugal pump. Perfusion culture performance is subsequently compared to that in a 5L BR and effectiveness of scaling is evaluated.

Chapter 6 presents a summary of the main conclusions established, alongside recommendations for future work.

Chapter 7 summarises additional outcomes of the thesis, including the scope for validation and commercialisation of the presented work, as well as a short economic and environmental appraisal.

2. CHAPTER 2: MATERIALS AND METHODS

2.1. Introduction

In this chapter, experimental techniques for cell culture, analytics and engineering characterisation are described. Section 2.2 describes cell culture preparation, expansion and storage. Sections 2.3, 2.4 and 2.5 describe batch, fed-batch and perfusion cultures in shake flasks and microwell plates (MWP). The design of a 250mL bioreactor (BR) is described in Section 2.6, and subsequent cell culture in batch, fed-batch and perfusion modes is described in Section 2.7. Further cell culture in 5L BRs is described in Section 2.8, with analytical techniques and derived growth parameters for all cell culture experimentation outlined in Section 2.9. Engineering characterisation of MWPs, 250mL BRs and 5L BRs are described in Sections 2.10-2.13, including rheological characterisation, and determination of mixing time, power input and oxygen mass transfer coefficient.

2.2. Cell culture

2.2.1. Cell line used

A single GS-CHO K1 cell line producing an IgG monoclonal antibody, supplied by Lonza Biologics (Slough, UK), was used for all studies. Cells were cultured in CD-CHO media (Thermo Fisher Scientific, Massachusetts, USA) supplemented with methyl sulphoximine (MSX) at 25 μ M. The mechanism of GS enables the growth of high expressing cells only in glutamine-free CD-CHO media, which metabolise glutamate and ammonia in the medium to produce sufficient glutamine to support cell proliferation (Kingston, 2002).

2.2.2. Revival of cells from liquid nitrogen

A working cell bank vial containing 1mL of frozen cells, stored in liquid nitrogen, was thawed in a water bath (SWB15D; Stuart, Staffordshire, UK) at 37°C for 3 minutes. The

thawed vial was transferred into 9mL CD-CHO medium at 37°C before being centrifuged (Universal 32; Hettich, Tuttlingen, DE) at 450g for 5 minutes. The supernatant was discarded and the cell pellet re-suspended in a total volume of 50mL of CD-CHO medium at 37°C in a 250mL vent cap Erlenmeyer flask (Corning, New York, USA) to achieve a cell density of approximately 0.3×10^6 viable cells mL^{-1} . The flask was placed in a CO₂ incubator (MCO-19AIC; Sanyo, Osaka, JP) at 37°C under 5% CO₂, and was agitated on one of two shakers; the first with an orbital diameter of 25mm, shaken at 130rpm (Certomat MOII; Sartorius, Göttingen, DE), and the second with an orbital diameter of 19mm shaken at 180rpm (CO₂ Resistant Shaker; Thermo Fisher Scientific).

Cells were sub cultured every 3-4 days by dilution into fresh media with a target seeding density of 0.3×10^6 viable cells mL^{-1} in 250mL Erlenmeyer vent cap flasks with a working volume of 50mL.

2.2.3. Preparation of working cell bank

Cells were expanded into 1L Erlenmeyer vent cap flasks with a working volume of 200mL at a seeding density of 0.3×10^6 viable cells mL^{-1} and cultured for 72 hours. The cell suspension was transferred into 50mL centrifuge tubes and centrifuged in a Universal 32 centrifuge at 450g for 5 minutes. Cells were re-suspended in solution of 90% CD-CHO and 10% DMSO (Sigma, Missouri, USA) at a concentration of 1.5×10^6 cells mL^{-1} and subsequently 1mL of solution was transferred into 1mL sterile cryovials (Nalgene™ Cryogenic Tubes; Thermo Fisher Scientific). The vials were placed into a freezing container (Nalgene™ Mr Frosty™; Thermo Fisher Scientific) with isopropanol in a fridge at 4°C overnight, before being transferred into a -80°C freezer for 48 hours. Following this, cryovials were transferred into a liquid nitrogen dewar for long term storage.

2.3. Shake flask culture

Shake flask cultures were performed in 250mL Erlenmeyer vent cap flasks with a working volume of 50mL at a seeding density of 0.3×10^6 viable cells mL⁻¹. Cultures were placed in a CO₂ incubator (MCO-19AIC; Sanyo) at 37°C under 5% CO₂, and were agitated on one of two shakers; the first with an orbital diameter of 25mm, shaken at 130rpm (Certomat MOII; Sartorius, Göttingen, DE), and the second with an orbital diameter of 19mm shaken at 180rpm (CO₂ Resistant Shaker; Thermo Fisher Scientific). For fed-batch cultures, feeding commenced on day 3 for 6 consecutive days. Feeding involved the addition of 2.5mL (5% volume) Efficient Feed B, followed by an addition of 1.25mL (2.5% volume) of bicarbonate solution to control pH. Bicarbonate solution was made up using 0.75M Na₂CO₃ (Sigma) and 0.5M NaHCO₃ (Sigma).

2.4. Microwell culture

All microwell cultures were performed in Standard Round Well Ultra-Low Attachment microwell plates (MWP) (CLS3483 Costar®; Corning) sealed with a Duetz sandwich lid (CR1524/CR1524a; EnzyScreen, Heemstede, NL) to maintain sterility and minimise evaporation whilst maximising headspace air exchange. Cultures were incubated in a humidified Sanyo incubator with CO₂ maintained at 5% and were shaken at 220rpm and at an orbital diameter of 25mm (Certomat MOII; Sartorius). All fed-batch and pseudo-perfusion microwell cultures were inoculated at densities between $0.2 - 2 \times 10^6$ viable cells mL⁻¹ and operated at a working volume of 1.2mL, unless otherwise stated.

2.4.1. Fed-batch culture in 24-well MWPs

Fed-batch cultures included daily feeding, commencing on day 3 for 5 consecutive days. Feeding involved a 60µL (5% volume) bolus addition of Efficient Feed B (Thermo Fisher Scientific), a nutrient rich feeding media, followed by an addition of 30µL (2.5% volume) of bicarbonate solution to control pH. Bicarbonate solution was made up using 0.75M Na₂CO₃ (Sigma) and 0.5M NaHCO₃ (Sigma) (Silk et al., 2010), and subsequently diluted

ten-fold for ease of liquid handling and to ensure the liquid volume is kept constant during evaporation. Due to the limited volume available in microwell systems, sampling was achieved using a sacrificial well approach. Average evaporation across the plate was monitored via daily weight measurements, before and after sampling.

2.4.2. Determination of evaporation in 24-well MWPs

Due to the sacrificial well approach used, evaporation in each well was quantified to ensure consistency across the plate and check the presence of edge effects. Evaporation was determined based on the change in concentration of blue dye over time, measured using optical density (OD) at 630nm. A stock solution of blue dye was added to 24-well MWPs at a fill volume of 1.2mL and covered with a Duetz sandwich lid. Culture conditions were simulated in a Sanyo humidified incubator at 37°C, shaken at 220rpm and at an orbital diameter of 25mm, for 8 days. The OD of each well was determined by transferring 100µL into a microtitre plate and measuring the absorbance at 630nm on a plate reader (FLUOstar Omega; BMG Labtech, Ortenberg, DE). Ultrapure water (Milli-Q®; Merck-Millipore, Darmstadt, DE) was utilised as a blank to enable the calculation of fold evaporation using **Equation 2.1** following Doig et al. (2006):

$$Fold\ Evaporation = \frac{(A_{630,d_n} - A_{630,blank})}{(A_{630,stock} - A_{630,blank})} \quad (2.1)$$

Where A_{630,d_n} is the absorbance of the well at day n, $A_{630,blank}$ is the absorbance of ultrapure water, and $A_{630,stock}$ is the absorbance of the blue dye initial stock solution.

2.5. Perfusion microwell culture

2.5.1. Development of quasi-perfusion techniques in 24-well MWPs

Media exchanges in quasi-perfusion cultures commenced on day 3 and continued until the termination of the culture. Media exchanges were preceded by a cell retention step, utilising either sedimentation or centrifugation to separate the cells from the

supernatant. A defined volume of supernatant was subsequently removed, and cells were re-suspended in fresh media. The volume of fresh media was calculated as the volume of supernatant removed plus an additional 36 μ L to account for 3% daily evaporation, ensuring a constant volume. The media used for exchange was CD-CHO, CD-CHO supplemented with glucose at 9 or 12g/L or with CD-CHO blended with Efficient Feed B at 5, 15, 30 or 45% v/v.

2.5.2. Determination of sedimentation time and centrifugation conditions for quasi-perfusion cultures

Methods for cell retention were developed such that they provided sufficient separation whilst minimising detrimental impact to cells. In the sedimentation protocol, plates are removed from the shaker and allowed to settle in the incubator at 37°C, 5% CO₂. Settling time was initially calculated using Stokes law, **Equation 2.2**;

$$V_t = \frac{gd^2(\rho_p - \rho_m)}{18\mu} \quad (2.2)$$

Where V_t is settling velocity, g is acceleration due to gravity, d is particle diameter, μ is viscosity of medium and ρ_p and ρ_m are the densities of the particle and the medium respectively. The medium was assumed to have the properties of water at 37°C. Settling velocity can then be used to calculate settling time using **Equation 2.3**;

$$t_s = \frac{H_L}{V_t} \quad (2.3)$$

Where t_s is settling time and H_L is liquid height.

From **Equations 2.2** and **2.3** a calculated settling time of 10 minutes was determined for cultures with a working volume of 1.2mL. The accuracy of Stokes law relies on several assumptions, including the particle being spherical and rigid, and there being no particle nearby that would affect the flow pattern. These assumptions are not necessarily

applicable to cells in a high cell density culture, and therefore the calculated settling time was validated experimentally. To achieve this, cells were seeded at a high concentration, 40×10^6 cells mL^{-1} , into 24-well MWP at 1.2mL and allowed to settle. Every 3 minutes, half of the volume (0.6mL) was taken from the top of the liquid level in a sacrificial well and the cell density measured. Separation efficiency with time was calculated from the cell concentration in the supernatant.

Figure 2.1 shows a separation efficiency for the calculated separation time of approximately 70%. Increasing the separation time to 24 minutes generate efficiencies greater than 95% without impacting cell viability. A sedimentation time of 28 minutes was selected and utilised for cell retention in all sedimentation quasi-perfusion cultures.

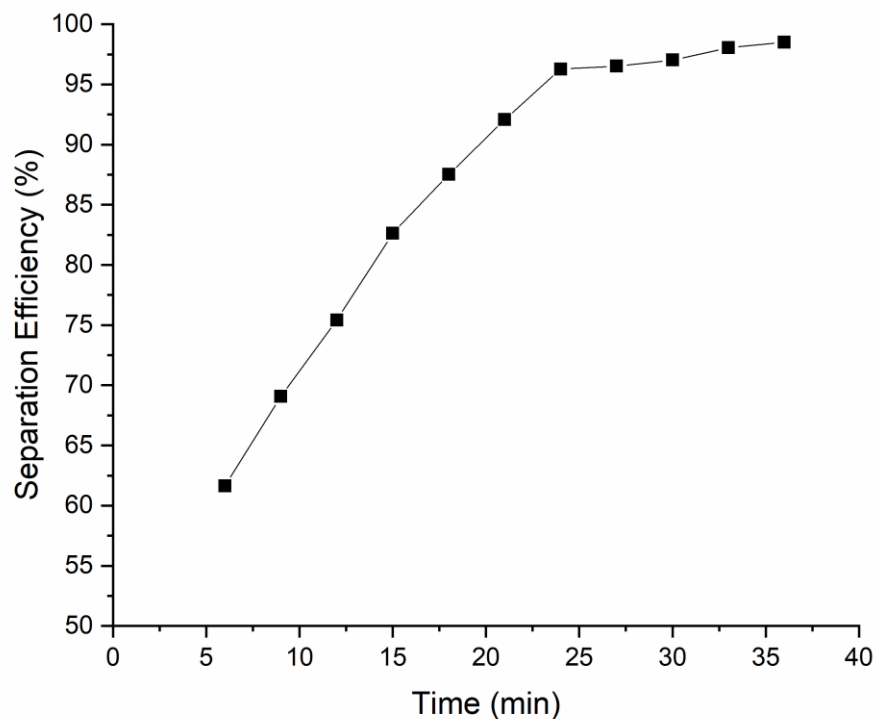


Figure 2.1 - Separation efficiency with time for cell culture seeded at 40×10^6 and allowed to settle via gravity. Data represents triplicate wells.

In cultures that utilised centrifugation for cell separation, MWPs were centrifuged in a Universal 32 centrifuge (Hettich) fitted with a plate rotor. The centrifuge speed was set

as the minimum that provided adequate cell separation, which was found to be $50 \times g$. In quasi-perfusion centrifugation cultures, plates were spun at $50 \times g$ for 5 minutes prior to media exchange.

2.5.3. Media exchange for consistent VVD

Perfusion rates between 0.5 and 1.8 VVD were evaluated for both sedimentation and centrifugation cell retention techniques. This was achieved by varying the volume of exchanged media from 600 – 1100 μ L and by repeating exchanges up to 1-2 \times daily to achieve the desired perfusion rate. For sedimentation cultures, the cell pellet is less tightly packed, so the maximum volume per exchange was set at 75% to ensure that cell separation efficiencies were maintained above 95%. This meant that the maximum perfusion rate for sedimentation cultures over 2 daily exchanges was 1.5 VVD. The use of centrifugation for media exchange resulted in a more tightly packed cell pellet, meaning that the entire volume of the supernatant could be removed during each exchange without impacting cell separation efficiencies, generating perfusion rates up to 1.8 VVD.

2.5.4. Media exchange to maintain constant cell specific perfusion rate (CSPR)

For several cultures, media exchange was carried such that a constant CSPR was maintained throughout. In order to achieve this, a sample was taken prior to exchange and cell concentration was measured. The volume to be exchanged each day was calculated using the following **Equation 2.4**;

$$V_{ex,n} = C_{cells} \times V_{well} \times CSPR \quad (2.4)$$

Where $V_{ex,n}$ is the volume to exchange on day n (mL day⁻¹), C_{cells} is the measured concentration of cells (cells mL⁻¹), V_{well} is the volume of the well (mL) and CSPR is the desired cell specific perfusion rate (mL cell⁻¹ day⁻¹). The CSPR was set between 0.02 – 0.06 nL cell⁻¹ day⁻¹ for both sedimentation and centrifugation cultures and was kept

constant throughout. Where calculated exchange volume exceeded the maximum exchange volume, up to 2 daily exchanges were carried out.

2.6. Design and fabrication of novel 250mL bioreactor

Cell culture in 250mL bioreactors was carried out in batch, fed-batch and perfusion modes in a novel bioreactor geometry specifically designed for small scale perfusion cultures. The bioreactor was designed and fabricated to meet the requirements of a perfusion culture, including additional ports to allow for cell retention connection, placed to minimise shear and foaming, and the inclusion of baffles and dual impellers to encourage O₂ transfer and CO₂ stripping. A schematic of the reactor design is depicted in **Figure 2.2**. The dimensions and geometries can be found in **Table 2.1**.

Table 2.1 - Reactor geometry and design specification

Dimensions		
D _T	6.7	cm
H _T	10	cm
H _L	7.4	cm
W _V	250	mL
Baffles		
D _B	0.35	cm
W	0.05	cm
H	8	cm
Spacing	7	cm
Impellers		
Type	Dual Rushton-Style & Pitch Blade	
D _i OD	3	cm
H _{I1-I2}	2.5	cm
H _{I1-BASE}	2	cm
Sparger		
Type	L-sparger	
Length	8.5	cm
Hole number	7	
Hole size	0.5	mm

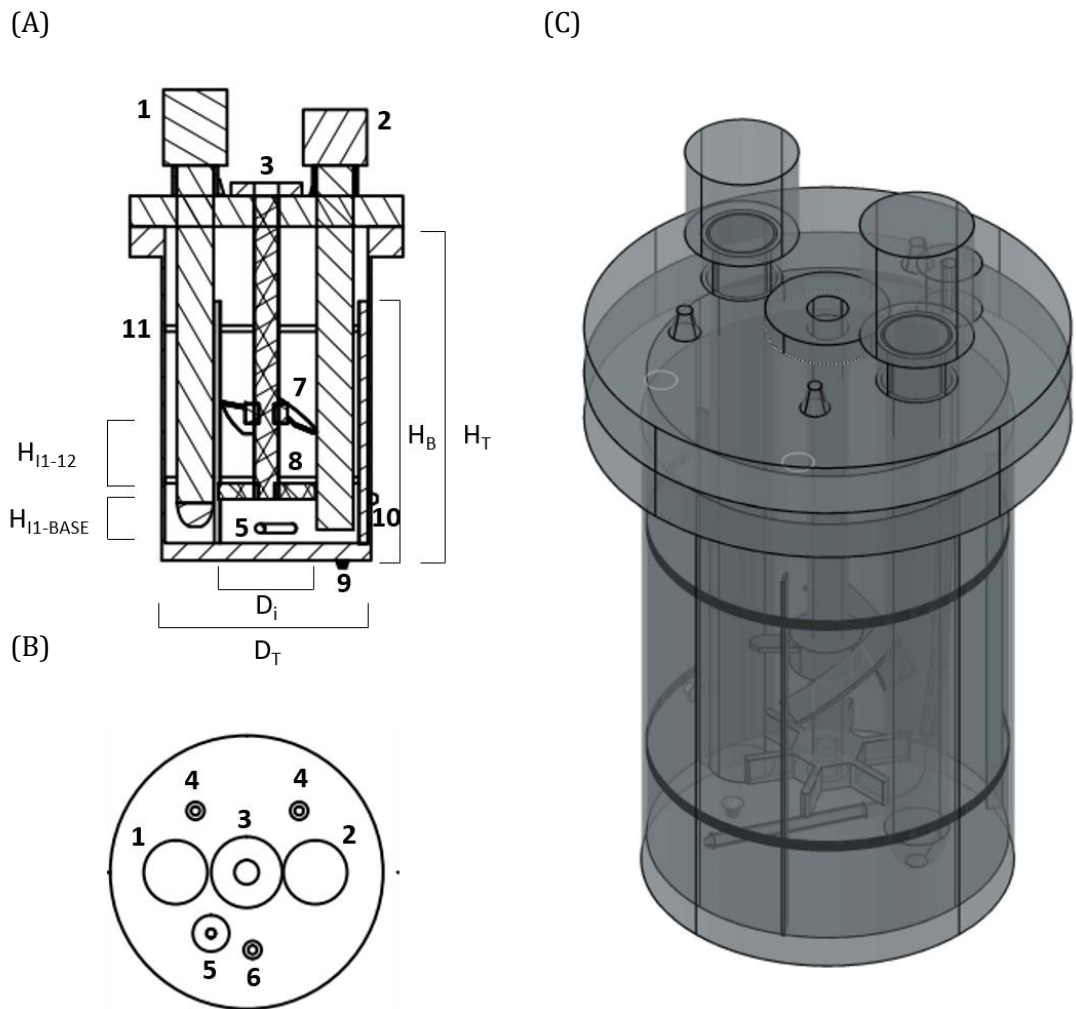


Figure 2.2 - Reactor geometry and design drawing. (A) 2-D cross-section (B) 2-D headplate (C) 3-D view with X-ray allowing observation of internal components (1) pH probe port (2) DO probe shaft (3) Impeller shaft (4) Liquid addition (5) Sparger (6) Gas outlet (7) Pitch-blade impeller (8) Rushton-style impeller (9) Connection to cell retention device - outlet (10) Connection to cell retention device - inlet (11) Baffles

The bioreactor has a flat bottom, with a diameter of 6.7cm and height of 10cm, and was designed such that that ratio of $H_T:D_T$ is approximately 1.5:1. $H_T:D_T$ was selected on the basis of increasing residence time within the reactor while retaining a large headspace surface area (Clapp, 2018). The liquid height for the working volume of 250mL is 7.4cm. The tank contains 3 baffles, each with a diameter of 0.35cm, calculated following **Equation 2.5**.

$$D_B = 0.05D_T \quad (2.5)$$

Where D_B is the diameter of the baffle. The baffle height (H_B) is 8cm, such that $H_B > H_L$ at the operating volume, where H_L is liquid height. The baffles were evenly spaced in the tank, with a spacing of 7cm between each. The impellers consisted of a 6-blade flat blade turbine impeller below a 3-blade pitched-blade impeller with a 30° pitch (Eppendorf, Hamburg, Germany). The flat blade turbine impeller is similar to a Rushton turbine since it contains 6 flat blades at 90°, however does not contain a disk. For simplicity the 6-blade flat blade turbine will herein be referred to as “Rushton-style”. Rushton style impellers are associated with high shear with high impeller power number of ~5 (Ravi, 2017) and are typically utilised in fast growing cultures of cells that are less shear sensitive, such as bacteria and yeast (Flickinger, 2010). Pitched blade impellers provide axial flow and are associated with low shear, with impeller power numbers ~0.75 (Ravi, 2017), and are commonly implemented in processes where mass transfer demands are lower, such as mammalian cell cultures (Flickinger, 2010). Very HCD perfusion cultures have unique characteristics whereby demand for O_2 transfer, bubble dispersion, and CO_2 stripping is high but CHO cells are somewhat shear sensitive, although several recent studies have shown that shear sensitivity in CHO cells is more closely linked to bubble bursting (Nienow, 2006) and Kolmogoroff Eddy size concepts (Flickinger, 2010). Considering these requirements, and the additive nature of power number (Ravi, 2017, Fitchen, 2019) when utilising multiple Rushton turbines, it was decided that a dual impeller configuration consisting of a Rushton-style turbine and a pitched blade, would provide adequate mass transfer and bubble dissipation, capable of supporting HCD perfusion cultures, without inducing shear stress beyond that tolerated by CHO cells. Both the Rushton-style and pitched blade impeller had an outer diameter (D_i) of 3cm, according to the following **Equation 2.6**.

$$D_i = 0.4D_T \quad (2.6)$$

The internal spacing of the impellers was calculated such that the distance from the first impeller to the base was $0.33 D_T$ and the spacing between the impellers was approximately equal to the impeller diameter. The impeller shaft has a diameter of 8cm, sufficient to avoid large oscillations at high rotational speed.

The sparger is an L-shape, designed to sit 0.5cm below the impellers, drilled with 7 holes with a diameter of 0.5mm, to maximise gas transfer by reducing bubble size and therefore increasing surface area available for mass transfer compared to open hole spargers.

The top plate is fitted with 3 hose barb connectors for media additions, base additions for pH control and for outlet gas, each with a diameter of 3.2mm. The top plate includes two elevated housings with a 12mm diameter for the placement of pH (EasyFerm; Hamilton, NV, USA) and electrolyte DO (OxyFerm; Hamilton) probes with a length of 120mm and a diameter of 12mm could be fitted within the vessel. Connection to the cell retention device was achieved by a hose barb connector at the base of the vessel, with a diameter of 3.2mm, and returned into the side of the vessel at a height of 2.5cm from the base. The cell retention connection location on the reactor base is comparable to large scale systems and alleviates over-cluttering on the headplate. Additionally, the return of cell broth below the liquid level reduces foaming compared to return from the headplate and reduces shear stress caused by the recirculation loop.

Temperature was monitored externally via a thermowell temperature sensor (New Brunswick, Eppendorf). Correlation between the measured temperature outside and the temperature inside is shown by **Equation 2.7**.

$$T_{in} = T_{out} + 3.5 \quad (2.7)$$

Where T_{in} is the temperature inside the vessel, T_{out} is the measured temperature outside the vessel, and temperatures are measured in °C.

The reactor was fabricated in the UCL Biochemical Engineering Workshop and is made of stainless steel. To enable engineering characterisation of the 250mL BR, a mimic was fabricated in the UCL Biochemical Engineering Workshop, made of acrylic. Acrylic is transparent and allows for observation of internal BR conditions, however, is not easily sterilised and therefore is unsuitable for cell culture applications. The acrylic mimic, shown in **Figure 2.3**, has identical internal dimensions to the stainless steel culture BR, and identical placement of recirculation flow ports on the base and the side. Additionally, impeller shaft, type and position and baffles were replicated from the stainless steel culture BR. Despite having identical internal dimensions, the acrylic mimic has flat external walls, to increase the quality of images taken in characterisation studies by reducing refraction of light from the external surface of the mimic. **Figure 2.4** shows photographs of (A) stainless steel bioreactor and (B) acrylic mimic.

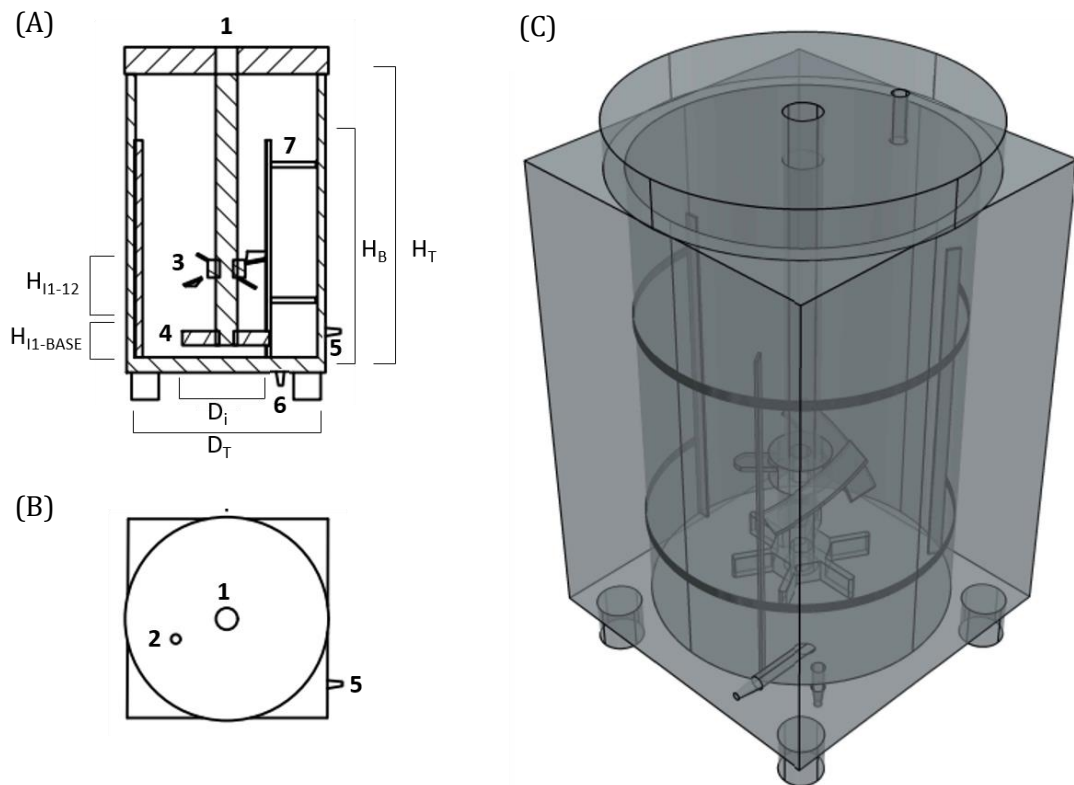
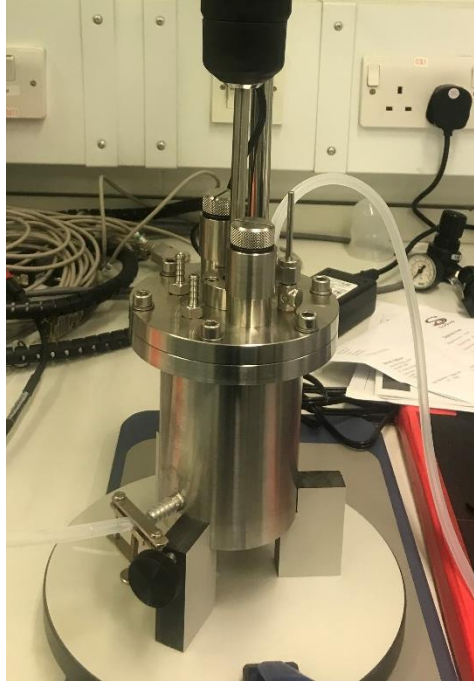


Figure 2.3 - Acrylic mimic reactor design drawing. (A) 2-D cross-section (B) 2-D headplate (C) 3-D view with X-ray allowing observation of internal components (1) Impeller shaft (2) Liquid addition port (3) Pitched blade impeller (4) Rushton-style impeller (5) Connection to cell retention device - inlet (6) Connection to cell retention device - outlet (7) Baffles

(A)



(B)

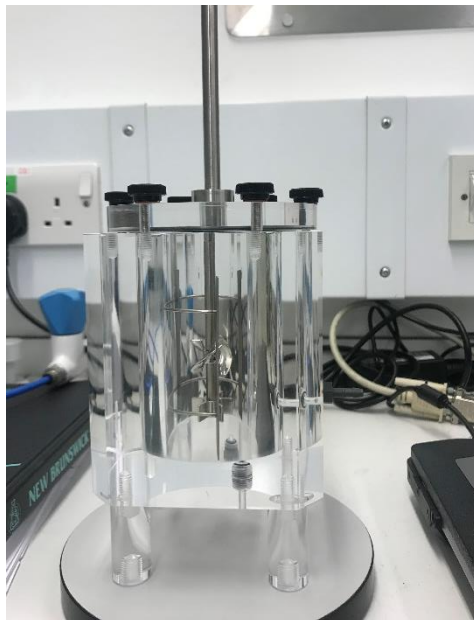


Figure 2.4 Photographs of 250mL BRs, fabricated by UCL Biochemical Engineering Workshop. (A) Stainless steel cell culture bioreactor. (B) Acrylic mimic for hydrodynamic analysis

2.7. Culture in novel 250mL bioreactor

The bioreactor was connected to a BioFlo110 controller (New Brunswick, Eppendorf) with 4-Gas blending. The control of pH was achieved via the sparging of CO₂ and base additions, with CO₂ additions restricted to a maximum flowrate equivalent to 20% of

total air flowrate. Electrolyte DO sensors within the reactor continually measure DO concentration related to the calibration of raw signals utilising offset and slope measurements. DO is maintained by sparge on demand oxygen enrichment cascades, altering the percentage of N₂, O₂ or air to maintain the desired setpoint while maintaining a constant air flowrate. Temperature was controlled using a 5 × 15 cm silicone heating mat (RS Components, UK) adapted by the UCL electrical workshop for compatibility with the controller. An overhead stirrer (Pro40 Digital Overhead Stirrer; SciQuip, UK), independent of the controller, was utilised for agitation. Prior to each bioreactor run, pH was calibrated by placing the probe into pH 4 solution, followed by pH 7 solution (Mettler Toledo, Ohio, USA). The bioreactor was sterilised at 121°C for 15 minutes containing 250mL MilliQ water. DO was calibrated after sterilisation by sparging air at the desired air flowrate and agitation rate overnight until a stable signal is achieved, and subsequently sparging N₂ until a stable signal is achieved, approximately 1 hour. Following calibration, MilliQ water was aseptically removed.

All cell cultures in the bioreactor were cultured at 37°C (T_{in}), with a pH setpoint of 7.2 ±0.1 and DO controlled at 30%, unless otherwise stated. The working volume across all culture modes was 250mL. Air flowrate into the bioreactor was 50 mL³ min⁻¹, a volumetric flowrate of 0.2 VVM. Cells were seeded at 2 × 10⁶ viable cells mL⁻¹. Base control was achieved with automatic additions of 1M NaOH (Sigma). Foam was controlled with a 1mL addition of 1% antifoam (Antifoam C Emulsion; Sigma) as required.

2.7.1. Batch and fed-batch

Figure 2.5 shows the bioreactor set-up for batch and fed-batch modes. Agitation rate in batch and fed-batch modes was set at $N = 250\text{rpm}$. In batch mode, cells were seeded at the target cell density in 250mL CD-CHO. In fed-batch mode, cells were seeded at the target density in 162.5mL of CD-CHO. Feeding commenced on day 3 and involved a 12.5mL (5% volume) addition of Efficient Feed B until day 9, when the working volume of 250mL was reached. Cell retention connector ports were closed off and utilised as sampling ports.

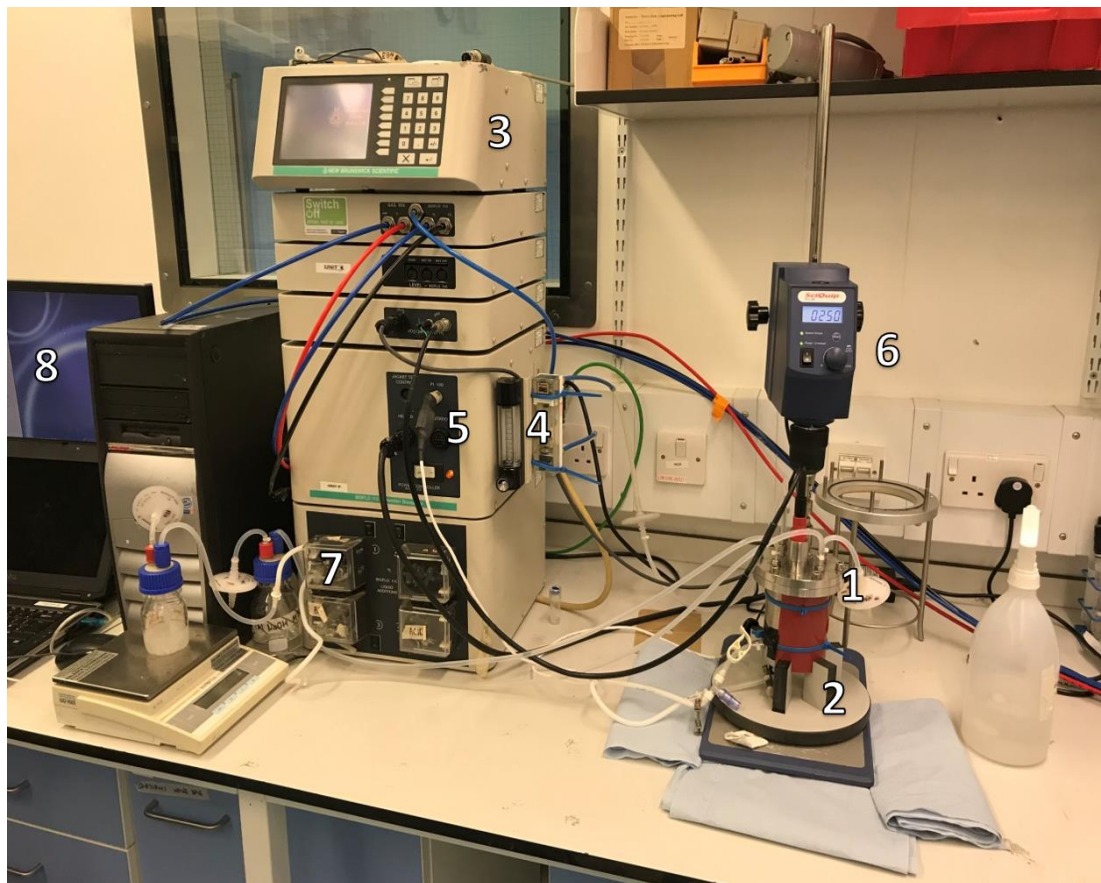


Figure 2.5 - Bioreactor configuration for batch and fed-batch operation. (1) 250mL BR: H=10cm W=6.7cm. Dual Rushton and marine impeller, 3 baffles, L-sparger, oxyferm DO and easyferm pH probe (Hamilton). (2) Stand (3) Control tower (New Brunswick) (4) Air flow rate control (5) Temperature and heating jacket control (6) Agitation motor (Rockwell automation) (7) Liquid addition pumps (8) Computer for monitoring and data logging (Dell)

2.7.2. Bioreactor perfusion operation

Figure 2.6 shows the bioreactor set-up for perfusion. Cell retention for perfusion cultures was achieved with a tangential flow filter (TFF). A hollow fibre mPES TFF with a surface area of 88cm², length of 20cm and internal diameter of 1mm (Spectrum® MidiKros; Repligen, Massachusetts, USA) was connected via the base and side connections. During perfusion operation, cell culture was circulated at flowrate of 80mL min⁻¹ using a PuraLev® i30SU pump with sterile, single use pumphead (PuraLev® i30 SU; Levitronix, CH). The recirculation rate was calculated such that shear rates of 1000s⁻¹ were generated, consistent with shear rate targets in the range of 1000 - 2000s⁻¹ for use with fragile cell lines. Shear rate promoted by the pump was not considered, as while peristaltic pumps in TFF systems are considered the major contributor to shear stress (Wang et al., 2017), the low shear factor of the Levitronix pump was considered negligible in this work. Media inlet and supernatant outlet flow rates were controlled using identical peristaltic pumps (101U/R; Watson-Marlow, Cornwall, UK).

For perfusion mode cultures, cells were seeded at the target density in 250mL of CD-CHO. Agitation rate was initially set at 250rpm and DO at 30%. Perfusion commenced on day 3, when cell recirculation was initiated. CD-CHO blended with 15% v/v Efficient Feed B was attached to the media inlet and fed into the bioreactor between 0.09 - 0.625 mL min⁻¹, generating perfusion rates of 0.5 - 1.8VVD. Supernatant was simultaneously removed at an identical flowrate, maintaining constant volume in the vessel. During the culture, as cell density increased, the air flow rate and agitation setpoints were incapable of maintaining DO. To enable maintenance of the DO setpoint, the agitation rate was increased stepwise by 30 rpm per day, as required, to maximum of 500rpm. During perfusion culture, 1mL of antifoam was added daily to control foam levels.

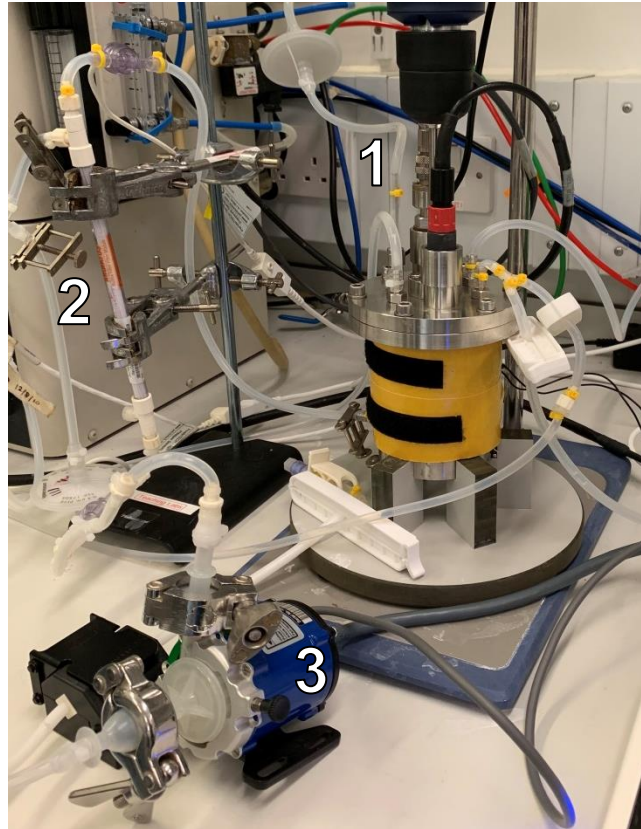


Figure 2.6 - Bioreactor configuration for perfusion mode operation, with cell retention achieved by TFF (1) 250mL BR: H=10cm W=6.7cm. Dual Rushton and marine impeller, 3 baffles, L-sparger, oxyferm DO and easyferm pH probe (Hamilton). (2) Hollow fiber filter module. PES, 0.2 μ m pore diameter. SA 88cm² (Spectrum labs) (3) PuraLev® i30SU magnetic centrifugal pump (Levitronix)

2.8. Cell culture in commercial 5L bioreactor

A 5L stirred bioreactor (Biostat B-DCU; Sartorius, Epsom, UK) was operated at 37°C, with a pH setpoint of 7.2 \pm 0.1 and DO controlled at 30%. Temperature was controlled using an electrical heating jacket. pH was controlled using a combination of CO₂ sparging and base additions, while DO was controlled by sparging air, N₂ and O₂ using a horse shoe sparger. Base control was achieved through additions of 1M NaOH. Air flow rate was 200 mL min⁻¹, a volumetric flow rate of 0.08 VVM. Agitation was provided by a three blade pitched impeller with a 45° pitch. Prior to each reactor run, the pH probe was calibrated in pH 4 buffer, followed by pH 7. Sterilisation took place at 121°C for 15 minutes, with the vessel containing 2.5L of MilliQ water. Calibration of the optical DO probe (InPro; Mettler Toledo) took place after sterilisation; sparging air until saturation,

approximately 1 hour, followed by sparging N₂. Aseptic removal of MilliQ water followed DO calibration.

2.8.1. Fed-batch

Cells were seeded into 2 parallel Biostat B-DCU units, at 0.3×10^6 viable cells mL⁻¹ at an initial volume of 2.5 L. Agitation rate was set at N = 260 rpm. Feeding commenced on day 3 and involved the addition of 125 mL (5% volume) Efficient Feed B daily, until the total volume reached 3.25 L on day 9. Foaming was controlled with 10mL additions of antifoam as required.

2.8.2. Perfusion

Cells were seeded into a single Biostat B-DCU unit at 2×10^6 viable cells mL⁻¹ in 2.5 L of CD-CHO. Perfusion was initiated on day 3. Agitation rate was initially set at 260 rpm and was increased stepwise by 7 rpm, as required during perfusion operation to maintain DOT, to a maximum of 320 rpm. Cell retention connection was achieved using tangential flow filtration (TFF); attached through a dip tube, typically used for media removal, and returned through the headplate. The hollow fibre mPES TFF had a length of 20cm, an internal diameter of 1cm and an area of 480cm² (Spectrum® MiniKros; Repligen). A PuraLev® i30SU pump was used for recirculation at a rate of 400mL min⁻¹, generating a shear rate of 1000s⁻¹. Media in and supernatant out were pumped at 1.7mL min⁻¹ using identical peristaltic pumps, a perfusion rate of 1VVD. Perfusion media was CD-CHO blended with Efficient Feed B at 15% v/v. Antifoam (Antifoam C emulsion; Sigma) was used to control foaming with a daily addition of 20 mL.

2.9. Cell culture analytical techniques

2.9.1. Determination of cell number and viability

Cell counts were performed in a Vi-Cell XR automated viability analyser (Beckman Coulter, California, USA), with samples diluted in PBS (Gibco, Thermo Fisher Scientific) as required.

2.9.2. Determination of metabolite concentration

Metabolite concentrations were determined using NOVA Bioprofile FLEX (Nova Biomedical, Deeside, UK). Prior to analysis, samples were centrifuged at 16200 rpm for 5 minutes and the supernatant frozen at -20°C until required. PBS was used for dilution of samples, to bring metabolite concentrations into the analysis range and to conserve the limited sample volume.

2.9.3. IgG quantification

IgG titre was determined using HPLC (HPLC Agilent 1100 series; Agilent, Santa Clara, USA). A 1mL Protein G column (HiTrap Protein G HP; GE Healthcare, Chicago, USA) was used to quantify IgG concentration against a calibration curve. The calibration curve was made up using a known concentration of IgG diluted in running buffer, to enable the conversion of absorbance on the chromatogram into concentration. Samples were loaded onto the column in running buffer, 20 mM sodium phosphate ($\text{NaH}_2\text{PO}_4 \cdot \text{H}_2\text{O}$, Na_2HPO_4 ; Sigma) at pH 7, and eluted using 20mM glycine (Sigma) at pH 2.8.

2.9.4. Determination of osmolality

Osmolality was determined using a freezing point osmometer (Osmomat 3000; Gonotec, Berlin, DE).

2.9.5. Gel analysis

Presence of aggregates and low or high molecular weight proteins was determined using SDS-PAGE. Samples in LDS sample buffer (Thermo Fisher Scientific) were loaded onto a

NuPAGE Bis-Tris gel (Thermo Fisher Scientific) and run in MES LDS running buffer (Thermo Fisher Scientific). Gels were then stained using InstantBlue™ Coomassive stain (Merck-Millipore) and imaged using an Amersham Imager 600 (GE Healthcare).

2.9.6. Derived growth parameters for batch and fed-batch cultures

The integral of viable cell density (IVCD), specific glucose consumption (q_{gluc}), specific lactate consumption (q_{Lac}) and specific productivity (q_{Ab}) were calculated according to **Equations 2.8-2.11**.

$$IVCD_n = IVCD_{n-1} + \left(\frac{VCD_n + VCD_{n-1}}{2} \right) \times (t_n - t_{n-1}) \quad (2.8)$$

Where VCD is viable cell density and $IVCD_n$ and $IVCD_{n-1}$ are integrated viable cell densities calculated for time t_n and t_{n-1} . The specific glucose consumption was calculated following **Equation 2.9**.

$$q_{gluc} = \frac{c_{gluc,n-1} + m_{gluc} - c_{gluc,n}}{\Delta IVCD_n} \quad (2.9)$$

Where $c_{gluc,n}$ and $c_{gluc,n-1}$ are glucose concentrations measured in the media at time t_n and t_{n-1} respectively and m_{gluc} is the concentration of glucose in exchanged media. The specific lactate consumption and productivity was determined using **Equation 2.10**.

$$q_x = \frac{(p_{x,n} - p_{x,n-1})}{\Delta IVCD_n} \quad (2.10)$$

Where x is the product (Ab) or lactate (Lac) and $p_{x,n}$ and $p_{x,n-1}$ are product or lactate concentration.

Volumetric productivity was calculated according to **Equation 2.11**.

$$Vol. Productivity = \frac{\sum_{t=0}^{t=n} p_{Ab} \times V_s}{V \times t_n} \quad (2.11)$$

Where V_s is the volume of product containing supernatant and V is the volume of cell culture.

2.9.7. Derived growth parameters for perfusion cultures

Integral of viable cell density (IVCD) and volumetric productivity were calculated following **Equations 2.8 and 2.11**. Specific glucose consumption (q_{gluc}), specific lactate consumption (q_{Lac}) and specific productivity (q_{Ab}) were calculated following Villiger-Oberbek et al. (2015), according to **Equations 2.12-2.13**.

$$q_{gluc} = \frac{(c_{gluc,n-1} \times (1 - D_n) + (m_{gluc} \times D_n)) - c_{gluc,n}}{\Delta IVCD_n} \quad (2.12)$$

Where D_n is the daily dilution at time t_n and is determined by dividing the exchanged volume on day n by the vessel volume. Specific lactate consumption and productivity was determined using **Equation 2.13**.

$$q_x = \frac{(p_{x,n} - (p_{x,n-1} \times (1 - D_n)))}{\Delta IVCD_n} \quad (2.13)$$

Cell specific perfusion rate (CSPR) was calculated following Ozturk (1996) according to **Equation 2.14**.

$$CSPR = \frac{D}{VCD_n} \quad (2.14)$$

Where D is dilution rate.

2.10. Rheological characterisation

2.10.1. Viscosity measurement

Viscosity of cell culture was estimated measured using a rotational rheometer (Kinexus Lab +; Malvern Instruments, Malvern, UK). Cells were expanded in 1L Erlenmeyer flasks for 3 days before being centrifuged at 450rpm for 5 minutes and re-suspended in fresh

CD-CHO media at concentrations between 20–100 × 10⁶ viable cells mL⁻¹. Measurements were then performed on a 1mL sample at 37°C, between 50mm parallel plates with a 0.4 mm gap size.

Measured shear rate ranges were calculated based on expected average shear within the bioreactor, using **Equation 2.15** defined by Metzner and Otto (1957).

$$\gamma = kN \quad (2.15)$$

Where γ is shear rate, k is a non-dimensional constant, dependant on impeller geometry and N is the rotational speed. k for the dual impeller configuration was estimated to be comparable to the Rushton impeller constant, as determined by Metzner and Otto (1957), 10.9. A range of shear rates between 10 – 1000 s⁻¹ were then measured, and viscosity determined using **Equation 2.16**:

$$\mu = \frac{\tau}{\gamma} \quad (2.16)$$

Where μ is viscosity and τ is shear stress. Following measurement of concentrated cell cultures, the viscosity of NaAlg (Sodium Alginate) solutions was measured in order to find a solution capable of mimicking the rheological properties of HCD cell cultures. NaAlg was dissolved in MilliQ water and at concentrations between 0.085 and 0.25 g L⁻¹ and 1mL samples were measured at room temperature using the plates, gap, and shear rate range used in cell culture measurements.

Experimentally determined viscosity measurements were subsequently compared to a model suggested by Gibilaro et al. (2007) to determine the viscosity of a fluidized bed, following **Equation 2.17**.

$$\mu_{pf} = \mu_f \mathcal{E}^{-2.8} \quad (2.17)$$

Where μ_{pf} and μ_f is the viscosity of the pseudo fluid and the fluid respectively. The pseudo fluid represents the cell culture broth, and the fluid is the cell culture medium. And ε is the concentration of the fluid, determined by **Equation 2.18**.

$$\varepsilon = \frac{V_t - V_c}{V_t} \quad (2.18)$$

Where V_t is the total volume of the pseudo fluid, and V_c is the volume of cells in the fluid, estimated from average cell diameter in the sample, assuming cells are spherical.

2.11. Mixing time determination

Mixing time characterisation was carried out in an acrylic mimic of the 250mL bioreactor, using the Dual Indicator System for Mixing Time (DISMT) first described by Melton et al. (2002). The acrylic mimic has the same dimensions to the bioreactor, found in **Table 2.1** and was fitted with identical baffles and impeller configuration. A port 2.5cm from the reactor wall was included on the headplate of the acrylic mimic to ensure addition were from the same location. Agitation was achieved with the same Pro 40 Digital Stirrer used for cell culture. Images were taken with a high-speed camera (NET NS4133CU iCube; Net, Finning, DE) with 1280 × 1024 pixel resolution, positioned to include the entire working volume of the reactor. **Figure 2.7** shows the experimental set up for mixing time.

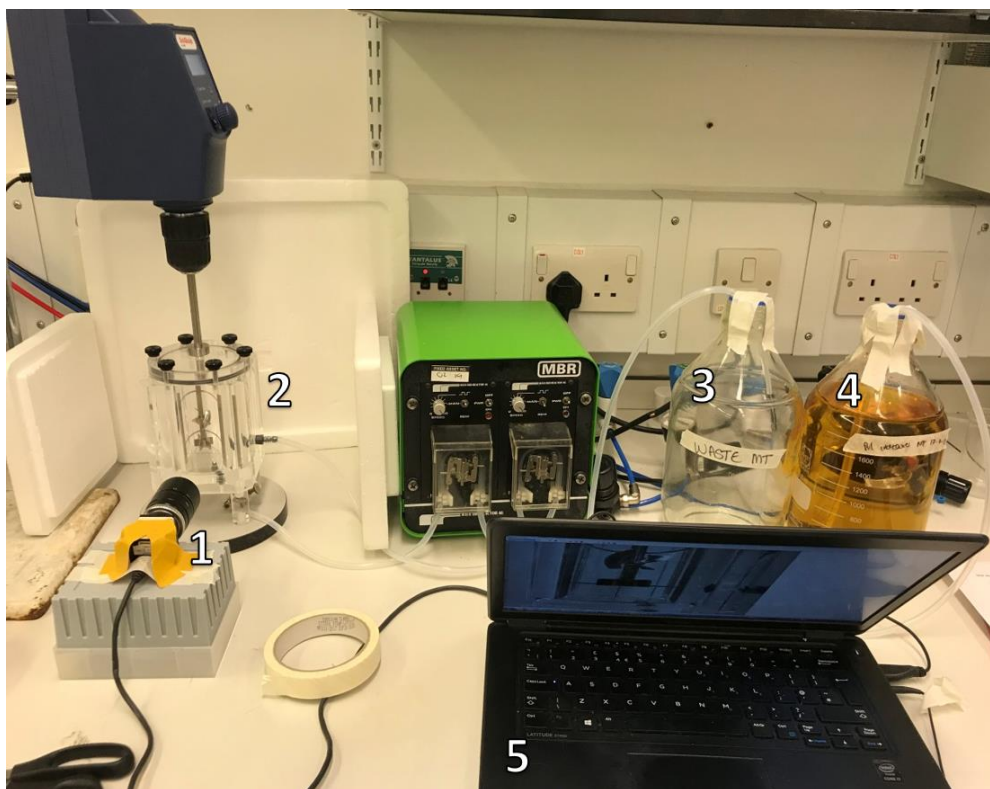


Figure 2.7 – Experimental set up for mixing time experiments. (1) iCube camera (Net) (2) Acrylic mimic (3) Waste (4) Reservoir of DISMT (5) Computer to capture images (Dell)

2.11.1. DISMT reagent preparation

The DISMT method uses two pH indicators, Methyl Red and Thymol Blue, that change colour during a rapid reaction between NaOH and HCl. Methyl Red is red under acidic conditions, while Thymol Blue is blue under basic conditions, with both indicators showing yellow in the neutral pH range of 5.6-8.0.

Stock solutions of Thymol Blue and Methyl Red were prepared in 70% EtOH at a concentration of 1.38 and 1.52 mg mL⁻¹ respectively. For the standard DISMT solution, stock solutions were added to MilliQ water at a concentration of 4.67 mL L⁻¹ Thymol Blue and 4.26 mL L⁻¹ Methyl Red, before the incremental addition of 0.75M NaOH until a colour change to bright yellow was observed. For the HCD mimic DISMT solution, the standard DISMT solution was made up at the same concentration of Thymol Blue and Methyl Red. NaAlg was then dissolved in the solution at a concentration of 0.085g L⁻¹, before addition of NaOH until a colour change to yellow was observed.

2.11.2. Experimental mixing time measurements

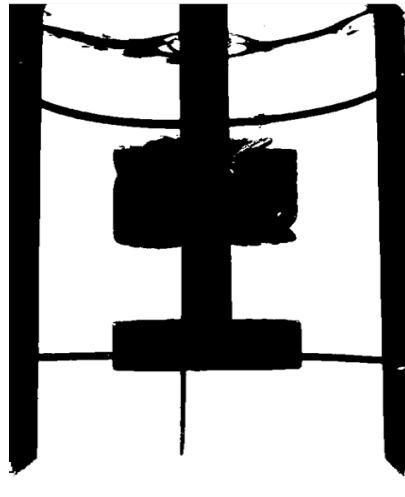
For mixing time measurements, 250mL of DISMT solution were added to the acrylic mimic and acidified with 15 μ L of 0.75 M HCl and mixed until a uniform red colour was achieved. Agitation was then set at the desired rate, with N between 50 and 600 rpm, before initiating measurement on the iCube camera. For measurements that included recirculation to mimic perfusion, the recirculation pump was initiated simultaneously with the agitation. After initiation of image capture, 15 μ L of 0.75 M NaOH was added through the addition port, and images were captured until a colour change to yellow was achieved and maintained consistently for 30 seconds. Images were captured at a rate of 10 - 20 fps, with lower frame rates used slower agitation speeds. All mixing time analysis was performed at agitation rates between 50 – 600 rpm.

The standard DISMT solution was used to determine mixing time at two impeller heights for the dual impeller configuration, 2.5cm and 1cm from the base. The measurements using NaAlg-DISMT solution, mimicking high cell density, used a fixed impeller height of 2.5cm. Perfusion recirculation was mimicked for some NaAlg-DISMT measurements, using the Puralev® i30SU, with recirculation from either the side port or headplate port at a rate of 40 – 140 mL min⁻¹. Images were analysed and mixing time determined using a purposely-written MATLAB code (Mathworks, Massachusetts, USA), which measured the change in red, green and blue (RGB) pixels in the images over time. Impeller and baffle areas were masked to enable accurate analysis of the liquid. An example of image masking and RGB graph generated from image analysis can be found in **Figure 2.8**. Mixing time (t_m) is defined as the time when the green pixel value is 95% of the stable final value, when the colour is yellow, meaning that the solution is 95% homogenous at t_m .

2.11.3. Production of mixing maps

Images taken for mixing time measurements were subsequently processed through a second purposely-written MATLAB code to generate a mixing map. The code measures the rate of change in intensity of red, green and blue within each individual pixel within the image. Impellers and baffles were masked as shown in **Figure 2.8**. Rate of change within a single pixel is compared to average rate of change across the vessel, in order to obtain mixing efficiencies of individual regions within the BR, and the identification of well-mixed and poorly-mixed zones.

(A)



(B)



(C)

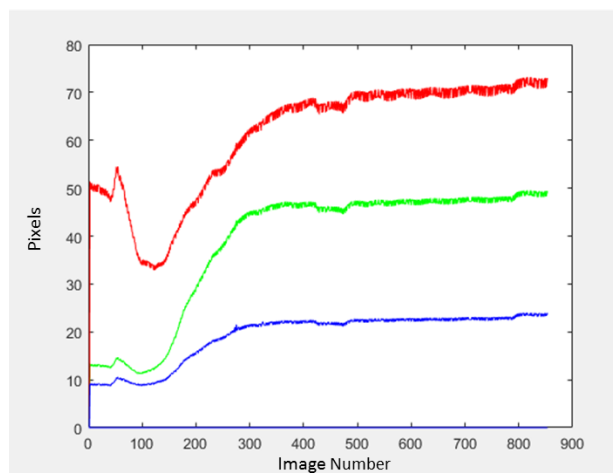


Figure 2.8 (A) Binarised mask generated from image of 250mL mimic. (B) Mask imposed on reactor image filled with DISMT solution. (C) RGB graph showing number of red, green and blue pixels in the image with time.

2.12. Determination of power input and impeller power number

2.12.1. Calculation of power input

Power input per unit volume in 24-well MWP were calculated based on **Equation 2.19**, as described by Klöckner et al. (2012).

$$\frac{P}{V} = 9g^{-0.42}\rho^{0.83}d^{3.34}N^{3.67}\mu^{0.17}V_L^{-0.56}d_o^{0.42} \quad (2.19)$$

Where g is acceleration due to gravity, ρ is liquid density, d is the microwell diameter, N is shaking frequency, μ is liquid viscosity, V_L is the volume of the liquid and d_o is the orbital shaking diameter.

Power input for stirred tank bioreactors was calculated for un-gassed systems following **Equation 2.20**.

$$P_{ug} = N_p \rho N^3 d_i^5 \quad (2.20)$$

Where P_{ug} is un-gassed power number N_p is impeller power number, N is rotational speed and d_i is impeller diameter. Power input for gassed systems was subsequently calculated following **Equation 2.21**.

$$P_g = 0.72 \left(\frac{P_{ug}^2 N d_i^3}{Q^{0.56}} \right)^{0.45} \quad (2.21)$$

Where P_g is gassed power, 0.72 is a constant related to conversion of gassed power (Doran, 1995), and Q is volumetric gas velocity.

2.12.2. Determination of impeller power number in 250mL bioreactor

Impeller power number was determined experimentally using the 250mL bioreactor mimic clamped into chuck jaws on an air bearing. The baffled mimic was fitted with the dual impeller configuration on an extended impeller shaft, connected to a MP-Series Low inertia Servo motor (Rockwell Automation, Milwaukee, US), raised above the headplate

with an impeller clearance of 2.5cm. The motor was controlled using Ultraware software (Rockwell Automation).

The vessel was filled with 250mL of MilliQ water, glycerol or water-glycerol solutions. Pure glycerol and glycerol solutions were used for reduced turbulence conditions, when Reynolds number is ≤ 1000 . A force gauge (Omega DG55; Omega, Manchester, UK) was positioned horizontally such that the sensor rod contacts the jaw, and the distance between the centre of the impeller shaft and contact point measured. The force gauge was set to zero prior to each measurement, initiating a delay time of 30 s. The motor was set at agitation rates between 50 – 750 rpm during the delay, either clockwise (down-pumping) or counter-clockwise (up-pumping). The force gauge then measures average force over 45 s after the initial delay. Force is converted to power using the following **Equations 2.22-2.23**.

$$T = rF \quad (2.22)$$

Where T is torque, r is lever arm length, the distance from the centre impeller shaft and contact point, and F is measured force. From torque, power can be calculated using the following **Equation 2.23**.

$$P = 2\pi NT \quad (2.23)$$

Where P is power and N is rotational speed. From power, impeller power number was calculated using the following **Equation 2.24**.

$$N_p = \frac{P}{\rho N^3 d^5} \quad (2.24)$$

Where N_p is impeller power number, ρ is liquid density, and d is impeller diameter.

2.13. Determination of oxygen mass transfer coefficients

2.13.1. Calculation of $k_L a$ in MWPs

The $k_L a$ in shaken 24-well MWPs was calculated based on the sequence of **Equations 2.25 – 2.28**, described by Doig et al. (2005).

$$k_L a = 33.35 D a_i Re^{0.68} Sc^{0.36} Fr^x Bo^y \quad (2.25)$$

Where D is the diffusion coefficient of oxygen into water, a_i is the initial specific surface area, Re is Reynolds number, Sc is Schmidt number, Fr is Froude number, Bo is bond number and x and y are Froude and Bond coefficients respectively related to the specific geometry of the microwell plate.

Reynolds number was calculated using the following **Equation 2.26**.

$$Re = \frac{\rho N d^2}{\mu} \quad (2.26)$$

Where ρ is the liquid density, N is the shaking speed, d is the microwell diameter and μ is the dynamic viscosity. Schmidt number was calculated using **Equation 2.27**.

$$Sc = \frac{\mu}{\rho D} \quad (2.27)$$

And Bond number was calculated using **Equation 2.28**.

$$Bo = \frac{\rho d^2 g}{W} \quad (2.28)$$

Where g is acceleration due to gravity and W is wetting number. The calculations described by Doig et al. (2005) were experimentally validated, and found to have an error of $\pm 30\%$. The minimum $k_L a$ was therefore determined to be 70% of that calculated from the previous **Equations 2.25-2.28**.

2.13.2.Determination of k_La in bioreactors

The gas-liquid mass transfer coefficient, k_La , in the 250mL bioreactor was experimentally determined using the static gassing out method. Air flow rates between 25–100 mL min⁻¹ were investigated, at agitation rates between 50–600 rpm. The basis of the dynamic gassing out method is to sparge N₂ at the desired flowrate until DO reaches < 5%, followed by sparging air at the desired flowrate and agitating until DO reaches > 50%. k_La can then be determined from the slope generated by plotting the natural log of measured data. The static gassing out method is applicable when probe response time is sufficiently low. Probe response (τ_p) time is determined as the time taken for the electrode to reach a 63% step change, and if $\tau_p \ll k_La^{-1}$ then probe response time is negligible (Lamping et al., 2003). The test liquid was 250mL CD-CHO at 22 and 37°C to simulate cell culture conditions. The experimentally determined k_La was used to determine the coefficients of the following **Equation 2.29**, using regression analysis.

$$k_La = K \left(\frac{P}{V} \right)^a W_{sg}^B \quad (2.29)$$

Where P is power input, V is volume, W_{sg} is superficial gas velocity and K, a and B are coefficients specific to the system. k_La was calculated for comparison in 5L bioreactor (Biostat B-DCU; Sartorius, Epsom, UK) following **Equation 2.29**, using the following coefficients: K = 1.64, a = 0.55, B = 0.81. Coefficients were assumed following Karimi et al. (2013) from the impeller geometry and sparger type, in 5L BR; single pitched blade impeller and horseshoe sparger.

3. CHAPTER 3: ESTABLISHMENT OF QUASI-PERFUSION METHODS IN MICROWELL PLATES

3.1. Introduction

Perfusion cultures have historically been a popular method for the production of unstable proteins, however recent technological advancements, resulting in reduced failure rates, has increased industry interest in implementing perfusion in a wide range of process applications. Advantages associated with perfusion cultures include greater productivity, reduced CoGs, decreased facility footprints and increased flexibility. For the success of perfusion cultures, cell lines, medium and perfusion rates must be carefully selected in order to maximise productivity whilst minimising cost. Media must provide adequate nutritional depth to support desired cell densities, with an osmolality appropriate to the cell line, while perfusion rates are often reduced to levels of < 1 VVD, to reduce liquid burden on downstream processing steps while maximising titre.

The utilisation of mL scale parallel bioreactors offers the possibility to screen for the best-performing cell lines and media in combination with perfusion rates in order to identify the optimal conditions for a particular process. A literature search has demonstrated that MWPs have been used successfully for the optimisation of fed-batch cultures, and while recent studies have demonstrated development of techniques to mimic perfusion cultures, these are in early phases of development (Bielser et al., 2019, Karst et al., 2016, Villiger-Oberbek et al., 2015). Current early phase development studies on perfusion cultures are mainly based on L-scale benchtop bioreactors, which are resource intensive and low-throughput. Several mL-scale quasi-perfusion techniques have been described to address the technology gap, incorporating cell retention and discrete media exchanges into pre-existing fed-batch processes for CHO cell culture. Examples include spin tubes (Bielser et al., 2019, Wolf et al., 2018, Villiger-

Oberbek et al., 2015), mL scale bioreactors (Kreye et al., 2019, Matteau et al., 2015, Sewell et al., 2019, Karst et al., 2018) and, more recently, MWP (Bielser et al., 2019).

Spin tubes are commonly operated between working volumes of 10-20 mL and shaken at frequencies between 220 and 320 rpm. Cell retention is achieved via centrifugation prior to media exchanges of 40-100% of the working volume. Villiger-Oberbek et al. (2015), Bielser et al. (2019) and Wolf et al. (2018) reported maximum VCDs for quasi-perfusion methodologies in spin tubes of up to 50×10^6 cells mL⁻¹, while Karst et al. (2018) maintained a stationary phase culture at 15×10^6 cells mL⁻¹ to perform dynamic metabolic analysis. Ambr15® microbioreactors have been utilised to mimic perfusion cultures utilising several techniques. The most common is the addition of sedimentation as a cell retention mechanism (Kreye et al., 2019, Sewell et al., 2019), but recent developments have incorporated 3D-printing elements to the bioreactor system or transfer of cell culture broth into falcon tubes to enable the use of centrifugation as a cell retention step (Gagliardi et al., 2019). Sedimentation methodologies involve a settling period of 40-60 minutes to allow settling followed by shutdown of pH, DO and stirrer controls before supernatant removal and pulse media additions up to 8 times per day. Extended periods of control shutdown cause pH and DO spikes that can become detrimental to cell health and proliferation as the culture progresses. Centrifugation methods involve the removal of the bioreactors from the system into a custom 3D-designed basket, prior to centrifugation. Maximum VCDs of 35×10^6 cells mL⁻¹ have been reported using centrifugation and sedimentation modes in ambr15® systems.

Recent papers (Bielser et al., 2019) have described the utilisation of 96 DSW MWPs for high-throughput development studies of perfusion cultures, incorporating centrifugation as a cell retention step, and reporting comparable μ_{\max} to 5L bioreactors and cell densities of up to 35×10^6 cells mL⁻¹. The use of MWPs involves a significant cost

reduction compared to microbioreactors and a significantly increased experimental throughput compared to shake flasks.

While emerging studies outline the use of quasi-perfusion techniques in MWP, cell retention techniques are not directly compared, and are often selected arbitrarily. In this chapter, the development of a quasi-perfusion methodology in MWPs is described, incorporating both sedimentation and centrifugation methodologies for cell retention. The integration of sedimentation or centrifugation methodologies is compared and critically evaluated for associated advantages and potential applications.

3.2. Results

3.2.1. Determination of evaporation profiles and cell culture variability in 24-well MWP cultures

Evaporation profiles of microwell plate (MWP) were investigated as described in section 2.3.2. A stock blue dye solution was added to each well of a 24-well MWP to a volume of 1.2mL, covered with a Duetz sandwich lid and placed in a humidified incubator at 220 RPM, 37°C and 5% CO₂ for 8 days. The change in concentration of the initial stock solution was measured for each well to determine fold evaporation. The plate was divided in three zones as shown in **Figure 3.1 A** and named “centre”, “edge” and “corner”. **Figure 3.1 B** shows the fold evaporation measured for 8 days in each zone. MWPs were covered with a Duetz sandwich lid and placed under culture conditions, as outlined in section 2.3, for 8 days. There is an average of 1.45±0.03 fold evaporation across the plate, with 4% deviation between the three zones. Volume loss was consistent at 60±12 µL day⁻¹ per well. Consistent well-to-well volume loss allowed for the monitoring of well volume in subsequent experiments via daily weight measurements, assuming all weight deviation is due to liquid loss, and the density of the cell culture broth is comparable to water at 1000 kg m⁻³.

The consistency of cell culture performance was determined using the methods described in section 2.3, following an approach initially outlined by Silk et al. (2010) **Figure 3.1 C** shows the VCD and viability variation with time for a fed-batch culture seeded at 0.3×10^6 cells mL⁻¹ and 0.2×10^6 cells mL⁻¹ in 250mL shake flasks (SF) and MWP, respectively. Fill volumes were 50mL and 1.2 mL, respectively, for SF and MWP, which were placed under culture conditions, as described in Section 2.3 and 2.4. Feeding commenced on day 3 for 5 consecutive days. In MWPs, one sample from each of the centre and edge zones was taken daily. The corner zone is limited to 4 wells, meaning samples from this location were taken at days 2, 4, 6 and 8 only. VCD and viability was taken as the average from each zone sampled. Maximum cell densities of 6.4 ± 0.5 and $6.5 \pm 0.3 \times 10^6$ cells mL⁻¹ were achieved for SF and MWP, respectively. Cell culture kinetics was similar between SF and MWP and consistent between positions within the MWP for the duration of the culture.

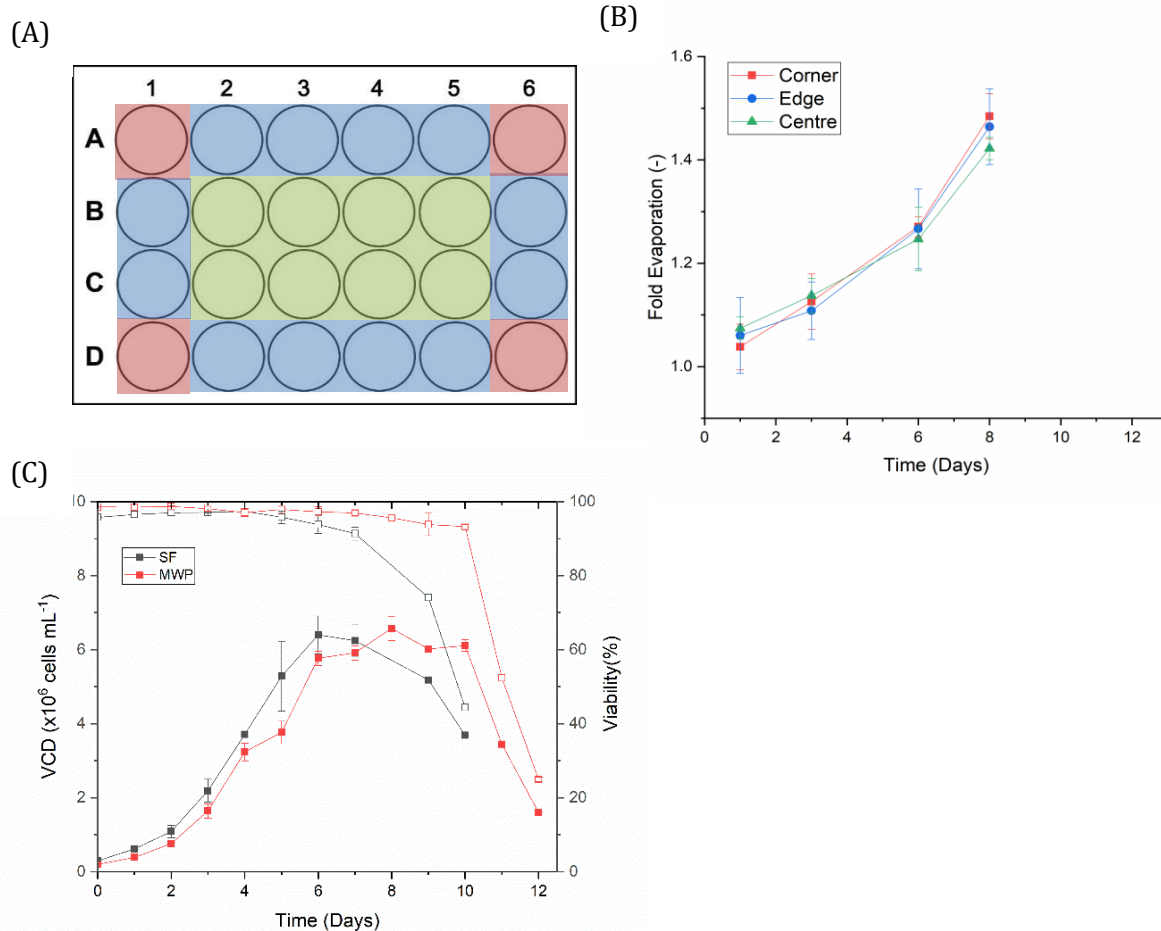


Figure 3.1 - Characterisation of cell growth environment in 24-well MWPs. (A) Definition of 3 distinct “zones” within the MWP, named “centre”, “edge” and “corner”. (B) Fold evaporation experienced within the MWP zones. MWPs were filled with a stock blue dye solution, placed in an incubator at 37°C, covered with Duetz sandwich lid, N=220RPM. The optical density of stock solution was monitored with time, and fold evaporation for each zone was calculated following Equation 2.1. (C) VCD (filled symbols) and viability (empty symbols) of fed-batch CHO cell culture in SF and MWPs. SF cultures were seeded at 0.3×10^6 cells mL^{-1} and placed in a shaken incubator at 37°C at 140 RPM. MWP cultures were seeded at 0.2×10^6 cells mL^{-1} , covered with a Duetz sandwich lid and placed in a shaken incubator at 37°C at 220 RPM. SF data represents 3 cultures \pm s.d. MWP data is averaged from each zone across 2 cultures \pm s.d.

Since MWPs are limited to small volumes, sampling is often achieved with a sacrificial well approach to allow the harvest of adequate volume for analytics (Micheletti et al., 2006). In order to implement such approach, it must be assumed that the sample well is representative of each well across the plate, and thus well-to-well variation is minimal. Deviations between zones of MWPs can occur due to an edge effect (Micheletti and Lye, 2006, Barrett et al., 2010) where evaporation in the outer wells is greater than internal

wells, leading to increased osmolality, concentration of cells in the media and therefore altered culture performance. In this system, evaporation profiling showed minimal edge effect and consistent cell culture performance, so it was appropriate to implement a sacrificial well sampling approach. Cell culture was performed following Silk et al. (2010), who implemented a comparable feeding regime for a GS-CHO line, seeding at 0.2×10^6 cells mL⁻¹ in identical MWPs, covered with a Duetz sandwich lid at a fill volume of 0.8mL. A maximum cell density of 8×10^6 cells mL⁻¹ was reported on day 10, comparable to the maximum reported of 6.5×10^6 cells mL⁻¹. Small deviations can be attributed to the deviation in working volume and feeding regimes between the two systems. Working volume was increased from 0.8 mL following Silk et al. (2010) to 1.2 mL to enable greater flexibility for volume manipulations in future quasi-perfusion cultures. The impact of utilising an increased working volume was found to be not statistically significant, $p=0.11$. Cell growth data can be found in Appendix 1.

3.2.2. Development of batch and fed-batch cultures in 24 MWP

The suitability of sealing membranes for cell culture was investigated and evaporation rates measured in batch MWPs under standard culture conditions, as described in section 2.3. **Figure 3.2 A** shows the change in well volume with time for batch microwell plates under standard culture conditions covered with either a Duetz sandwich filter lid (CR1524) or a Duetz sandwich silicone lid (CR1524a). Evaporation is greater in cultures covered with the filter lid, which results in a volume decrease from 1200 μ L to 975 ± 55 μ L on day 7, a volume loss of 19%. In comparison, cultures covered with silicone lids had a volume of 997 ± 88 μ L on day 7, a volume loss of 17%. Filter lids facilitate a greater rate of headspace air exchange compared to silicone lids, at 1.1 mL min^{-1} and 0.25 mL min^{-1} respectively (Duetz et al., 2000). **Figure 3.2 B** shows VCD and viability with time for batch microwell plates under standard culture conditions covered with either filter or silicone lids. Both filter and silicone lids achieve comparable performance, with a

maximum VCD on day 5 of $2.52 \pm 0.07 \times 10^6$ cells mL^{-1} and $2.29 \pm 0.17 \times 10^6$ cells mL^{-1} for filter and silicone lids, respectively.

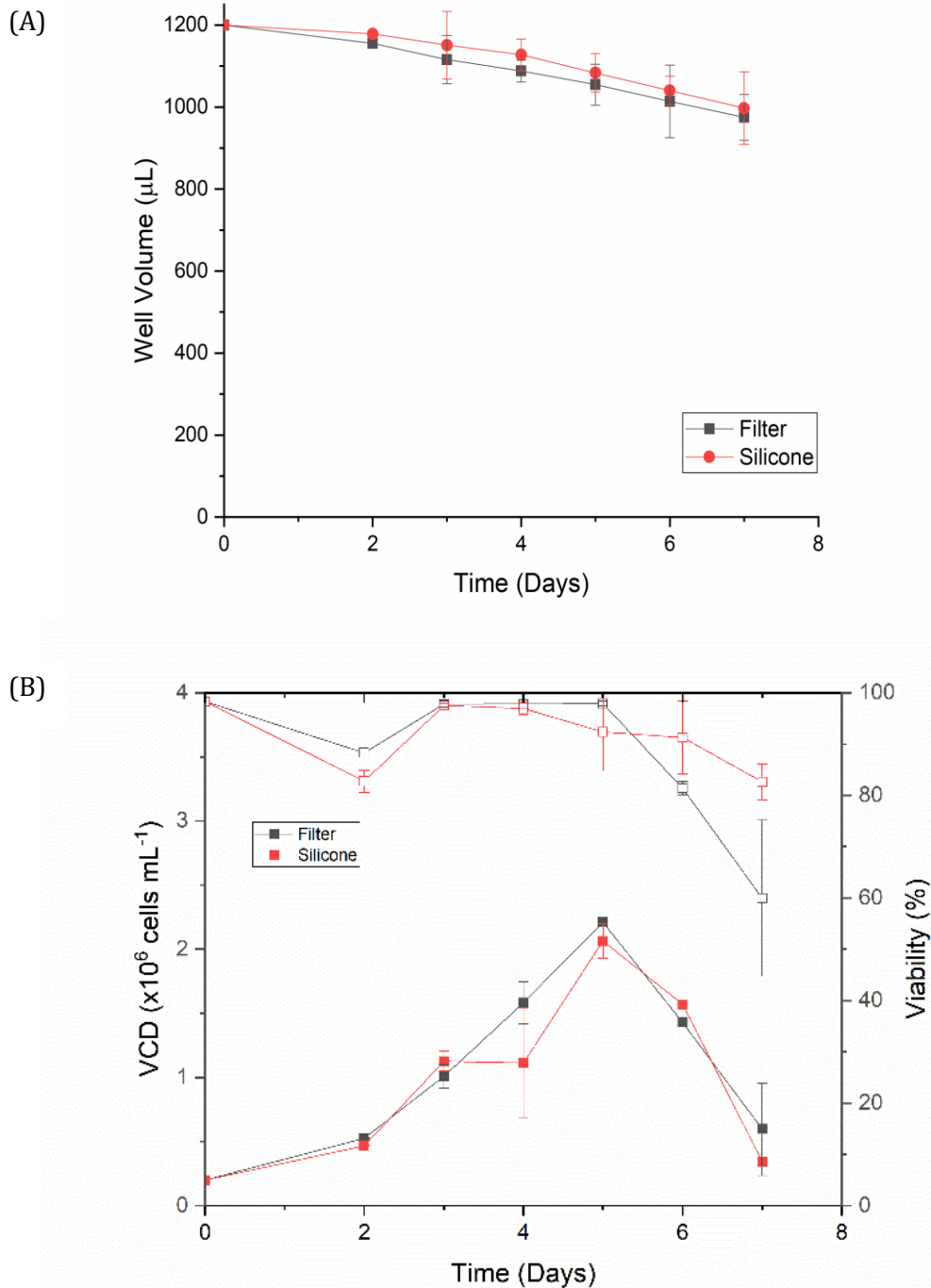


Figure 3.2 - Comparison of evaporation and CHO cell culture performance in 24-well MWP covered with filter or silicone based Duetz sandwich lids. Cell cultures were incubated at 37°C at an initial seeding density of 0.2×10^6 cells mL^{-1} , N=220 RPM (A) Well volume with time (B) VCD (filled symbols) and viability (empty symbols) with time. Data represents 2 cultures \pm s.d.

The impact of seeding density on cell culture performance was considered in fed-batch mode, as described in section 2.3.1. **Figure 3.3** shows VCD variation with time for fed-batch cultures under standard culture conditions, with cells seeded at densities between 0.2 and 2×10^6 cells mL^{-1} . Seeding at the lowest density of 0.2×10^6 cells mL^{-1} generates the lowest peak VCD of 6.5×10^6 cells mL^{-1} on day 8. Increased seeding densities between $0.4 - 1.4 \times 10^6$ cells mL^{-1} reach comparable peak cell densities, between $7.85 - 8.78 \times 10^6$ cells mL^{-1} on day 9. The greatest seeding density, 2×10^6 cells mL^{-1} achieves the highest peak VCD of 11×10^6 cells mL^{-1} on day 7. Viability is maintained comparably throughout the culture for all seeding densities.

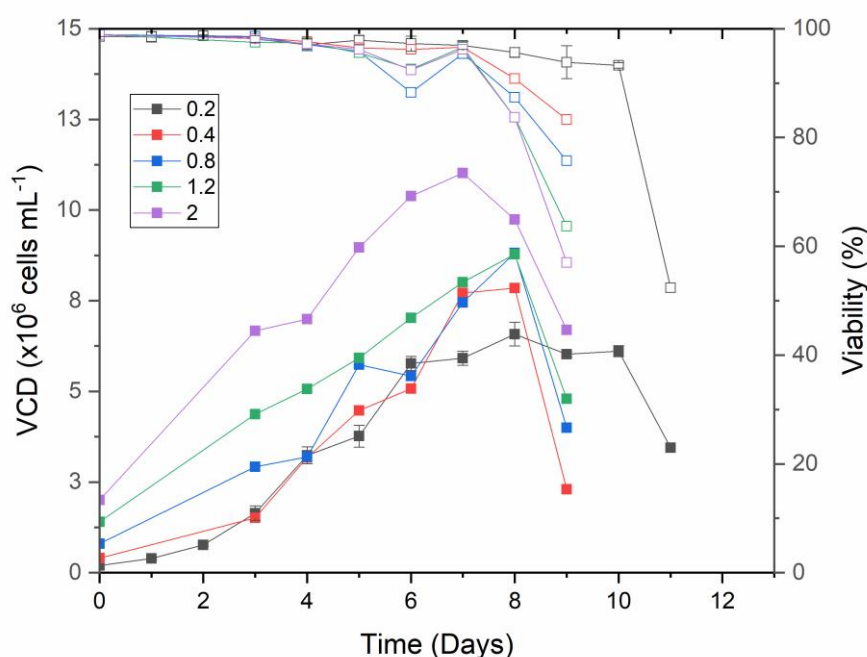


Figure 3.3 - VCD and viability of fed-batch CHO cell culture in 24-well MWP, seeded at a range of densities between 0.2 - 2×10^6 cells mL^{-1} . Cultures were covered with a Duetz sandwich lid, incubated at 37°C , $N=220$ RPM. Data at a seeding density of 0.2×10^6 cells mL^{-1} is averaged from each zone across 2 cultures \pm s.d. All other data points represent 1 culture, with one well sampled per day per condition utilising a sacrificial well sampling approach.

Table 3.1 shows maximum specific growth rate (μ_{max}) for each of the fed-batch microwell cultures. μ_{max} decreases with increased seeding density between 0.2 and 1.4×10^6 cells mL^{-1} , from 1.7 to 0.7×10^{-3} hrs^{-1} , but a slight increase can be observed for cultures seeded at 2×10^6 cells mL^{-1} to 0.8×10^{-3} hrs^{-1} .

Table 3.1- Maximum specific growth rate (μ_{\max}) for fed-batch CHO cultures in MWP with seeding densities between $0.2\text{-}2 \times 10^6$ cells mL^{-1} .

Seeding Density ($\times 10^6$ cells mL^{-1})	μ_{\max} (hrs^{-1})
0.2	1.7×10^{-2}
0.4	1.3×10^{-2}
0.8	9.3×10^{-3}
1.4	6.6×10^{-3}
2	7.9×10^{-3}

It is expected that seeding density increases result in lower μ_{\max} due to suppressed nutrient consumption rates caused by a reduction in the relative available nutrients in the media (Rodriguez, 2001), this effect is particularly pronounced during the early phase of exponential cell growth prior to the initiation of feeding on day 3 in fed-batch cultures. The relative availability of O_2 in high seeding density cultures is expected to compound the impact of nutrient availability beyond the initiation of nutrient feeding resulting in reduced maximal growth rates. Previous studies have shown comparable results with respect to the impact of seeding density on cell growth. Ozturk (1990) reported that deviations in seeding density impact maximum viable cell concentration, however large variations in seeding density were required, 10 fold, to achieve a small increase in maximum cell density, up to a 20% increase. Additionally, Rodriguez (2001) reported that μ_{\max} decreased as seeding density increased in CHO cell lines.

Standard culture conditions were selected to provide optimal, robust performance for future expansion into quasi-perfusion cultures. Comparing filter and silicone lids, there is little impact on using either lid in terms of cell culture performance in batch mode. To enable quasi-perfusion cultures, O_2 limitation at high cell densities must be taken into consideration alongside evaporation. The increased evaporation rate when using the filter lid was not deemed to be significant, particularly when considering fed-batch and perfusion cultures where volume additions can be manipulated to maintain a constant volume. Filter lids were therefore selected as the preferred sealing membrane for all

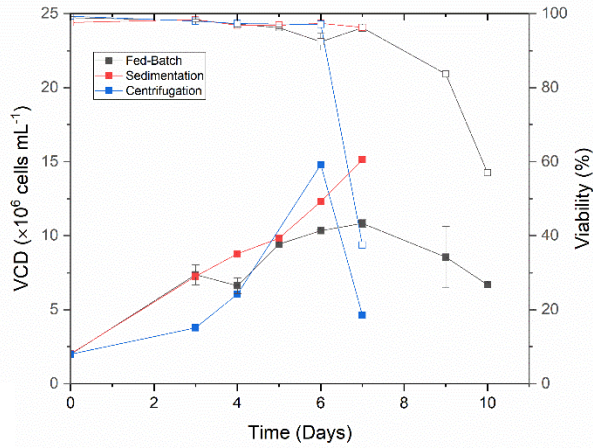
subsequent microwell cultures, due to the 4 times increase in headspace air exchange in comparison to silicone lids. A seeding density of 2×10^6 cells mL⁻¹ was the best performing during the seeding density screen, generating the highest cell densities whilst maintaining a μ_{\max} comparable to lower seeding density cultures. Subsequent MWP cultures were seeded at 2×10^6 cells mL⁻¹.

3.2.3. Quasi-perfusion proof of concept studies

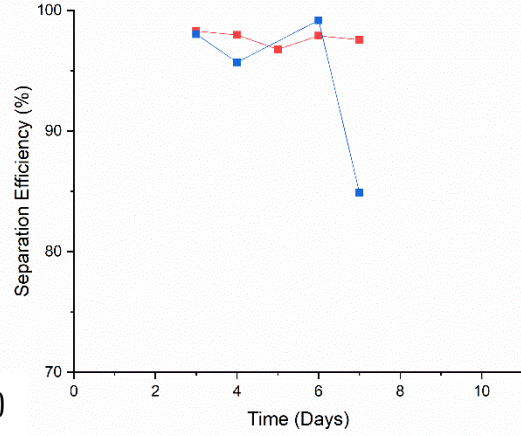
Following the successful establishment of optimised fed-batch protocols in microwell plates format, sedimentation and centrifugation methodologies were established in MWPs for quasi-perfusion, as described in sections 2.4.1 and 2.4.2. **Figure 3.4 A** shows VCD and viability variation with time for fed-batch and quasi-perfusion sedimentation cultures and quasi-perfusion centrifugation cultures. CD-CHO media was exchanged at a rate of 1 VVD for both sedimentation and centrifugation cultures. Perfusion rate was achieved with 2 daily exchanges equal to half the liquid volume in sedimentation cultures and 1 daily exchange of the entire liquid volume in centrifugation cultures. The maximum volume per exchange for sedimentation cultures are limited to 75% of the working volume (900 μ L), due to a larger packed cell density after cell settling compared to centrifugation cultures. Volume exchanges above 900 μ L causes disruption of the cell pellet and reduced separation efficiencies. The tightly packed cell pellet after centrifugation enables the entire liquid volume to be removed without disrupting the cell pellet and affecting separation efficiency. Maximum cell densities of 14.8 and 15.1×10^6 cells mL⁻¹ were achieved for centrifugation and sedimentation cultures, respectively. Viability is maintained above 97% until day 6 in centrifugation cultures and until day 7 for sedimentation cultures. **Figure 3.4 B** shows the separation efficiencies for the quasi-perfusion cultures. Both sedimentation and centrifugation methods maintain high separation efficiencies above 96% for the duration of the culture. **Figures 3.4 C and D** show the corresponding glucose and lactate profiles, respectively, for quasi-perfusion cultures. Periodic media exchanges mean that glucose concentration is not steady state

and fluctuates between exchanges. While the volume exchanged per day in quasi-perfusion culture was consistent, the feeding regime and therefore the cell metabolism is shown to vary. In centrifugation cultures, where the entire culture volume is exchanged daily, the available glucose concentration increases to 6 g L^{-1} post exchange. Comparatively, sedimentation cultures are exchanged with half the culture volume twice daily, reducing the maximum glucose concentration during cell growth to 4.5 g L^{-1} . Despite media exchanges, in both centrifugation and sedimentation cultures glucose is depleted by day 7, with low concentrations observed prior to exchange from day 6 in centrifugation cultures. Lactate concentration with time across each regime is typical, with high production in the early phases of exponential growth (Zagari et al., 2013). For fed-batch cultures, net consumption is observed in the stationary phase, while in both sedimentation and centrifugation cultures, the rate of lactate production decreases with time as relative glucose availability is reduced and cell growth rate slows. It is expected that wider fluctuations in glucose availability in centrifugation cultures in 24 hours between exchanges compared to sedimentation cultures influences the glucose utilisation with time and therefore lactate production, with yield of lactate on glucose elevated in centrifugation cultures compared to sedimentation cultures. It has been previously reported that up to 90% of glucose utilisation in CHO cells is involved in lactate production (Mulukutla, 2010), with a theoretical yield of lactate from glucose of 2 mols lactate produced per 1 mol glucose consumed. Yield of lactate on glucose is approximately 0.6:1 and 0.4:1 mol;mol for centrifugation and sedimentation cultures respectively. It is therefore expected that some consumption of lactate is occurring in quasi-perfusion cultures between sampling points, and maximum concentrations of lactate observed are not necessarily maximum concentrations experienced by cells in culture.

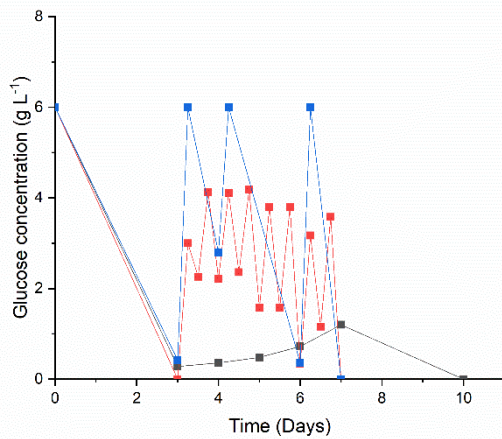
(A)



(B)



(C)



(D)

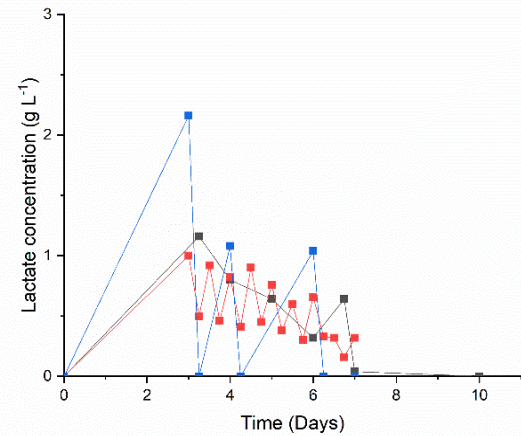


Figure 3.4 - Fed-batch, sedimentation quasi-perfusion and centrifugation quasi-perfusion cultures in 24-well MWP. Cultures were seeded at 2×10^6 cells mL^{-1} incubated at 37°C , $N=220$ RPM and covered with Duetz sandwich lids. Quasi-perfusion cultures were exchanged with CD-CHO media from day 3 at a rate of 1 VVD. (A) VCD (filled symbols) and viability (empty symbols) for fed-batch, sedimentation quasi-perfusion and centrifugation quasi-perfusion cultures. (B) Separation efficiency for sedimentation quasi-perfusion and centrifugation quasi-perfusion cultures. (C) Glucose concentration for fed-batch, sedimentation quasi-perfusion and centrifugation quasi-perfusion cultures. (D) Lactate concentration for fed-batch, sedimentation quasi-perfusion and centrifugation quasi-perfusion cultures. Fed-batch data represents triplicate cultures \pm s.d. All other data points represent 1 culture, with one well sampled per day per condition utilising a sacrificial well sampling approach.

Implementation of quasi-perfusion techniques in MWP generates cell densities 1.5 times greater than fed-batch. Both centrifugation and sedimentation methods maintain high separation efficiencies where exchanged volume is less than or equal to the maximum. Viability and cell densities in quasi-perfusion cultures are maintained until day 7, when sudden drops in viability are observed. The observed drop in viability corresponds to the depletion of glucose, which suggests that viabilities could be maintained and cell densities increased by improving the nutritional depth of the exchanged media.

3.2.4. Media development for quasi-perfusion methodologies at 1VVD

Media development was undertaken in order to increase the nutritional depth of chemically defined CHO medium (Thermo Fisher) to enable the support high cell density cultures. GS CHO systems rely on glutamine-free media to select on the basis of clones which highly express GS and are therefore able to produce sufficient glutamine to support cell growth, which is linked to high expression and production of product. GS expression systems produce glutamine through conversion of glutamate and ammonia, which are therefore vital media components in GS-CHO expression systems alongside glucose (Kingston, 2002). In media design, concentration of CD-CHO media and blending with high-concentration feeding media was investigated, in order to increase concentration of available glucose, glutamate and ammonia, alongside the supplementation with additional glucose only.

3.2.4.1. Concentrated CD-CHO

Initial development was undertaken by exchanging sedimentation and centrifugation quasi-perfusion cultures with 1.5 times and 2 times concentrated CD-CHO at a rate of 1 VVD, as described in sections 2.4.1 and 2.4.2. **Figure 3.5 A** shows VCD and viability variation with time for quasi-perfusion cultures exchanged with concentrated media compared to fed-batch. Peak VCDs for concentrated medias are comparable to those achieved in fed-batch, at 10.7 and 7.87×10^6 cells mL⁻¹ for 1.5 times and 2 times

concentrations, respectively. **Figure 3.5 B** shows the osmolality changes in the culture with time. Osmolality sharply increases in cultures exchanged with concentrated media from day 3, the time at which exchanges begin. Osmolality reaches a peak of 658 and 487 m Osm kg⁻¹ for 1.5 times concentrations, respectively.

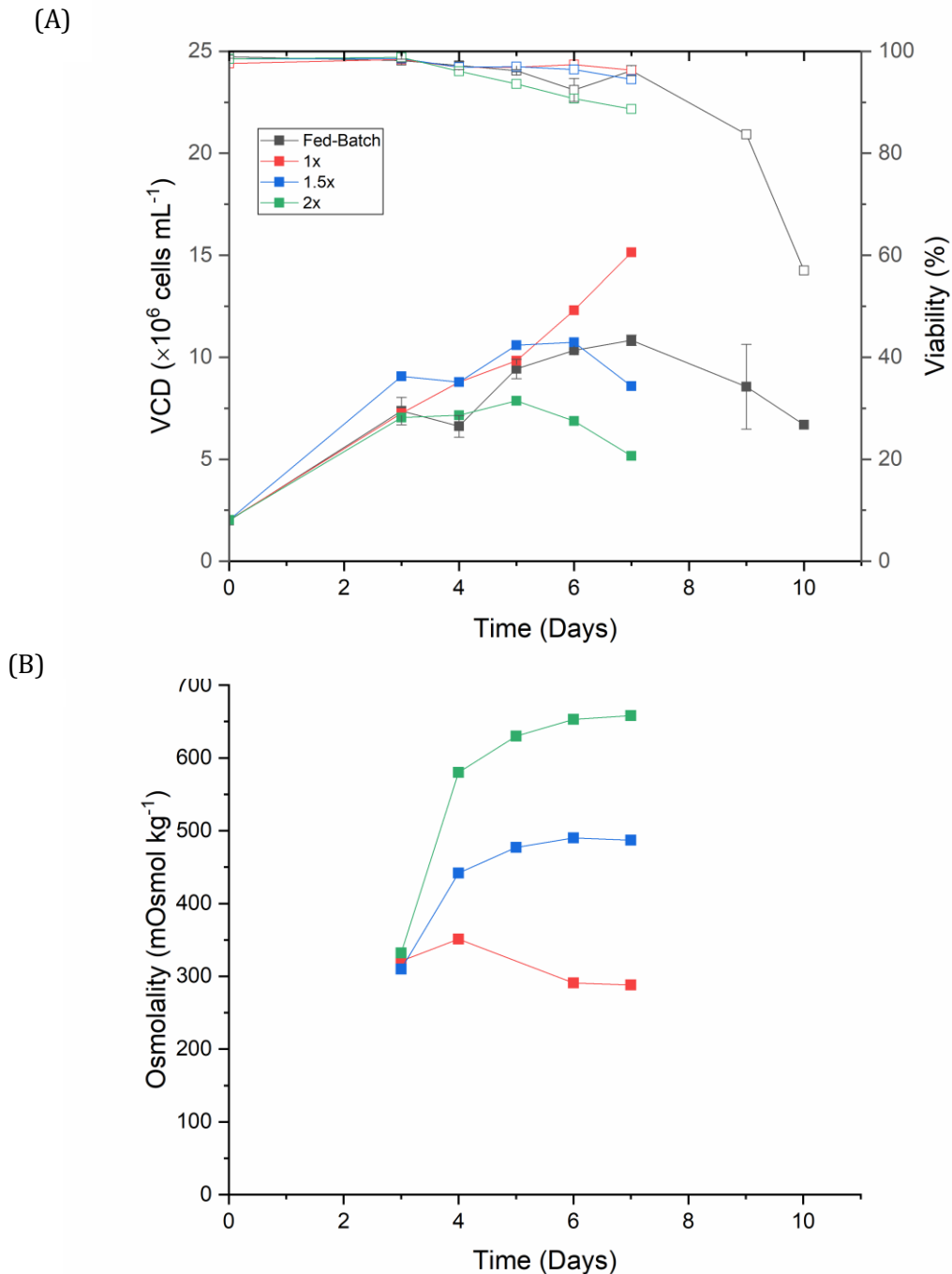


Figure 3.5 - Fed-batch and centrifugation quasi-perfusion cultures exchanged with 1, 1.5 and 2 times concentrated CD-CHO medium at a rate of 1 VVD. Cultures were seeded at 2×10^6 cells mL⁻¹ incubated at 37°C, N= 220 RPM and covered with Duetz sandwich lids. (A) VCD (filled symbols) and viability (empty symbols) of fed-batch and centrifugation quasi-perfusion cultures (B) Osmolality of centrifugation quasi-perfusion cultures exchanged with 1, 1.5 and 2 times concentrated medium. Fed-batch data represents triplicate cultures \pm s.d. All other data points represent 1 culture, with one well sampled per day per condition utilising a sacrificial well sampling approach.

Cell cultures exchanged with concentrated CD-CHO suffered from poor growth performance, with generated VCDs more comparable to fed-batch than quasi-perfusion exchanged with un-supplemented CD-CHO. Measured osmolality in the medium and the cell culture for both concentrations was above 450 m Osm kg⁻¹, which is considered to be the point at which osmolality becomes toxic, damaging cell growth and viability (Zhu, 2005, Takago, 2000).

3.2.4.2. CD-CHO supplemented with glucose

Glucose was aseptically added to CD-CHO to provide increased nutritional depth without increasing osmolality. CD-CHO was supplemented with glucose at 9 and 12 g L⁻¹ and used for exchange of quasi-perfusion cultures at 1 VVD.

Figure 3.6 A shows VCD and viability with time for quasi-perfusion cultures exchanged with CD-CHO supplemented to 9 and 12 g L⁻¹ of glucose at 1 VVD. Peak VCD for both 9 and 12 g L⁻¹ CD-CHO are comparable to cultures exchanged with un-supplemented CD-CHO at 15.8 and 15.5 × 10⁶ cells mL⁻¹ respectively. **Figure 3.6 B and C** shows the corresponding glucose and lactate profiles respectively for glucose supplemented and un-supplemented quasi-perfusion cultures. Glucose depletion is observed in cultures exchanged with CD-CHO and CD-CHO supplemented to 9 g L⁻¹ by day 7. Supplementing media to 12 g L⁻¹ generates a surplus of glucose, at a concentration of 5.88 g L⁻¹ on day 7. Lactate production is greater in the cultures exchanged with 12 g L⁻¹ CD-CHO, resulting in a lactate concentration of 1.3 g L⁻¹ on day 7. While lactate production is lower for cultures exchanged with CD-CHO supplemented to 9 g L⁻¹, lactate is continuously produced to a final lactate concentration of 0.5 g L⁻¹. Comparatively, cultures exchanged with un-supplemented CD-CHO have a net lactate production of 0 by day 7, remaining at 0 g L⁻¹ after the final exchange on day 6.

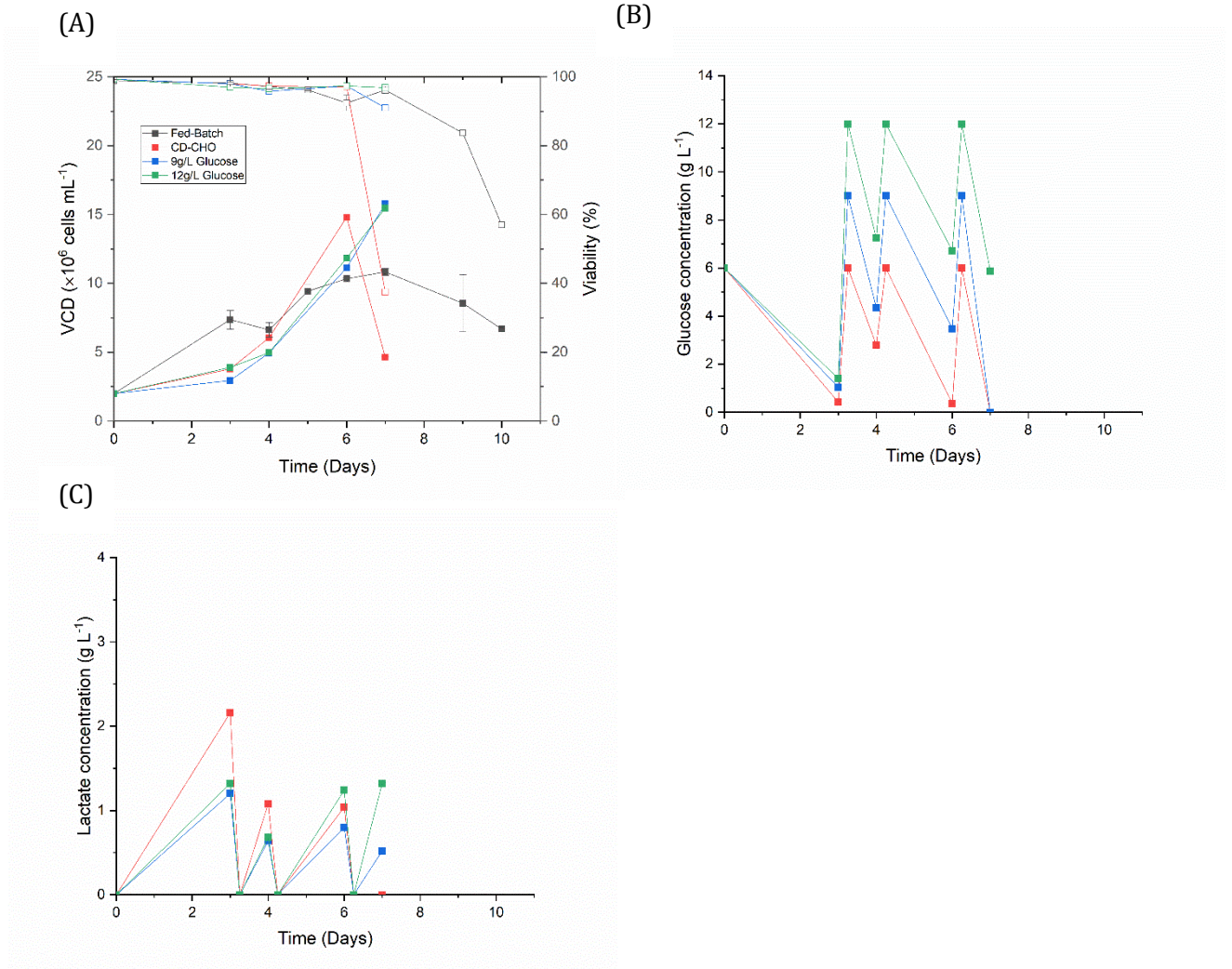


Figure 3.6 - Fed-batch, sedimentation quasi-perfusion and centrifugation quasi-perfusion cultures in 24-well MWP. Cultures were seeded at 2×10^6 cells mL^{-1} incubated at 37°C , $N=220$ RPM and covered with Duetz sandwich lids. Quasi-perfusion cultures were exchanged from day 3 at 1 VVD with CD-CHO and glucose-supplemented CD-CHO media at 9 and 12 g L^{-1} . (A) VCD (filled symbols) and viability (empty symbols) (B) Glucose concentration (C) Lactate concentration. Fed-batch data represents triplicate cultures \pm s.d. All other data points represent 1 culture, with one well sampled per day per condition utilising a sacrificial well sampling approach.

Glucose supplemented CD-CHO medium has an osmolality below toxic levels, between 270 - 321 m Osm kg^{-1} . For supplemented CD-CHO, cell viability is maintained for an increased number of days compared to un-supplemented cultures, but maximum VCDs are comparable. Cultures exchanged with CD-CHO have a net 0 lactate production on day 7, suggesting that the lactate shift has occurred, and cells are consuming rather than producing lactate due to exhaustion of metabolites.

3.2.4.3. CD-CHO blended with feeding media

The supplementation of a nutrient-rich feeding media, Efficient Feed B (Feed B), into CD-CHO was subsequently investigated to increase the concentration of glucose as well as glutamine, glutamate, ammonia and other trace metabolites. Media blends of 5, 15, 30 and 45% Feed B were investigated. The osmolality of all media studied are between 320-355 m Osmol kg⁻¹ and therefore osmotic effects are not considered in this study. Quasi-perfusion cultures were carried out in sedimentation and centrifugation modes, as outlined in section 2.4.3. Media exchanges commenced on day 3 at a rate of 1 VVD, with two daily exchanges of 50% volume required for sedimentation cultures and one daily exchange of the entire volume for centrifugation cultures.

Figures 3.7 A and B show VCD and viability with time for sedimentation and centrifugation, respectively, compared to optimised fed-batch culture, seeded at 2×10^6 cells mL⁻¹. **Figures 3.7 C and D** show corresponding glucose profiles for sedimentation and centrifugation quasi-perfusion cultures respectively supplemented with Feed B. **Figures 3.7 E and F** show lactate profiles for sedimentation and centrifugation quasi-perfusion cultures, respectively, supplemented with Feed B. For fed-batch cultures, optimised as described in section 3.2.2, maximum VCD was 10.6×10^6 cells mL⁻¹ and viability starts dropping after 7 days of cultivation. Quasi-perfusion techniques using media blends generate VCDs greater than fed-batch and achieve comparable performance for all but the lowest and highest supplementation of Feed B.

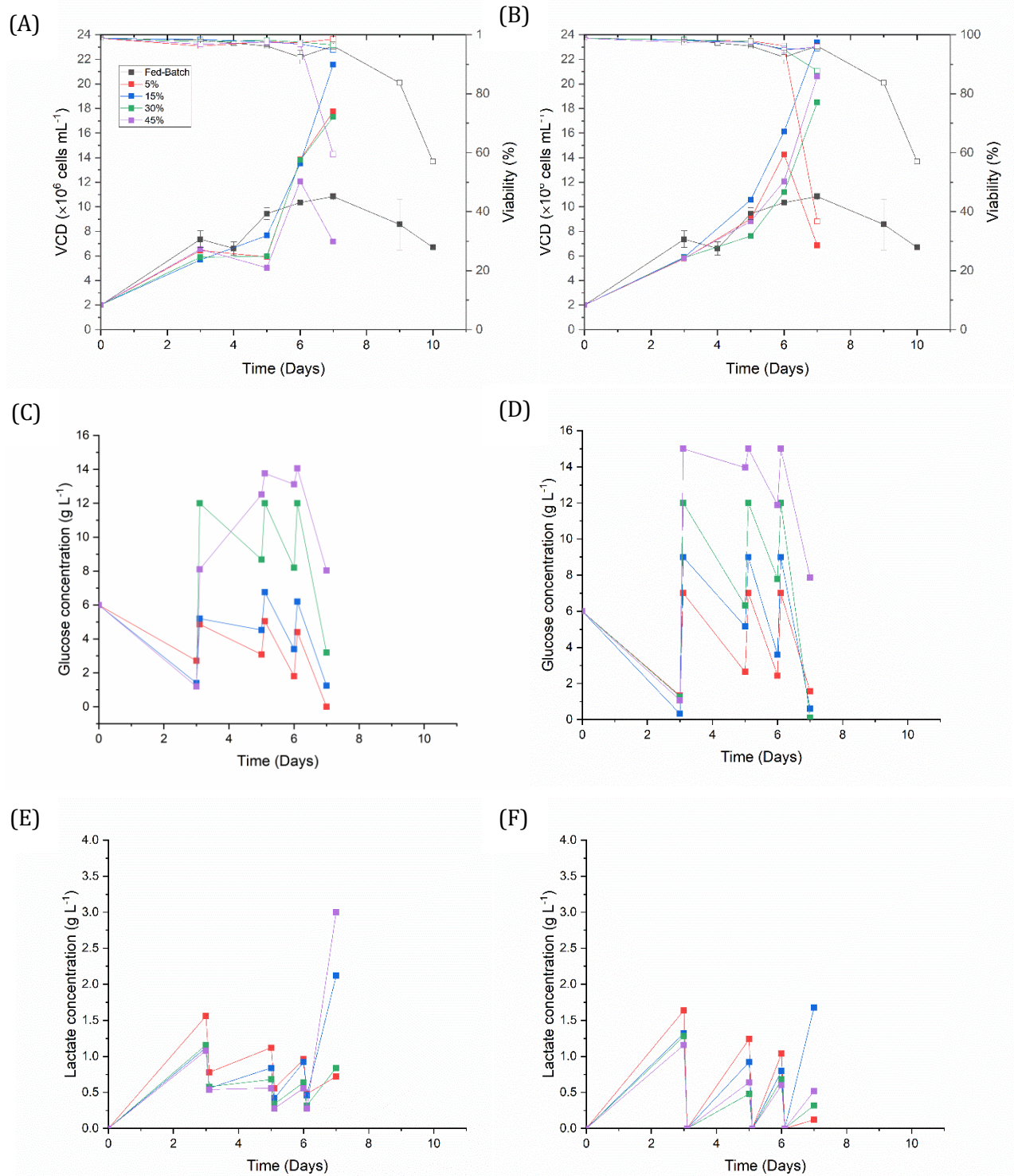


Figure 3.7- Fed-batch, sedimentation quasi-perfusion and centrifugation quasi-perfusion cultures. Cultures were seeded at 2×10^6 cells mL^{-1} incubated at 37°C , $N = 220$ RPM and covered with Duetz sandwich lids. Quasi-perfusion cultures were exchanged from day 3 at a rate of 1 VVD with CD-CHO media blended with Efficient Feed B at 5, 15, 30 and 45% volume/volume. (A) VCD (filled symbols) and viability (empty symbols) for fed-batch and sedimentation quasi-perfusion cultures. (B) VCD (filled symbols) and viability (empty symbols) for fed-batch and centrifugation quasi-perfusion cultures. (C) Glucose concentration for sedimentation quasi-perfusion cultures. (D) Glucose concentration for centrifugation quasi-perfusion cultures (E) Lactate concentration for sedimentation quasi-perfusion cultures (F) Lactate concentration for centrifugation quasi-perfusion cultures. Fed-batch data represents triplicate cultures \pm s.d. All other data points represent 1 culture, with one well sampled per day per condition utilising a sacrificial well sampling approach.

For sedimentation cultures, all media blends show comparable media performance until day 6, with deviations observed from day 7. Media blends containing 45% Feed B see a significant decline in VCD from a maximum of 12.1×10^6 cells mL⁻¹ and a viability drop of 96% on day 6 to 7×10^6 cells mL⁻¹ and 59% viability on day 7. The observed decrease in viability can be attributed to consistent over supplementation of glucose, which reaches a maximum of 13 g L⁻¹ in the culture on day 6 prior to media exchange. Sustained high glucose concentration and unbalanced amino acids cause high q_{Lac} (Reinhart et al., 2015), resulting in a lactate spike on day 7 to 3 g L⁻¹. Elevated lactate concentration causes a pH shift to values less than 6.5, which detrimentally impacts cell growth and proliferation.

Blends containing 30% Feed B are also limited, to a lesser extent, by high glucose concentrations of 8 g L⁻¹, causing lactate concentration to spike to 2.1 g L⁻¹ on day 7. Viability is maintained, despite the lactate spike, at 95%, and maximum cell density is 17.3×10^6 cells mL⁻¹ on day 7. Cultures exchanged with 5% Feed B are glucose depleted on day 6, reaching a maximum cell density comparable to cultures exchanged with 30% Feed B, at 17.8×10^6 cells mL⁻¹. Media supplemented with 15% Feed B generates optimal performance, reaching a maximum VCD of 21.6×10^6 cells mL⁻¹ on day 7, and maintains a viability greater than 96%. Glucose concentration is well controlled between 1.2- 4.5g L⁻¹ for the duration of the culture.

Performance of media blends in centrifugation cultures are comparable to sedimentation cultures under otherwise identical conditions for 15 and 30% blends, but variation is seen in 5 and 45% Feed B blends. Blends containing 5% Feed B are glucose depleted on day 6, causing a drop in cell density and viability from a maximum of 16.1×10^6 cells mL⁻¹ and 95% on day 6 to 6.9×10^6 cells mL⁻¹ and 37% on day 7. Blends containing 45% Feed B maintain viability >95% for the culture duration and reach a maximum cell density of 20.6×10^6 cells mL⁻¹ on day 7. Media supplemented with 15%

Feed B, similarly to sedimentation cultures, produce the greatest VCD of 23.4×10^6 cells mL^{-1} and maintain a viability of greater than 96% for the duration of the culture. Glucose concentration is well controlled between days 1-6, fluctuating between 1-3.6 g L^{-1} prior to exchange, however elevated VCD and less frequent media exchange compared to sedimentation cultures leads to near-depletion at 0.12 g L^{-1} on day 7.

Exchanging with media supplemented with Feed B produce VCDs twice as much as fed-batch approach. The less frequent media exchanges required to achieve a 1 VVD perfusion rate in centrifugation cultures result in deviations compared to the same media in sedimentation cultures, for medias containing extreme high or low glucose concentrations. The consumption of glucose over a 24 hour period, rather than a 12 hour period, causes wider fluctuations in glucose concentrations. This is advantageous for high concentration medias, such as those in the 45% media blends, as elevated glucose concentrations are not consistently maintained, resulting in lower q_{Lac} , and reduced pH fluctuations. The wide glucose fluctuations when exchanging medias with a low glucose concentration cause elongated periods of glucose depletion, which detrimentally impacts cell proliferation and viability.

Figure 3.8 A and B shows mAb concentration of fed-batch and sedimentation and centrifugation quasi-perfusion cultures, respectively, exchanged with media blended with 5-45% Feed B. **Figure 3.8 C** shows the volumetric productivity for fed-batch culture and for sedimentation and centrifugation quasi-perfusion cultures. All blends produce up to a 2 fold greater mAb per litre of culture per day compared to fed-batch. Centrifugation cultures have improved performance compared to corresponding sedimentation cultures, with 15% media blends producing the greatest volumetric productivity across both quasi-perfusion modes. From these results it is clear that productivity is not directly reliant on VCD, with 5% media centrifugation cultures producing some of the greatest volumetric productivity.

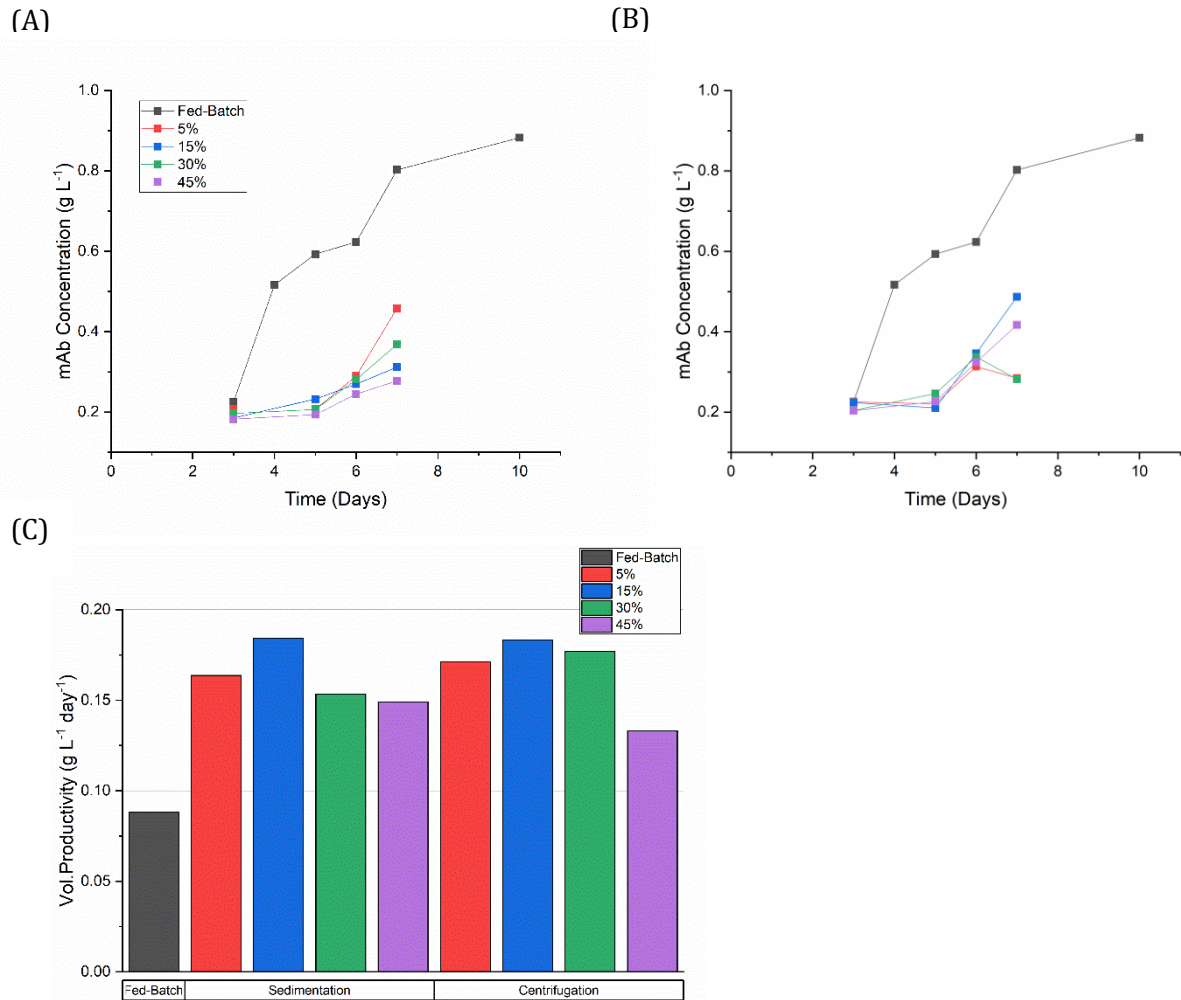


Figure 3.8 - Productivity of fed-batch, sedimentation quasi-perfusion and centrifugation quasi-perfusion cultures. Cultures were seeded at 2×10^6 cells mL⁻¹ incubated at 37°C, N= 220 RPM and covered with Duetz sandwich lids. Quasi-perfusion cultures were exchanged from day 3 at a rate of 1 VVD with CD-CHO media blended with Efficient Feed B at 5, 15, 30 and 45% volume/volume. (A) mAb concentration for fed-batch and sedimentation quasi-perfusion cultures (B) mAb concentration for fed-batch and centrifugation quasi-perfusion cultures (C) Volumetric productivity for fed-batch, sedimentation quasi-perfusion and centrifugation quasi-perfusion cultures. Fed-batch data represents triplicate cultures \pm s.d. All other data points represent 1 culture, with one well sampled per day per condition utilising a sacrificial well sampling approach.

The purpose of conducting a media screen was firstly to identify an appropriate media for subsequent quasi-perfusion and perfusion studies in bioreactor, and secondly to demonstrate the capabilities of the quasi-perfusion system as a screening tool. Media development is a vital phase of cell culture development, with selection parameters such as cost, consumption rate, nutritional depth and osmolality considered. Quasi-perfusion methodologies were found to be sensitive to changes in media composition, a promising

characteristic for the utilisation for early-phase media screening. In the study, consistent over-feeding of glucose leads to spikes in lactate above 3 g L⁻¹ for both sedimentation and centrifugation cultures exchanged with 45% media blends. It has been observed that lactate concentrations above 2 g L⁻¹ can cause acidification of pH to less than 6.5 in fed-batch cultures where control is achieved via media buffer capacity (Hsu et al., 2012). Media exchanges in quasi-perfusion cultures will reduce lactate concentration by half every 12 hours in sedimentation cultures and to 0 g L⁻¹ every 24 hours in centrifugation cultures. This will provide limited control of pH but cells will be exposed to unfavourable pH for extended time periods, particularly in centrifugation cultures.

The impact of periodic media exchanges every 12-24 hours is highlighted as an important system limitation. With infrequent media exchanges, concentration of nutrients, such as glucose, are not kept constant, and toxic by-products, such as lactate, accumulate prior to exchange. The result is glucose and lactate concentration fluctuations between media exchanges, as reported in alternative quasi-perfusion methodologies (Bielser et al., 2019, Wolf et al., 2018). While this limitation can be mitigated by increasing the number of media exchanges to achieve the desired perfusion rate, a large number of plate manipulations per day could become detrimental to culture performance, increases the risk of contamination and, without automation, would reduce the number of plates to be feasibly managed by one technician, thus reducing throughput.

Overall, comparable performance is observed between sedimentation and centrifugation cultures for media containing between 9-12 g L⁻¹ of glucose. Promising increases in VCD compared to fed-batch have been shown for a range of conditions, alongside 2 fold improvements in volumetric productivity. Media blends containing 15% Feed B represented the best performing recipe across sedimentation and centrifugation cultures and has therefore been selected as the standard for all subsequent cultures. The

key cause of deviation between sedimentation and centrifugation methodologies is thought to be the variation in feeding strategies, resulting in deviations in the dilution ratio of fresh to spent media after each exchange. To enable greater comparability, all subsequent sedimentation and centrifugation methodologies have matched the number of daily exchanges in order to enable comparable dilution ratios.

3.2.5. Process optimisation using quasi-perfusion methodologies at varying perfusion rates 0.5-1.8 VVD

In order to assess how robust quasi-perfusion methodologies are for use as a tool for early phase development, the volume and frequency of media exchanges were varied to study the impact on consistency and cell culture performance. **Figure 3.9 A** shows VCD and viability for quasi-perfusion sedimentation cultures, at exchange rates between 0.5 and 1.5 VVD. **Figure 3.9 B** shows VCD and viability for quasi-perfusion centrifugation cultures, at exchange rates between 0.5 and 1.8 VVD. Sedimentation and centrifugation cultures at each perfusion rate were exchanged with media containing 15% Feed B. **Figure 3.9 C and D** show corresponding glucose profiles for sedimentation and centrifugation cultures respectively. **Figure 3.9 E and F** show corresponding lactate profiles for sedimentation and centrifugation cultures, respectively. One daily exchange was required to generate a perfusion rate of 0.5 and 0.75 VVD. Two exchanges of half the total volume were necessary to facilitate perfusion rates of 1.5 and 1.8 VVD. To avoid the disruption of the cell pellet in sedimentation cultures, supernatant removal was capped at 75% of the volume per exchange, meaning a perfusion rate of 1.8 VVD was performed in centrifugation mode only.

Growth kinetics for sedimentation and centrifugation cultures under otherwise identical conditions are comparable until day 7 for all exchange rates analysed. VCDs for sedimentation cultures on day 7 are between $20.7\text{-}22.8 \times 10^6$ cells mL⁻¹ for all perfusion rates, with viabilities maintained above 94%. Centrifugation cultures maintain close

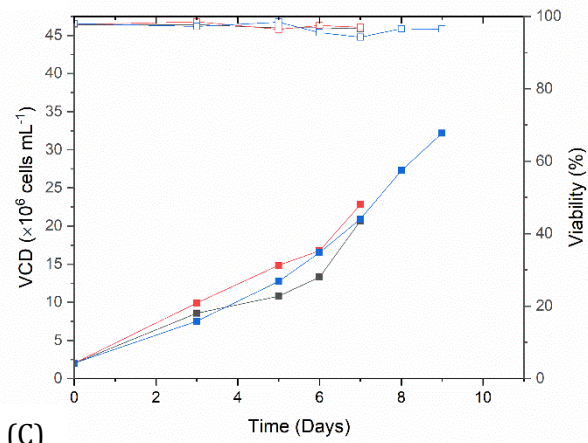
comparability until day 5 at all perfusion rates, but deviations of up to 25% are observed from day 6. VCDs on day 7 lie between $21.4\text{-}25.2 \times 10^6$ cells mL^{-1} , with viability maintained above 91%. Several cultures were maintained for an extended growth period, until day 9, and all show continued improvements in VCD with maintenance of viability. Low exchange rate centrifugation cultures at 0.5 and 0.75 VVD maintain high viabilities of 95.5 and 91.1%, respectively, and achieve maximum VCDs of 33.3×10^6 cells mL^{-1} on day 9. Comparing sedimentation and centrifugation cultures at a rate of 1.5 VVD sees a maximum VCD on day 9 of 32.2 and 34.2×10^6 cells mL^{-1} respectively. Increasing the perfusion rate further to 1.8 VVD in centrifugation cultures generates a 23% improvement in VCDs compared to all other conditions, generating a maximum VCD of 42.2×10^6 cells mL^{-1} at a viability of 96.1% on day 9.

Figures 3.9 G and H show separation efficiencies for sedimentation and centrifugation cultures, respectively, exchanged at perfusion rates between 0.5-1.8 VVD. Sedimentation cultures have more variable separation efficiencies than centrifugation cultures, which is expected due to the fragile cell pellet being more easily disrupted. Despite the wider variability, separation efficiencies for all perfusion rates across both modes is >93% for the duration of the culture. Centrifugation cultures maintain consistent concentration of cells in the supernatant throughout a range of exchange rates, meaning separation efficiencies increase as VCD increases. The separation efficiencies of sedimentation cultures are inversely related to VCD, with increases in VCD causing a larger settled cell volume, leading to poorer separation. This is particularly prominent for cultures with the greatest volume per exchange, 0.75 and 1.5 VVD. Additionally, the delicate pellet of separated cells is easily disrupted during manual supernatant removal, causing more inconsistent efficiencies compared to centrifugation cultures.

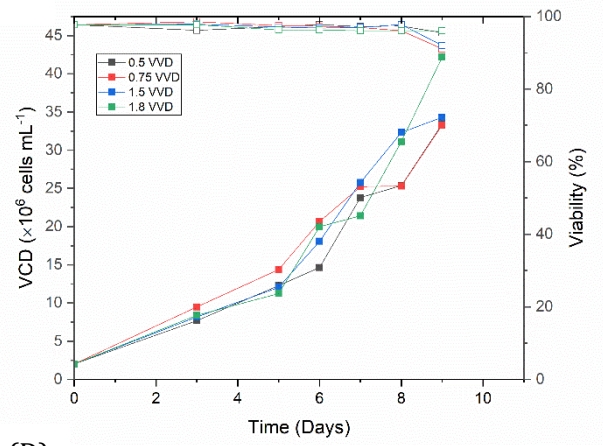
Figure 3.9 I and J shows the CSPR for sedimentation and centrifugation cultures at perfusion rates between 0.5 and 1.8 VVD and exchanged with media containing between

5-30% Feed B. For all culture conditions, as cell density increases exponentially in the growth phase of the culture, cultures experience an inverse exponential decline. This trend is particularly apparent in high perfusion rate cultures, where initial perfusion rate is high in comparison to the VCD. Towards the later stages of the culture, in days 7 – 9, VCD is greater and growth rate slower in proportion to the exchange volume, leading to the CSPR curve to flatten. $CSPR_{min}$ for higher perfusion rates of 1.5 and 1.8 VVD lie between 0.05–0.06 nL cell⁻¹ day⁻¹ for sedimentation and centrifugation cultures. Lower perfusion rates see less dramatic changes to CSPR for the culture duration, with cultures exchanged at 0.5 and 0.75 VVD generating $CSPR_{min}$ between 0.02-0.03 nL cell⁻¹ day⁻¹. The low CSPRs in low VVD cultures could be a contributing factor to the limitation of maximum VCD (Kreye et al., 2019), with the maximum VCD achieved across all modes operated under 1VVD being 33.4×10^6 cells mL⁻¹. This is agreement with Villiger-Oberbek et al. (2015), who state that CSPRs below 0.05 nL cell⁻¹ day⁻¹ are considered unfeasible for the support of cells at concentrations over 40×10^6 cells mL⁻¹.

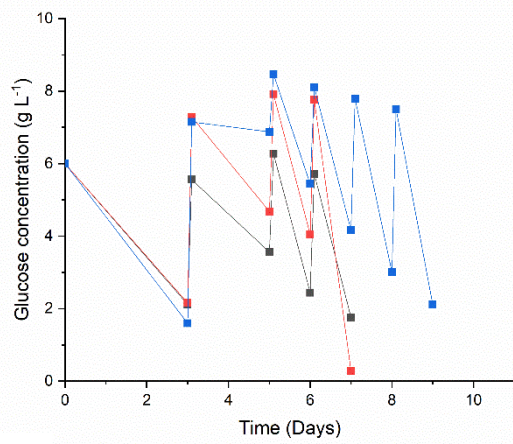
(A)



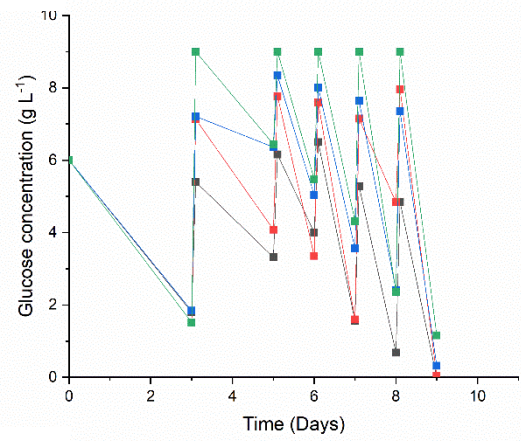
(B)



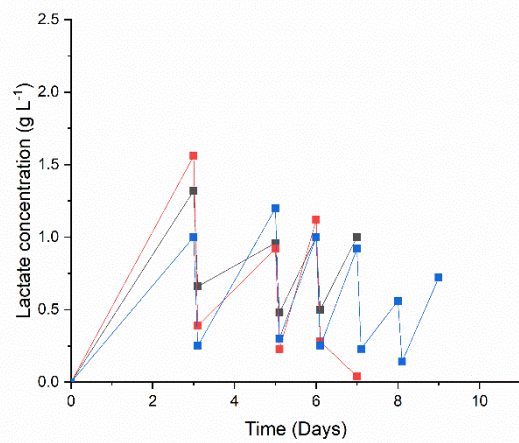
(C)



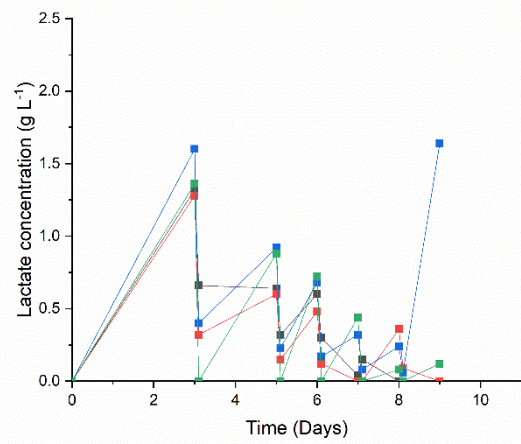
(D)



(E)



(F)



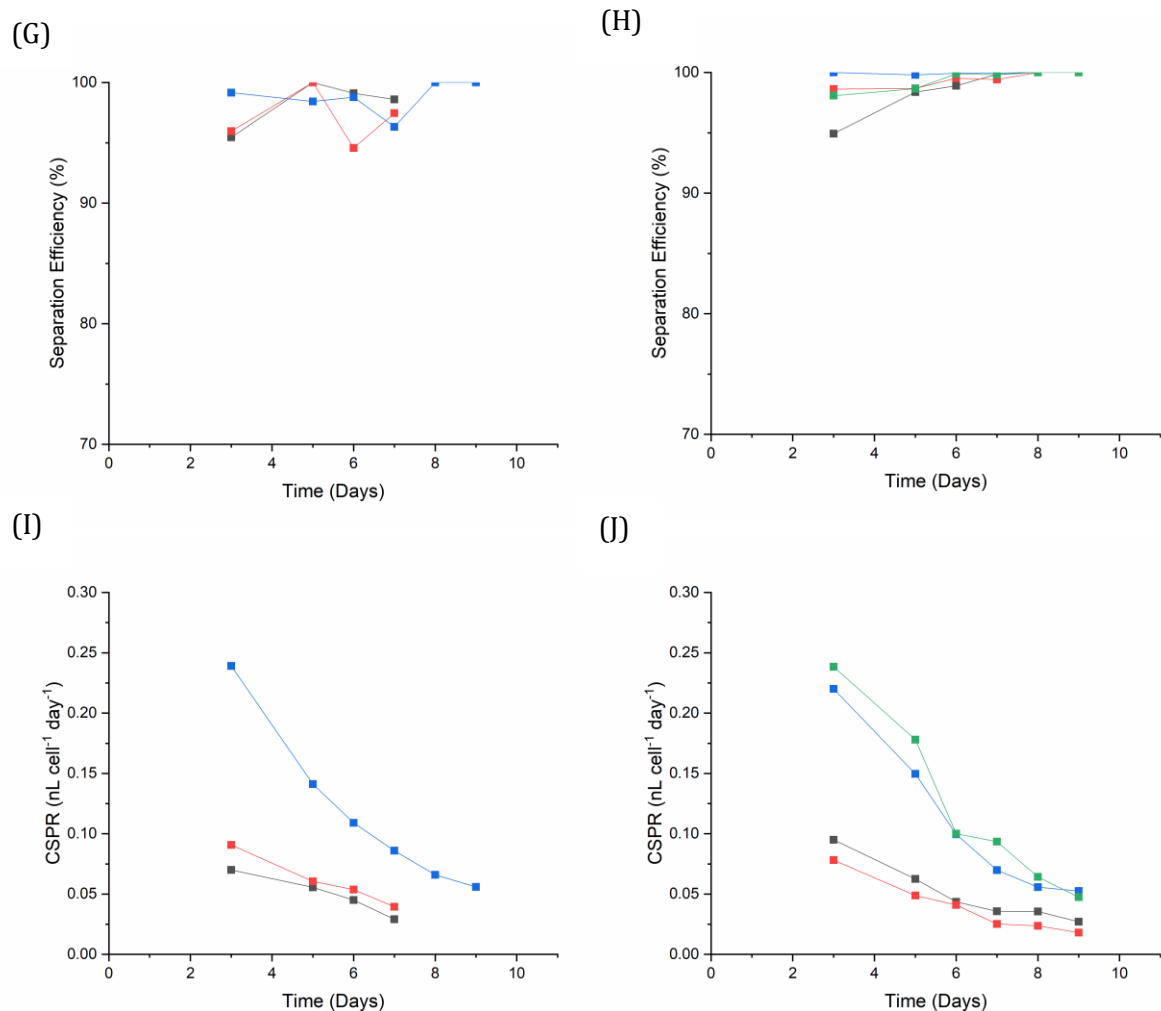


Figure 3.9 - Sedimentation quasi-perfusion and centrifugation quasi-perfusion cultures exchanged at rates between 0.5-1.8 VVD. Cultures were seeded at 2×10^6 cells mL⁻¹ incubated at 37°C, N= 220 RPM and covered with Duetz sandwich lids. Quasi-perfusion cultures were exchanged from day 3 with CD-CHO media blended with 15% Efficient Feed B at exchange rates between 0.5-1.8 VVD. (A) VCD (filled symbols) and viability (empty symbols) for sedimentation quasi-perfusion cultures. (B) VCD (filled symbols) and viability (empty symbols) for centrifugation quasi-perfusion cultures. (C) Glucose concentration for sedimentation quasi-perfusion cultures. (D) Glucose concentration for centrifugation quasi-perfusion cultures. (E) Lactate concentration for sedimentation quasi-perfusion cultures (F) Lactate concentration for centrifugation quasi-perfusion cultures (G) Separation efficiency for sedimentation quasi-perfusion cultures (H) Separation efficiency for centrifugation quasi-perfusion cultures (I) CSPR for sedimentation quasi-perfusion cultures (J) CSPR for centrifugation quasi-perfusion cultures. Data represents 1 culture per condition, with one well sampled per day per condition utilising a sacrificial well sampling approach.

Media blends containing 15% Feed B represented the best performing media during media screening at 1 VVD, however it is important to note that perfusion rate and nutritional depth of media are dependant variables. For the optimisation of perfusion cultures, the nutritional depth of the media should be considered alongside perfusion rate. Therefore, low glucose blend media were considered in high perfusion rate

cultures, and higher glucose blends were considered for low perfusion rate cultures. **Figure 3.10 A and B** shows VCD and viability for sedimentation and centrifugation cultures respectively, exchanged at perfusion rates between 0.5-1.8 VVD. **Figure 3.10 C and D** show corresponding glucose profiles for sedimentation and centrifugation cultures, respectively. **Figure 3.10 E and F** show corresponding lactate profile for sedimentation and centrifugation cultures, respectively. Low perfusion rate cultures of 0.5 and 0.75 VVD were exchanged with media blends containing 30% Feed B, and high perfusion rates of 1.5 and 1.8 VVD were exchanged with 5% Feed B blends. Sedimentation cultures for both media and all perfusion rates perform comparably for the duration of the culture. Maximum VCDs for sedimentation cultures exchanged with 5% and 30% media are between $18.7-19.1 \times 10^6$ cells mL⁻¹ on day 7, a slight reduction in those achieved using the same perfusion rates and exchanging with 15% blend media. In centrifugation cultures, VCD is between $18.8-23.4 \times 10^6$ cells mL⁻¹ for all conditions on day 7. Continued growth in centrifugation cultures is shown until day 9 for all perfusion rates. Cultures exchanged at 0.5 VVD and 0.75 VVD exchanged with 30% blend media achieve a maximum VCD of 33.1 and 41.4×10^6 cells mL⁻¹ respectively on day 9. Maximum VCDs for 0.5 VVD cultures are comparable using 15 and 30% media blends, which both see glucose limitation, at low concentrations between 0.16-0.68 g L⁻¹ prior to exchange, from day 8. For 0.75 VVD cultures, the use of 30% media blend compared to 15% media improves the VCD achieved on day 9 by 20%.

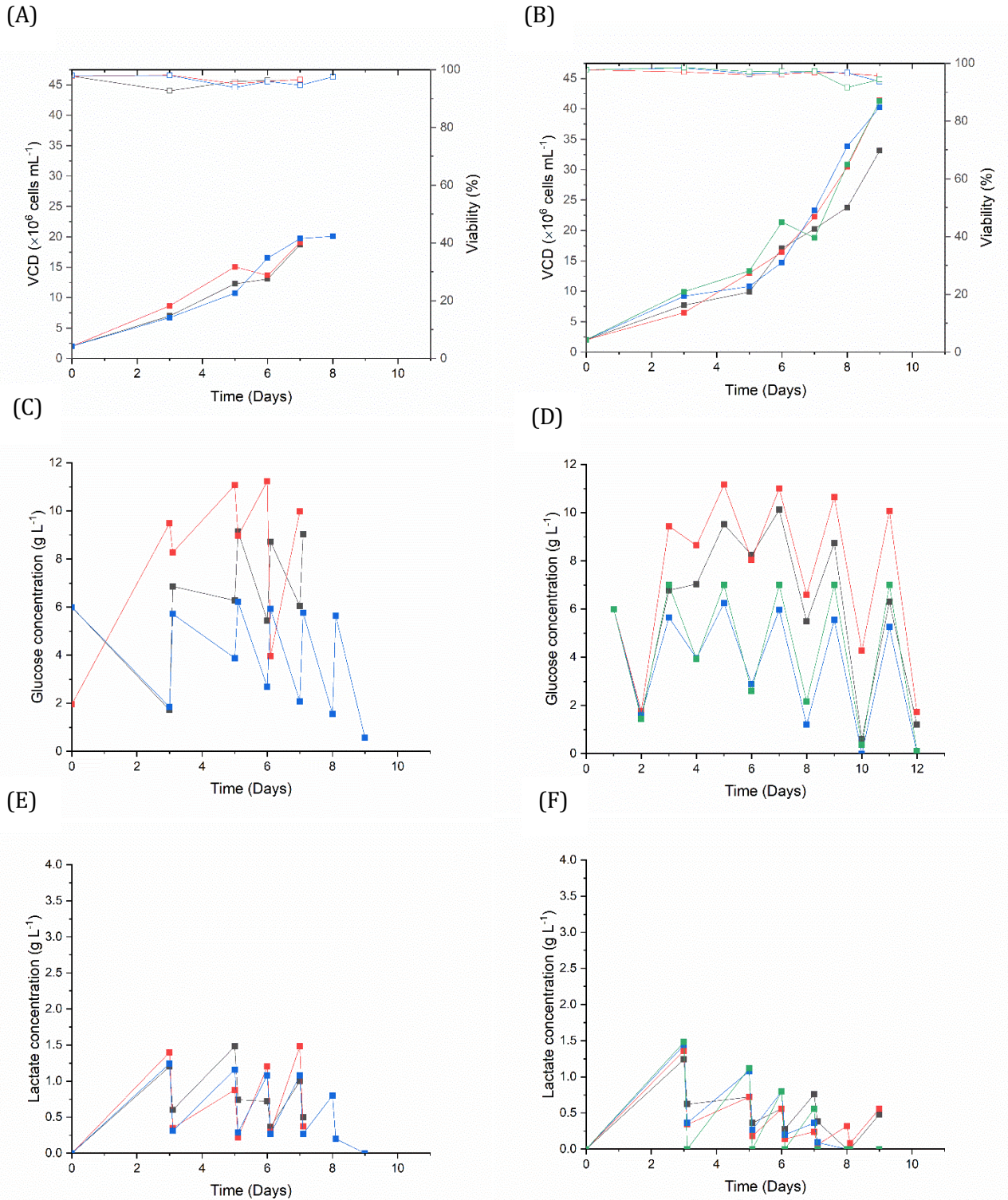


Figure 3.10- Sedimentation quasi-perfusion and centrifugation quasi-perfusion cultures exchanged at rates between 0.5-1.8 VVD. Cultures were seeded at 2×10^6 cells mL^{-1} incubated at 37°C , $N= 220$ RPM and covered with Duetz sandwich lids. Quasi-perfusion cultures were exchanged from day 3 with CD-CHO media blended with 30% Efficient Feed B at an exchange rate of 1.5 and 1.8 VVD, or CD-CHO media blended with 5% Efficient Feed B at an exchange rate of 0.5 and 0.75 VVD. (A) VCD (filled symbols) and viability (empty symbols) for sedimentation quasi-perfusion cultures (B) VCD (filled symbols) and viability (empty symbols) for centrifugation quasi-perfusion cultures (C) Glucose concentration for sedimentation quasi-perfusion cultures (D) Glucose concentration for centrifugation quasi-perfusion cultures (E) Lactate concentration for sedimentation quasi-perfusion cultures (F) Lactate concentration for centrifugation quasi-perfusion culture. Data represents 1 culture per condition, with one well sampled per day per condition utilising a sacrificial well sampling approach.

Figure 3.11 shows volumetric productivity and maximum titre for quasi-perfusion sedimentation and centrifugation cultures exchanged at perfusion rates between 0.5 – 1.8 VVD with 5, 15 and 30% blend media. While all quasi-perfusion methodologies produce higher volumetric productivities than fed-batch, lower volumetric productivities and titres are consistently observed in sedimentation cultures in comparison to centrifugation cultures under otherwise identical conditions. For sedimentation cultures at the lowest exchange rate, 0.5 VVD, maximum titres of 0.8 and 0.66 g L⁻¹ are achieved when exchanging with 15 and 30% media, respectively. In comparison, centrifugation cultures at 0.5 VVD generate maximum titres of 1.2 g L⁻¹ for both 15 and 30% blend medias, an up to 50% increase compared to sedimentation. It is worth noting that sedimentation cultures at 0.5 and 0.75 VVD were maintained for 7 days, in comparison to 9 days achieved for centrifugation cultures, which has an impact on volumetric productivity, however for all cultures the maximum titre was achieved on or before day 7, so direct comparisons can be made between titres. As expected, an increase in perfusion rate for 0.5-0.75 VVD to 1.5-1.8 VVD cultures generally is seen to decrease titre across both sedimentation and centrifugation modes. The decrease in titre for high VVD cultures correlates to an increased number of exchanges to twice daily, meaning that volumetric productivities generally increase as perfusion rate increases. In general, media tested generate comparable volumetric productivities under otherwise identical conditions, with maximum deviations of 10%. The exceptions to this are (i) sedimentation cultures at 0.5 VVD, where a 25% increase in volumetric productivity is observed when using 15% blend media and (ii) centrifugation cultures at 1.5 VVD where a 25% increase in volumetric productivity is observed when exchanging with 5% blend media compared to 15% blend media.

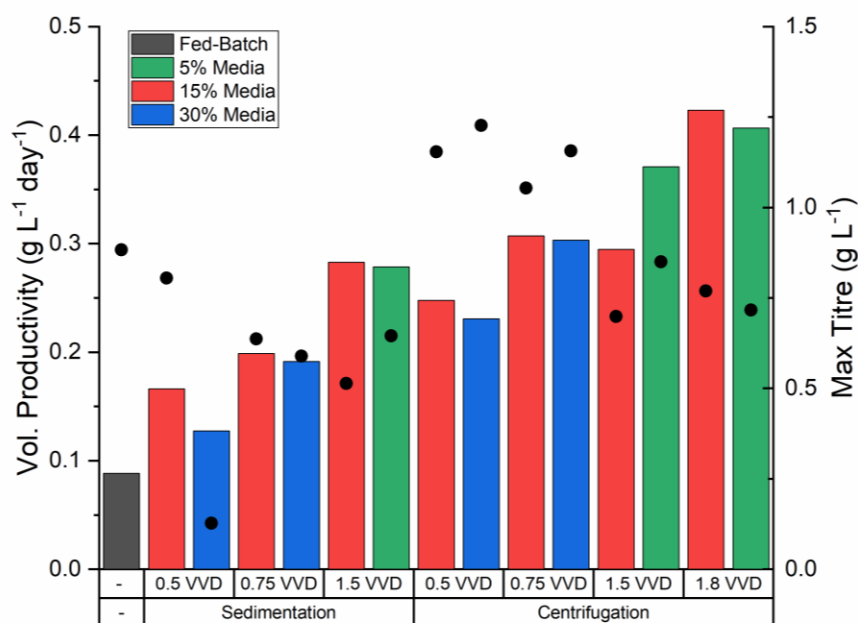


Figure 3.11- Volumetric productivity (bars) and maximum titre (scatter) for fed-batch, sedimentation quasi-perfusion and centrifugation quasi-perfusion cultures exchanged at perfusion rates between 0.5-1.8 VVD with CD-CHO medium blends with Efficient Feed B at 5, 15 and 30%. Volumetric productivity was calculated following Equation 2.11. Fed-batch data represents triplicate cultures. All other data represents 1 culture per condition, with cumulative mAb calculated from each well sampled per day per condition utilising a sacrificial well sampling approach.

Table 3.2 show specific glucose consumption, and lactate and antibody production for fed-batch culture. Table 3.3 shows (A) sedimentation and centrifugation quasi-perfusion cultures exchanged at perfusion rates between 0.5-1.8 VVD with 15% blend media and (B) 5 and 30% blend media, respectively. Specific glucose consumption increases with an increased availability of glucose, whether from an increased perfusion rate or an exchange with higher concentration media blends. Higher q_{Lac} is also associated with increased availability of glucose with high VVD cultures exchanged at 1.5 and 1.8 VVD producing up to 3 times more lactate than corresponding low VVD cultures. Specific antibody production is generally greater in sedimentation cultures compared to centrifugation cultures, however any increase in q_{Ab} in sedimentation cultures is outweighed by the increased VCD in centrifugation cultures, which maintain the greatest volumetric productivities.

Table 3.2 - Specific glucose consumption (q_{Gluc}), and lactate (q_{Lac}) and antibody (q_{Ab}) production rates for fed-batch cultures

Fed-Batch	
q_{Gluc} (pg cell ⁻¹ day ⁻¹)	721
q_{Lac} (pg cell ⁻¹ day ⁻¹)	35.8
q_{Ab} (pg cell ⁻¹ day ⁻¹)	52.0

Table 3.3 - Specific glucose consumption (q_{Gluc}), and lactate (q_{Lac}) and antibody (q_{Ab}) production rates for (A) Sedimentation quasi-perfusion and centrifugation quasi-perfusion cultures exchanged a perfusion rates between 0.5-1.8 VVD with media blended with 15% Efficient Feed B and (B) Sedimentation quasi-perfusion and centrifugation quasi-perfusion cultures exchanged at perfusion rates of 0.5 and 0.75 VVD exchanged with media blended with 5% Efficient Feed B and at perfusion rates of 1.5 and 1.8 VVD exchanged with media blended with 30% Efficient Feed B

(A)

15% Media						
	Sedimentation			Centrifugation		
VVD	q_{Gluc} (pg cell ⁻¹ day ⁻¹)	q_{Lac} (pg cell ⁻¹ day ⁻¹)	q_{Ab} (pg cell ⁻¹ day ⁻¹)	q_{Gluc} (pg cell ⁻¹ day ⁻¹)	q_{Lac} (pg cell ⁻¹ day ⁻¹)	q_{Ab} (pg cell ⁻¹ day ⁻¹)
0.5	221	44.9	24.7	207	21.2	21.9
0.75	172	47.0	19.2	225	22.8	23.9
1.5	354	63.0	31.0	366	62.2	31.9
1.8	-	-	-	410	60.7	39.9

(B)

5% and 30% Media						
	Sedimentation			Centrifugation		
VVD	q_{Gluc} (pg cell ⁻¹ day ⁻¹)	q_{Lac} (pg cell ⁻¹ day ⁻¹)	q_{Ab} (pg cell ⁻¹ day ⁻¹)	q_{Gluc} (pg cell ⁻¹ day ⁻¹)	q_{Lac} (pg cell ⁻¹ day ⁻¹)	q_{Ab} (pg cell ⁻¹ day ⁻¹)
0.5	166	44.9	7.76	223	23.3	18.0
0.75	133	120	53.2	258	32.7	15.8
1.5	443	101	43.5	302	56.9	34.4
1.8	-	-	-	1250	55.1	135

The use of quasi-perfusion in microwell plates has been expanded in this work to include the screening of perfusion rates alongside media screening, previously described in section 3.2.6. Perfusion rates can be screened independently of media, or it is possible to screen several media for each perfusion rate to combined optimisation. In this study, a small pool of the best performing media were taken forward from the media screen for investigation at varying perfusion rates. While it has been shown that a wide range of perfusion rates can be tested, in this study 0.5 – 1.8 VVD, further increases to the perfusion rate are limited by the feasible number of daily exchanges. Increasing the

perfusion rate for both sedimentation and centrifugation cultures increases the maximum VCD and volumetric productivity of the cultures. This can be attributed in part to the increased number of daily exchanges, which mean toxic by-products are more frequently removed, glucose concentration is more stable, and pH is better controlled. The advantages of increasing the number of daily exchanges outweigh potential disadvantages that come from increasing the number of cell retention steps, which has been found to be detrimental to cell proliferation (Kreye and Zoro, 2016).

Kreye et al. (2019) conducted quasi-perfusion cultures in the ambr15, shutting down agitation, air sparging and pH controls and allowing cells to sediment for between 45 to 60 minutes prior to media exchange. Peak VCDs of 15×10^6 cells mL⁻¹ were reported in the study, because the complete shutdown of all controls for up to 60 minutes caused spikes in pH and DO concentrations to fall significantly. The prolonged exposure to high pH and low DO conditions through multiple daily exchanges slowed cell growth and caused viability to decline. While these fluctuations are experienced in MWP, a smaller liquid height means a settling time is approximately half, reducing length of exposure. Additionally, MWPs sediment inside the incubator, where air exchange can still occur through the lid, and 5% CO₂ continues to provide some pH control, minimising the severity of pH and DO fluctuations. Similarly, the implementation of centrifugation as a cell retention step reduces the time cells are exposed to high pH and low DO conditions by 5.6 times compared to sedimentation cultures, while the low rpm utilised means that limited shear is exerted (Hutchinson, 2006). The reduction in the severity of and exposure to high pH and low DO conditions in MWP means that viability is maintained, and cells proliferate throughout the culture duration across both cell retention modes. Sedimentation cultures have a longer cell retention step compared to centrifugation cultures, which is a contributing factor to the lower VCDs consistently achieved in sedimentation cultures compared to centrifugation cultures under otherwise identical conditions.

While some perfusion cultures are operated at a fixed perfusion rate, a ramp-up approach to perfusion rate is often utilised in order to maintain a constant CSPR. The maintenance of CSPR enables a more consistent culture environment, particularly during the cell growth phase of the culture. Similar methodologies, maintaining constant VVD in quasi-perfusion cultures, have been described in shake tubes (Wolf et al., 2018, Villiger-Oberbek et al., 2015) and 96 DSW plates (Bielser et al., 2019). Each method utilised centrifugation as the cell retention step prior to media exchange. Wolf et al. (2019) described the use of shake tubes at a fixed perfusion rate of 1 VVD, focused on determining the $CSPR_{min}$. CSPRs were reported to drop as cell density increased from 0.25 to 0.04 nL cell⁻¹ day⁻¹, which is comparable to the CSPR profiles reported in high VVD cultures exchanged at 1.5 and 1.8 VVD. Wolf et al. (2019) suggest that as CSPRs tend to 0.04 nL cell⁻¹ day⁻¹, maximum specific growth rates are variable and, in some cases, negative, suggesting CSPRs in these ranges do not allow for stable growth. Contrary to this, all quasi-perfusion cultures carried out in sedimentation and centrifugation modes show continued growth throughout the culture duration, despite low perfusion rates of 0.5 and 0.75 VVD reaching a $CSPR_{min}$ of 0.02 nL cell⁻¹ day⁻¹ on day 9.

3.2.6. Expansion of quasi-perfusion methodologies to enable maintenance of constant cell-specific perfusion rates

In order to align the developed quasi-perfusion technology with large scale systems, a ramp up approach was incorporated to enable the maintenance of constant CSPR throughout the culture duration, as described in section 2.4.4. Prior to media exchange, VCD was measured and exchange volume calculated using **Equation 2.4**, to generate CSPRs between 0.02 – 0.06 nL cell⁻¹ day⁻¹. **Figure 3.12 A and B** show VCD and viability for quasi-perfusion sedimentation and centrifugation cultures, respectively, at constant CSPRs between 0.02-0.06 nL cell⁻¹ day⁻¹, exchanged with media blends containing 15% Feed B. **Figure 3.12 C and D** show corresponding glucose profiles for sedimentation and

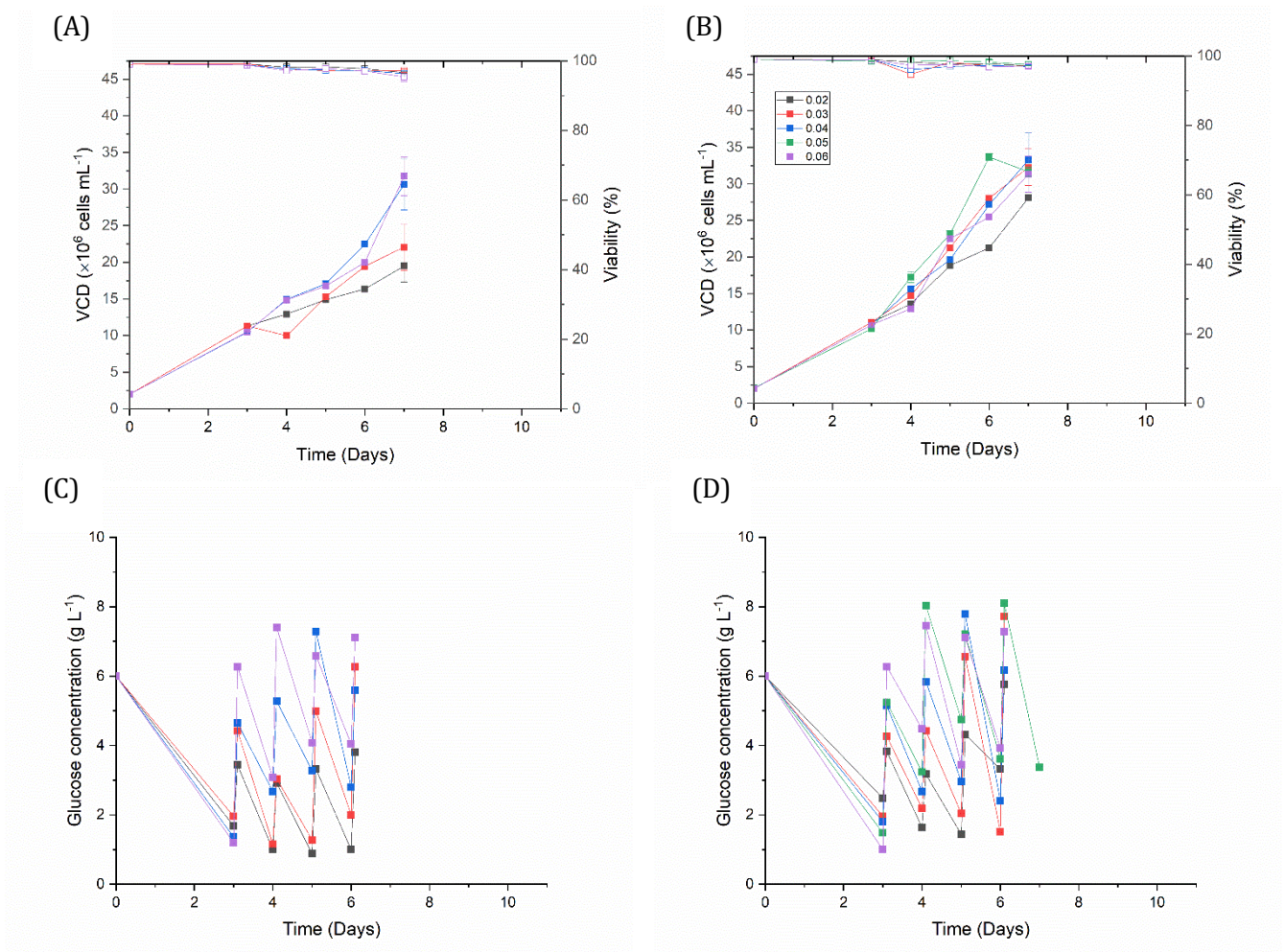
centrifugation cultures respectively. **Figure 3.12 E and F** show corresponding lactate profiles for sedimentation and centrifugation cultures respectively.

While centrifugation cultures show comparable performance for all CSPRs, sedimentation cultures show deviations between low CSPRs, 0.02 and 0.03 nL cell⁻¹ day⁻¹ and high CSPRs, 0.04 and 0.06 nL cell⁻¹ day⁻¹. Maximum VCD for sedimentation cultures exchanged at 0.02 and 0.03 nL cell⁻¹ day⁻¹ are 19.5 and 22.1 × 10⁶ cells mL⁻¹ respectively, with viability maintained above 95% throughout the duration. Comparatively, cultures exchanged at 0.04 and 0.06 nL cell⁻¹ day⁻¹ reach maximum VCDs of 30.6 and 31.8 × 10⁶ cells mL⁻¹ respectively. Centrifugation cultures exchanged at CSPRs between 0.03 – 0.06 nL cell⁻¹ day⁻¹ achieve maximum VCDs between 31.7 – 33.2 × 10⁶ cells mL⁻¹, with the lowest exchange rate of 0.02 nL cell⁻¹ day⁻¹ generating a maximum VCD of 28.1 × 10⁶ cells mL⁻¹. All conditions maintain a high viability of >95% for the culture duration. Glucose concentration fluctuates throughout the culture duration during media exchanges, with higher exchange rates experiencing greater glucose concentrations. Glucose is maintained above 1 g L⁻¹ for the duration of the culture for all conditions across sedimentation and centrifugation modes, and therefore is not considered to be a limiting factor. Similarly, lactate is controlled below 2 g L⁻¹ across all conditions, meaning the buffer capacity of the media should provide adequate control of pH, avoiding shifts to below 6.5 (Hsu et al., 2012).

Figure 3.12 G and H shows the volume exchanged with time of quasi-perfusion cultures maintained at constant CSPR between 0.02-0.06 nL cell⁻¹ day⁻¹ for sedimentation and centrifugation cultures, respectively. For cultures exchanges at CSPRs at or above 0.03 nL cell⁻¹ day⁻¹. exchange volume increases exponentially as VCD increases. On day 7, sedimentation cultures exchanged at 0.06 nL cell⁻¹ day⁻¹ and centrifugation cultures exchanged at 0.05 and 0.06 nL cell⁻¹ day⁻¹ reach the maximum exchange volume achievable with 2 daily exchanges, of 1.6 and 2.1 mL day⁻¹ respectively. Maintenance of

these CSPRs beyond day 7 would require additional daily exchanges. The higher VCDs achieved in centrifugation cultures under otherwise identical conditions mean that exchange volume is consistently greater under otherwise identical conditions.

Figure 3.12 I and J shows separation efficiencies with time of quasi-perfusion cultures maintained at constant CSPR between 0.02-0.06 nL cell⁻¹ day⁻¹ for sedimentation and centrifugation cultures, respectively. Sedimentation cultures show less consistent separation efficiencies across all CSPRs, with cultures exchanged at 0.06 nL cell⁻¹ day⁻¹, with the greatest volume taken per exchange, show the greatest variation. Separation efficiencies below 75% on day 4 will provide unwelcome cell bleeding. Centrifugation cultures are more consistent across all CSPRs, with efficiencies maintained above 95% for all conditions except for the final exchange of 0.06 nL cell⁻¹ day⁻¹, in which separation efficiencies fall below 85%.



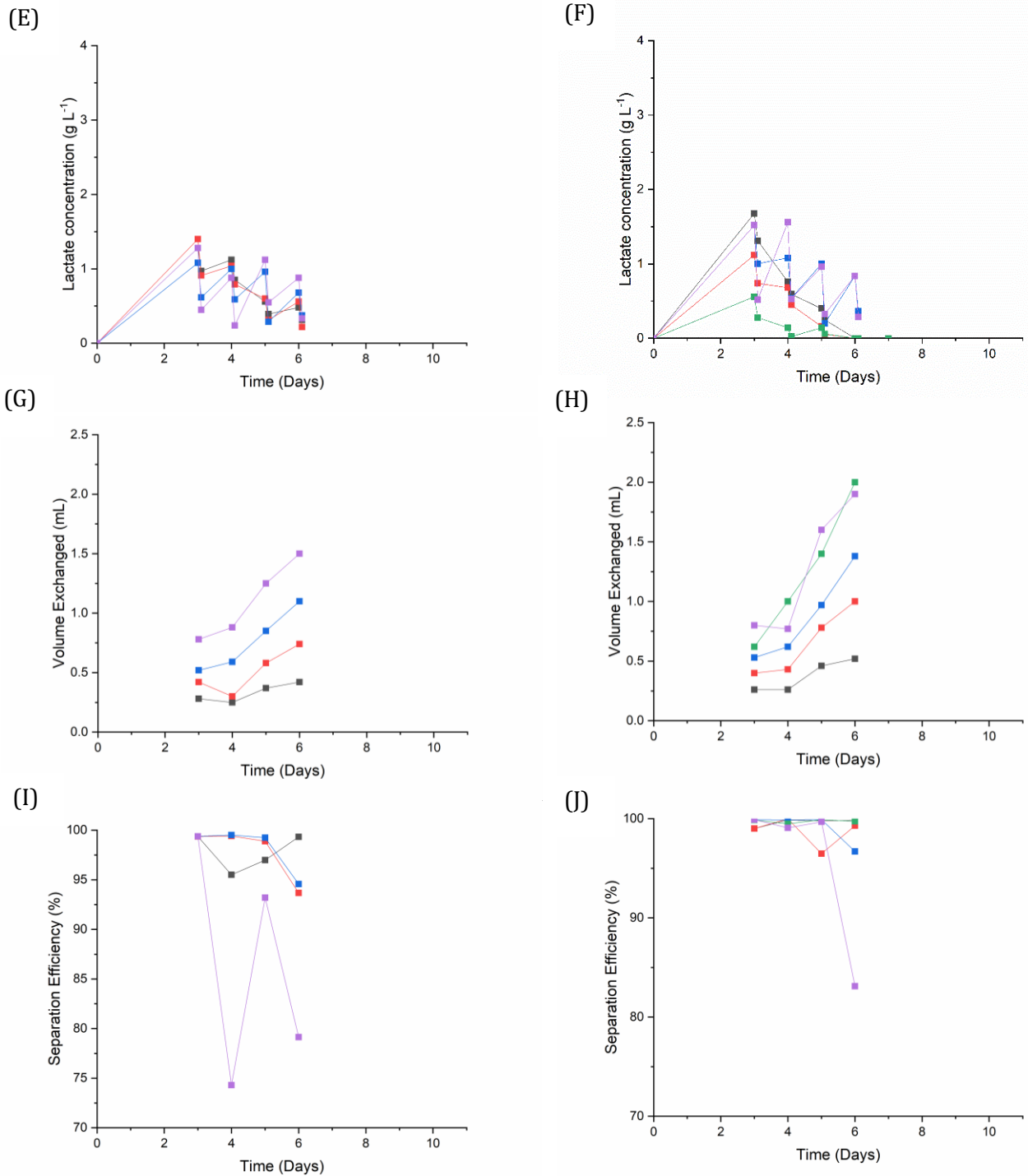


Figure 3.12 - Sedimentation quasi-perfusion and centrifugation quasi-perfusion cultures exchanged at constant CSPRs. Cultures were seeded at 2×10^6 cells mL⁻¹ incubated at 37°C, N= 220 RPM and covered with Duetz sandwich lids. Quasi-perfusion cultures were exchanged from day 3 with CD-CHO media blended with 15% Efficient Feed B at rates calculated to maintain CSPR between 0.02 – 0.06 nL cell⁻¹ day⁻¹. (A) VCD (filled symbols) and viability (empty symbols) for sedimentation quasi-perfusion cultures (B) VCD (filled symbols) and viability (empty symbols) for centrifugation quasi-perfusion cultures (C) Glucose concentration for sedimentation quasi-perfusion cultures (D) Glucose concentration for centrifugation quasi-perfusion cultures (E) Lactate concentration for sedimentation quasi-perfusion cultures (F) Lactate concentration for centrifugation quasi-perfusion cultures (G) Volume exchanged for sedimentation quasi-perfusion cultures (H) Volume exchanged for centrifugation quasi-perfusion cultures (I) Separation efficiency for sedimentation quasi-perfusion cultures (J) Separation efficiency for centrifugation quasi-perfusion cultures. Data represents 2 cultures per condition \pm s.d., with one well sampled per day per condition for each replicate utilising a sacrificial well sampling approach.

Figure 3.13 shows the volumetric productivity and maximum titre of quasi-perfusion cultures exchanged at a constant CSPR between 0.02-0.06 nL cell⁻¹ day⁻¹ in sedimentation and centrifugation modes. Lower CSPRs generate high maximum titres of 0.7 g L⁻¹ in both sedimentation and centrifugation cultures, which then decline as CSPR increases. CSPR rates of 0.02 nL cell⁻¹ day⁻¹ in sedimentation and centrifugation cultures have volumetric productivities comparable to those achieved in fed-batch of approximately 0.1 g L⁻¹ day⁻¹. Volumetric productivity increases as CSPR increases in both sedimentation and centrifugation cultures reaching the peak when exchanging at 0.06 nL cell⁻¹ day⁻¹ at a volumetric productivity 0.2 and 0.28 g L⁻¹ day⁻¹ respectively.

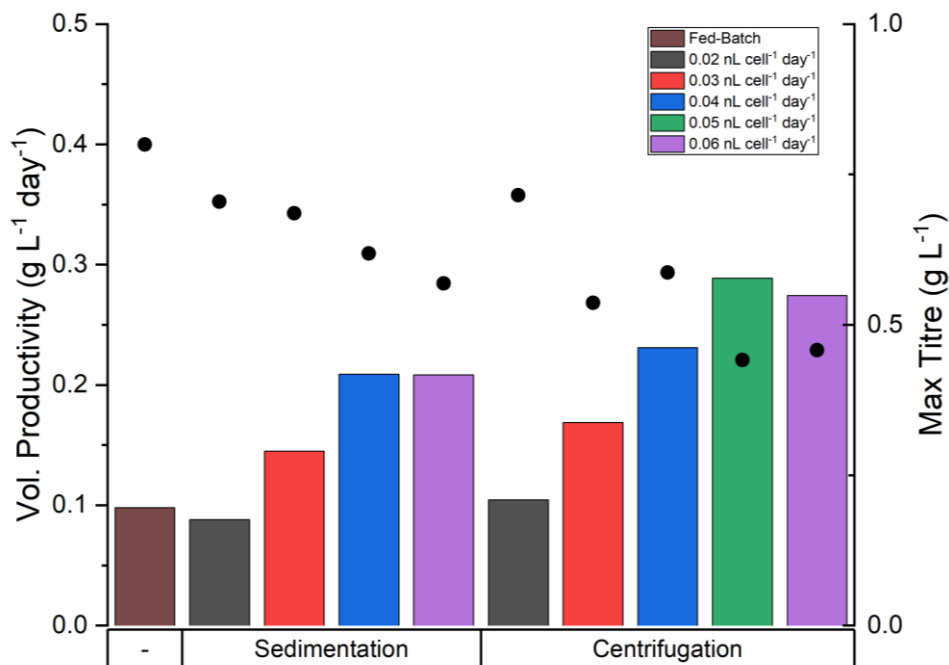


Figure 3.13 - Volumetric productivity (bars) and maximum titre (scatter) for fed-batch, sedimentation quasi-perfusion and centrifugation quasi-perfusion cultures exchanged at CSPRs between 0.02 and 0.06 nL cell⁻¹ day⁻¹. Volumetric productivity was calculated following Equation 2.11. Fed-batch data represents triplicate cultures. All other data represents 2 cultures per condition, with cumulative mAb calculated from each well sampled per day per condition utilising a sacrificial well sampling approach.

Table 3.4 shows specific glucose consumption and lactate and antibody production for sedimentation and centrifugation quasi-perfusion cultures exchanged at a constant CSPR. Specific glucose consumption and lactate production increases with increased

availability of glucose, at higher CSPRS, comparable to trends observed in fixed VVD cultures. Despite following comparable trends, constant CSPR cultures see q_{Lac} of up to 100 times lower than constant VVD cultures. Specific antibody production is comparable across all sedimentation cultures at constant CSPR, but centrifugation cultures generally see an increase in q_{Ab} as CSPR increases. Growth kinetics are comparable across centrifugation cultures at varying CSPRs, meaning that elevated volumetric productivities are caused by the increase in volume exchanged and from an increased q_{Ab} and exchange volume.

Table 3.4 - Specific glucose consumption (q_{Gluc}), and lactate (q_{Lac}) and antibody (q_{Ab}) production rates for sedimentation quasi-perfusion and centrifugation quasi-perfusion cultures exchanged at constant CSPR, between 0.02 and 0.06 nL cell⁻¹ day⁻¹.

CSPR	Sedimentation			Centrifugation		
	q_{Gluc} (pg cell ⁻¹ day ⁻¹)	q_{Lac} (pg cell ⁻¹ day ⁻¹)	q_{Ab} (pg cell ⁻¹ day ⁻¹)	q_{Gluc} (pg cell ⁻¹ day ⁻¹)	q_{Lac} (pg cell ⁻¹ day ⁻¹)	q_{Ab} (pg cell ⁻¹ day ⁻¹)
0.02	600	0.60	25.9	523	-36.8	21.3
0.03	841	13.4	27.5	770	-4.80	19.9
0.04	964	64.0	25.8	982	65.9	22.7
0.05	-	-	-	1160	8.30	31.9
0.06	1380	109	24.4	1290	133	25.5

Figure 3.14 shows the VCD achieved on day 7 of culture for quasi-perfusion cultures maintained at constant CSPRs between 0.02-0.06 nL cell⁻¹ day⁻¹ and for quasi-perfusion cultures at constant exchange rates between 0.5–1.8 VVD, exchanged with 15% blend media. Centrifugation cultures consistently achieve greater VCDs than sedimentation cultures in otherwise identical conditions. Each culture maintained at a constant CSPR attains a greater VCD on day 7 than cultures exchanged at a fixed perfusion rate. CSPRs of 0.04 nL cell⁻¹ day⁻¹ and above see the greatest improvement in VCD, with an improvement of up to 40% compared fixed VVD cultures. While CSPRs of 0.03 nL cell⁻¹ day⁻¹ and below attain lower VCDs on day 7 compared to high CSPRs, improvements of up to 15% are achieved compared to high VVD cultures, despite exchange volume being up to 4 times greater in high VVD cultures compared to low CSPR cultures.

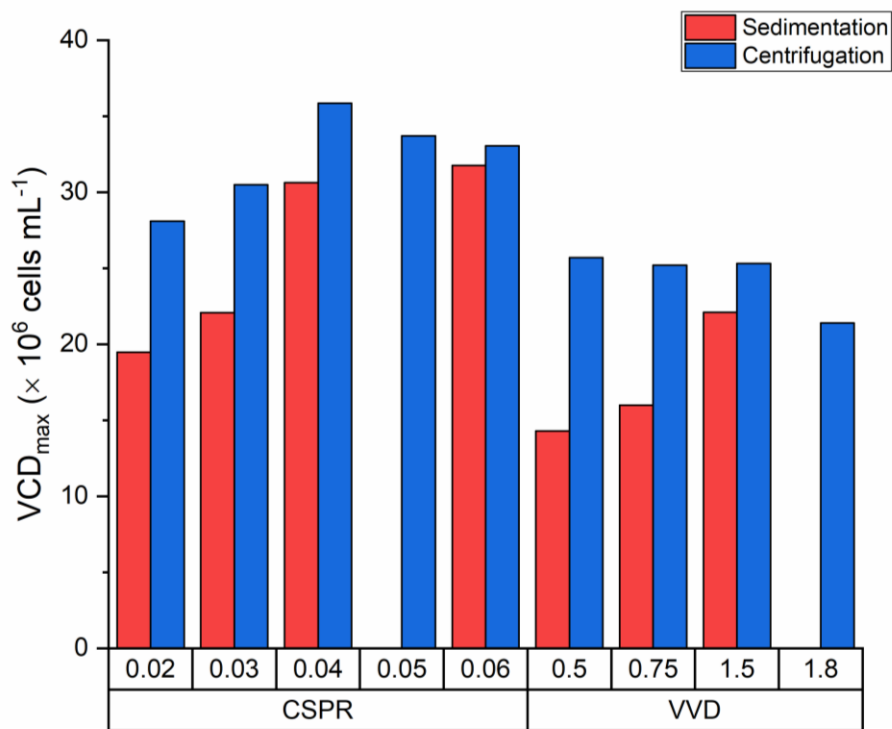


Figure 3.14 - Maximum VCD achieved on day 7 for sedimentation quasi-perfusion and centrifugation quasi-perfusion cultures exchanged with CD-CHO with 15% Efficient Feed B at constant CSPR between 0.02-0.06 nL cell⁻¹ day⁻¹ or a constant exchange rate between 0.5-1.8 VVD. Data represents 2 cultures per condition, with one well sampled per day per condition utilising a sacrificial well sampling approach for each replicate.

The maintenance of constant CSPR has been successfully implemented into the developed quasi-perfusion techniques in both sedimentation and centrifugation modes. This is believed to be the first such instance of incorporating a constant CSPR, commonly implemented in production bioreactors, into a mL-scale quasi-perfusion scale-down system. Utilising fixed CSPRs is the only technique where deviation is seen in performance between sedimentation and centrifugation cultures. While sedimentation cultures at fixed VVD generate lower VCDs and volumetric productivities compared to centrifugation cultures, the performance ranking of conditions has been consistent across modes. In constant CSPR mode, sedimentation cultures see a clear deviation in performance between lower CSPRs ≤ 0.03 nL cell⁻¹ day⁻¹ and higher CSPRs ≥ 0.04 nL cell⁻¹ day⁻¹ whereas comparable performance is observed in centrifugation cultures across all CSPRs. This suggests that CSPR_{min} is higher in sedimentation cultures, at 0.04 nL cell⁻¹

$^1 \text{ day}^{-1}$, agreeing with Wolf et al. (2019) who suggest a CSPR_{min} of $0.04 \text{ nL cell}^{-1} \text{ day}^{-1}$ for CHO cell perfusion cultures. By comparison, centrifugation cultures which continue to perform favourably at CSPRs as low as $0.02 \text{ nL cell}^{-1} \text{ day}^{-1}$.

CSPR cultures were executed for a maximum of 7 days, compared to a target of 9 days in fixed VVD cultures. Further increases in VCD expected on days 8 and 9 of culture mean that in order to maintain target CSPRs, particularly those at or above $0.04 \text{ nL cell}^{-1} \text{ day}^{-1}$, the number of daily exchanges would have to increase above 2 times daily. Increasing the number of daily exchanges is feasible, however its implementation will reduce the feasible number of plates handled per technician. Additionally, increased manipulations have the potential to disrupt cell growth kinetics, particularly in sedimentation cultures, where each manipulation lasts for 30 minutes. This effect is already observed when comparing sedimentation with centrifugation cultures, with the shorter manipulation time centrifugation cultures consistently outperforming equivalent sedimentation cultures. While this impact is small for cultures exchanged 1-2 times daily, it is expected that further increases to exchange number will increase deviations in growth kinetics.

Comparing maximum VCDs and volumetric productivities between cultures operated at fixed CSPR and cultures operated at constant VVD shows vastly improved performance in fixed CSPR cultures. VCD on day 7 in CSPR cultures are between 10-40% greater than constant VVD cultures, even when comparing the lowest CSPR to greatest VVD cultures. Volumetric productivities are comparable between CSPR cultures to VVD cultures that exchange an approximately equivalent volume on day 7. Centrifugation cultures that exchange 2 mL on day 7, at rates of $0.06 \text{ nL cell}^{-1} \text{ day}^{-1}$ or 1.8 VVD have average volumetric productivities of 0.27 and $0.28 \text{ g L}^{-1} \text{ day}^{-1}$ respectively. Performance improvements when implementing CSPR are achieved by providing a steady state environment for cells, compared to constant VVD cultures which experience up to 10 fold declines in CSPR from day 3 until day 9 of culture. The steady state environment

reduces the extremity of glucose fluctuations during media exchanges, and in turn reduces q_{Lac} . Lactate is in turn controlled below 2 g L^{-1} in both sedimentation and centrifugation cultures which reduce pH fluctuations and allow the media to provide some control through buffering capacity (Hsu et al., 2012). The cell culture environment is therefore better controlled and more favourable throughout the culture, improving the cell culture performance compared to constant VVD cultures.

3.3. Summary

A quasi-perfusion methodology was developed in MWP by incorporating cell retention techniques and periodic media exchanges to existing batch protocols. Quasi-perfusion methodologies consistently produce VCDs 3.3-4.2 fold greater and volumetric productivities up to 1.9 fold greater compared to optimised fed-batch protocols. Quasi-perfusion methodologies were shown to be sensitive to changes in media composition, with media development undertaken to identify optimal nutrient composition to ensure high productivity and generate elevated VCD. In this study, CD-CHO blended with 15% Feed B was identified as the best performing of the tested media across a range of perfusion rates in both sedimentation and centrifugation modes. Two modes of cell retention, commonly implemented in alternative quasi-perfusion methodologies (Bielser et al., 2019, Gagliardi et al., 2019, Kreye and Zoro, 2016, Kreye et al., 2019, Villiger-Oberbek et al., 2015, Wolf et al., 2018) but rarely directly compared, were implemented. The two methodologies, sedimentation and centrifugation, were shown in screening studies generate comparable performance results under otherwise identical conditions, while ensuring the same number of daily exchanges. Minor deviations in VCD and productivity between modes can be attributed to elongated manipulation time and lower packed cell density in sedimentation cultures, which achieve lower peak VCDs and volumetric productivity despite achieving comparable q_{Ab} .

Quasi-perfusion cultivations at constant VVD until day 9 demonstrate sedimentation and centrifugation techniques can produce comparable VCDs compared to previously published alternatives. The maximum VCD of 42.2×10^6 cells mL⁻¹ described in this chapter in centrifugation cultures at 1.8 VVD is similar to performance reported by Villiger-Oberbek et al. (2015), who reported a maximum VCD of 50×10^6 cells mL⁻¹ in spin tubes, and Bielser et al. (2019), who reported a maximum VCD of 35×10^6 cells mL⁻¹ in 96 DSW plates. Culture performance in MWP is comparable to those previously described in spin tubes, despite representing an 8 fold decrease in volume, and to recently reported MWP alternatives.

Quasi-perfusion in MWPs with cell retention utilising centrifugation techniques present favourable characteristics compared to those utilising sedimentation techniques, both in terms of growth kinetics and in terms of ease of handling. Elevated cell densities and increased productivity are achieved utilising centrifugation techniques over a range of conditions including perfusion rate and nutritional depth of the media. Additionally, centrifugation cultures represent a reduction in manipulation time compared to sedimentation, which allows an increased number of plates to be manipulated per operator, increasing throughput and therefore the power as a screening tool for early-phase development.

The maintenance of constant CSPR is commonly implemented in scale-up, meaning monitoring and, where necessary, maintaining CSPR is important for perfusion scale-down devices. CSPRs reported for perfusion cultures are typically between 0.5-0.04 nL cell⁻¹ day⁻¹ (Croughan et al., 2015), with the lowest CSPRs considered unfeasible for the support of very HCD cultures of $>40 \times 10^6$ cells mL⁻¹ (Clincke et al., 2013). CSPR is simple to calculate within the described quasi-perfusion system, either to study changes in CSPR from maintenance of constant VVD, or to calculate exchange volume to maintain a constant target. Ensuring a constant CSPR generates a consistent environment

throughout the culture duration, including maintaining consistent relative availability of nutrients throughout the culture duration. This has been shown to improve productivity and VCD compared to constant VVD cultures within quasi-perfusion systems across a range of media with varying nutritional depths and exchange rates.

Quasi-perfusion methodologies in microwell plates have been shown to be robust and high throughput and have potential applications as a tool for the early phase development and screening of perfusion cultures. While a range of methodologies were successful in generating the specific characteristics of perfusion culture by implementing cell retention techniques, maintaining a constant CSPR and utilising centrifugation for cell retention is recommended as the optimal culture methodology for small scale quasi-perfusion studies for CHO cell cultures. While it is expected that comparable trends will be observed when implementing these techniques across cell lines with comparable growth characteristics, for example HEK293 or hybridoma cell lines, the actual performance will be dependent on several factors including oxygen consumption rates, shear-sensitivity and specific growth, consumption and production rates of the chosen cell line.

4. CHAPTER 4: DETERMINATION OF ENGINEERING ENVIRONMENT AND HYDRODYNAMIC ANALYSIS IN MWP, 250ML AND 5L BIOREACTORS

4.1. Introduction

Scaling between bioreactors of different sizes and geometries is notoriously a challenging task, especially when very different types of motions are involved at either scales. As discussed in Chapter 1, scaling is historically achieved by keeping constant variables across scales, thus ensuring the same hydrodynamic environment. Many variables have been suggested for the scaling of stirred tank bioreactors including, but not limited to; gassed power input per unit volume (P/V), gas-liquid mass transfer coefficient (k_{La}), mixing time (t_m) and constant tip speed (u_{tip}) (Oosterhuis and Kossen, 1985). The selection of a scaling parameter inherently impacts other parameters, as discussed in Section 1.2.2.1, and therefore successful scale up is dependent on the appropriate selection of such scaling criteria. In this work engineering characterisation was carried out in the novel 250mL BR with the aim to experimentally determine the impeller power number (N_p) and P/V values at different conditions, k_{La} and t_m . The 5L BR and 24 round-well MWPs have been previously characterised (Klößner et al., 2012, Rodriguez et al., 2013) and therefore comparative parameters for both systems were calculated as defined in **Equations 2.19 - 2.21** (Power input), **2.25** and **2.29** (k_{La}) and **2.26** (Reynolds number).

Designing appropriate scaling conditions for perfusion cultures includes the additional consideration of viscosity changes during the culture as cell density increases above traditional levels for fed-batch culture and it is crucial to understand whether the fluid becomes non-Newtonian during the process and at which cell densities, given the impact the viscosity has on the flow characteristics. The engineering characterisation studies

carried out in this work not only enabled the identification of appropriate scaling criteria, but they also allowed a feasible range of operation to be identified. A thorough characterisation can help reduce the timescales associated with optimisation of process conditions, by narrowing the range of parameters to investigate.

4.2. Results

4.2.1. Design Considerations

A novel 250mL BR was designed to enable cost-effective small-scale process development of perfusion cultures. **Figure 4.1** shows a schematic drawing of the 250mL BR utilised for bench-scale cell culture (**A,B**) and the acrylic mimic utilised for hydrodynamic analysis (**C,D**). While it is common for bench top/laboratory scale BRs to be fabricated from glass, limitations in fabrication material meant that stainless steel was selected for our sub-L reactor. Stainless steel is biocompatible with cell culture operation, is sterilisable and allowed for flexibility to fulfil exact design specifications. A working volume of 250mL was selected, comparable to several small-scale fed-batch BRs including the Ambr@250 from Sartorius and the DASBOX from Eppendorf. Reactor dimensions were selected to enable the maintenance of a height to diameter ratio of approximately 1.5:1 (Doran, 1995, Ravi, 2017), whilst ensuring a liquid height of approximately $\frac{3}{4}$ of the BR height (Doran, 1995, Ravi, 2017), allowing headspace for foaming whilst maximising the utilisation of the vessel. To improve mass transfer, increase $k_L a$ and reduce mixing time (Alok, 2014) to optimise reactor performance for HCD perfusion cultures, baffles with a diameter of 0.35 cm were incorporated into the reactor, sized at approximately $0.05 D_T$ (Doran, 1995, Ravi, 2017).

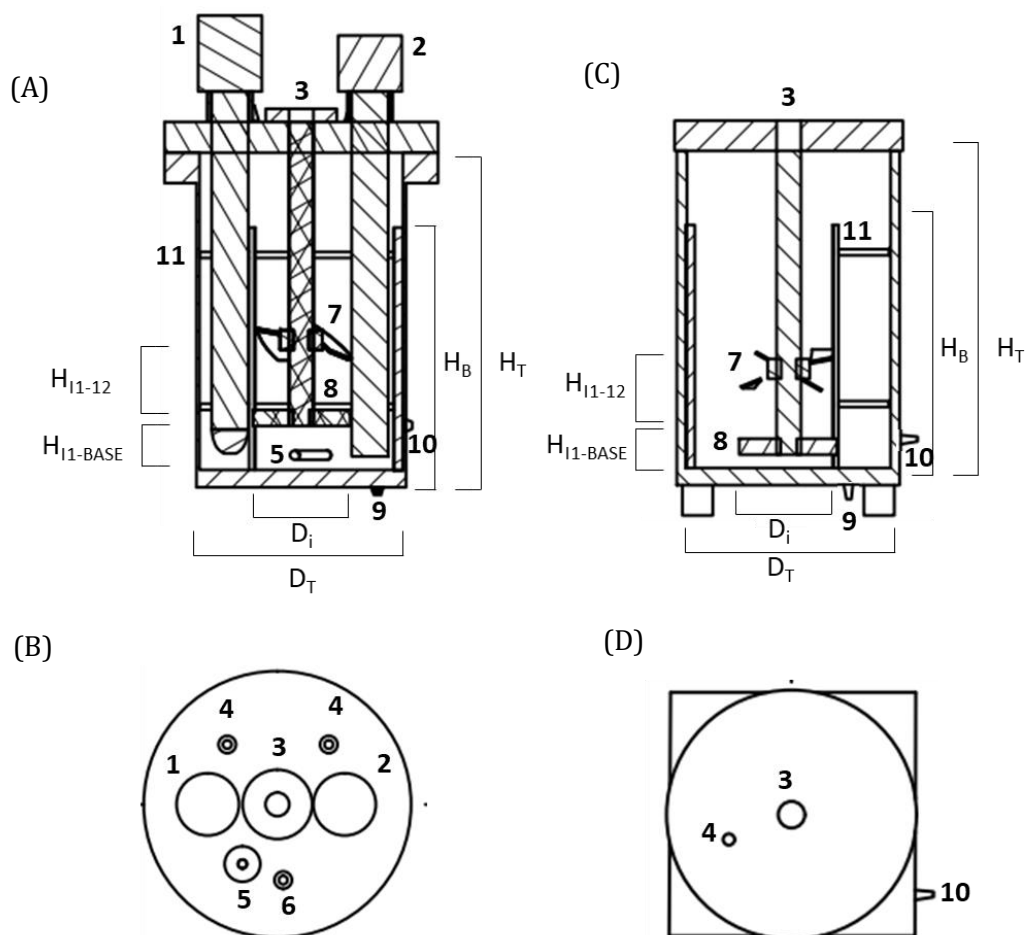


Figure 4.1 – Schematic diagram 250mL novel bioreactor (A) 2-D cross-section (B) Headplate and Acrylic mimic (A) 2-D cross-section and (B) Headplate. Labelled components as follows: (1) pH probe port (2) DO probe shaft (3) Impeller shaft (4) Liquid addition (5) Sparger (6) Gas outlet (7) Pitch-blade impeller (8) Rushton-style impeller (9) Connection to cell retention device - inlet (10) Connection to cell retention device - outlet (11) Baffles

The 250mL BR was designed to enable the operation of perfusion cultures at sub-litre scale by maximising the efficiency of mixing and optimising hydrodynamics within the tank. One method of scaling is to maintain geometric similarity, including aspect ratio and impeller type, position and geometry. However, since the 250mL was designed to maximise the efficiency of the hydrodynamic environment, some deviations in geometries are observed between scales. **Table 4.1** summarises key BR geometries compared to 24 round well MWP and 5L New Brunswick BRs. Aspect ratio, the ratio of

tank diameter to liquid height, is greater in the 5L BR compared to the 250mL BR at 1.3:1 and 1.1:1, respectively. Larger aspect ratios facilitate longer residence time within the BRs, which maximises potential oxygen transfer, and additionally allow for improved temperature controls due to a greater surface area to volume ratio (Jossen et al., 2017). Typically, cell culture BRs have an aspect ratio between 1-1.5 (Kadic and Heindel, 2010), therefore it is expected that the small deviation between 250mL and 5L BRs will not significantly impact mass transfer and mixing (Nienow, 1997).

Table 4.1- Key geometries of MWP, 250mL BR and 5L BR

	MWP	250mL BR	5L BR
H_T (cm)	1.9	10	34.5
D_T (cm)	1.5	6.7	16
H_L (cm)	0.58	7.4	21.5
V_v (m³)	1.2×10 ⁻³	0.25	2.5
H_T:D_T	0.36:1	1.1:1	1.3:1
V_L:V_v	1:0.36	1:0.75	1:0.36
Impeller Type		Dual Pitched Blade and Rushton-Style	Pitched Blade
D_i (cm)		3	6.2
D_{shaft} (cm)		0.8	0.62
D_i:D_T		0.44:1	0.39:1
H_T:H_i		1:0.25	1:0.29
Sparger Type		L-shape	Horseshoe

Impeller geometry, including blade thickness and impeller diameter to tank diameter ratio additionally influence hydrodynamics within the vessel. Studies of Rushton turbines have found that power number is sensitive to blade thickness but independent of impeller diameter to tank ratio (Bujalski et al., 1987), and for pitched blade impellers the opposite is true, with power numbers sensitive to impeller diameter to tank ratio but independent of blade thickness (Chapple et al., 2002). The impeller diameter to tank

diameter ratio is comparable in the 5L and 250mL BR at 0.44:1 and 0.39:1, suggesting that power number for the pitched blade impellers in each vessel will be comparable. It is worth noting that the ratio of blade thickness to impeller diameter is often greater in small scale BRs compared to benchtop BRs due to limitations of fabrication at small scale (Rutherford et al., 1996). While differences in blade thickness would be expected to cause deviations when comparing vessels with otherwise identical impeller configurations, direct comparisons between 250mL and 5L BRs based on impeller geometry are challenging since the 250mL BR has a multiple impeller design, Rushton-style and pitched blade, while the 5L BR contains a single pitched blade impeller only. A multiple impeller design in the 250mL BR was selected to increase mass transfer, in particular to maximise oxygen mass transfer to support high cell density perfusion cultures. Karimi et al. (2013) suggest optimal gas transfer is achieved in systems with multiple Rushton turbines, however Rushton turbines can induce high shear stress, and taking the shear sensitivity of mammalian cell culture into account led to the selection of dual impeller system comprising of a down-pumping pitched blade above a Rushton-style impeller.

Notable deviations in geometry observed between 250mL BR and 5L BR include the shape of the base, round-bottomed in the 5L and flat in the 250mL. The bottom shape does not significantly impact gas-liquid mass transfer or gas dispersion, however round bottoms are preferred for solid suspensions and mixing (Oldshue, 1983). Additionally, round bottom bases reduce the dead volume when removing water, media or cell culture. A flat base was selected in the 250mL reactor for ease of fabrication, with connectors to a cell retention device placed in the base, facilitating water and media removal and the dual impeller system improves mixing and suspension dynamics. Additionally, sparger type is varied across scales, with a horse shoe sparger in the 5L BR and an L-sparger in the 250mL BR. Spargers of different geometries have varied bubble sizes, and potential $k_L a$ will depend on geometry. In general, a greater number of holes

with a smaller diameter will increase the maximum potential k_La (Sardeing et al., 2004, Karimi et al., 2013). There are several geometric similarities between scales, including aspect ratio and ratio of impeller diameter to tank diameter. However, there are some notable deviations including base geometry and impeller geometries, including blade thickness. Therefore, to ensure successful scaling between vessels, engineering characteristics must be determined and implemented as a scaling tool.

For scaling of vessels, in particular those which are not geometrically similar, engineering characteristics with a significant impact on culture performance, such as power input per unit volume, k_La , and mixing time must be determined and their variation with operational conditions must be understood. In addition, process conditions specific to application must be understood, for example by characterising viscosity and density changes with time, and understanding the limiting factors of specific processes, for example shear sensitivity of cell processes limiting the feasible rotational speed of impellers.

Equations to determine engineering characteristics in a variety of vessels, such as MWPs and BRs of specific geometries, are available in literature. These equations expand beyond engineering rules of thumb to enable the accurate calculation of engineering characteristics in a particular vessel, with a specific geometry and impeller configuration (Diaz and Acevedo, 1999, Nienow et al., 2013, Xu et al., 2017). While these equations can be utilised to gain understanding of environment within a particular vessel, they show that engineering rules of thumb, while providing an estimation, do not necessarily accurately represent conditions in a vessel, and factors such as impeller geometry, size ratios and internal components can influence coefficients. This highlights the importance of conducting thorough engineering characterisation in novel BRs.

4.2.2. Oxygen Mass Transfer Coefficient ($k_{L,a}$)

Oxygen mass transfer coefficient ($k_{L,a}$) in the 250mL BR was experimentally determined using the static gassing out method, as described in Section 2.13.2. **Figures 4.2 A and B** show experimental $k_{L,a}$ in the BR with increasing RPM at RTP and 37°C respectively, at gas flowrates between 25-100 mL min⁻¹. Increasing $k_{L,a}$ is observed with increasing RPM and gas flowrate across each temperature analysed. A $k_{L,a}$ of 6 hrs⁻¹ is achieved at operating conditions of 37°C, N=250 RPM and a gas flowrate of 50 mL min⁻¹. Bareither et al. (2013) report $k_{L,a}$ in the range of 2.5-8.5 hrs⁻¹ for cell culture BRs fitted with a pitched blade impeller at 250mL scale, with $k_{L,a}$ in the 250mL BR within this expected range. From experimental measurements, the $k_{L,a}$ coefficients; K, a constant, a, an exponent relating to power input per unit volume and b, an exponent relating to superficial gas velocity in **Equation 2.29** were determined at RTP and 37°C using regression analysis. Variables that can affect $k_{L,a}$ values include temperature, gas bubble size, determined by sparger diameter, and mixing characteristics, determined by impeller geometry (Middleton, 1997). Impeller geometry is fixed across temperatures studied, with gas bubble size expected to decrease as rotational speed increases. It is therefore expected that $k_{L,a}$ will increase with increasing RPM due to smaller bubble size, by increasing the residency time in the BR and increasing the surface area available for oxygen transfer. Temperature increases inversely affects the oxygen solubility (Middleton, 1997), facilitating rapid stripping during the static gassing-out method implemented in experiments, and thus increasing $k_{L,a}$ with temperature. It is additionally worth noting that experimentally determined $k_{L,a}$, utilising media or water as the model fluid, is not always representative of real conditions during cell culture. This is due to the presence of nutrients, consumption of oxygen for cell growth, metabolite production and surface active agents (Garcia-Ochoa and Gomez, 2005).

Table 4.2 summarises coefficients determined at RTP and 37°C, alongside published coefficients in comparable reactor systems; 2-2600 L aerated STRs fitted with multiple

impeller types (Van't Riet, 1979), Ambr250® fitted with a single pitched blade impeller (Xu et al., 2017), 5L STRs fitted with two flat blade paddle impellers (Vasconcelos et al., 1998) and 5L STRs fitted with dual flat blade and pitched blade impellers (Arjunwadkar et al., 1998). Coefficients obtained at RTP mimic those reported in literature, however coefficients obtained in experiments at 37°C see are much larger than those previously reported. Variations observed could be a function of sparger geometry: L-sparger in 250mL BR vs. open hole in Ambr250®, and impeller geometry: dual pitched-blade and Rushton-type in 250mL BR vs. a single pitched blade impeller in Ambr250®. **Figure 4.2 C and D** compare experimentally determined k_La with calculated k_La for experiments conducted at RTP and 37°C respectively. k_La was calculated as defined in **Equation 2.29**, utilising coefficients previously determined and defined in **Table 4.2**. Utilising defined coefficients in the Van't Riet k_La equation is shown to provide an accurate prediction of experimental results, with the majority of experimentally determined k_La falling within a confidence interval of $\pm 5\%$, for both RTP and 37°C at > 50 RPM and at gas flowrates investigated. Experimentally determined k_La at RTP and 50 RPM fall outside the confidence interval but are within prediction bands.

Table 4.2- Summary of published coefficients correlating experimentally determined k_La to the equation: $k_La = K(P/V)^a Wsg^b$ compared to experimentally determined coefficients in 250mL BR.

	K	a	b
Van't Riet (1979)	0.021	0.40	0.50
Xu et al. (2017)	0.030	0.25	0.61
Vasconcelos et al. (1998)	-	0.62	0.49
Arjunwadkar et al. (1998)	-	0.68	0.4-0.58
250mL BR - RTP	0.037	0.46	0.59
250mL BR - 37°C	3.8	1.07	1.37

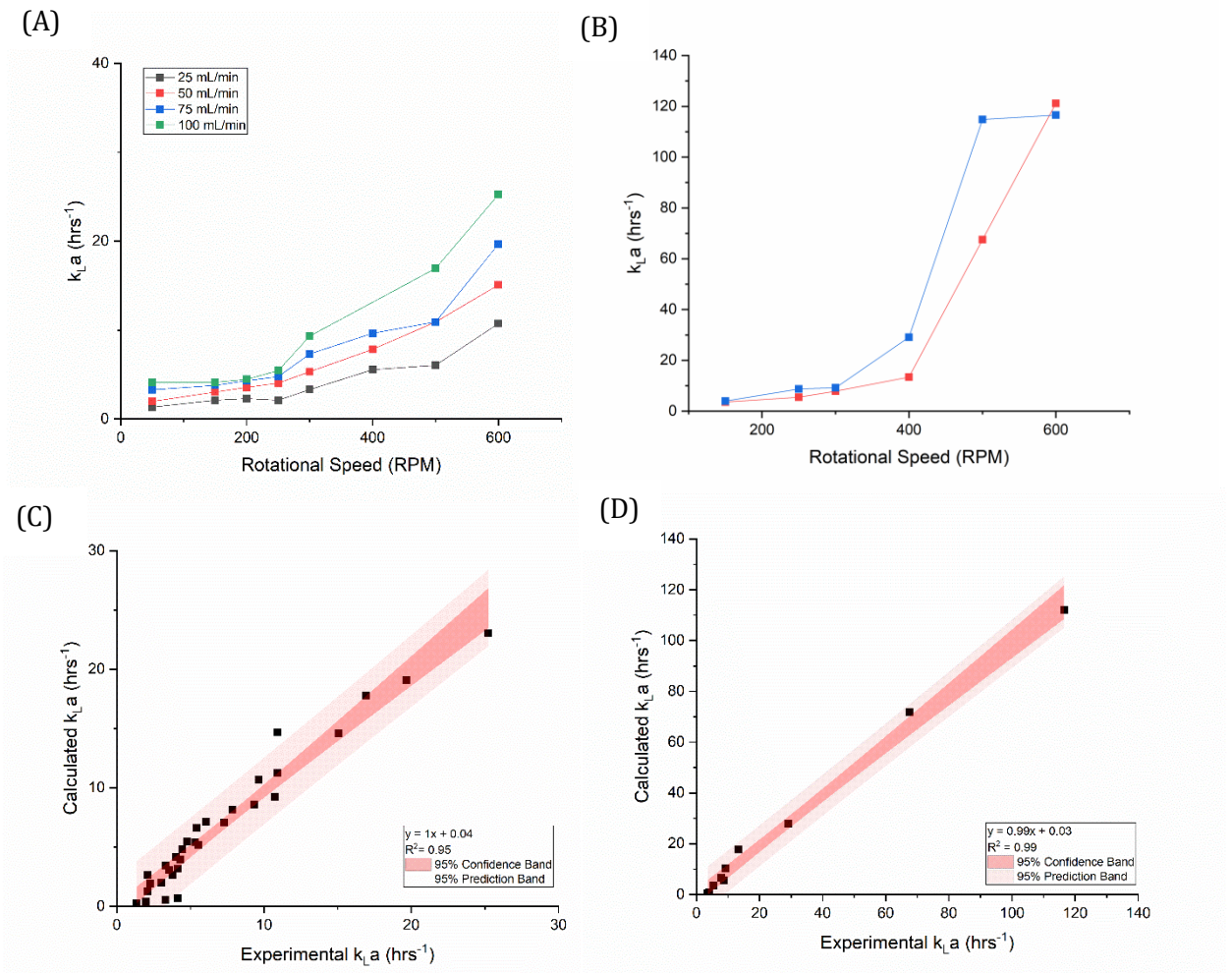


Figure 4.2 - Determination of oxygen mass transfer coefficient ($k_{L,a}$) in novel 250mL BR. $k_{L,a}$ was determined using the static gassing out method, as described in section 2.13, at gas flow rates of 25, 50, 75 and 100 mL min⁻¹, N=100-600 RPM. (A) $k_{L,a}$ at RTP (B) $k_{L,a}$ at 37°C. Comparison of $k_{L,a}$ calculated from exponents obtained to fit Equation 2.29 by regression analysis and experimentally determined $k_{L,a}$ at (C) RTP (D) 37°C. Data represents 2 replicates per condition.

The maintenance of constant $k_{L,a}$ is commonly implemented as a scaling tool for cell culture processes (Diaz and Acevedo, 1999, Razali, 2007, Minow et al., 2014), and as such, experimentally determined $k_{L,a}$ in the 250mL BR system is compared to $k_{L,a}$ in MWP and 5L BR. **Figure 4.3** compares $k_{L,a}$ across scales at increasing rotational speeds. $k_{L,a}$ in the 5L BR was calculated following **Equation 2.29** and utilising the Van't Riet coefficients defined in **Table 4.2**, and in MWP was calculated following Doig et al. (2005), as described in **Equation 2.25**. In order to enable the support of comparable cell densities, $k_{L,a}$ in MWP is required to be 5 times greater than in BRs (Zhu, 2017), since

BRs are capable of sparging pure oxygen at a partial pressure of 1 atm, whereas MWP can only achieve a maximum partial pressure of 0.21 atm, the concentration in air (Wolf et al., 2019). To enable appropriate comparison between scales, calculated $k_{L,a}$ in MWPs were reduced by a factor of 5, such that reported $k_{L,a}$ represents the same capacity for support of cell cultures (Ozturk, 1996). Gas flowrate in the 250mL and 5L BRs were fixed at operational conditions, at 50 and 280 mL min⁻¹ respectively.

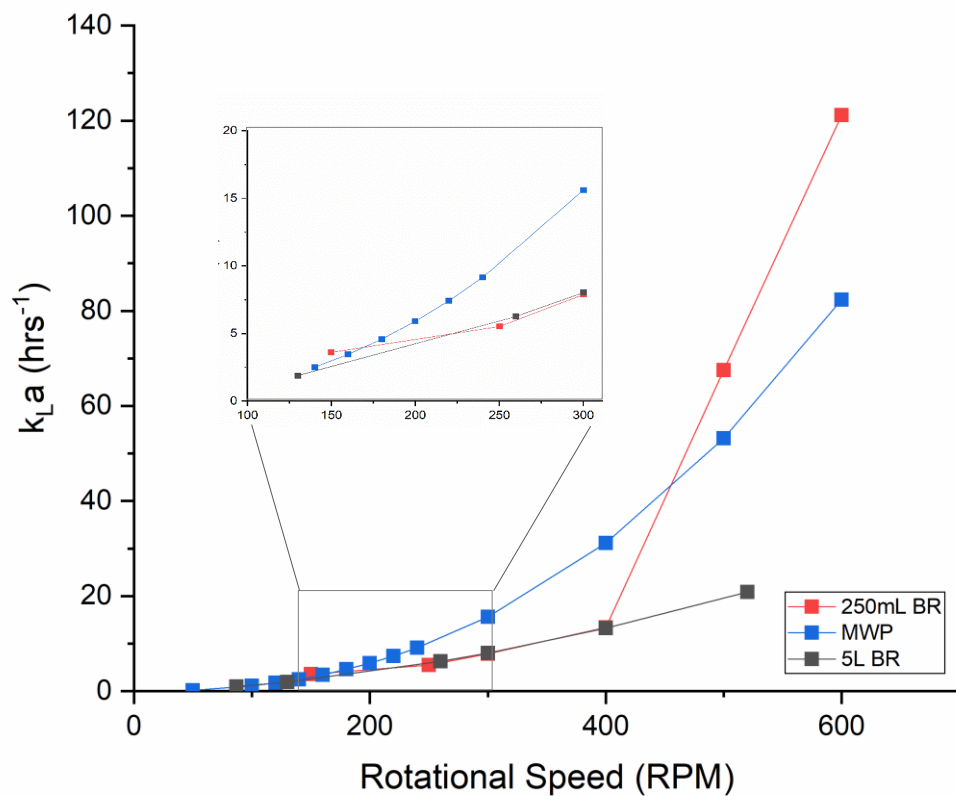


Figure 4.3 - Comparison of $k_{L,a}$ across scales. $k_{L,a}$ in 250mL BR was experimentally determined at $Q = 50 \text{ mL min}^{-1}$, $T = 37^\circ\text{C}$. $k_{L,a}$ in 5L BR was calculated following $k_{L,a} = K(P/V)^a W_{sg}^b$ assuming; $K = 1.64$, $a = 0.55$, $B = 0.81$. $k_{L,a}$ in MWP was calculated following Doig et al. (2006), outlined in Equations 2.25-2.27. Data for 250mL BR represents 2 replicates.

$k_{L,a}$ at each scale is shown to be comparable at the operating conditions; 6, 6.2 and 7.4 hrs⁻¹ in 250mL BR, 5L BR, and MWP respectively. $k_{L,a}$ has been shown to be comparable across scales at operating conditions, with a maximum deviation of 1.4 hrs⁻¹. It is worth noting that calculated $k_{L,a}$ in MWPs are subject to a high degree of error $\pm 30\%$ (Doig et

al., 2005), and therefore while $k_L a$ in MWP can serve as an estimation, it is not considered an accurate prediction.

4.2.3. Power Input

The impeller power number in the 250mL vessel was experimentally determined as described in Section 2.12. Impeller power number is a dimensionless number related to impeller blade thickness, ratio of impeller diameter to tank diameter and type of impeller(s) used. Impeller blade thickness is expected to influence power input particularly in Rushton turbines, and impeller to tank diameter ratio has an impact in pitch blade impeller systems (Chapple et al., 2002). In small scale bioreactors, the ratio of impeller blade thickness to impeller diameter is greater than observed in larger scale bioreactors, due to convenience of fabrication (Rutherford et al., 1996). Reported power numbers for Rushton turbines vary between 4.5-6.5 and for pitched blade impellers are expected to be in the range of 0.25-0.75 (Doran, 1995, Nienow, 2006, Nienow and Miles, 1971), hence for the 250mL BR fitted with dual impellers, it was important to experimentally determine an accurate power number. **Figures 4.4 A and B** shows power input at increasing rotational speeds using water, glycerol and water/glycerol mixes in the 250mL BR when rotating impellers in down-pumping and up-pumping modes respectively. Glycerol and water/glycerol mixtures were utilised in experiments when the RPM was sufficiently low that force could not be accurately measured with water, and fluids with increased viscosity were required. Power input with increasing RPM is comparable across down-pumping and up-pumping methodologies, with each liquid demonstrating increasing power input with increasing RPM. Comparability between up-pumping and down-pumping impellers is expected in dual impeller systems, particularly due to the Rushton-type impeller which have higher power numbers (Nienow and Miles, 1971) and is expected to be the dominating factor influencing power input. Since fluids with varying rheological properties were used, **Figure 4.4 C** shows power input with increasing Reynolds number, calculated following **Equation 2.26**, for the 250mL BR in

down-pumping and up-pumping. Viscosity of glycerol and water-glycerol mixtures was measured at RTP, at 7.9×10^{-4} and $3.6 \times 10^{-5} \text{ m}^2 \text{ s}^{-1}$ for pure glycerol and 75% glycerol, 25% water mixtures respectively. Comparing power input with Reynolds number confirms that up-pumping and down-pumping configurations perform comparably across each RPM investigated. **Figure 4.4 D** shows power number with increasing Reynolds number in the 250mL BR in down-pumping and up-pumping configurations. Power number was calculated following **Equation 2.24**. Power curves follow the expected pattern of decreasing with increasing Reynolds number through the laminar and transitional flow regime, and before reaching a constant in the turbulent flow regime. Overall impeller power number (N_p) for the dual impeller configuration in both up-pumping and down-pumping mode was found to be 4.9 ± 0.2 , which was utilised in all subsequent equations for the 250mL BR. Impeller power number is within the range expected for Rushton turbines, of 4.5-6.5 (Nienow and Miles, 1971), however comparable studies in literature of dual Rushton-type and pitched blade impellers are not available to facilitate direct comparison.

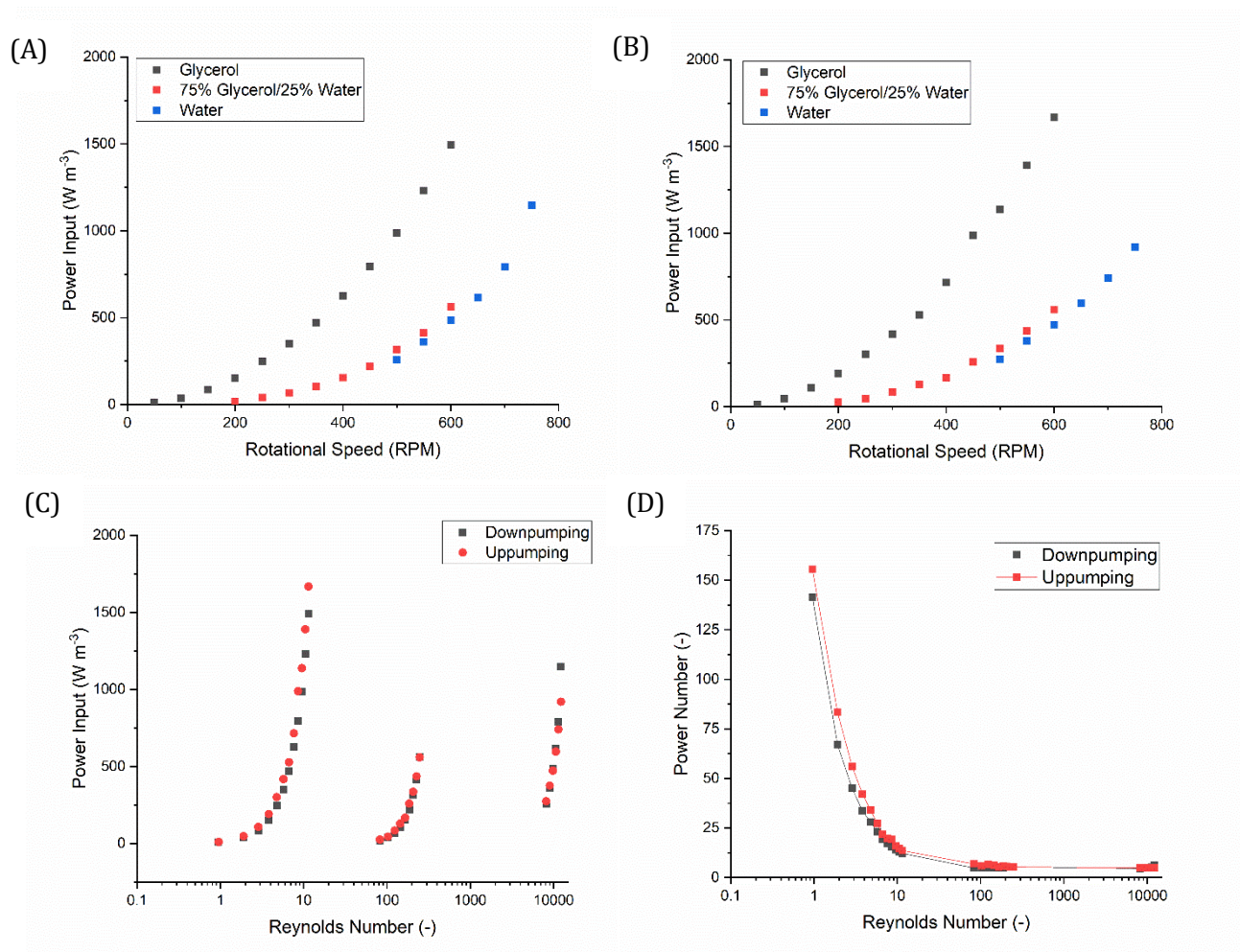


Figure 4.4 - Power input measured in the 250mL BR, determined experimentally by rotating the BR on an air bearing and measuring the force applied at $N = 50-700$ RPM. BR was filled with glycerol, water, and water and glycerol mixtures to enable adequate force applied at low Re with impellers rotated in down-pumping or up-pumping configurations. (A) Power input vs rotational speed, down-pumping (B) Power input vs rotational speed, up-pumping (C) Power input vs Re , down and up-pumping (D) Power number vs Re , down and up-pumping. Data represents 2 replicates.

Figure 4.5 shows the gassed power input per unit volume for 250mL and 5L BRs, and power input per unit volume for MWPs. Gassed power input per unit volume was calculated in BRs following **Equation 2.21** and following **Equation 2.19** for MWPs. Power input is comparable in BRs at operating conditions, at 22.6 and 23.2 hrs⁻¹ for 250mL and 5L BRs respectively. To enable calculation of power input in 5L BR, N_p for the pitched blade impeller was assumed to be 0.75 (Doran, 1995, Nienow, 2006, Nienow and Miles, 1971). Power input in the MWP is within the same order of magnitude and within 42% of BRs, at 14 hrs⁻¹ at a shaking speed of 220 RPM. Increasing the shaking

frequency to 240 RPM increases the power input to 21 hrs⁻¹, more comparable to the BRs for scaling. Early experiments to increase shaking frequency in MWP's showed that $N > 220$ RPM at a fill volume of 1.2mL caused over-spilling and therefore wetting of the sterile membrane causing contaminations. A shaking frequency of 220 RPM was therefore maintained for scale-down cultures, with power input at 220 RPM considered sufficiently similar.

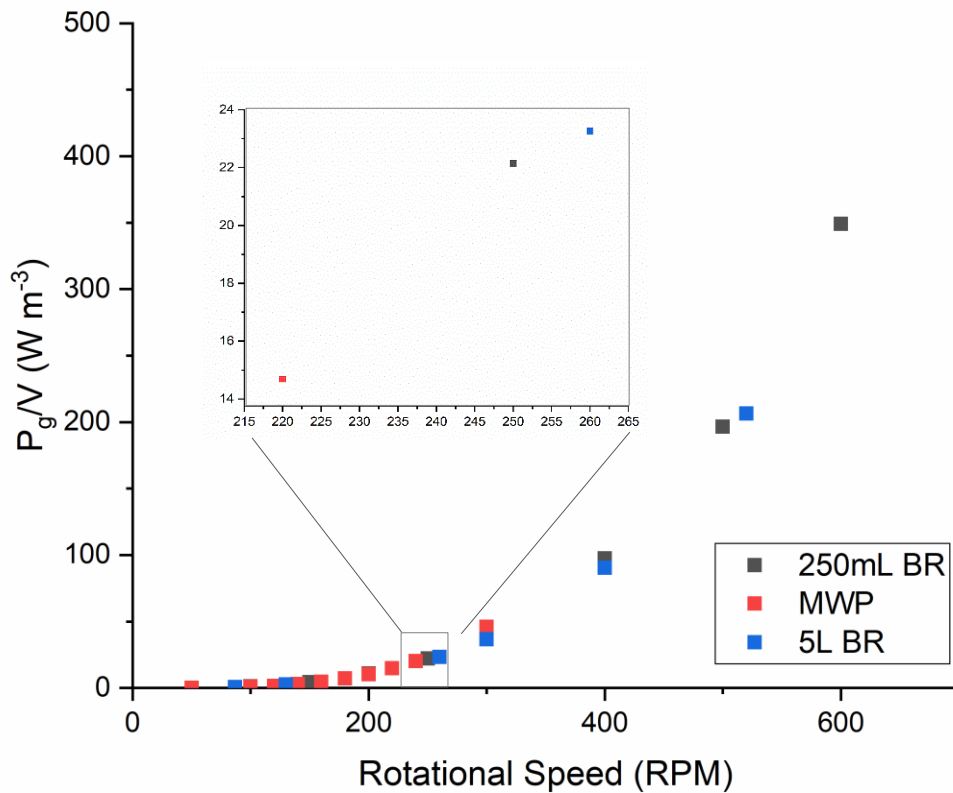


Figure 4.5 - Comparison of gassed power input per unit volume (P_g/V) across scales. P_g/V in 250mL and 5L BRs were calculated following Equations 2.18-2.19; $N_p = 4.9$, 250mL; $N_p = 0.75$, 5L. P/V in MWP was calculated following Equation 2.17.

4.2.4. Evaluation of impact of H_i on mixing time in 250mL BR

Mixing time (t_m) is another constant often determined to better quantify mixing efficiency and support scaling. Factors influencing t_m include the impeller position and geometry, and operational conditions such as rotational speed. t_m was measured in the

250mL BR at varying impeller heights (H_i) to determine the optimal configuration for the BR for processing HCD cell culture. **Figure 4.6 A** shows t_m with 2 impeller configurations vs impeller speed. Flat bottom vessels, such as the 250mL BR, can be prone to the presence of dead-zones when hydrodynamics are not properly considered (Samaras et al., 2020). An impeller off-bottom clearance of 0.25:1 $H_i:H_T$ ($H_i=2.5\text{cm}$) was calculated based on engineering principles, and a clearance of 0.1:1 $H_i:H_T$ ($H_i=1\text{cm}$) were trialled to assess the homogeneity of mixing. t_m is comparable for both impeller heights at $N > 150$ RPM, plateauing at t_m between 3-6 s^{-1} . Some deviation in mixing is observed between impeller heights at low RPM, with faster t_m observed at elevated H_i . This is expected in the dual impeller system, with marine impellers operating in down-pumping mode, mixing is improved with increased liquid heights below the impellers. **Figure 4.6 B** shows $t_m \times N$ vs Reynolds number for mixing experiments at $H_i = 1$ and 2.5cm. $t_m \times N$ is comparable for both H_i investigated, with increasing $t_m \times N$ observed throughout the transitional flow regime in the BR. $t_m \times N$ is more consistent at $H_i = 2.5$ cm, between 14-26, compared to $H_i = 1$ cm, with $t_m \times N$ between 14-34. **Figures 4.6 C and D** show mixing maps at $N=250$ RPM in the 250mL BR with impeller configurations of $H_i= 2.5$ and 1 cm respectively. A region of comparatively slow mixing is observed above the pitched blade impeller, since the impeller is configured to operate in down-pumping mode. A small region is observed at $H_i=2.5\text{cm}$, with t_m between 9-12 s, significantly greater than the vessel t_m of 6 s. This region is greater in BRs with $H_i=1\text{cm}$, with regions near the liquid surface experiencing mixing times of up to 15 s. Increased consistency at $H_i = 2.5$ cm meant that this impeller height was fixed for cell culture experiments with working volumes of 250mL. However, it is feasible to reduce H_i to facilitate smaller working volumes if required. Data obtained determining t_m in the 250mL BR fitted with a single Rushton-style impeller at $H_i=2.5\text{cm}$ shows that when utilising a single impeller system,

t_m is significantly increased. t_m at operational RPM=250 is 10 ± 1 s, a 100% increase compared to 3-5 s obtained in dual impeller systems. Data can be found in Appendix 2.

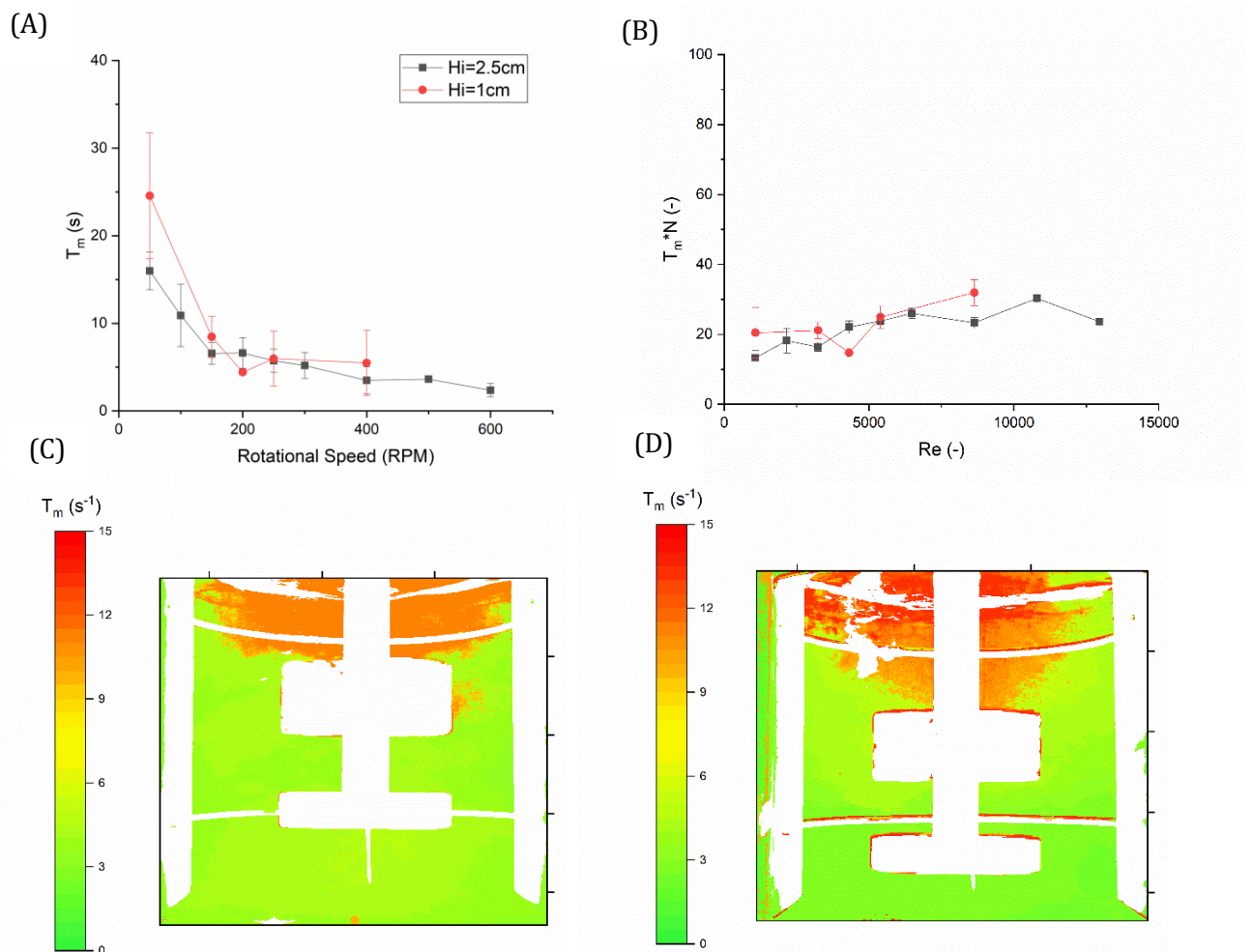


Figure 4.6 - Mixing in 250mL BR fitted with dual pitched-blade and Rushton-type impellers at $H_i = 1$ and 2.5 cm, measured using DISMT method. (A) t_m at $N = 50$ -600 RPM for $H_i = 1$ and 2.5 cm (B) $t_m \cdot N$ vs Re for $H_i = 1$ and 2.5 cm (C) Mixing map generated at $H_i = 2.5$ cm, $N = 250$ RPM (D) Mixing map generated at $H_i = 1$ cm, $N = 250$ RPM. Data <150 RPM represents 8 replicates \pm s.d. Data 150-300 RPM represents 5 replicates \pm s.d. Data >300 RPM represents 3 replicates \pm s.d.

4.2.5. Viscosity in HCD CHO cell cultures

When considering hydrodynamics, it is important to consider the rheological properties of the liquid. While CHO cell suspensions at typical fed-batch VCDs are considered to have comparable rheological properties to water, viscosity of very HCD cultures is expected to vary, however exact rheological properties of CHO suspension at increasing VCDs have not been reported in literature. To ensure an accurate mimic of HCD cultures

during mixing time experiments, the viscosity of a range of HCD CHO cell cultures was measured. **Figure 4.7 A** shows viscosity vs shear rate (γ) for CHO cell cultures at 20-100 $\times 10^6$ cells mL⁻¹, measured at 37°C. High variability is observed between $\gamma = 10$ -40 s⁻¹ across all cell densities measured due to γ lying outside the range of accuracy measured in the rheometer for low viscosity liquids. Cell densities up to 40 $\times 10^6$ cells mL⁻¹ show comparable rheological properties to water, at 0.8 - 1 $\times 10^{-3}$ Pa s for $\gamma = 10$ - 1000 s⁻¹. Elevated VCDs > 40 $\times 10^6$ cells mL⁻¹ exhibit a shear-thinning behaviour, with viscosity decreasing with γ . Viscosities of up to 3 \times greater are observed in HCD cultures compared to lower CD cultures at $\gamma < 40$ s⁻¹. As γ increases, viscosity decreases, to a minimum of 0.98, 1 and 1.3 $\times 10^{-3}$ for 60, 80 and 100 $\times 10^6$ cells mL⁻¹ suspensions respectively. Measured viscosity for cell suspensions at 100 $\times 10^6$ cells mL⁻¹ was utilised for all calculations relating to HCD cultures in BRs. Average shear rate was calculated following Equation 2.15, and was 45.4 s⁻¹ for the 250mL BR at operational conditions, relating to a viscosity of 1.8 $\times 10^{-3}$ Pa s. Viscosity for CHO suspensions was calculated following **Equations 2.17 - 2.18** and correlated to experimentally determined viscosity. **Figure 4.7 B** shows a parity plot comparing experimentally determined and calculated viscosity. Viscosity was calculated assuming viscosity of water at 37°C was 6.9 $\times 10^{-4}$, cell diameter is 16 μ m and cells are spherical. Experimental viscosity was taken as an average between $\gamma = 39.81$ - 1000 s⁻¹, where viscosity is accurately measured in the rheometer. The parity plot shows calculated viscosity is capable of predicting experimentally determined viscosity, within a 95% confidence interval. While calculated viscosity is comparable to average viscosity, it is not possible to predict the maximum viscosity and the rate of shear thinning.

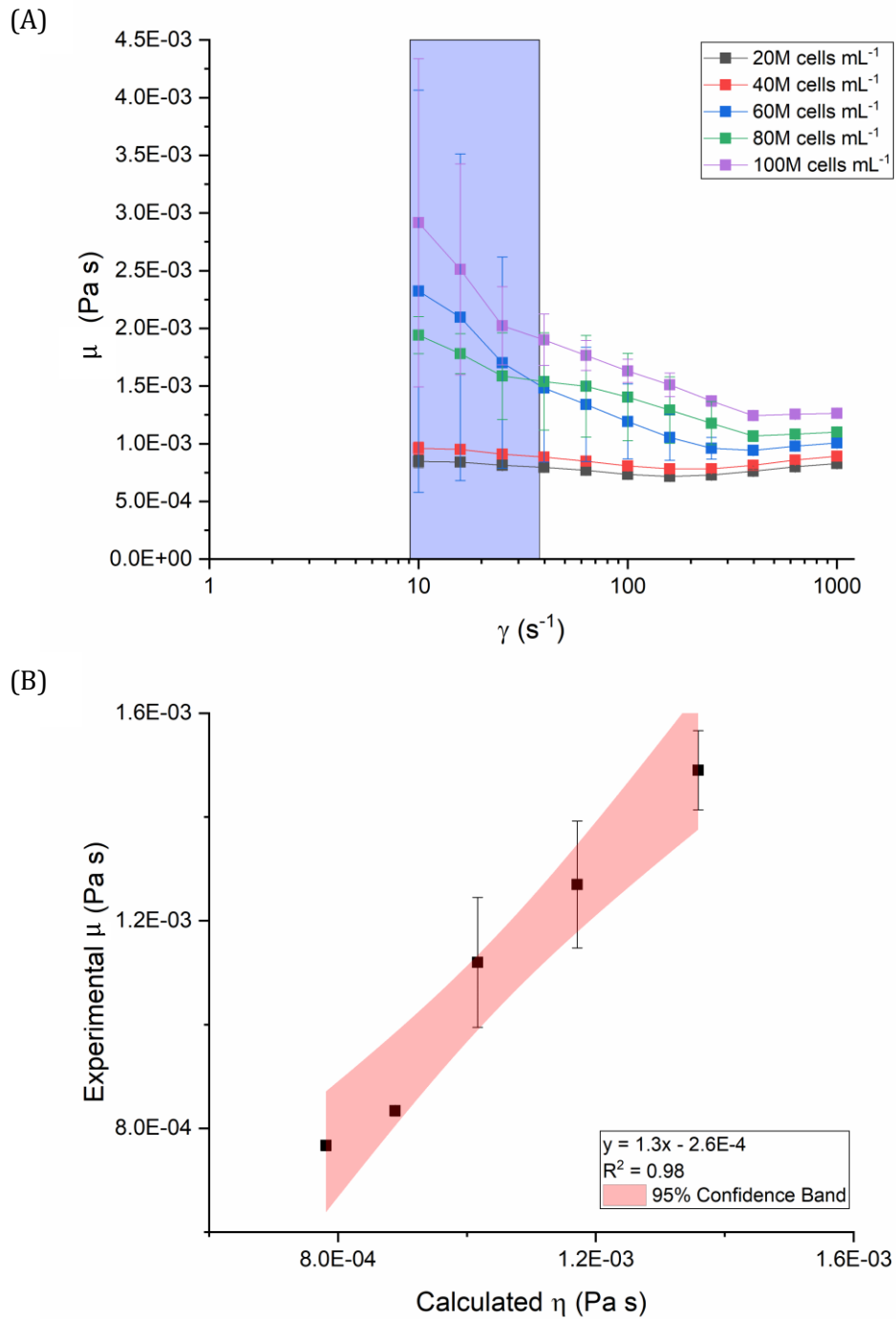
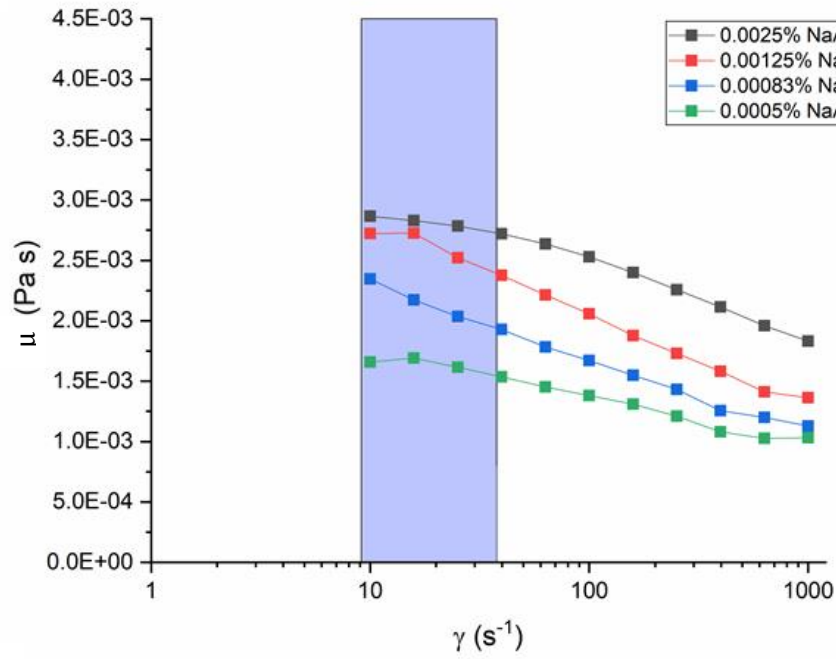


Figure 4.7 - Viscosity of CHO cell suspensions at densities 20-100 $\times 10^6$ cells mL^{-1} . (A) viscosity (μ) vs shear rate (γ), shaded region represents $\gamma < 40 s^{-1}$ where measurements are subject to a high degree of variability. Data points represent 3 measurements \pm s.d. (B) Comparison of experimentally determined μ to μ calculated following Equation 2.17. Data represents 3 replicates \pm s.d.

The viscosity of HCD CHO cell suspensions at operating conditions is approximately twice that of water, meaning that model fluids used in previous mixing time experiments is not hydrodynamically similar to HCD cell culture. Therefore, to ensure an appropriate estimation of mixing dynamics, a model fluid is required that is transparent and has identical rheological properties. Sodium alginate (NaAlg) is a shear thinning solution, and therefore multiple concentrations in solution were analysed for similarity. **Figure 4.8 A** shows viscosity with γ for dilute NaAlg solutions between 5×10^{-4} – 2.5×10^{-3} % V/V. Similarly to CHO suspensions, shear thinning properties are observed with increasing γ . **Figure 4.8 B** compares NaAlg solutions at 8.3×10^{-4} % to CHO cell cultures at 100×10^6 cells mL⁻¹. Close comparability is observed in viscosity at $\gamma > 37$ s⁻¹, with some deviation observed in viscosity at $\gamma < 37$ s⁻¹, however still maintained within the range of error. Solutions of 8.3×10^{-4} % NaAlg were subsequently utilised to enable accurate mimicking of HCD cultures in subsequent mixing time experiments.

(A)



(B)

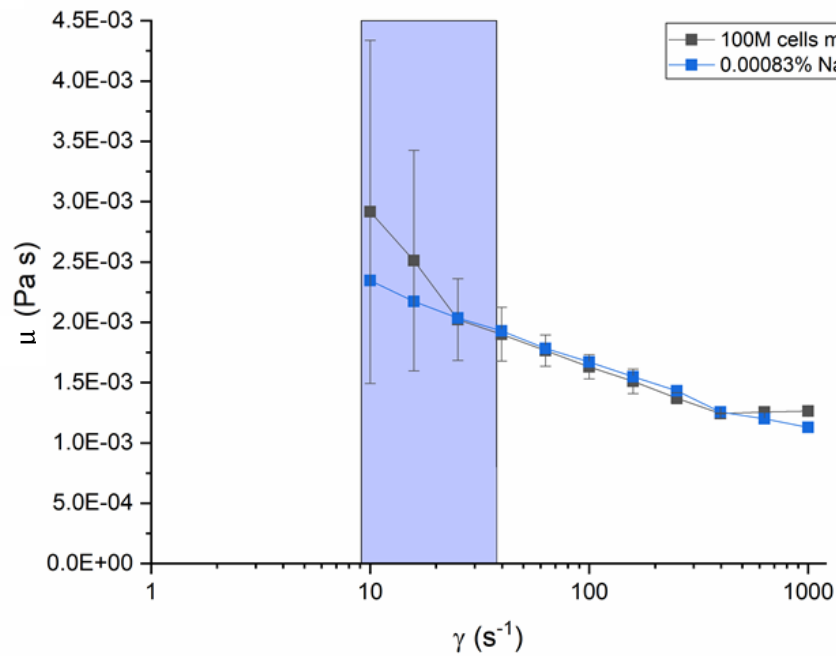


Figure 4.8 - Development of model fluid to mimic CHO cell suspensions at densities of 100×10^6 cells mL^{-1} . (A) μ vs γ NaAlg solutions. Shaded region represents $\gamma < 40 s^{-1}$ where measurements are subject to a high degree of variability. (B) Viscosity comparison of CHO cell suspensions at of 100×10^6 cells mL^{-1} and 0.0083% NaAlg solution. Data represents 3 replicates \pm s.d.

4.2.6. Impact of HCD on mixing dynamics

Sodium alginate solutions at $8.3 \times 10^{-4}\%$ were incorporated into the DISMT system to enable the prediction of mixing hydrodynamics at high cell density. **Figure 4.9 A** shows the viscosity of HCD mimic and water vs rotational speed in the 250mL BR. DISMT solution utilised in mixing time studies as previously discussed, has rheological properties comparable to water, which maintains a viscosity of 8 Pa s throughout increasing γ due to increasing RPM. Very HCD CHO cell cultures, and the resulting HCD mimic, are shear thinning at increasing rotational speeds, from 2.4×10^{-3} Pa s at 50 RPM, to 1.6×10^{-3} Pa s at 600 RPM. **Figure 4.9 B** and **C** show mixing time with increasing rotational speed and Reynolds number respectively for solutions with water-like viscosity and HCD mimic. t_m is comparable with increasing rotational speed across water-like and HCD mimics, for $N > 100$ RPM. At low rotational speeds, the low shear environment and therefore elevated viscosity results in significantly longer t_m in HCD mimics. At the operational $N = 250$ RPM, t_m is 5.7 ± 1.3 s for water-like viscosities and 6.1 ± 1.1 s for HCD mimics. To enable greater O_2 transfer during HCD perfusion culture, N is increased step-wise by 30 RPM to a maximum of 400 RPM. t_m at 400 RPM remains comparable, at 3.5 ± 1.5 and 3.5 ± 0.5 s for water and HCD mimics respectively. It is reassuring that in very HCD perfusion cultures, viscosity increases relating to HCD will not affect the t_m of the system at the operational conditions, meaning mass transfer should remain consistent as cell density increases. Comparing t_m against Reynolds number for water-like and HCD viscosity liquids in **Figure 4.9 C** shows that while t_m is consistent at identical rotational speeds, increases in viscosity for HCD mimics significantly impacts Reynolds number, with Reynolds at the maximal operating N of 400 RPM is 5400 and 3500 for water and HCD mimics respectively. **Figure 4.9 D** compares $t_m \times N$ with Reynolds number, for water and HCD mimics. $t_m \times N$ is consistent with Reynolds number across water and HCD mimics. $t_m \times N$ for $Re < 5600$ is in the range of 13-24 and 18-29 for water and HCD mimics repetitively. **Figures 4.9 E** and **F** show

mixing maps at $N=250$ RPM in the 250mL BR for DISMT solutions with a water-like and HCD-like viscosities respectively.

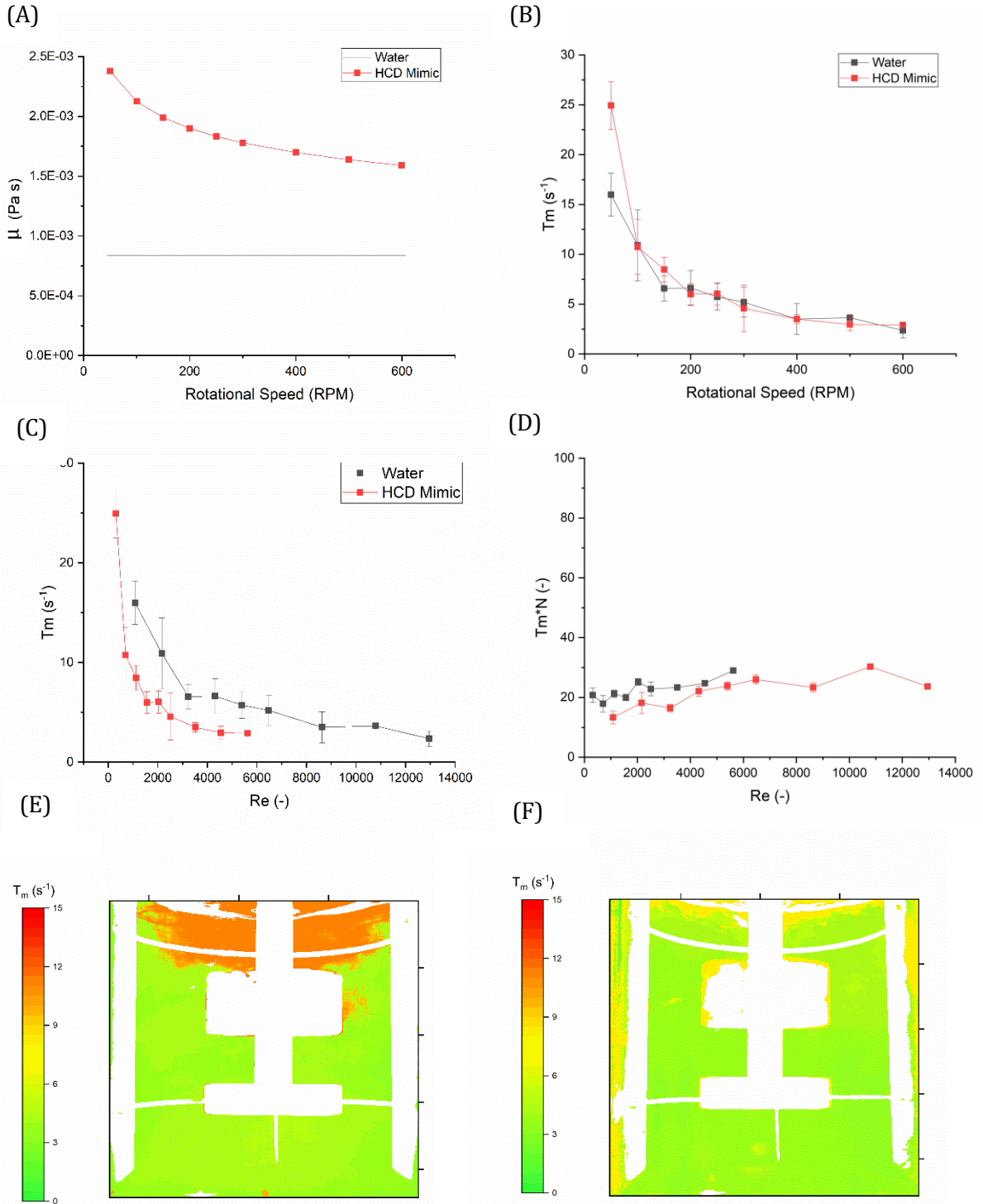


Figure 4.9 - Influence of elevated viscosity HCD on mixing dynamics. $H_i = 2\text{ cm}$ (A) μ of water-like and of HCD mimic, 0.0083% NaAlg, DISMT solutions at $N = 50\text{-}600$ RPM. (B) t_m vs N for water and HCD mimic solutions. (C) t_m vs Re for water and HCD mimic solutions. (D) $t_m \cdot N$ vs Re for water and HCD mimic solutions (E) Mixing map for DISMT solution, $N = 250$ RPM (F) Mixing map for HCD mimic DISMT solution, $N = 250$ RPM. Data <150 RPM represents 8 replicates \pm s.d. Data 150-300 RPM represents 5 replicates \pm s.d. Data >300 RPM represents 3 replicates \pm s.d.

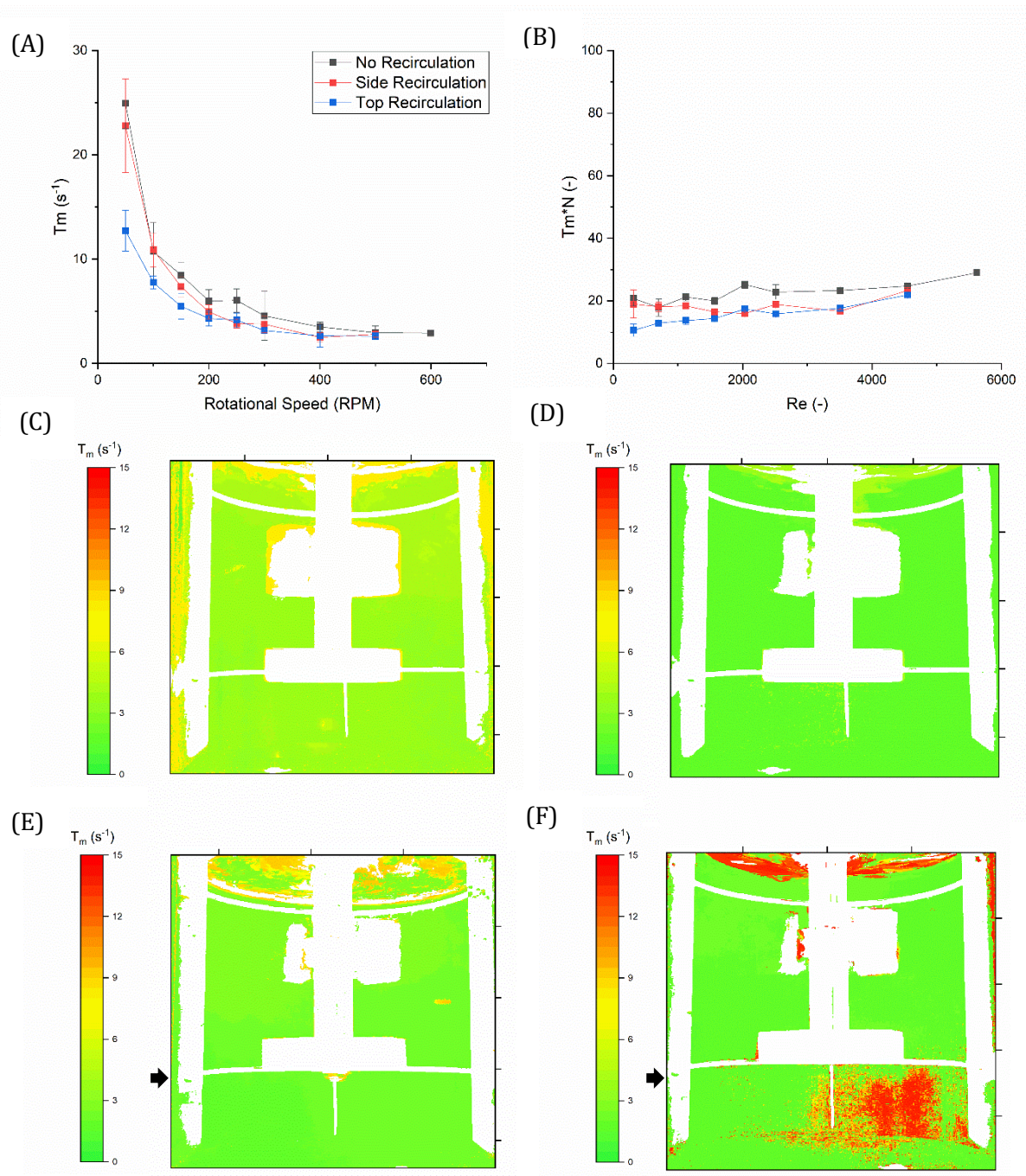
t_m for the bulk liquid for HCD mimics is slightly elevated compared to water-like viscosity liquid, however mixing maps show more homogenous mixing is achieved, with peak t_m of 8 s observed in slow mixing zones. Interestingly, while slow mixing regions in water like BRs are observed above the pitched-blade impeller, slowest mixing in HCD-mimics are observed close to the vessel walls. Slowest mixing near the vessel walls is expected, since the HCD-mimic is shear thinning and lowest shear, and therefore highest viscosities, will be experienced near the vessel walls. Overall, viscosity increases in HCD cultures have been shown to have a negligible impact on mixing time in the 250mL BR. This instils confidence that mixing is homogenous throughout the duration of the culture. However, Reynolds number is much lower when considering viscosity changes in HCD cultures, important when considering mass transfer characteristics between fed-batch like cell density and very HCD in perfusion cultures.

4.2.7. Impact of perfusion recirculation loop on mixing time

Unlike fed-batch cultures, perfusion cultures have the addition of a cell retention loop, constant circulation of cell broth into a cell retention device, where supernatant is taken, and cells are returned to the BR. Cell return is often below the liquid level in large scale systems (Martens et al., 2014), but can be from above the liquid level from the headplate, and is often placed here in small scale BR systems due to space limitations inside the vessel. t_m for cell recirculation loops from the headplate, above the liquid level, and from the side port, below the liquid level, was investigated to determine the impact of loop placement on vessel hydrodynamics. **Figure 4.10 A** shows t_m with rotational speed in the 250mL BR with no recirculation, and recirculation from under and above the liquid height. Recirculation rate was 80 mL min⁻¹, the operational flowrate. Recirculation from under the liquid height, from the side port, results in comparable t_m to the vessel with no recirculation, across the range of rotational speeds investigated. At 50 RPM, t_m is 22±4.4 and 23±2.4 s for vessels with side recirculation and no recirculation respectively. Comparatively, t_m with top recirculation at low RPM is significantly lower, at 12±1.9 s

when $N = 50$ RPM. At elevated $N > 150$ RPM, t_m is comparable across all configurations, with minor t_m elevation observed between configurations with no recirculation compared to both top and side port recirculation. t_m at operational conditions was 6 ± 1.1 , 3.8 ± 0.5 and 4.1 ± 0.7 for no, side and top recirculation configurations respectively, $N = 250$ RPM. **Figure 4.10 B** shows $t_m \times N$ with increasing Reynolds number for the 250mL vessel with no, side and top recirculation configurations. When calculating Reynolds number, recirculation flowrate was considered to have a negligible impact on flow regime in the vessel when agitated. $t_m \times N$ is consistent for side and top recirculation configurations at $Re > 2000$, below which lower $t_m \times N$ is observed in top recirculation configurations, due to increased turbulence induced from cell return above the liquid level compared to return below the liquid level. Vessels without recirculation have elevated $t_m \times N$ across the range of Reynolds numbers, suggesting that recirculation affects the hydrodynamics of the system, including for the operating conditions; $N = 250$ RPM, $Re = 2032$. To better understand the impact of the recirculation loop on vessel hydrodynamics, mixing time was determined at a range of recirculation flowrates with no additional agitation. **Figures 4.10 C, D** and **E** show mixing maps for the 250mL BR at $N = 250$ RPM mixed utilising HCD mimic, with no recirculation, side and top recirculation respectively, with recirculation flowrate at 80 mL min^{-1} . t_m in the bulk liquid is slightly elevated for configurations with no recirculation, however no significant impact to overall mixing profiles is observed. Maximum t_m s of 7-8 s are observed across all configurations. **Figures 4.10 F, G** and **H** show mixing maps for the 250mL BR at $N = 400$ RPM mixed utilising HCD mimic, with no recirculation, side and top recirculation respectively, with recirculation flowrate at 80 mL min^{-1} . While recirculation configurations at 250 RPM have a negligible impact on mixing profiles, minor deviations are observed at 400 RPM. Recirculation from the side port results in a slower mixing zone near to the return, suggesting that at high RPM, when t_m for the bulk liquid is lower, t_m is limited by the recirculation loop. This is observed to a lesser extent for top

recirculation configurations, where return from above the liquid height induces turbulence at the surface.



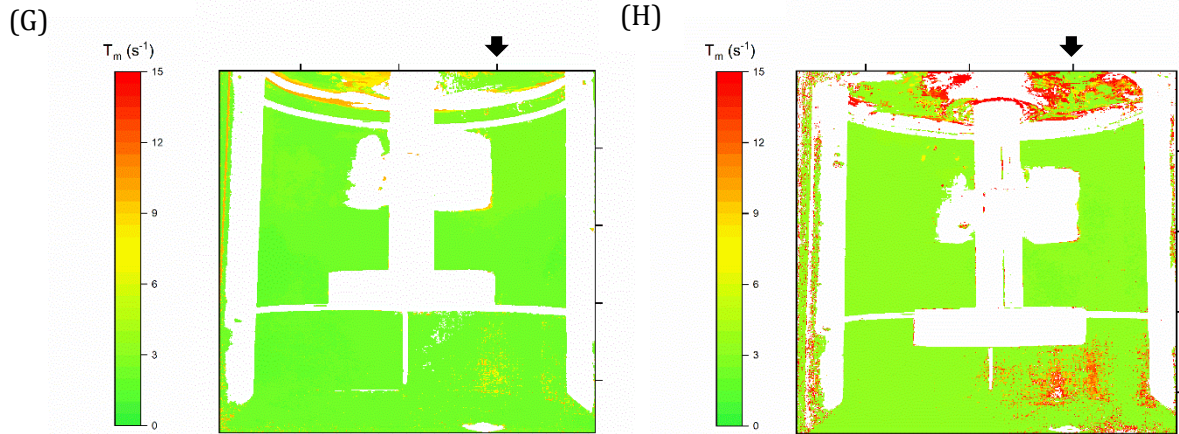


Figure 4.10 - Influence of perfusion recirculation with return from side or top ports at 80 mL min^{-1} on mixing dynamics. $N = 50 - 600 \text{ RPM}$, $H_i = 2 \text{ cm}$, mixed with DISMT HCD mimic solution. (A) t_m vs N with recirculation from the side, top or no recirculation. (B) $t_m * N$ vs Re with recirculation from the side, top or no recirculation. (C) Mixing map at $N = 250 \text{ RPM}$, no recirculation. (D) Mixing map at $N = 400 \text{ RPM}$, with no recirculation (E) Mixing map at $N = 250 \text{ RPM}$, with side recirculation (F) Mixing map at $N = 400 \text{ RPM}$, with side recirculation (G) Mixing map at $N = 250 \text{ RPM}$, with top recirculation (H) Mixing map at $N = 400 \text{ RPM}$, with top recirculation. Arrows represent point of return into vessel during recirculation through the side port (E,F) or top (G,H). Data $<150 \text{ RPM}$ represents 8 replicates \pm s.d. Data $150\text{-}300 \text{ RPM}$ represents 5 replicates \pm s.d. Data $>300 \text{ RPM}$ represents 3 replicates \pm s.d.

Figure 4.11 A shows t_m with recirculation rate for configurations returning at flowrates between $40\text{-}140 \text{ mL min}^{-1}$ from the side port and at the operational flowrate, 80 mL min^{-1} from the top port. For side port recirculation, increasing flowrates reduces the mixing time, from $240 \pm 41 \text{ s}^{-1}$ at a recirculation rate of 40 mL min^{-1} , to $50 \pm 7 \text{ s}^{-1}$ at 140 mL min^{-1} . Recirculation from the top port results in lower t_m at a recirculation rate of 80 mL min^{-1} , at $32 \pm 8 \text{ s}^{-1}$ compared to $102 \pm 28 \text{ s}^{-1}$ for side port recirculation. **Figures 4.11 B and C** show mixing maps for side and top recirculation configurations respectively at $N=0 \text{ RPM}$ and a recirculation flowrate of 80 mL min^{-1} . Several slow mixing zones up to 220 s are observed in side port recirculation configurations, compared to relatively homogenous mixing profiles when utilising top port recirculation. Reduced mixing time and homogenous mixing maps for top port recirculation configurations suggests that increased turbulence is introduced when recirculating from above the liquid level compared to return from the side port, below the liquid level. While the reduced t_m for top recirculation configurations is significant compared to side port recirculation in non-agitated systems, the relatively slow t_m compared to agitated systems means that impact

of recirculation loop position is reduced. Despite having little impact on t_m , side port recirculation was utilised for all perfusion experiments in the 250 mL BR, to reduce over crowding headplate and to reduce turbulence experienced by cells during the culture. Reducing turbulence experienced in cell cultures is beneficial, reducing foaming during cell culture. Reduced foaming reduces the number of cells damaged by the bubble bursting effect, and secondary impacts to cell health from increased osmolality due to the utilisation of antifoaming agents is limited.

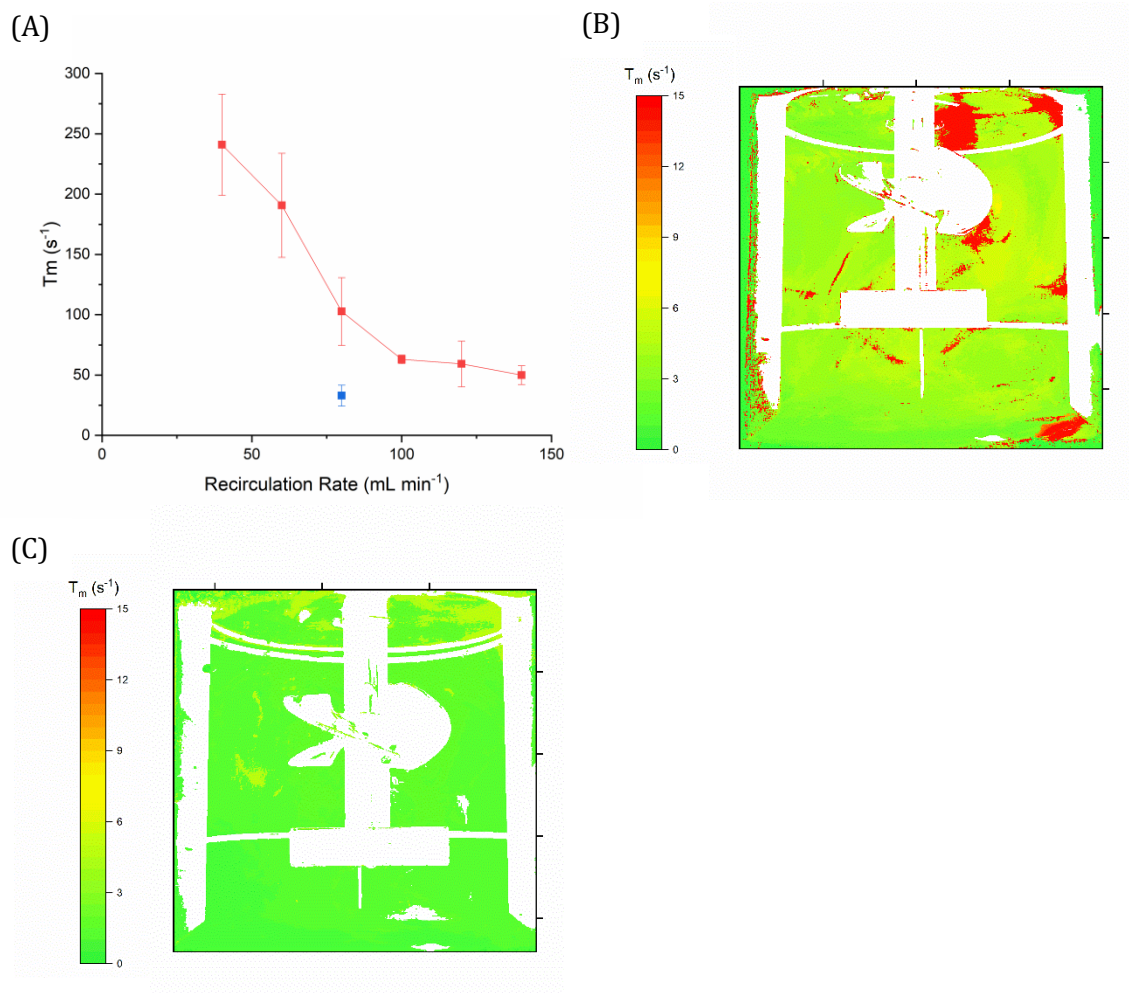


Figure 4.11 - Influence of perfusion recirculation with return from side port at 40 – 140 mL min⁻¹ and from the top port at 80 mL min⁻¹, N = 0 RPM. (A) t_m vs recirculation rate, recirculation from side and top ports (B) Mixing map for side recirculation at 80 mL min⁻¹, N = 0 RPM. (C) Mixing map for top recirculation at 80 mL min⁻¹, N = 0 RPM. Data represents 3 replicates \pm s.d.

4.2.8. Selection of scaling criteria

Following engineering characterisation, the utilisation of several scaling criteria was compared to determine the most appropriate. In order to identify the most suitable scaling criteria, parameters at operating conditions in the 250mL BR were calculated and each set as constants in a series of scaling scenarios. **Table 4.3 (A)** shows P/V , u_{tip} , $k_{L,a}$, t_m , N and Re in the 250mL BR at operating conditions; $N=250$ RPM, airflow rate = 50 mL min^{-1} . **Table 4.3 (B)** shows subsequent values in MWP and 5L BR, calculated on the basis of maintaining a single variable; P/V , u_{tip} , $k_{L,a}$, t_m or Re constant across scales. Scaling based on constant P/V requires reasonable shaking frequencies in MWP and stirring speeds in the 5L BR, at 240 and 260 RPM respectively. Reynolds number is transitional in MWP and the 250mL BR, and turbulent in the 5L BR, as expected with increasing volumes. Additionally, $k_{L,a}$ remains comparable, between $5.5\text{-}9 \text{ hrs}^{-1}$ across each scale. Scaling based on constant u_{tip} is only possible in stirred tank vessels, meaning that this technique is inappropriate when scaling between shaken and stirred vessels. Considering scale-up between the 250mL and 5L BR based on constant u_{tip} results in low $k_{L,a}$, at 1.9 hrs^{-1} in the 5L BR, and a reduction in power input per unit volume by approximately ten-fold compared to scaling with constant P/V . Maintaining constant $k_{L,a}$ generates operating parameters across MWPs and 5L BRs comparable to those observed when maintaining constant P/V . Reynolds number, N and power input are maintained within feasible ranges across scales. Finally, scaling based on the maintenance of constant Re is investigated. In MWPs, this method results in impossibly high N , at 925 RPM, generating a high specific power input and $k_{L,a}$. Conversely, in the 5L BR, maintenance of Re requires a considerably lower N , at 58 RPM. This results in a reduction of power input of approximately 100-fold compared to maintenance of constant P/V and a low $k_{L,a}$, incapable of supporting elevated cell density cultures, at 0.4 hrs^{-1} .

Table 4.3 -(A) Summary of power input, impeller tip speed, k_{La} , mixing time, impeller speed and Reynolds number in the 250mL BR at operating conditions. (B) Summary of the impact of selection of scaling parameters on key process variables when scaling from 250mL BR into 5L BR and MWPs.

(A)

250mL BR					
P/V (Wm ⁻³)	u_{tip} (ms ⁻¹)	k_{La} (hrs ⁻¹)	t_m (s ⁻¹)	N (RPM)	Re (-)
22.6	0.39	5.5	5	250	5397

(B)

Constant	MWP					5L BR				
	P/V (Wm ⁻³)	u_{tip} (ms ⁻¹)	k_{La} (hrs ⁻¹)	N (RPM)	Re (-)	P/V (W m ⁻³)	u_{tip} (ms ⁻¹)	k_{La} (hrs ⁻¹)	N (RPM)	Re (-)
P/V	22.6	-	9	240	1397	22.6	0.81	6	255	23972
u_{tip}	-					2.62	0.39	1.9	130	11986
k_{La}	10	-	5.5	200	1164	18	0.72	5.5	240	22128
Re	2856	-	232	925	5397	0.21	0.17	0.4	58	5397

5. CHAPTER 5: ESTABLISHMENT AND SCALE COMPARISON OF CELL CULTURE PROTOCOLS IN BATCH, FED-BATCH AND PERFUSION CULTURE MODES

5.1. Introduction

The utilisation of mL-scale devices to perform perfusion cultures has been demonstrated in Chapter 3, and such tools provide great promise for the screening of a large range of process conditions. Following initial screening, a small subset of best-performing process conditions can be selected for further investigation. To enable rapid, cost effective investigation at the laboratory scale and under controlled conditions, different mL-scale bioreactors (BRs) have been described, retrofitting pre-existing reactor systems and linked to cell retention devices to enable perfusion culture operation.

Examples of mL-scale BR systems utilised for perfusion include the 250mL DASBOX BR, where CHO cell densities of up to $80 \times 10^6 \text{ cells}^{-1} \text{ mL}^{-1}$ were achieved, utilising ATF and TFF filtration systems for cell retention (Chotteau, 2017). More recently, perfusion cultures have been described in the Ambr®250, incorporating single-use hollow fibre filters into the Ambr® parallel bioreactor system and reporting maximum VCDs of $40 \times 10^6 \text{ cells}^{-1} \text{ mL}^{-1}$ (Zoro and Tait, 2017).

While these examples go some way to fulfil the requirement for small scale perfusion culture in BRs, there are several limitations. Small scale BR systems, such as the DASBOX, inherently lack space on the headplate due to the high number of ports required for process monitoring and control, in addition to media and gas additions and motors for impellers. Because of this, additional unused ports are not common and as such when retrofitting from BRs previously designed for use in batch and fed-batch cultures. This means that the cell return is commonly placed on the headplate, where high recirculation flowrates can cause increased turbulence and trigger excessive foaming. Conversely,

systems such as the Ambr®250, have been specifically designed for perfusion processes and include additional ports for cell retention placement, however single use devices have a high consumable cost, and integrated cell retention devices do not allow for flexibility.

In order to address these limitations, a novel 250mL BR has been designed in this work specifically for scale-down perfusion cell culture processes. Design has been optimised to ensure capacity to enable flexibility to connect multiple cell retention devices, with cell retention inlet taken from the base of the bioreactor, and outlet returned below the liquid level. Return below the liquid level has been demonstrated in Section 4.2.7 to improve the homogeneity of mixing profiles and reduce turbulence within the BR. Additionally, a dual impeller system was fitted to ensure sufficient oxygen transfer to support HCD perfusion cultures. In this chapter, the optimisation of the novel BR system across multiple culture modes is described, including the incorporation of perfusion culture methodologies with cell retention achieved via a tangential flow filter (TFF). Cell culture performance in the novel 250mL BR is compared to performance in a 5L BR system and in the previously described MWP system in batch, fed-batch and perfusion modes.

5.2. Results

5.2.1. Development and optimisation of cell culture techniques in novel 250mL BR in batch and fed-batch modes

Preliminary development of cell culture protocols in the 250mL BR was undertaken in batch and fed-batch modes. Batch cultures were inoculated at 2×10^6 cells mL⁻¹ in 250mL CD-CHO media, controlled at 37°C, 30% DO and pH 7.2 as described in **Section 2.6**. **Figure 5.1 A** shows VCD and viability with time in the 250mL BR in batch mode. **Figure 5.1 B** shows corresponding glucose and lactate concentration with time. Peak VCDs of 7×10^6 cells mL⁻¹ were achieved on day 4, which corresponds to the time at which glucose

is depleted. Following glucose depletion, a shift to lactate consumption is observed and viability drops, to 40% on day 7. Cell culture performance was replicated consistently across multiple runs. **Figure 5.1 C** shows the pH, DO and temperature control profiles for a single batch cell culture run. Temperature is well controlled throughout the culture duration at $33.5 \pm 0.2^\circ\text{C}$ ($T_{\text{in}}=37^\circ\text{C}$). Placement of the external temperature probe however leads to temperature drops to 31.5°C during sampling, leading to subsequent over-heating, and unstable temperature for up to 30 minutes before re-equilibrating at the setpoint. Large fluctuations in DO are observed throughout the culture duration, initially oscillating between 25-100% before increasing to 10-180% on day 7. The DO setpoint of 30% is most closely achieved between days 3-4 where DO is maintained between 25-60%. While fluctuations in oxygen concentration are expected in BRs due to the dynamic nature of cell culture, impact of probe response time and poor proportional integral derivative (PID) control can cause the excessive fluctuations observed. The PID control implemented was previously optimised for a larger vessel with lower $k_{\text{L}}a$ and prolonged mixing time, and therefore was the focus of subsequent optimisation. pH is generally well controlled around the setpoint of 7.2 for the culture duration, however a notable rise in pH to 8 is observed between days 3 and 4. The control of pH, similarly to DO, was optimised for a larger vessel, and requires a balance between the addition of CO_2 gas for down-regulation and the addition of 1M NaOH for up-regulation. While down-regulation benefits from allowing a large percentage of CO_2 gas addition, up-regulation requires only a small volume of NaOH. Large additions of NaOH with time will increase the osmolality, and reactor volume above the maximum working volume. Additionally, large NaOH additions might cause pH increase to the point where CO_2 cannot adequately down-control. The aforementioned event caused the pH rise between days 3 and 4, where eventually pH control was manually overridden to regain equilibrium. Despite the fluctuations, process control is sufficient to sustain batch cell cultures consistently, with VCD is limited by glucose depletion.

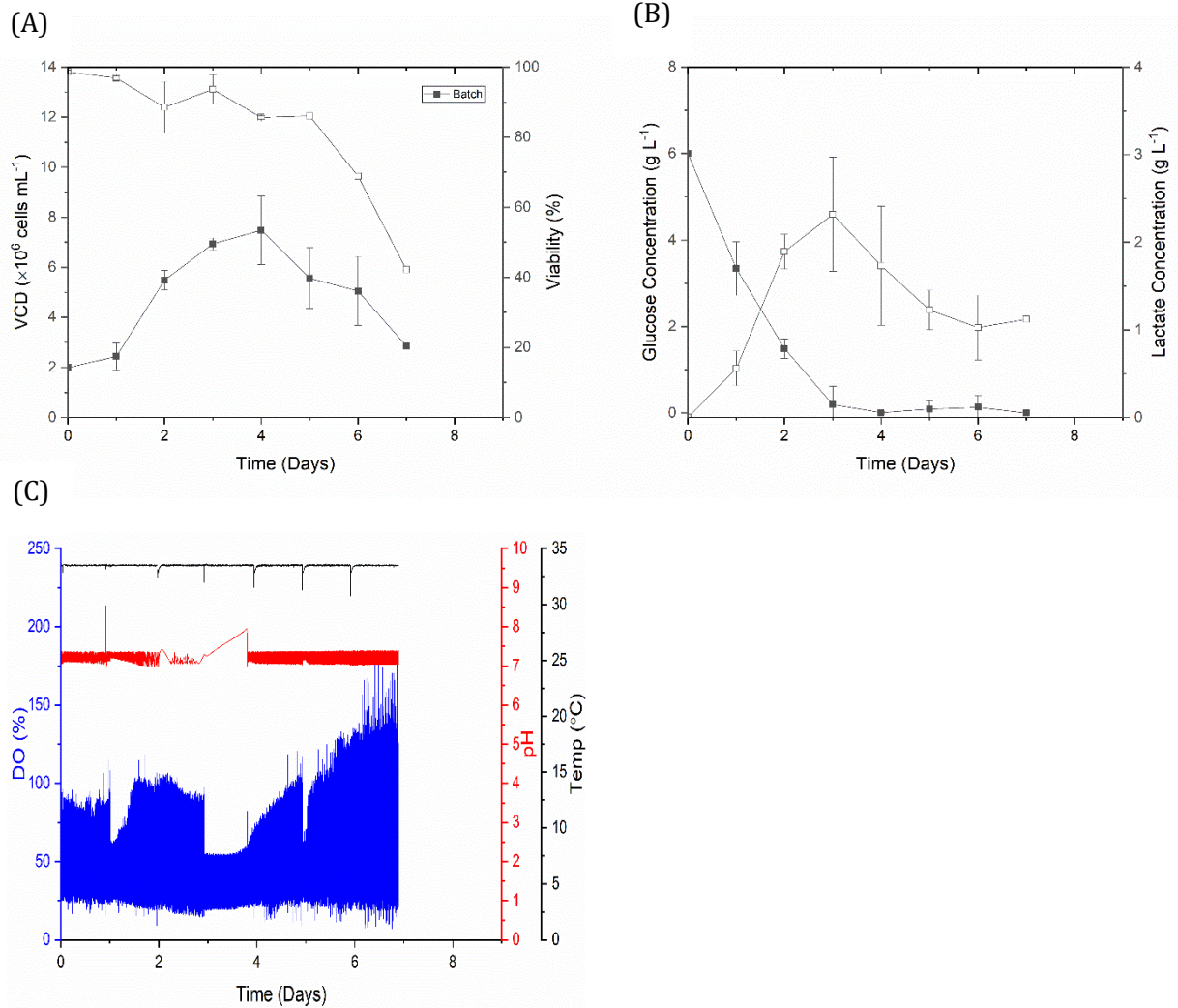


Figure 5.1 - Batch CHO cell culture in 250mL BR. Cultures were seeded at 2×10^6 cells mL^{-1} and maintained at 37°C , pH 7.2, DO 30%, $N = 250$ RPM. (A) VCD (filled symbols) and viability (empty symbols) (B) Glucose concentration (filled symbols) and lactate concentration (empty symbols) (C) BR control profile; DO concentration (blue), pH (red), temperature (black). VCD and metabolite data represents 3 cultures \pm s.d., control profiles represent a single BR run.

Improvements to PID settings were introduced step-wise during fed-batch culture in the 250mL bioreactor. Fed-batch cultures were inoculated at 2×10^6 cells mL^{-1} in 162.5mL of CD-CHO, with feeding commencing on day 3 for 6 consecutive days, as described in Section 2.6.1. **Figure 5.2 A** shows VCD and viability with time for 3 consecutive fed-batch cell culture with improving PID controls. **Figures 5.2 B, C and D** show corresponding glucose, lactate and antibody concentration respectively with time for fed-batch cell culture runs.

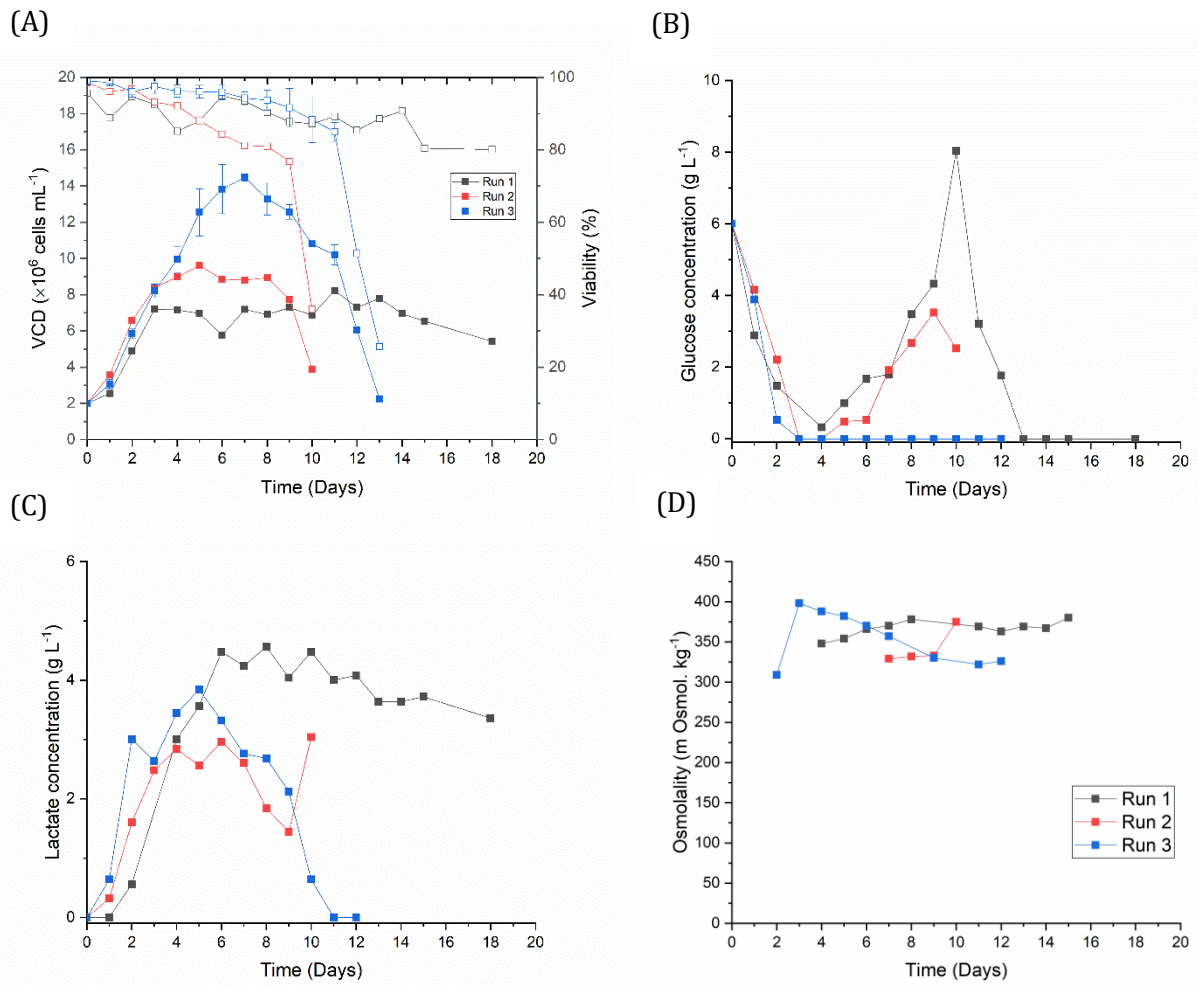


Figure 5.2 - Fed-batch CHO cell culture in 250mL BR with step-wise improvements to PID control. Cultures were seeded at 2×10^6 cells mL^{-1} and maintained at 37°C , pH 7.2, DO 30%, $N = 250$ RPM. Feeding commenced on day 3 and involved a 5% daily addition of Efficient Feed B. (A) VCD (filled symbols) and viability (empty symbols) (B) Glucose concentration (C) Lactate concentration (D) Osmolality. Data for Run 1 and Run 2 culture represent a single BR run. Run 3 data represents 2 cultures \pm s.d.

Run 1 shows an elongated stationary phase from day 3-14 and comparable peak VCD to those previously reported in batch cultures, at 7.3×10^6 cells mL^{-1} on day 10. Glucose is significantly over-fed during the feeding phase of the culture, reaching a peak concentration of 8 g L^{-1} on day 10. **Figure 5.3 A** shows the pH, DO and temperature control profiles for the initial fed-batch run. Improvements to PID control yielded an initial reduction in the scale of DO fluctuations, allowing the maintenance of a DO of $30 \pm 5\%$ until day 8 of the culture. During the late stationary phase of the culture on days 8-12, larger DO fluctuations between 25-170% are observed. Temperature profiles are comparable to those previously observed in batch cultures, with temperature drops to

31.5°C observed during sampling. Optimisation of pH control setpoints has resulted in improved performance, with pH well controlled around the setpoint at pH 7.2 for the duration of the culture. Improvements were made by limiting the pH response to 20% of the maximal response, which was the lowest percentage that provided adequate control, limiting the volume of NaOH being pumped into the vessel without hindering the capabilities of down-regulation by CO₂.

Run 2 generates improved peak VCDs, reaching a maximum of 9.6×10^6 cells mL⁻¹ on day 6. Glucose concentration increases during the feeding phase of the culture until day 9, reaching a peak concentration of 3.8 g L⁻¹ on day 9. **Figure 5.3 B** shows the pH, DO and temperature control profiles for fed-batch Run 2. While observed fluctuations in DO and pH are within acceptable ranges, large variations are seen in the temperature profile. Temperature fluctuates between 33.5-37°C ($T_{in}=37-40.5^\circ\text{C}$) for the duration of the culture. Poor temperature control is caused by inadequate insulation, and external probe placement. In subsequent cultures, insulation was placed around the BR in addition to the heating jacket to extend the heating jacket lifetime, and a permanent external temperature well was created to reduce temperature fluctuations.

All improvements in PID and temperature control previously discussed were incorporated into process control in Run 3. Further improvements in VCD are achieved, with a peak VCD of 14×10^6 cells mL⁻¹ observed on day 7. Cell culture shows consistent performance over 2 identical runs, with maximum deviations in VCD of 10%. Glucose is completely consumed at 0 g L⁻¹ from day 3, meaning that consumption is occurring same rate as addition during the feeding phase of the culture. Lactate is produced until day 5, reaching a peak concentration of 4 g L⁻¹, following which a lactate shift is observed, with consumption until day 12. **Figure 5.3 C** shows the pH, DO and temperature control profiles for fed-batch Run 3. Temperature is well controlled throughout the duration of the culture, maintaining $33.5 \pm 0.2^\circ\text{C}$. Additionally, pH is well controlled around 7.2 ± 0.1

for the duration of the culture. Despite observing fluctuations in DO during the exponential growth phase of the culture between 20-160% on days 2-5, DO is otherwise well controlled at $30 \pm 10\%$.

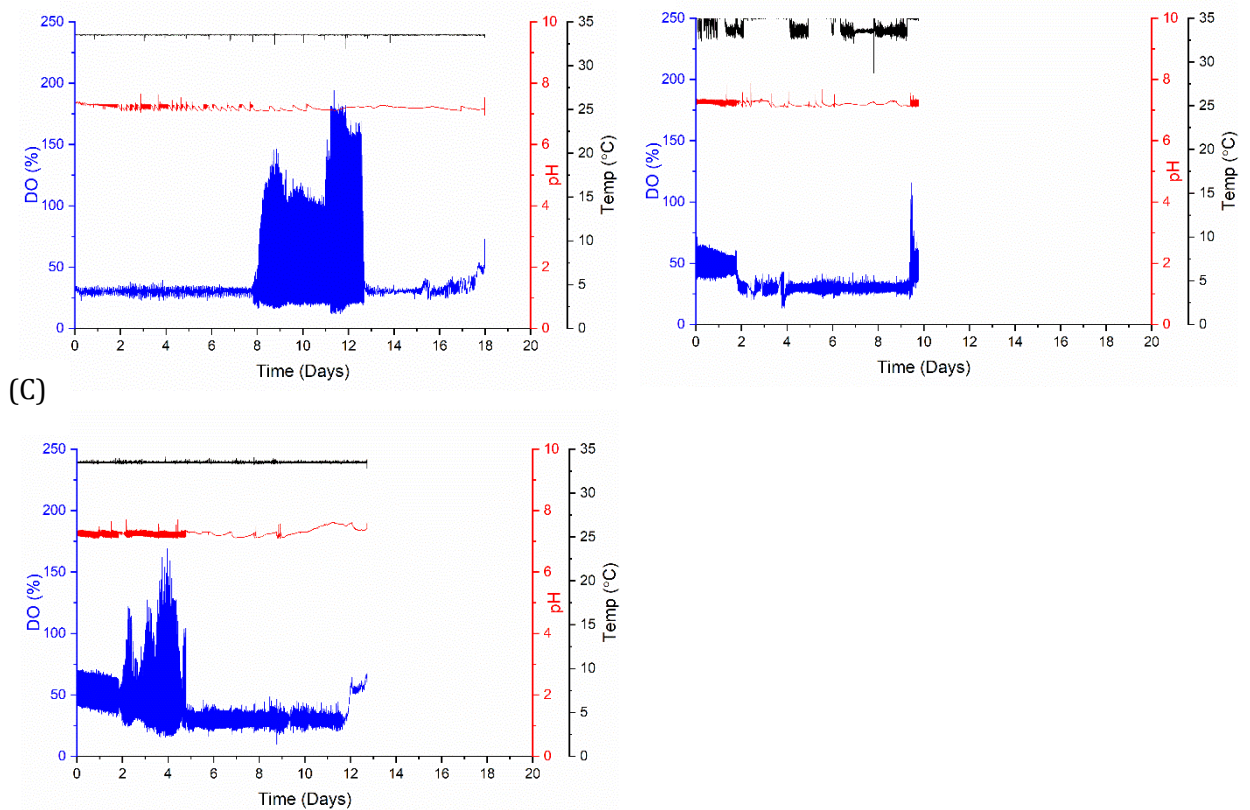


Figure 5.3 -Control tracers for fed-batch CHO cell culture in the 250mL BR: DO concentration (Blue), pH (Red), Temperature (Black).Control tracers represent a single BR run.

The retrofitting of the New Brunswick controller, previously used for 5L BRs, for use in the 250mL novel BR led to poor control of pH and DO, due to incompatible pH and DO PID settings. P and I set points were optimised utilising manual tuning techniques. Manual tuning techniques are conducted in situ, starting with low proportional (P-gain) and no integral (I-gain). P-gain was doubled until oscillation in output was observed, and then halved. A small I-gain was then implemented and similarly tuned until oscillations were maintained within an acceptable range (Ravi, 2017, Doran, 1995). PID settings for pH control were optimised by reducing both the P and I gain to allow for faster response

to changes in pH, but with a smaller output. This is necessary in smaller vessels in comparison to larger ones because of the shorter mixing time, meaning homogenous changes in pH are observed more rapidly after additions of CO₂ or NaOH and pH dead zones due to poorly mixed regions in the BR are uncommon. Smaller outputs avoid accumulation of NaOH over time and toxic increases in osmolality and vessel over-filling. DO fluctuations were similarly controlled by reducing the P and I gain, allowing for rapid response to changes but reducing the volumes of O₂ sparged into the vessel. Initial runs included the sparging high volumes of O₂ which create a feedback loop and in turn the large fluctuations in DO between 25-175%, as observed in Run 1. Optimisation of the P and I gain lead to a vast reduction in fluctuations observed, with DO controlled for the majority of the culture of 30±10% as observed in Run 3. The final improvement to temperature control was largely achieved by improvements to physical aspects, such as the jacket and insulation, and providing a permanent thermowell outside the reactor to monitor temperature.

Improvements in PID and temperature control have facilitated improved cell culture performance, with peak VCDs of 2× greater and maintenance of elevated viability in Run 3 compared to Run 1. PID settings and probe placements were fixed and utilised for all subsequent experiments in the 250mL BR.

5.2.2. Comparison of cell culture performance across scales in batch and fed-batch modes

In order to ensure the culture performance in the 250mL BR is representative of commercially available BRs and to compare with the performance of previously described MWP systems, batch and fed-batch cultures were performed across scales. **Table 5.1** summarises the hydrodynamic conditions within the BRs and MWPs, at operational conditions. Reynolds number, P/V and k_La for MWP and 5L BR calculated as described in Section 4.2, k_La in 250mL BR experimental determined as described in

Section 4.2.2. Scale-up was performed on the basis of constant power input per unit volume.

Table 5.1 - Reynolds number, k_{La} , power input and u_{tip} at operational conditions in MWP and 250 mL and 5L BRs.

	Re (-)	k_{La} (hrs ⁻¹)	P/V (W m ⁻³)	u_{tip} (m s ⁻¹)
MWP	1.28×10^{-3}	7.4	14.7	-
250mL BR	5.40×10^{-3}	8.7	22.1	0.18
5L BR	2.40×10^{-4}	6.3	25.4	0.79

Figure 5.4 A shows VCD and viability with time for MWP and 250mL BR batch cultures, as described in Sections 2.4 and 2.7 respectively. **Figures 5.4 B and C** show corresponding glucose and lactate profiles, respectively, for MWP and 250mL BR batch cultures. Comparable performance is observed between MWP and 250mL BRs, which reach peak VCDs of 9 and 7.4×10^6 cells mL⁻¹, respectively. Glucose concentration profiles in MWP and BRs are comparable, with depletion of glucose observed from day 4. Additionally, lactate concentrations are comparable, with lactate produced until day 3 before being consumed. Peak lactate concentrations of 1 and 2.4 g L⁻¹ are generated in MWP and 250mL BR, respectively. Maximum growth rates are comparable between the two scales, at 0.024 and 0.021 hr⁻¹ for MWP and BR, respectively. Overall, cell culture performance in the 250mL BR has been shown to be in good agreement to that of MWPs in batch mode.

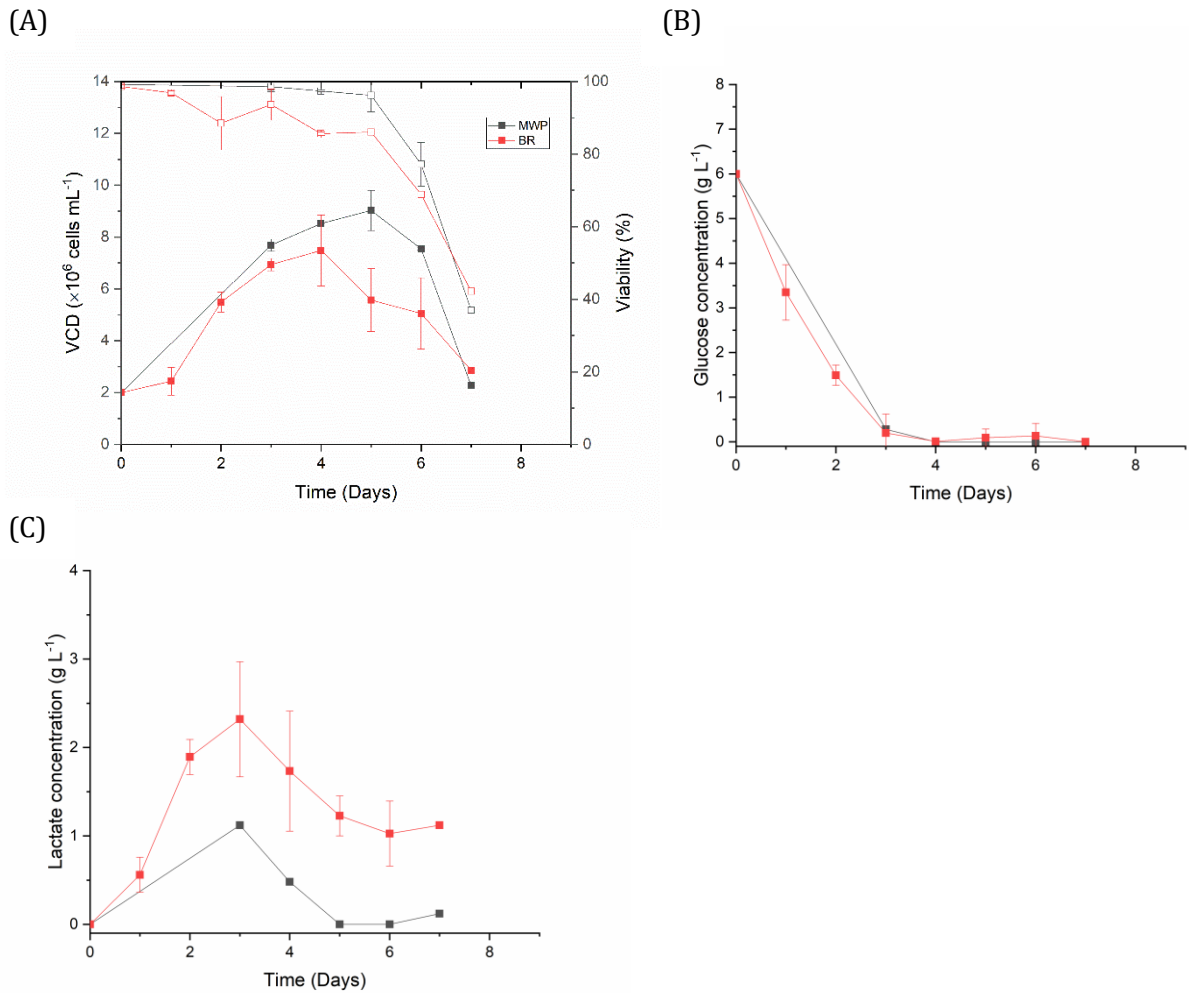


Figure 5.4 - Comparison of batch CHO cell culture performance in MWP and 250mL BR. Cultures were seeded at 2×10^6 cells mL^{-1} and maintained at 37°C, pH 7.2, DO 30%. N = 220 RPM in MWP, N = 250 RPM in 250mL BR. (A) VCD (filled symbols) and viability (empty symbols) (B) Glucose concentration (C) Lactate concentration. Data represents 3 cultures \pm s.d.

Fed-batch cultures extend the complexity of operations compared to batch cultures by introducing daily feeding for glucose and metabolite supplementation. Fed-batch cultures were conducted in a 5L BR in addition to MWP and 250mL BR. Cell culture in the 5L BR¹ was inoculated at a concentration of 0.3×10^6 cells mL^{-1} in accordance with standard cell culture protocols. Fed-batch cultures were fed from day 3 for 6 consecutive

¹ Conducted in collaboration with Ricardo Suarez Heredia and Milena Rivera-Trujillo, UCL Department of Biochemical Engineering

days with 5% volume additions of Efficient Feed B, as described in Section 2.4 and Section 2.7 for MWP and BRs respectively.

Figure 5.5 A shows VCD and viability variation with time for fed-batch cultures in MWP, 250mL BR and 5L BR. MWP cultures involved the additional bolus addition of buffer, since pH is not controlled as in BR systems. **Figures 5.5 B, C and D** show corresponding glucose, lactate and antibody concentrations, respectively, for fed-batch cultures.

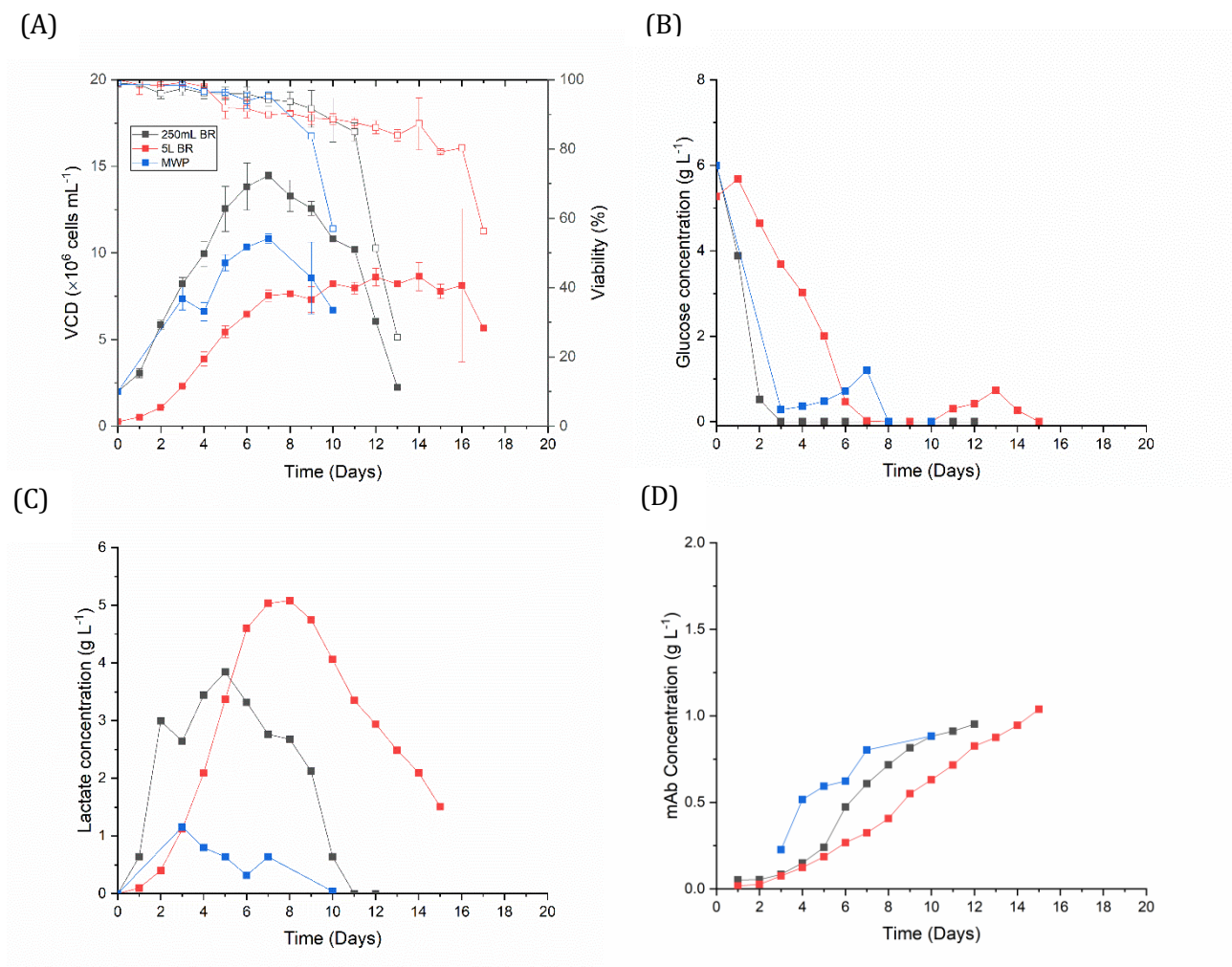


Figure 5.5 - Comparison of fed-batch CHO cell culture performance in; MWPs and 250mL and 5L BRs. Cultures in MWP and 250mL BRs were seeded at 2×10^6 cells mL^{-1} and in 5L BR were seeded at 0.3×10^6 cells mL^{-1} . Cultures across scales were maintained at 37°C , pH 7.2, DO 30%. Feeding commenced on day 3 and involved a 5% addition of Efficient Feed B. N = 220, 250 and 260 RPM in MWPs, 250mL BR and 5L BR respectively. (A) VCD (filled symbols) and viability (empty symbols) (B) Glucose concentration (C) Lactate concentration (D) mAb concentration. 250mL BR and MWP data represents 3 cultures \pm s.d. 5L BR data represents 2 cultures \pm s.d.

Table 5.2 shows μ_{\max} , volumetric productivity and q_{Ab} for fed-batch cultures in BRs and MWP. Variation is observed in growth performance between the two scales of BRs and MWPs. The peak VCD in the 5L BR of 8.6×10^6 cells mL^{-1} achieved on day 10, is significantly lower than the peak VCD of 14×10^6 cells mL^{-1} in 250mL BR on day 7. Performance in MWP lies between the two BR scales, with peak VCDs of 10×10^6 cells mL^{-1} reported on day 7. Despite variation in peak VCDs and growth profiles, BRs generate comparable μ_{\max} , of 0.021 and 0.023 hrs^{-1} in 250mL and 5L BRs respectively. Consistent μ_{\max} suggests that deviations in growth performance in BRs is a factor of the variable seeding density. Glucose concentration profiles are, as expected, a factor of growth performance, with the 5L BR at a lower VCD than alternative scales reaching glucose depletion prior to feeding on day 7. Comparatively, the 250mL BR and MWPs, which generate higher VCDs earlier in the culture, observe glucose depletion prior to feeding on day 3, with over supplementation of glucose up to concentrations of 1.3 g L^{-1} observed in MWPs during the feeding phase of the culture. Lactate is produced until day 8 in 5L BRs, reaching a concentration of 5 g L^{-1} before entering the consumption phase. Lactate production in the 250mL BR experiences a shift from production to on day 5, 2 days prior to achieving the peak VCD, equivalent to the timeline experienced in 5L BRs.

Table 5.2- Maximum specific growth rate (μ_{\max}), volumetric productivity (Vol Prod) and specific antibody production (q_{Ab}) for fed-batch cell cultures in MWP, 250mL BR and 5L BR

	$\mu_{\max} (\text{hr}^{-1})$	Vol Prod ($\text{g L}^{-1} \text{ day}^{-1}$)	q_{Ab} ($\text{pg cell}^{-1} \text{ day}^{-1}$)
MWP	0.018	0.088	52.0
250mL BR	0.021	0.079	7.67
5L BR	0.023	0.068	11.3

Antibody concentration is comparable in the 250mL BR and MWPs, where concentrations of 0.88 g L^{-1} are observed on day 10. 250mL and 5L BRs generate

comparable antibody concentration profiles until day 5, after which the antibody concentration diverges, with increasing concentration in the 250mL BR consistent with elevated VCD. Maximum titres of 0.95 g L^{-1} and 1 g L^{-1} is achieved in the 250mL and 5L, respectively. The extended duration of the 5L BR culture means that the maximum titre across scales is achieved on day 15, compared to on day 12 in the 250mL BR. Elevated q_{Ab} is achieved in the 5L BR, which produces comparable productivity to the 250mL BR despite having a reduced VCD.

Variation is observed in cell culture performance throughout each scale, particularly when considering VCD, with peak VCDs ranging between $8.6\text{--}14 \times 10^6 \text{ cells mL}^{-1}$. While differing VCDs are observed between the BRs, μ_{max} is comparable. From this, it can be concluded that the primary cause of the deviation is likely a function of the varying seeding density. Additional sources of variation include operational VVM, different impeller configurations between bioreactor scales and impeller tip speed (u_{tip}).

The 250mL BR is operated at an elevated VVM compared to the 5L BR, which as previously discussed, was necessary to ensure adequate control of pH and DO. In order to maintain a constant gassed power input per unit volume, RPM was subsequently adjusted across scales. An elevated VVM in a smaller vessel with a shorter mixing time allows for rapid response to changes in pH and DO. Interestingly, fed-batch culture performance in the 5L vessel is comparable to Run 1 in the 250mL vessel, shown in **Figure 5.2** and discussed in Section 5.2.1, which generated a peak VCD of $7.3 \times 10^6 \text{ cells mL}^{-1}$. Initial runs in the 250mL BR were undergoing improvements to PID control, with Run 1 shown to have some of the widest fluctuations and longest response times, the time taken from a spike or drop occurring to the return of pH or DO within the acceptable margin. The slow response in Run 1 could be effectively mimicking the larger vessel, which has an elongated mixing time, 15 fold greater (Vélez Suberbie, 2013) than 250mL

BR, meaning fluctuations of pH and DO in the bulk liquid are detected later and therefore are subject to an elongated response time.

Both the 5L and 250mL BRs are operated at comparable RPMs, with $N=260$ and 250 RPM, respectively. This means that u_{tip} for impellers in the 5L BR are 4× greater than in the 250mL BR, due to the larger impeller diameter. A high u_{tip} is related to high shear rate in the bulk liquid, which can damage shear-sensitive cells. Shear rate in both the 250mL and 5L BRs were calculated following **Equation 2.15**, which provides an estimate of average shear rate in the bulk liquid based on impeller geometry and rotational speed. Despite the greater u_{tip} in 5L BRs, shear rate experienced in the bulk liquid is not significantly greater, at $47.2s^{-1}$ compared to $45.4s^{-1}$ in the 250mL BR. GS-CHO cells have been shown to resistant to shear stress equivalent to $2000s^{-1}$ (Hu et al., 2011), which supports the conclusion that the increased impeller tip speed has a negligible impact on cell culture performance in this case.

Performance variations between MWPs and BRs are not suspected to be attributed to deviations caused by the nature of agitation, including turbulence and shear rate.. Despite MWPs having a k_La greater than the 250mL and 5L BRs, actual gas transfer is dependent on diffusion through the headspace only, and occurs through the covering membrane which will limit actual gas transfer in the system. Additionally, BRs are capable of controlling gas additions such that pure O_2 can be sparged if required. Conversely, MWPs exchange with atmospheric air, which contains approximately 21% O_2 . This means that actual k_La is approximately a fifth of the calculated k_La , and therefore will have a value of approximately 7 hrs^{-1} . Despite accounting for limitations in the MWP, k_La is not suspected to limit cell growth at VCDs in the order of $10\text{-}20 \times 10^6\text{ cells mL}^{-1}$. Reynolds number is shown to decrease as the scale of operation increases when power input per unit volume is used as scaling criteria, with the 250mL BR falling within the transitional phase and the 5L BR in the turbulent phase. Comparing BRs to MWP based

on flow regimes is difficult since laminar, transitional, and turbulent flow regimes in MWP are not well defined, and observed flow is very different compared to BRs. Running at high Reynolds number increases the rate of mass transfer within systems, which impacts availability of metabolites and O₂. In the transitional phase, turbulence is considered to provide adequate mass transfer in mL-scale systems, meaning the lower Reynolds number experienced in MWP should not limit cell culture performance with reduced mass transfer, since the volume is in the mL-scale.

The deviation in performance between MWPs and BRs can therefore be explained by the control methodologies used in the two systems. While BRs have online pH measurements and control, MWPs rely on arbitrary bolus feeding of buffer during the feeding phase of the culture. Despite MWPs experiencing low concentrations of lactate, up to a maximum concentration of 1 g L⁻¹, in which range pH shifts caused by lactate accumulation should be controlled by the buffering capacity of the media, it is expected that pH fluctuations will be experienced. Fluctuations in pH are particularly seen in batch and fed-batch cultures where media is not exchanged, as described in Section 3.2.2. Deviation from the optimal setpoint can limit cell capacity to proliferate, and hence is a potential cause of the limitation of peak VCDs in MWPs compared to 250mL BRs. It is worth noting that while MWP performance is limited compared to the 250mL BR, improved cell culture performance is observed in MWP compared to the 5L BR. This further strengthens the conclusion that cell culture performance in the 5L BR is likely the result of the lower seeding density.

5.2.3. Development of perfusion culture methodologies in novel bioreactor

Following optimisation of control parameters and culture performance in fed-batch mode, perfusion culture was conducted. Perfusion cultures were carried out as described in **Section 2.6.2**, with perfusion initiated on day 3 at an exchange rate of 1 VVD with CD-CHO blended with 15% Efficient Feed B. To achieve cell retention, a TFF

was connected via the base and side connections and recirculated at 80 mL min^{-1} . Media inlet and supernatant outlet flow was controlled using identical peristaltic pumps at a rate of 0.17 mL min^{-1} to achieve the desired exchange rate. **Figure 5.6 A** shows VCD and viability variation with time for cell culture in the 250mL BR in fed-batch and perfusion modes, exchanged at a rate of 1 VVD. **Figures 5.6 B, C and D** show corresponding glucose, lactate and antibody concentrations, respectively, with time. The introduction of perfusion culture methodologies generate peak VCDs of $86 \times 10^6 \text{ cells mL}^{-1}$ on day 11, an 8 fold improvement compared to fed-batch cultures. Additionally, viability is maintained above $>96\%$ for the duration of the culture until day 16.

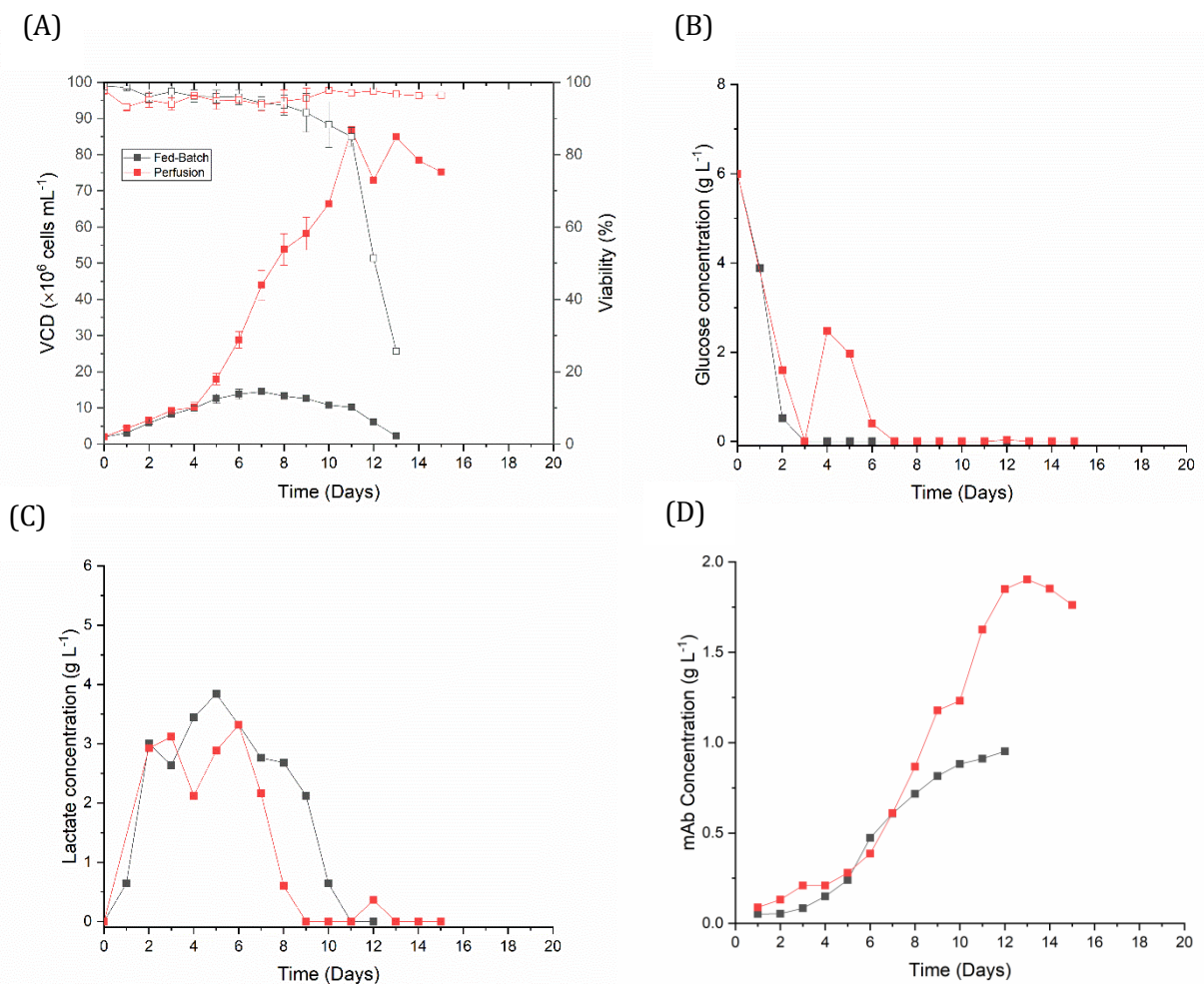


Figure 5.6 - Comparison of fed-batch and perfusion CHO cell culture in 250mL BR. Cultures were seeded at $2 \times 10^6 \text{ cells mL}^{-1}$ and maintained at 37°C , pH 7.2, DO 30%, N = 250 RPM. For fed-batch cultures, feeding commenced on day 3 and involved a 5% daily addition of Efficient Feed B. For perfusion cultures, perfusion was initiated on day 3 at a rate of 1 VVD, exchanging with CD-CHO media blended with 15% Efficient Feed B. Cell retention was achieved with TFF and a recirculation flow rate of 80 mL min^{-1} . (A) VCD (filled symbols) and viability (empty symbols) (B) Glucose concentration (C) Lactate concentration (D) mAb concentration. Data represents 2 cultures \pm s.d.

Glucose concentration in fed-batch and perfusion modes follows comparable trends, with glucose supplied at the same rate as consumption during the feeding phase of the fed-batch culture, and after day 6 in perfusion cultures. Lactate concentration is also comparable across fed-batch and perfusion culture modes, with peak concentrations of 3.8 and 3.3 g L⁻¹ achieved on days 5 and 6, respectively.

Peak antibody concentrations of 1.8 g L⁻¹ were observed in perfusion cultures are approximately 2-fold greater than those achieved in fed-batch. Perfusion cultures often produce lower titres compared to fed-batch, with supernatant removal diluting the product stream. However, the relatively low perfusion rate of 1 VVD and very HCDs achieved generate improvements in antibody concentrations in this case. Additionally, a 7 fold increase in volumetric productivity is observed for perfusion cultures compared to fed-batch, at 0.12 and 0.87 g L⁻¹ day⁻¹ respectively.

Figure 5.7 A shows the pH, temperature and DO concentration during perfusion culture at 1 VVD. The optimisation of temperature control previously described was sufficient to maintain a consistent temperature for the culture duration, maintaining the T_{out} setpoint of 33.5±0.2°C. pH is generally well controlled for the culture duration, at 7.2±0.1, a single spike to 7.6 is experienced during the exponential growth phase of the culture between days 1 and 2, which was corrected without the need for manual manipulation. It was noted during the exponential phase of the culture following initiation of media exchange that large quantities of NaOH were added into the system, up to 8% of the reactor working volume daily. While the media exchange reduces the osmotic effects, the cumulative addition of large volumes of NaOH will increase osmolality and suppress cell proliferation with time. To reduce the volume of NaOH additions, the pH dead-band was increased, to 7.2±0.2, which maintained adequate control whilst reducing the maximum volume of NaOH additions to 3% of the reactor volume daily. DO is well controlled until day 5, when VCD begins to deviate above that

achieved in fed-batch cultures. From day 6, DO begins to drop below the setpoint, to values <5%, which would limit cell growth if sustained for elongated periods of time. In order to increase the $k_{L,a}$, RPM was increased step-wise by 30 RPM per day, when DO begins to fall <5%, to a maximum of 400 RPM. During the culture, two RPM increases were required, on days 6 and 8, reaching a maximum rotational speed of 310 RPM. Increasing RPM when required ensures adequate O_2 supply to support very HCD perfusion cultures. **Table 5.3** summaries the $k_{L,a}$ at each RPM step, calculated following the Van't Riet equation, using experimentally determined coefficients as described in Section 4.2.2.

Table 5.3 - $k_{L,a}$ in the 250mL BR at step-wise RPM increases during perfusion culture. $k_{L,a}$ was calculated following the Van't Riet equation, utilising coefficients that were experimentally determined; $K = 3.8$, $a = 1.067$, $b = 1.371$

N (RPM)	$k_{L,a}$ (hrs ⁻¹)
250	3.5
280	5.2
310	7.4
340	10.2
370	13.6
400	17.8

Figure 5.7 B shows the RPM of the centrifugal recirculation pump, required to maintain a constant flowrate of 80 mL min⁻¹, with time. Initially it appears that as viscosity increases with increased VCD, the RPM required to maintain 80 mL min⁻¹ increases. However, a drop in RPM on days 6-8, whilst cells continue to proliferate and biomass increases, contradicts this conclusion. While viscosity changes might contribute to changes in RPM, it is more likely that changes within the filter, such as fouling and blockages, contribute more heavily to output RPM.

An additional complication with perfusion culture at mL-scale process volumes is maintaining a constant volume within the reactor. Despite utilising identical inlet and

outlet pumps, pressure differentials can cause deviations throughout the culture. The pressurised BR slows the flow of the inlet media stream, and the pressure of recirculation can cause high flowrates in the supernatant outlet. While the mL-deviations are negligible in L-scale systems, the cumulative impact of differential flow with time concentrates cell culture in the 250mL BR, impacting mass transfer. To ensure a constant volume in the opaque vessel, daily weight measurements were taken from the media inlet, supernatant outlet and NaOH, and corrections to volume were made by pulsing media in as necessary.

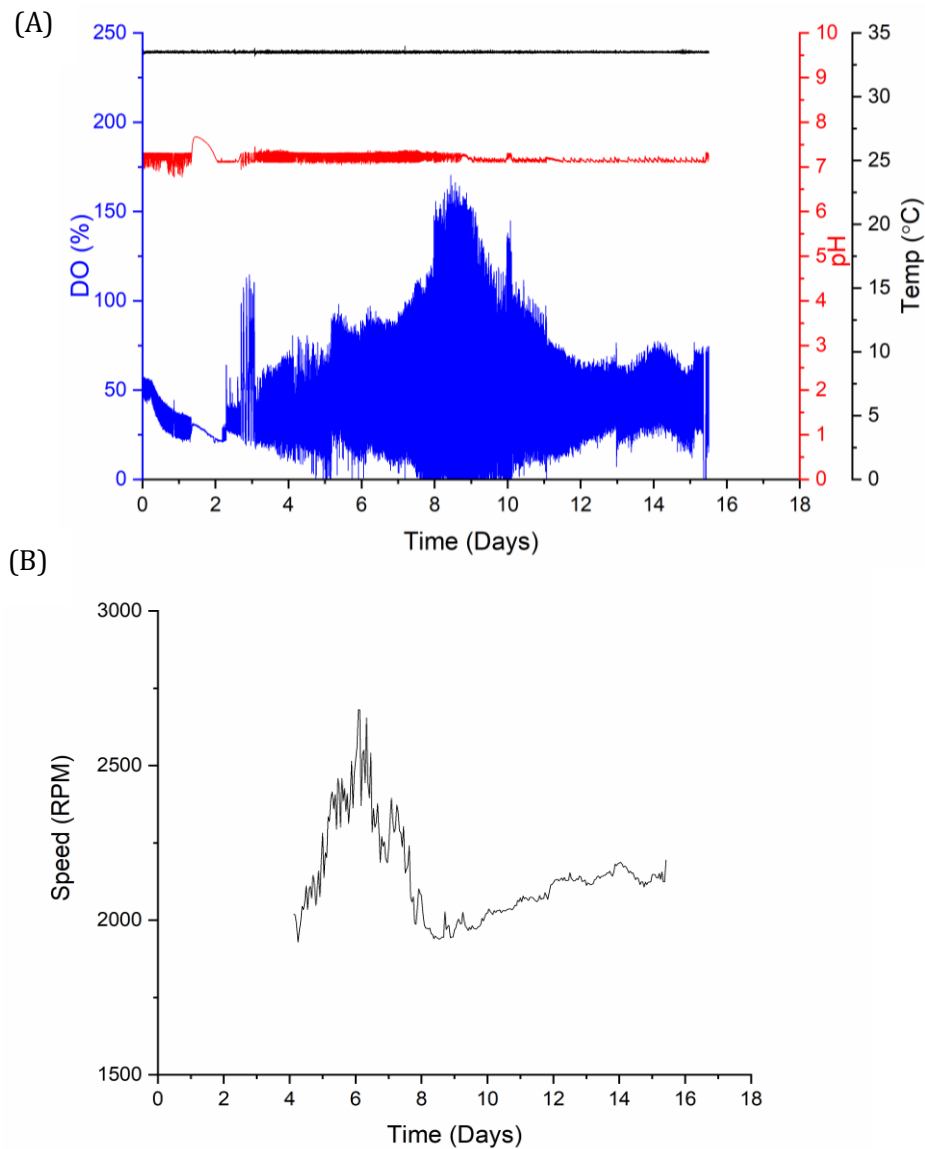


Figure 5.7 - Control profiles of perfusion CHO cell culture in the 250mL BR. (A) DO (blue), pH (red) and temperature (black) (B) Rotational speed of centrifugal pump to maintain a recirculation flowrate of 80 mL min⁻¹. Data represents 1 culture.

Perfusion culture was successfully conducted at a perfusion rate of 1 VVD in the 250mL BR. The BR design was shown to be capable of proliferating and supporting very HCD cultures up to 86×10^6 cells mL^{-1} , and extending duration of high viability >96% compared to fed-batch cultures. Performance is comparable to Chotteau (2017), who reported cell densities in GS-CHO cultures of 100×10^6 cells mL^{-1} in a DASBOX BR of identical scale. Media inlet and supernatant outlet flows were successfully balanced in order to maintain a constant volume for the culture duration. The L-sparger combined with dual impeller system provided adequate $k_{L,a}$ to enable the support of cells up to 20×10^6 cells mL^{-1} at $N=250$ RPM, with further increase in cell density supported by increasing the RPM step-wise to a maximum of 310 RPM on day 8. The TFF was capable of operating through the 16 day duration of the culture without observing pressure build ups indicative of pore clogging, and maintains a 100% separation efficiency. Perfusion culture was exchanged with 15% Feed B blend media, previously determined as the optimal media in quasi-perfusion cultures as described in Section 3.2.4. Exchange of Feed B at 1 VVD provides sufficient glucose to sustain HCD cultures, with glucose concentration in the media equivalent to consumption from day 7 until termination of the culture. The low concentration of glucose within the BR initiates a lactate shift, with consumption occurring from day 7. This suggests that, despite the HCD attained, cell density could be limited by glucose availability in cultures at 1 VVD.

Perfusion cultures in the 250mL BR were subsequently operated at varying perfusion rates. **Figure 5.8 A** shows VCD and viability with time for perfusion cultures in the 250mL BR exchanged at perfusion rates 0.5, 1 and 1.8 VVD. **Figure 5.8 B, C and D** show corresponding glucose, lactate and antibody concentrations respectively with time. **Table 5.4** shows q_{Gluc} , q_{Lac} , q_{Ab} and volumetric productivity for 250mL BR cultures exchanged at perfusion rates of 0.5, 1 and 1.8 VVD. Control profiles of pH, DO, temperature and of the centrifugal pump for cultures exchanged at 0.5 and 1.8 VVD can be found in Appendix 3 and 4, respectively.

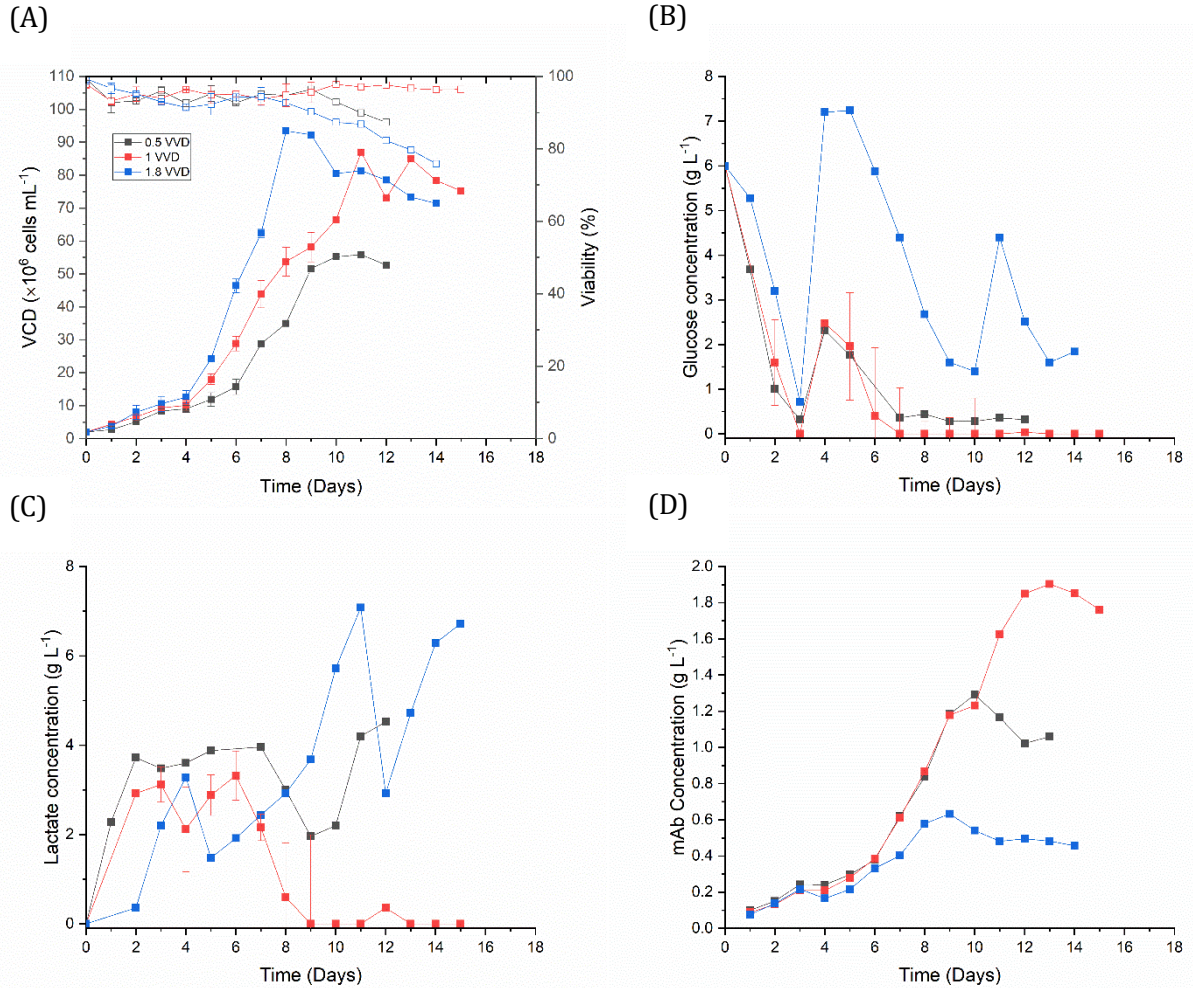


Figure 5.8 - Perfusion CHO cell culture in 250mL BR. Cultures were seeded at 2×10^6 cells mL⁻¹ and maintained at 37°C, pH 7.2, DO 30%, N = 250 RPM. Perfusion was initiated on day 3, exchanging with CD-CHO media blended with 15% Efficient Feed B at an exchange rate of 0.5, 1 or 1.8 VVD. Cell retention was achieved with TFF and a recirculation flow rate of 80 mL min⁻¹. (A) VCD (filled symbols) and viability (empty symbols) (B) Glucose concentration (C) Lactate concentration (D) mAb concentration. Data represents 2 cultures \pm s.d.

Table 5.4- Specific glucose consumption (q_{Gluc}), and lactate (q_{Lac}) and antibody (q_{Ab}) production rates and volumetric productivity for perfusion cultures in 250mL BR at perfusion rates of 0.5, 1 and 1.8 VVD with media blended with 15% Efficient Feed B.

	q_{Gluc} (pg cell ⁻¹ day ⁻¹)	q_{Lac} (pg cell ⁻¹ day ⁻¹)	q_{Ab} (pg cell ⁻¹ day ⁻¹)	Vol prod (g L ⁻¹ day ⁻¹)
0.5 VVD	485	363	23.7	0.32
1 VVD	114	100	22.1	0.87
1.8 VVD	3348	243	23.6	0.64

Cultures exchanged at 0.5 VVD generate peak VCDs of 55×10^6 cells mL^{-1} on day 11, a significant reduction compared to previously described cultures exchanged at 1 VVD and maintain a viability of $>88\%$ for the duration of the culture. Conversely, cultures exchanged at 1.8 VVD show an improved peak VCD of 93×10^6 cells mL^{-1} on day 8, but observe a decline in viability from day 8 to 75%. Glucose concentration profiles for 0.5 and 1 VVD cultures are comparable, with depletion observed from day 7 for the duration of the culture. High glucose concentrations are observed in the early perfusion phase of cultures exchanged at 1.8 VVD, with glucose concentration maintained above 1.5 g L^{-1} for the duration of the culture. Lactate concentration in 0.5 VVD cultures follows a comparable profile to 1 VVD, with lactate consumed from day 7 and a maximum concentration of 3.8 g L^{-1} . Comparatively, over-supplementation of glucose in cultures exchanged at 1.8 VVD causes high lactate concentrations of up to 7 g L^{-1} on day 11. Antibody concentration is greatest when exchanging at 1 VVD, with a maximum titre of 1.9 g L^{-1} . As expected, elevated perfusion rates of 1.8 VVD cause dilution of the product stream, generating lower titres of 0.6 g L^{-1} . Cultures exchanged at 0.5 VVD have a more concentrated product stream and therefore an increased titre compared to 1.8 VVD cultures, reaching a peak of 1.3 g L^{-1} . A comparable q_{Ab} is observed in cultures at each perfusion rate, meaning that as VCD in 0.5 and 1 VVD cultures deviates from day 8, antibody concentration deviates. Despite the lower titres generated in high VVD perfusion cultures, the elevated exchange volume improves productivity compared to low VVD cultures, at 0.64 and $0.32 \text{ g L}^{-1} \text{ day}^{-1}$ for 1.8 and 0.5 VVD cultures respectively. Volumetric productivity is greatest in cultures exchanged at 1 VVD, at $0.87 \text{ g L}^{-1} \text{ day}^{-1}$, where the improvements in maximum titre compared to 1.8 VVD cultures outweigh the decrease in product volume.

Perfusion cultures have been successfully implemented in the 250mL BR at a range of perfusion rates between 0.5 and 1.8 VVD. Maximum VCDs of 93×10^6 cells mL^{-1} are generated in cultures exchanged at 1.8 VVD. The increased media flowrate in 1.8 VVD

cultures increases the reactor foaming, which impacts cell viability directly, by bubble bursting (Walls et al., 2017), and indirectly by increases in osmolality due to higher rates of antifoam addition. Despite 1.8 VVD cultures generating elevated peak VCDs, 1 VVD cultures generate improved titres and volumetric productivities and therefore represent the best performing condition. It is promising that the 250mL BR is capable of supporting HCD cultures close to maximum cell density reported in perfusion cultures of 100×10^6 cells mL^{-1} (Chotteau et al., 2014). Changes to perfusion rate are managed by varying the media inlet and supernatant outlet flowrates, with the minimum feasible perfusion rate lying at 0.5 VVD. Further reductions to perfusion rate is hindered by flowrate fluctuations of $\pm 0.02 \text{ mL min}^{-1}$ in peristaltic pumps. With time, flowrate fluctuations will cause concentration or dilution of the cell culture broth within the reactor, with the greatest impacts observed at the lowest perfusion rates.

It is expected that the implementation of CSPR techniques in place of the maintenance of constant VVD would further improve cell culture performance, as experienced in MWP systems, discussed in Section 3.2.6, Improvements in VCDs are not expected in BR format due limitations of supply of O_2 during the later phase of the cell culture in cultures exchanged at rates equal to or greater than 1 VVD. However, the steady state achieved utilising CSPR techniques has the potential to improve culture performance by limiting available glucose concentration and thus reducing production of lactate, limiting the osmotic effect of base additions. The study of constant CSPR in BR format to enable comparison with performance in MWPs is recommended to be studied in further work, discussed in Section 6.2.

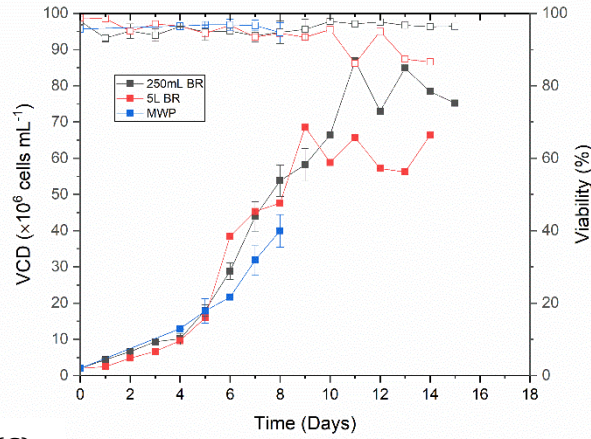
5.2.4. Comparison of culture performance across scales in perfusion mode

Performance of perfusion cultures was subsequently compared across scales, in MWPs, a novel 250mL BR and a commercial 5L BR. Perfusion cultures were carried out as described in Sections 2.5, 2.7.2 and 2.8.2 for MWP, 250mL BRs and 5L BRs, respectively.

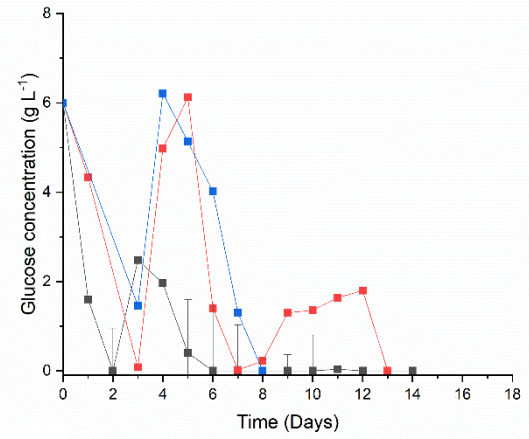
Cells were seeded at a density of 2×10^6 cells mL⁻¹ and perfusion was initiated on day 3 at a rate of 1 VVD, exchanging with CD-CHO blended with 15% Efficient Feed B. **Figure 5.9 A** shows VCD and viability with time for perfusion cultures in MWPs, and 250mL and 5L BRs exchanged at 1 VVD. **Figures 5.9 B, C and D** show corresponding glucose, lactate and antibody concentrations respectively with time. Cell growth is comparable across the BR scales until day 8, generating VCDs of 53 and 47×10^6 cells mL⁻¹ in 250mL and 5L BRs respectively. While cell density follows a comparable profile in MWPs, peak VCDs on day 8 of 40×10^6 cells mL⁻¹ are up to 25% lower compared to those generated in BRs. Continued growth is observed in the 5L BR until day 9, generating peak VCDs of 69×10^6 cells mL⁻¹, before entering the stationary phase. Glucose concentration is comparable in MWPs and 5L BRs, with consumption prior to initiation of perfusion on day 3 followed by a spike to 6 g L^{-1} from day 4. Comparatively, glucose concentration in the 250mL BR is maintained below 3 g L^{-1} for the duration of the culture. Lactate concentration profiles are comparable in BRs, with maximum concentrations of 3.3 and 3.4 g L^{-1} in 250mL and 5L BRs respectively. While lactate concentration is lower in MWPs at a peak of 1.5 g L^{-1} , comparable trends are observed between MWPs and BRs with production on days 2-6 followed by consumption. Production of antibody follows comparable trends in MWP and 250mL BRs until day 8, generating concentrations of 1 and 0.9 g L^{-1} respectively. Production of antibody is lower in 5L BRs, with maximum titres of 0.4 g L^{-1} on day 8. Volumetric productivities are comparable in MWPs and 5L BR, at 0.23 and $0.26 \text{ g L}^{-1} \text{ day}^{-1}$ respectively, while significant increases in antibody concentration cause $4\times$ greater volumetric productivity in the 250mL BR. **Figure 5.9 E** shows maximum specific growth rate (μ_{\max}) for each of the perfusion cultures at the three scales. Comparable μ_{\max} is observed between all scales, with a maximum deviation of 11% observed between the mL-scale MWP and the 5L BR. It can therefore be suggested that MWP quasi-perfusion cultures can provide appropriate prediction of μ_{\max} obtained in BRs. **Figure 5.9 F** shows specific glucose consumption (q_{Gluc}), specific lactate production (q_{Lac}) and specific

antibody production (q_{Ab}) for perfusion cultures at 1 VVD in MWP and 250mL and 5L BRs. Variation is observed in q_{Gluc} at varying scales, with MWP presenting the greatest consumption, 14% higher than the 5L BR. Lactate production in BRs at 250mL and 5L scales are closely comparable, with q_{Lac} in MWPs significantly lower. Reduction in q_{Lac} in MWPs is most likely a function of periodic media exchanges, meaning lactate concentration fluctuated between media exchanges and nutrient limitations prior to media exchange can initiate a shift to lactate consumption over production. Specific antibody production is closely comparable in the 250mL BR and MWP, with a minor deviation of 3%. Production in the 5L BR is comparatively lower, approximately half compared to the alternative scales. Reduced production in the 5L BR can be attributed to reduced viability during the stationary phase of the culture, caused by increased foam production from the placement of cell return into the BR.

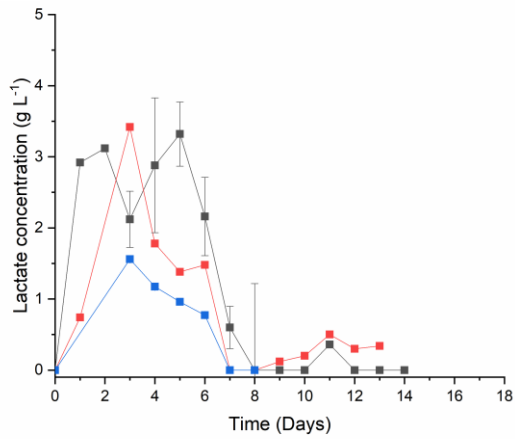
(A)



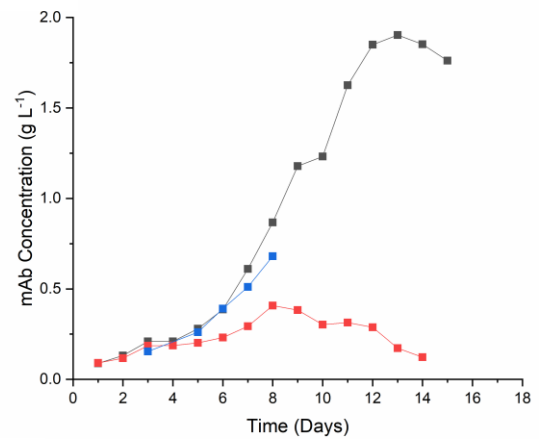
(B)



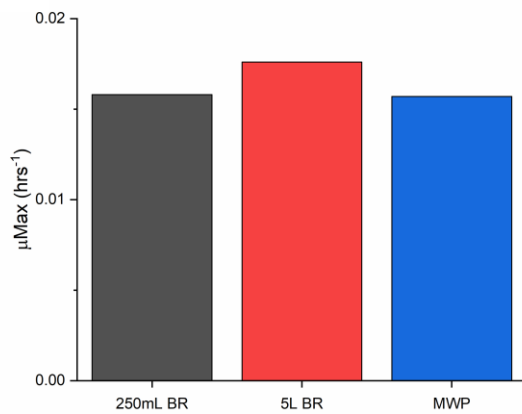
(C)



(D)



(E)



(F)

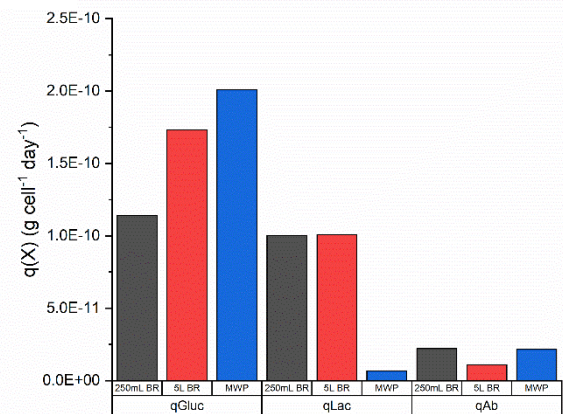


Figure 5.9 - Comparison of perfusion CHO cell culture performance in MWP, 250mL BR and 5L BR. Cultures were seeded at 2×10^6 cells mL^{-1} and maintained at 37°C , pH 7.2, DO 30%, perfusion was initiated on day 3 at a rate of 1 VVD, exchanged with CD-CHO media blended with 15% Efficient Feed B. Cell retention in 250mL and 5L BRs were achieved with TFF, and in MWP was achieved via discontinuous media exchanges following centrifugation. (A) VCD (filled symbols) and viability (empty symbols) (B) Glucose concentration (C) Lactate concentration (D) mAb concentration (E) μ_{max} (F) Specific glucose consumption, and lactate and antibody production. MWP data represents 3 cultures \pm s.d. 250mLBR data represents 2 cultures \pm s.d. 5L BR culture represents 1 culture.

Figure 5.10 shows DO, pH and temperature control in the 5L BR during perfusion culture at 1 VVD. Temperature is well controlled throughout the culture duration at $37\pm 0.5^\circ\text{C}$, and pH is maintained at 7.2 ± 0.1 . DO is well controlled at 30% until day 4, where increases in cell density cause depletion in oxygen saturation. Following comparable protocols implemented in the 250mL BR during perfusion mode, RPM was increased once daily as required to increase k_La and improve oxygen availability. RPM increases were calculated such that increases to u_{tip} were constant between 250mL and 5L BRs, and therefore increases of 8 RPM were implemented in the 5L BR to a maximum of 300 RPM, increasing k_La from 6.2 hrs^{-1} to 8.0 hrs^{-1} at 260 and 300 RPM, respectively. Despite RPM increases, oxygen concentration is low, between 2-7% from day 8 of the culture. The depletion of oxygen corresponds with the culture entering the stationary phase, suggesting that oxygen concentration limits cell proliferation. Rotational speed of the centrifugal pump to maintain a constant recirculation flowrate of 800 mL min^{-1} during perfusion culture in the 5L BR can be found in the Appendix 5.

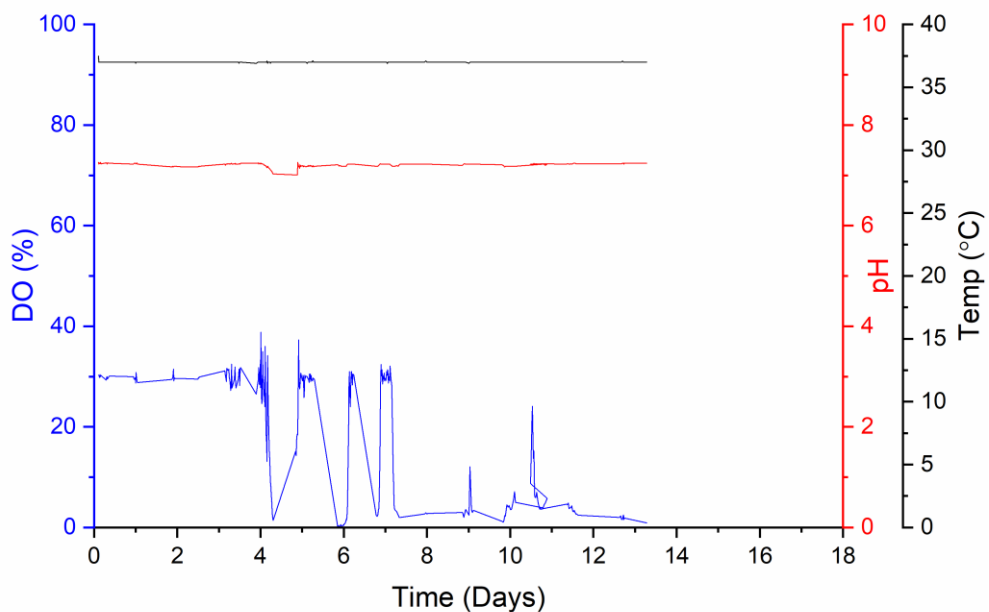


Figure 5.10 - Control profile in 5L BR during perfusion CHO cell culture at an exchange rate of 1 VVD. DO (blue), pH (red) and temperature (black). Data represents 1 culture.

Comparable perfusion culture performance has been demonstrated across scales until day 8 when scaling on the basis of constant power input per unit volume. Deviations in cell culture performance are observed between 250mL and 5L BRs from day 8, which can be attributed to reduced k_{La} causing oxygen limitations at very HCD in the 5L BR. Cell density in MWP are closely comparable to those achieved in BRs until day 5, after which minor deviations are observed. Performance deviation in MWP are attributed to comparable factors as described in fed-batch comparisons, and include pH fluctuations due to bolus control methodologies, and oxygen limitations. Differences in methodology from fed-batch to perfusion provides some advantages when comparing performance across scales. Since MWP have no on-line control of pH, quasi-perfusion cultures, where media is refreshed daily, limit lactate build up and therefore maintain lactate concentrations within the limits of media buffering capacity. Additionally, media exchange every 24 hours, reduces the exposure time to elevated concentrations of lactate. The benefits incurred from introducing media exchanges in MWP compared to fed-batch improve performance, generating cell growth curves more comparable to those achieved in BRs. While fed-batch protocols see a deviation of 30% in peak cell densities between MWP and BRs, deviation is reduced when utilising perfusion protocols to $\leq 25\%$. While it was predicted that increasing complexity of operation in MWP would further amplify the deviations between BRs, periodic media exchanges have helped to overcome some of the factors limiting performance in batch and fed-batch modes. Despite improvements, the ability to sparge pure oxygen into BRs facilitates the support of HCD cultures, and as such elevated cell densities are achieved in comparison.

Comparable performance is observed across scales in metabolite concentration and growth profiles, however a noteworthy difference is observed in product concentration between 250mL and 5L BRs. Lower antibody production can be attributed to reduced average cell density during the stationary phase, with additional q_{Ab} suppression likely

a function of reduced viability in the 5L BR during the stationary phase. Reduced viability in 5L reactor cultures is caused, as previously discussed, by oxygen limitations but additionally by increased foaming compared to 250mL BRs due to the position and increased flowrate of cell return of the cell retention loop. While foaming is minimised in the 250mL BR due to recirculation connection below the liquid level, the 5L reactor returns through the headplate, which increases foam production. Subsequent bubble bursting from excessive foaming in the 5L BR impacts the viability and therefore productivity. Therefore, it is expected that improvements in operation of the 5L BR, for example introducing a comparable dual impeller system to the 250mL BR to increase k_{La} and improving the placement of recirculation return to minimise foaming.

5.2.5. Validation of scale-down quasi-perfusion MWP mimic against novel BR at varying perfusion rates

Since the performance of the 250mL BR has been validated as a suitable scale-down model against a pre-existing 5L BR, the suitability of the 250mL BR and MWPs as a scale-down tool for process optimisation was investigated by varying perfusion rates between 0.5-1.8 VVD. Perfusion cultures were seeded at 2×10^6 cells mL^{-1} with perfusion initiated on day 3, exchanging with CD-CHO media blended with 15% Efficient Feed B. **Figure 5.11 A, B, and C** show VCD and viability with time for 250mL BR and MWPs exchanged at 0.5, 1 and 1.8 VVD respectively. For each perfusion rate, close comparison is observed in cell culture performance in the early phase of the culture, until days 5-7, dependant on the perfusion rate. Performance between 250mL BRs and MWPs in sedimentation and centrifugation modes are within the range of error, with VCDs between $21\text{-}28 \times 10^6$ cells mL^{-1} on day 7. Additionally, viability is maintained above 94% across all scales. For cultures exchanged at 1 VVD, close comparison is maintained until day 6, with VCDs between $20\text{-}28 \times 10^6$ cells mL^{-1} and comparable viability profiles above 96% for the culture duration. Cultures exchanged at 1.8 VVD show the least comparable performance, with close comparison until day 4 before deviations are observed. **Figure**

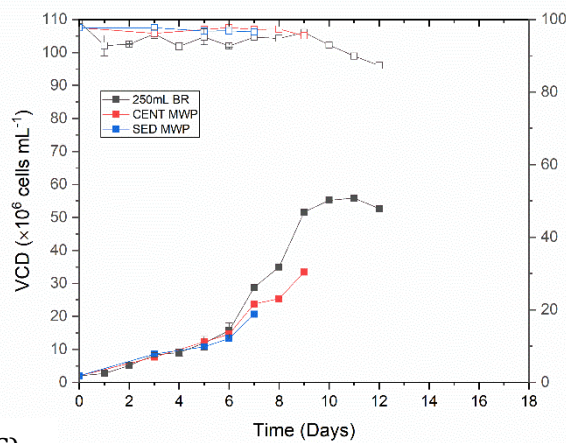
5.11 D compares maximum VCD achieved between the 250mL BR and MWPs in sedimentation and centrifugation mode. While maximum VCDs are not comparable, performance ranking between BRs and MWPs are consistent. Both the 250mL BR and MWPs show a trend between increasing perfusion rates generating increased maximum VCDs. Improvements in VCDs observed by increasing perfusion rates are comparable, with a 25 and 35% increase in maximum VCD when increasing perfusion rates from 0.5 to 1 VVD in MWPs and 250mL BR, respectively. Further increasing the perfusion rate from 1 to 1.8 VVD led to additional improvements to VCD, however in both the BR and MWP, percentage improvements are smaller at 8% in both 250mL BRs and MWPs. Both the rank of VCDs and the percentage increase in maximum VCD achieved at varying perfusion rates has been shown to be consistent between 250mL BRs and MWPs.

Figure 5.11 E shows μ_{\max} for 250mL BR and MWP cultures exchanged at perfusion rates between 0.5-1.8 VVD. μ_{\max} is shown to increase as perfusion rate increases, with each perfusion rate demonstrating comparable μ_{\max} across BRs and MWPs. Maximum deviations of 15% observed in cultures exchanged at 0.5 VVD, with cultures exchanged at 1 and 1.8 VVD showing 4% and 1% deviations respectively. Close comparability with minimal deviations between MWP and BRs suggests that μ_{\max} in BR cultures can be successfully predicted from MWP quasi-perfusion cultures at a range of perfusion rates.

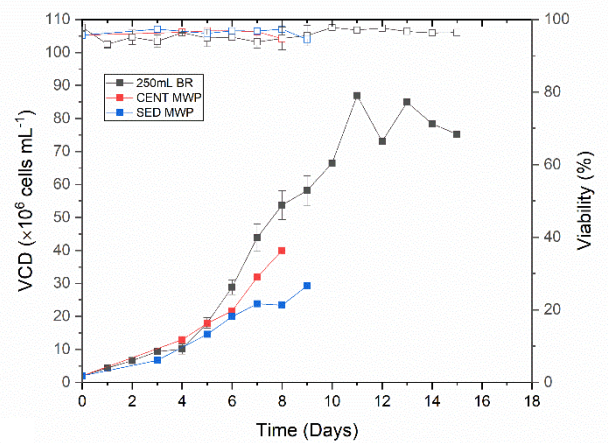
Biomass is an important factor to consider when designing a perfusion culture process, and the ability to predict loading into the cell retention device will enable appropriate size selection. **Figures 5.11 F, G and H** show biomass volume as a percentage of the reactor volume with time for cultures exchanged at 0.5, 1 and 1.8 VVD respectively. Biomass was calculated as described in Section 2.9.6 from VCD and average cell diameter. Biomass volume follows comparable trends to VCD, as previously discussed. Cultures exchanged at 0.5 VVD in the 250mL BR and microwell plates have comparable biomass volumes between 4.8-6.3 % on day 7, with a maximum of 11% observed in the

250mL BR on day 10. For cultures exchanged at 1 VVD, biomass remains comparable until day 6, at volumes between 4.7-6.2%. Continued growth in the 250mL BR generates biomass volumes of >18%. In cultures exchanged at 1.8 VVD, greater variation is observed in biomass volume between 250mL BR and MWPs, with a biomass of 9 and 4.4% respectively on day 6. Continued growth in the 250mL BR generates biomass volumes of 17% on day 8. Despite cultures at 1.8 VVD generating higher VCDs than 1 VVD cultures, a reduction in biomass volume is observed. Elevated growth rates and increased shear rates due to higher recirculation flowrates in 1.8 VVD cultures reduces the mean cell diameter, from 16 to 14.8 μm on day 14 for cultures exchanged at 1 VVD and 1.8 VVD respectively. Performance ranking for biomass production is identical for the 250mL BR and MWP, with 1 VVD cultures producing the greatest biomass volume in 250mL BRs on day 14 and on day 8 in MWPs.

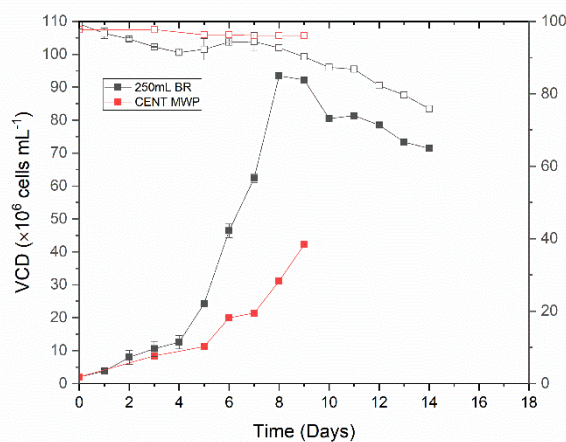
(A)



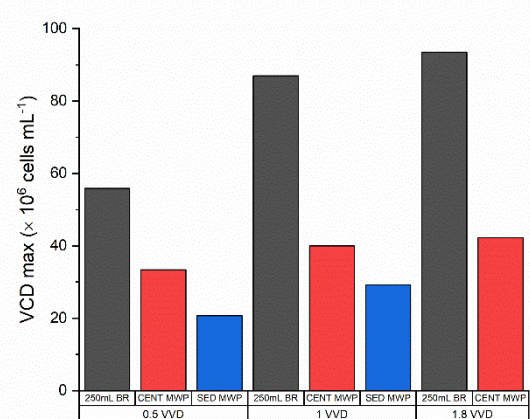
(B)



(C)



(D)



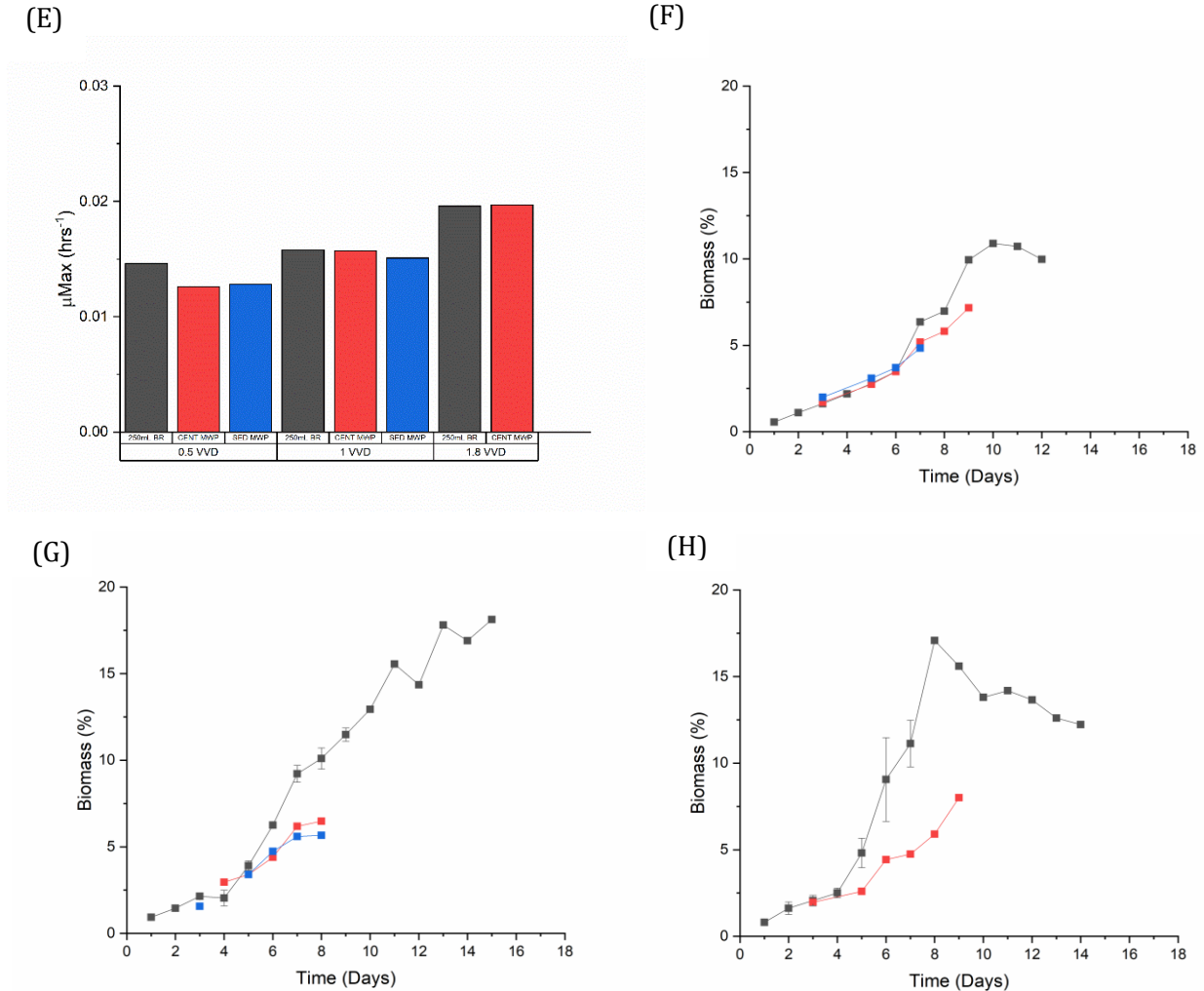
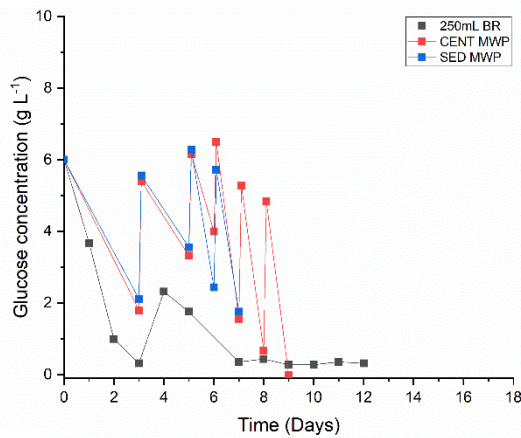


Figure 5.11 - Comparison of perfusion CHO cell culture performance in MWP, in quasi-perfusion sedimentation and quasi-perfusion centrifugation modes, and in 250mL BR at exchange rates of 0.5, 1 or 1.8 VVD. Cultures were seeded at 2×10^6 cells mL⁻¹ and maintained at 37°C, pH 7.2, DO 30%. N = 220 RPM in MWP, N = 250 RPM in 250mL BR. (A) VCD (filled symbols) and viability (empty symbols) for perfusion cultures exchanged at 0.5 VVD (B) VCD (filled symbols) and viability (empty symbols) for perfusion cultures exchanged at 1 VVD (C) VCD (filled symbols) and viability (empty symbols) for perfusion cultures exchanged at 1.8 VVD (D) Maximum VCD achieved in quasi-perfusion sedimentation, quasi-perfusion centrifugation and perfusion in 250mL BR at 0.5, 1 and 1.8 VVD. (E) μ_{max} in quasi-perfusion sedimentation, quasi-perfusion centrifugation and perfusion in 250mL BR at 0.5, 1 and 1.8 VVD. (F) Biomass for perfusion cultures exchanged at 0.5 VVD (G) Biomass for perfusion cultures exchanged at 1 VVD (H) Biomass for perfusion cultures exchanged at 1.8 VVD. Data represents 2 cultures \pm s.d.

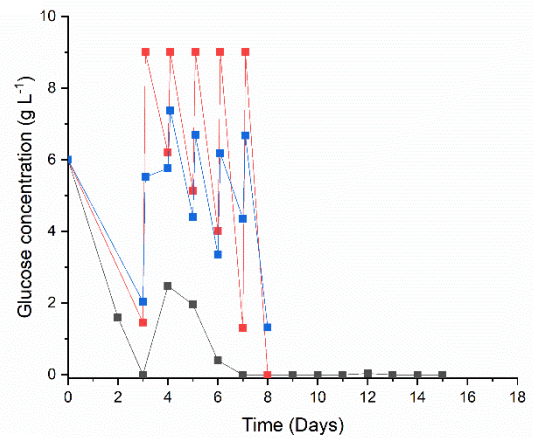
Figures 5.12 A, B and C show glucose concentration with time for 250mL BR and MWP cultures exchanged at perfusion rates of 0.5, 1 and 1.8 VVD respectively. Periodic media exchange in MWPs cause fluctuations in glucose concentrations as spent media is replaced by fresh media at 12 - 24 hours intervals. Despite deviations in glucose concentration profiles attributed to the nature of periodic media exchange in quasi-perfusion MWPs vs. constant exchange in 250mL BRs, glucose concentration profiles

follow comparable trends, particularly in cultures exchanged at 0.5 and 1.8 VVD. **Figures 5.12 D, E and F** show lactate concentration with time for 250mL BR and MWP cultures exchanged at perfusion rates of 0.5, 1 and 1.8 VVD respectively. Lactate production across all perfusion rates is greater in the 250mL BR compared to the MWP. In the 250mL BR, elevated lactate concentrations are observed, above 4 g L⁻¹ and 7 g L⁻¹ at a perfusion rate of 0.5 and 1.8 VVD respectively. Comparatively, MWPs maintain lactate concentrations below 1.5 g L⁻¹ for the duration of the culture.

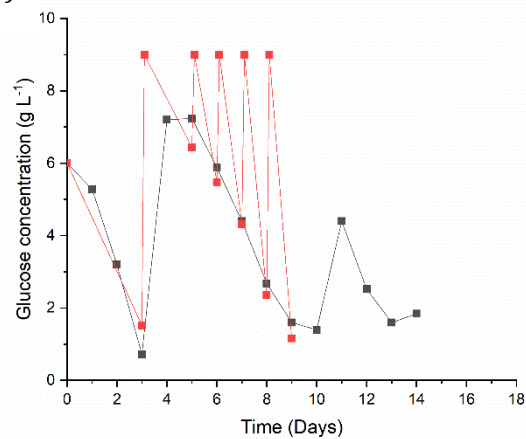
(A)



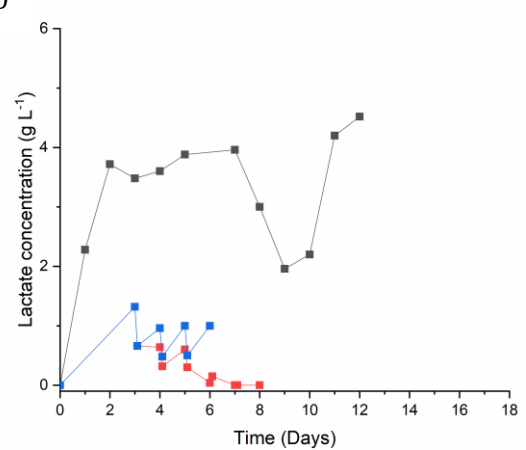
(B)



(C)



(D)



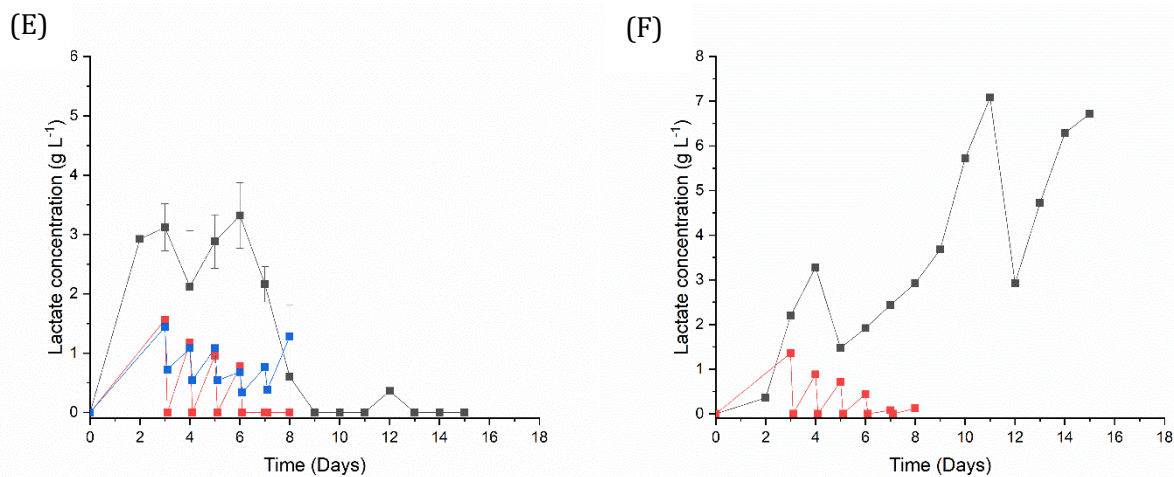


Figure 5.12 - Comparison of perfusion CHO cell culture performance in MWP, in quasi-perfusion sedimentation and quasi-perfusion centrifugation modes, and in 250mL BR at exchange rates of 0.5, 1 or 1.8 VVD. Cultures were seeded at 2×10^6 cells mL⁻¹ and maintained at 37°C, pH 7.2, DO 30%. N = 220 RPM in MWP, N = 250 RPM in 250mL BR. (A) Glucose concentration for cultures exchanged at 0.5 VVD (B) Glucose concentration for cultures exchanged at 1 VVD (C) Glucose concentration for cultures exchanged at 1.8 VVD (D) Lactate concentration for cultures exchanged at 0.5 VVD (E) Lactate concentration for cultures exchanged at 1 VVD (F) Lactate concentration for cultures exchanged at 1.8 VVD. Data represents 2 cultures \pm s.d.

Figure 5.13 A, B and C shows antibody concentration with time for 250mL BR and MWP cultures exchanged at 0.5, 1 and 1.8 VVD respectively. For each perfusion rate, close agreement in titre observed with time between BRs and MWPs. Cultures exchanged at 0.5 VVD see the greatest variation between titres at various scales, with titres between 0.6-1 g L⁻¹ on day 7. Titres in MWPs at an exchange rate of 0.5 VVD represent the maximum achieved in MWPs across all perfusion rates analysed. Maximum titres in BRs of 1.9 g L⁻¹ were achieved at a perfusion rate of 1 VVD, with MWP cultures maintaining close comparability until day 7. Peak VCDs in MWP at 1 VVD of 1 and 0.6 g L⁻¹ in centrifugation and sedimentation modes respectively represented the second greatest performance for respective modes in MWPs. Cultures exchanged at 1.8 VVD observe a close likeness for the duration of the culture, with maximum titres of 0.76 and 0.63 g L⁻¹ in BRs and MWPs respectively. While cultures exchanged at 1.8 VVD see the lowest titres, variable exchange volumes mean that volumetric productivities are not a direct function of titre. **Figure 5.13 D** shows volumetric productivity for cultures exchanged at rates between 0.5-1.8 VVD in BR and MWPs. Cultures exchanged at 0.5 VVD see the lowest

volumetric productivity in both BR and MWP, between 0.16-0.37 g L⁻¹ day⁻¹. MWP cultures exchanged at 1 VVD have the second greatest volumetric productivity at 0.25 g L⁻¹ day⁻¹ across both sedimentation and centrifugation modes. Conversely, the high titres achieved in BR when exchanging at 1 VVD lead to the greatest volumetric productivity in BRs of 1 g L⁻¹ day⁻¹, despite the reduced exchanged volume compared to 1.8 VVD cultures. Some deviation is observed when ranking antibody production with perfusion rates between MWPs and BRs. While cultures exchanged at 0.5 VVD generate the lowest volumetric productivities in MWPs and BRs, cultures exchanged at 1 VVD are the best-performing in BRs while cultures exchanged at 1.8 VVD represent the best performance in MWPs.

An additional consideration when considering the suitability of a scale-down system, in terms of productivity, is product quality. **Figure 5.13 E** shows an SDS-Page gel loaded with supernatant, normalised based on product concentration, for perfusion cultures at 0.5-1.8 VVD in MWPs and BRs at 250mL and 5L scale, and in fed-batch modes in 250mL BR and MWP for comparison. Across each scale in fed-batch and perfusion, the deepest band is observed at approximately 150kDa, the expected molecular weight of a mAb (Janeway et al., 2001). High molecular weight forms are observed across all scales, at a molecular weight of approximately 200 kDa. Multiple low molecular weight forms and fragments can be observed across scales, between 116.3-31 kDa. While in-depth product quality analysis was not possible, gel analysis provides an insight into protein sizes within supernatant, presence of aggregates and low/high molecular weight forms. Comparable ratios between mAb product and alternative forms are observed between sizes at each scale and in perfusion vs fed-batch.

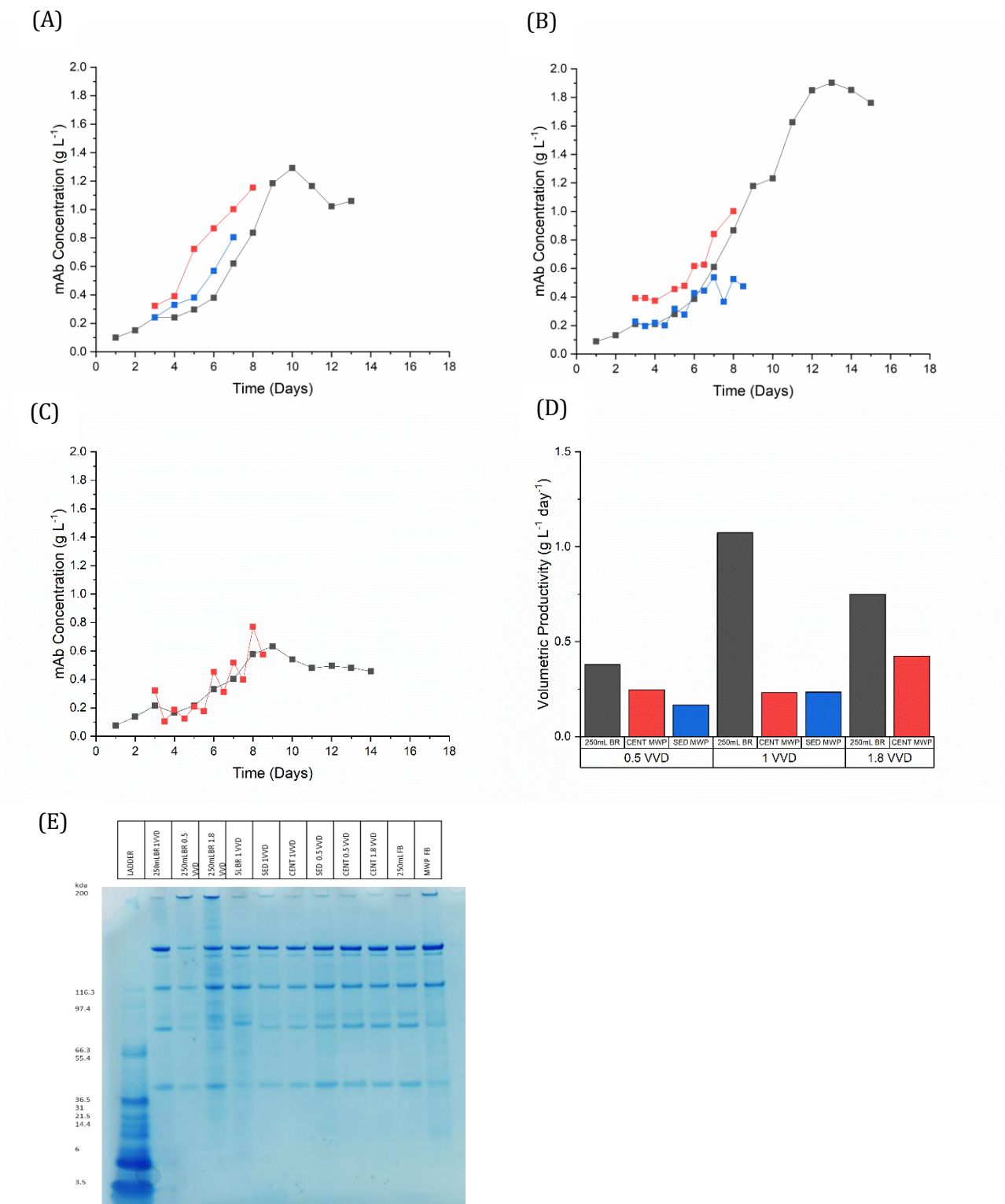


Figure 5.13 - Comparison of perfusion CHO cell culture performance in MWP, in quasi-perfusion sedimentation and quasi-perfusion centrifugation modes, and in 250mL BR at exchange rates of 0.5, 1 or 1.8 VVD. Cultures were seeded at 2×10^6 cells mL⁻¹ and maintained at 37°C, pH 7.2, DO 30%. N = 220 RPM in MWP, N = 250 RPM in 250mL BR. (A) mAb concentration for perfusion cultures exchanged at 0.5 VVD (B) mAb concentration for perfusion cultures exchanged at 1 VVD (C) mAb concentration for perfusion cultures exchanged at 1.8 VVD (D) Volumetric productivity for MWP quasi-perfusion sedimentation, quasi-perfusion centrifugation and 250mL BR at 0.5, 1 and 1.8 VVD (E) SDS-Page gel for MWP quasi-perfusion sedimentation, quasi-perfusion centrifugation and 250mL BR at 0.5, 1 and 1.8 VVD. Data represents 2 cultures.

Figure 5.14 A shows q_{Gluc} for perfusion cultures in MWP and 250mL BR. Variation is observed between MWP and BR systems at otherwise identical conditions. Greatest variation is observed at the lowest perfusion rate, with q_{Gluc} in both sedimentation and centrifugation MWPs approximately half of those observed in the BR. For higher perfusion rates, q_{Gluc} is over-estimated in MWP compared to BR, with the closest comparability observed at a perfusion rate of 1.8 VVD which sees a 20% increase in MWP q_{Gluc} compared to BR. It was expected that glucose consumption is a function of varying culture lengths in BRs compared to MWPs, while MWPs focus on the growth phase and run for a maximum of 9 days, extended cultures are carried out in BRs, into the stationary phase until day 15. However, comparing q_{Gluc} until day 9 in BRs to those obtained in MWP show comparable patterns. **Figure 5.14 B** shows q_{Lac} for perfusion cultures in MWP and 250mL BR. As observed in **Figures 5.12 D-E**, lactate production is significantly less in MWP compared to BR, which is reflected in reduced q_{Lac} . Reduced lactate production in MWP could be caused by several factors, including from impacts due to periodic media exchanges. Periodic media exchanged in MWP means that lactate concentration fluctuates with time, and glucose can be depleted prior to media exchange, initiating lactate consumption. **Figure 5.14 C** shows q_{Ab} for perfusion cultures in MWP and 250mL BR. Close agreement is observed in q_{Ab} across all scales and perfusion rates, with centrifugation cultures providing the most accurate and consistent prediction of q_{Ab} in the 250mL BR. Maximum deviations of 30% are observed between sedimentation and BR cultures at 1 VVD, with centrifugation cultures experiencing maximum deviation of 8% at 0.5 VVD.

Cell specific perfusion rate (CSPR) is an important process variable specific to perfusion cultures. Minimum CSPR (CSPR_{min}) is defined specifically for processes and is dependent on media composition, cell line and perfusion rate. Identifying minimum perfusion rates allows for the reduction of costs associated with media without impacting process performance. **Figure 5.14 D** shows CSPR_{min} for BR and MWP cultures exchanged

between 0.5-1.8 VVD. $CSPR_{min}$ was calculated as described in **Equation 2.19** and is related to maximum VCD achieved. For each perfusion rate, $CSPR_{min}$ is over estimated in MWPs compared to BRs, due to the shorter cultures and limitations to continued proliferation in MWPs, as discussed in Section 3.2.4. Despite variations, BRs and MWPs follow identical ranking, with the $CSPR_{min}$ a factor of the perfusion rate.

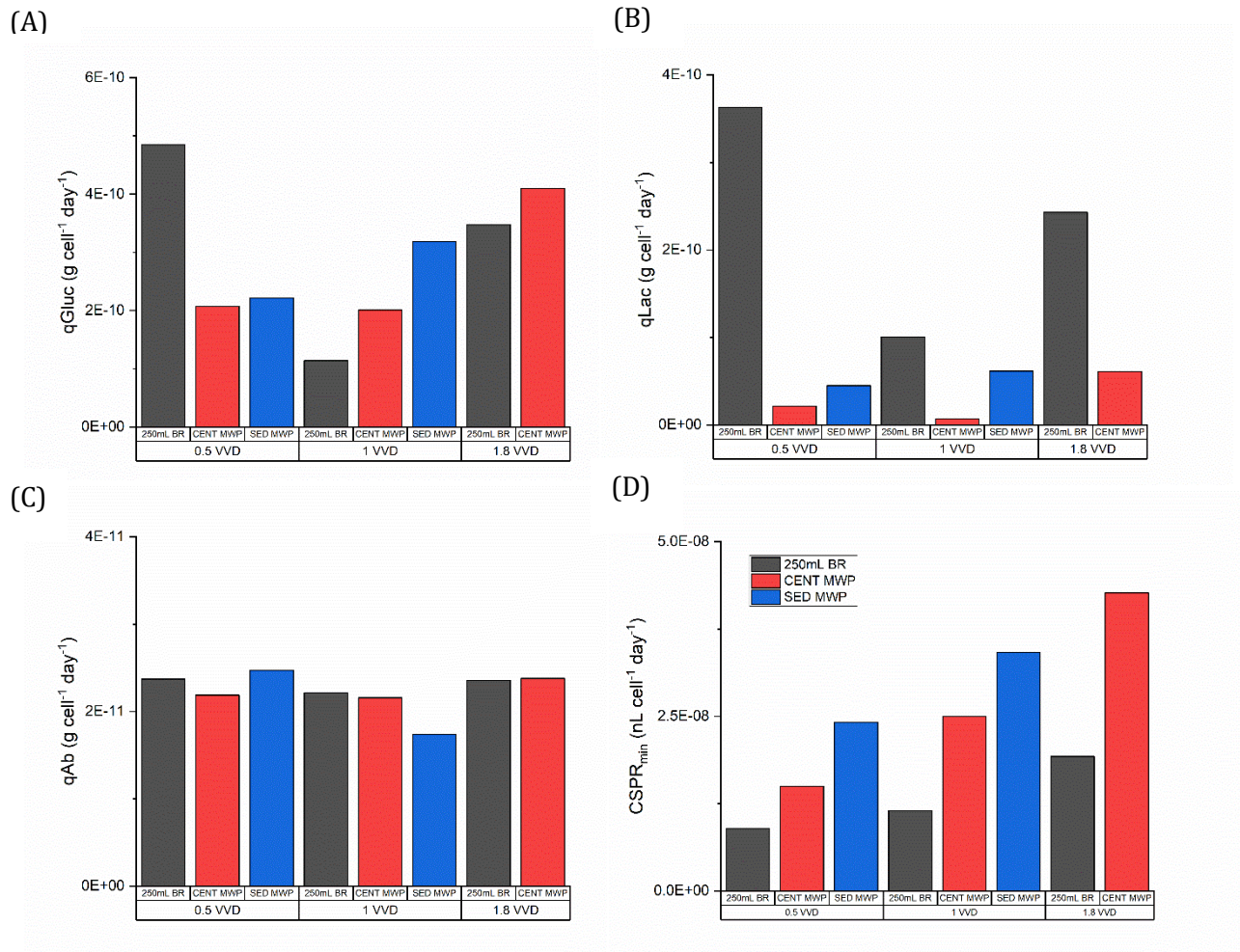


Figure 5.14- Comparison of perfusion CHO cell culture performance in MWP, in quasi-perfusion sedimentation and quasi-perfusion centrifugation modes, and in 250mL BR at exchange rates of 0.5, 1 and 1.8 VVD. Cultures were seeded at 2×10^6 cells mL^{-1} and maintained at 37°C, pH 7.2, DO 30%. N = 220 RPM in MWP, N = 250 RPM in 250mL BR. (A) Specific glucose consumption (q_{Gluc}) (B) Specific lactate consumption (q_{Lac}) (C) Specific antibody production (q_{Ab}) (D) $CSPR_{min}$. Data represents 2 cultures.

Overall, results obtained in MWPs have been shown to be indicative of performance in BR system across cell growth, metabolite consumption and lactate and antibody

production and perform comparably compared to previously published scale-down models for perfusion culture at mL-scale (Bielser et al., 2019, Wolf et al., 2018, Villiger-Oberbek et al., 2015). Performance in MWP is closely comparable to BRs until day 7, where deviations begin to be observed, due to the limitations of MWP caused by lack of instrumentation and periodic, rather than continuous, media exchange. Deviations between scales are most prominent in cultures exchanged at 1.8 VVD, the highest perfusion rate investigated. Because of the elevated exchange rate, cultures exchanged at 1.8 VVD are less inhibited by nutrient availability, and are less likely to experience high lactate concentrations. The alleviation of nutrient limitations across scales means that the oxygen limitations in MWP are more apparent compared to lower VVD cultures which observe nutrient limitations in both MWP and BRs. Despite variations observed in arbitrary performance, such as VCD, calculated performance metrics have been shown to demonstrate close comparability. Percentage volume of biomass with time is closely comparable, which enables the appropriate selection of the cell retention device in the large-scale process based on required solids loading capacity. Additionally, μ_{\max} in MWP are predictive of performance in BRs, with maximum deviations of 15% observed at the lowest perfusion rate, and error decreasing with increasing perfusion rate.

Specific consumption of glucose is under-estimated in low VVD cultures, and over-estimated in mid and high ranging VVDs, with closest comparison observed at 1.8 VVD, the highest perfusion rate investigated. Lactate production is also varied, with BRs producing significantly higher concentrations of lactate compared to MWP. It is expected that varying glucose consumption and lactate production between BR and MWP is related to periodic media exchanges in MWP cultures compared to constant exchange in BRs. The deviation in media feeding strategies has caused the most significant deviations between MWP and BRs, due to fluctuating concentrations of metabolites, product and by-products. Glucose consumption is greater in systems with greater glucose availability (Lu et al., 2005), such as the BR culture at 0.5 VVD which has

relatively low maximum VCDs compared to alternative cultures, and BR at 1.8 VVD. It therefore logical that MWPs follow comparable trends, with cultures exchanged at 0.5 VVD having the lowest glucose availability and 24 hour periods between exchange, experiencing the lowest q_{Gluc} . Comparing sedimentation and centrifugation cultures in MWP at 1 VVD supports this, with sedimentation cultures exchanged at 12 hour intervals, and therefore having more consistent glucose concentrations than centrifugation cultures exchanged every 24 hours, having elevated q_{Gluc} . Despite variations in glucose consumption, ranking of BR and MWP performance as a function of VVD, and therefore quantity of glucose added, is identical with increasing perfusion rates generated improved performance.

Performance metrics related to the production of mAb are comparable across BR and MWP, with q_{Ab} obtained in BR and MWPs at identical VVDs obtaining minor deviations to a maximum of 8% for centrifugation MWP cultures. Additionally, titres are comparable across perfusion rates for the duration of MWP cultures. Volumetric productivity, whilst higher in BRs due to the elongated cultures, shows comparable performance ranking. Gel analysis suggests that comparable product quality is achieved, with ratios of high and low molecular weight forms and fragments are observed across MWPs and BRs.

In conclusion, MWPs have been shown to generate a good scale-down model for perfusion culture performance in BRs. VCD, viability, biomass show comparable profiles with time until day 6 of the culture, with titre maintained for the duration of the MWP culture. Performance metrics such as μ_{max} and q_{Ab} in MWP is predictive of BR performance, with an acceptable maximum error of 8% for centrifugation cultures and 30% in sedimentation cultures.

5.3. Summary

A novel 250mL BR was developed to enable scale-down process design of perfusion cultures. Initial experiments focused on the set-up and optimisation of BR performance in batch and fed-batch modes. Improvements to PID control were implemented to enable consistent, accurate control of pH, DO and temperature for the duration of the culture. Improved PID settings were capable of maintaining pH at 7.2 ± 0.1 , temperature at $33.5\pm 0.2^\circ\text{C}$, ($T_{in}=37\pm 0.2^\circ\text{C}$) and DO at $30\pm 10\%$ in the early growth phase of the culture. Increasing VCDs in fed-batch cultures were observed with PID improvements, from initial runs generating maximum VCDs of 7.3×10^6 cells mL^{-1} to final runs achieving VCDs of 14×10^6 cells mL^{-1} . Comparing batch and fed-batch performance to MWPs and commercially available 5L BR generated comparable μ_{max} , glucose concentration profiles, and productivity; volumetric, titre, and q_{Ab} .

Perfusion was achieved via connection of TFF to the cell retention connectors on the base and the side of the reactor, with recirculation at 80 mL min^{-1} and an initial perfusion rate of 1 VVD. The novel 250mL BR was capable of supporting cell densities of up to 86×10^6 cells mL^{-1} and maintaining viability $>96\%$, comparable to alternative studies conducted in BR at similar scale, who report maximum VCDs of 90×10^6 cells mL^{-1} (Chotteau et al., 2014). Control settings were optimised for perfusion culture, which included the increase of impeller rotational speed during continued growth above 20×10^6 cells mL^{-1} , to increase k_La and allow for the maintenance of DO in HCD cultures. Performance in the 250mL BR, 5L BR and MWP at an exchange rate of 1 VVD is comparable, with VCD maintained until day 9 with a maximum deviation of 12%. Performance metrics including μ_{max} and q_{Ab} are comparable across all scales from mL to L. MWPs have significantly lower q_{Lac} compared to BRs, which show close comparison between 250mL and 5L scale. From experiments conducted at 1 VVD, it can be concluded that perfusion culture in the 250mL BR is comparable to and predictive of performance

in larger pre-existing vessels, with deviations in VCD related to gas transfer limitations and excessive foam production in the 5L BR.

Further experiments in the 250mL BR were carried out at perfusion rates of 0.5 and 1.8 VVD, which obtained maximum VCDs of 56 and 94×10^6 cells mL⁻¹ respectively. Performance was compared between the 250mL BR and in MWPs, previously described in Section 3.2, to determine the scale-up performance of MWPs. Analysis of performance in MWPs and 250mL BR at 0.5, 1 and 1.8 VVD show close comparison between MWPs and BRs across multiple performance metrics. Cell culture performance in MWPs is limited by periodic media exchanges and reliance on gas transfer by diffusion of air, meaning that VCD_{max} obtained in MWPs is lower than those generated in BRs. However, comparable μ_{max} , biomass, and viability profiles are obtained across MWPs and BRs at each perfusion rate. Specific glucose consumption was shown to vary between MWPs and BRs, with lower glucose consumption observed at low perfusion rates and elevated glucose consumption at higher perfusion rates. Lactate production was shown to be significantly under-estimated in MWPs at all perfusion rates analysed. Variation in q_{Gluc} and q_{Lac} is expected to be a function of periodic media exchanges rather than continuous, causing wide fluctuations in concentration in glucose and lactate between media exchanges, which in turn affects glucose consumption and lactate production rates. Production of antibody is shown to be comparable in MWPs and BRs, with comparable titres observed and equivalent q_{Ab} across each perfusion rate. Additionally, brief analysis of product quality demonstrates comparable ratios of high and low molecular weight forms, fragments and aggregates are present in MWPs and BRs. Performance in MWPs is limited by discontinuous media exchanges and reliance on headspace air for gas transfer. Performance could be more closely aligned with that achieved in the BR by increasing the frequency of media exchanges in order to more closely mimic the steady state environment of continuous perfusion culture in BRs, it would be beneficial to incorporate this via automated liquid handling systems. Additionally, to overcome

limitations in oxygen transfer limiting to cell growth in MWPs, introducing gas blending chambers to increase the concentration of oxygen and therefore the partial pressure available for diffusion via the headspace is expected to improve achievable VCDs. Comparing performance of both sedimentation and centrifugation quasi-perfusion methodologies in MWP to BR cultures confirms that centrifugation cultures represent a preferable tool for early phase screening, not only demonstrating improved performance, as discussed in Chapter 3, but also produces results more closely aligned conditions observed in BR cultures at 250mL and 5L scale, thus is shown to be the preferred methodology for scale-down perfusion studies.

The accurate prediction of a wide range of performance metrics allows for the prediction of cell culture performance in BRs from results obtained in MWPs at a range of conditions, enables performance ranking from screening experiments conducted in MWPs and therefore supports the use of MWPs as a reliable, accurate screening scale-down tool for perfusion cultures.

6. CHAPTER 6: CONCLUSIONS

6.1. Concluding remarks

Key objectives of this work included the establishment of sub-liter scale-down systems for perfusion cell culture processes. To fulfil this objective, two systems have been developed; (i) quasi-perfusion in 24-well MWP, described in **Chapter 3** and (ii) a novel 250mL BR, characterised in **Chapter 4** and utilised as a perfusion culture mimic in **Chapter 5**. Both systems achieved the key characteristics of perfusion culture by incorporating cell retention techniques, reaching elevated cell density and increased volumetric productivity compared to fed-batch operations within comparable vessels. Additionally, good scalability was demonstrated utilising constant power input per unit volume as a scaling parameter from 1.2mL scale in MWP, to the novel 250mL BR and to a 5L established bench-scale BR.

Quasi-perfusion methodologies in MWP incorporated two cell retention techniques; (i) sedimentation and (ii) centrifugation, with periodic media exchanges to achieve discontinuous perfusion culture. Both sedimentation and centrifugation methodologies generated VCDs 3.3-4.2 fold greater and volumetric productivities up to 1.9 fold greater compared to fed-batch protocols. Quasi-perfusion methodologies were utilised to screen a variety of media, including concentrated CD-CHO, and CD-CHO supplemented with glucose or nutrient-rich feeding media, Efficient Feed B. MWP methods are shown to be sensitive to changes in media composition, with CD-CHO blended with 15% v/v Feed B representing the best performing media of all those analysed, generating peak VCDs of 21.6 and 23.4×10^6 cells mL⁻¹ on day 7 at a perfusion rate of 1 VVD for sedimentation and centrifugation cultures respectively. In addition to utilising quasi-perfusion techniques to screen a variety of media at 1 VVD, a range of perfusion rates between 0.5-1.8 VVD and the interaction between nutrient density of the media and perfusion rates were investigated. As expected, increasing the perfusion rate generates the greatest cell

density, at 32.2 and 34.2×10^6 cells mL^{-1} on day 9 for sedimentation and centrifugation cultures respectively exchanged at 1.5 VVD with media blended with 15% Feed B, with further improvements of 23% for centrifugation cultures exchanged at 1.8 VVD, to a maximum of 42.2×10^6 cells mL^{-1} whilst maintaining viabilities $>95\%$. The introduction of constant CSPR quasi-perfusion cultures demonstrates the capability of the 1.2mL scale quasi-perfusion MWP system to incorporate more complex processing techniques implemented at pilot scale. Maintaining CSPR generates a steady state cell culture environment, and the benefits of this are reflected in process performance, with constant CSPR cultures attaining VCDs between 10-40% greater on day 7 compared to constant VVD cultures.

The investigation of two methods of cell retention implemented in alternative scale-down quasi-perfusion methodologies allowed for the techniques to be compared and for the identification of performance deviations and relative advantages. It was found that the increased manipulation time associated with sedimentation cultures resulted in a cumulative impact on cell health over time, achieving slightly lower VCDs and viability with time compared to centrifugation cultures under otherwise identical conditions. Additionally, cell separation via sedimentation results in a larger packed cell volume than centrifugation methodologies, meaning the exchange rate is fixed to a maximum of 75% of the total well volume per exchange, limiting the range of perfusion rates that can feasibly be investigated, compared to centrifugation where almost the entirety of the well volume can be exchanged. Overall, quasi-perfusion methodologies were shown to be a robust tool for high throughput screening of media and exchange rate for early phase development of perfusion culture.

Engineering characterisation is an important step in the development of bioprocess methodologies in order to; identify process limitations, such as poor mixing zones, to define a range of feasible process parameters, and to gain a deep understanding of

hydrodynamics within the system to support successful scaling. Oxygen mass transfer coefficient, $k_{L,a}$, was calculated using pre-defined correlations in MWP and the 5L BR and experimentally determined in the novel 250mL BR system since the dual impeller configuration and the geometry is unique, and as such no correlations currently exist in literature for a similar geometry. $k_{L,a}$ was found to be between 6-7.4 hrs^{-1} across each system at operational process conditions, and experimentally determined $k_{L,a}$ was fitted to the Van't Riet equation via regression analysis with exponents comparable to those published in similar reactor systems. An impeller power number of 4.9 was experimentally determined for the dual impeller 250mL BR configuration, with this value being between the expected range for single turbine Rushton (4.5-6.5) and pitched blade (0.25-0.75) impellers. Power input was calculated at $22.6 \pm 7 \text{ W m}^{-3}$ at operational conditions in MWP, and 250mL and 5L BRs.

Mixing dynamics in the 250mL BR were investigated at a range of configurations to ensure homogeneous mixing and to maximise mass transfer for support of very high cell density perfusion cultures. Impeller base clearances, H_i , of 2.5 and 1 cm generated comparable t_m , at 3-6 s^{-1} for $N > 150$ RPM, however more homogenous mixing was achieved at $H_i = 2.5$ cm which was fixed for all subsequent experiments. Perfusion cell cultures at very high cell density present additional challenges compared to fed-batch cultures since cell densities of $> 40 \times 10^6$ cells mL^{-1} are more viscous than lower cell density cultures and exhibit shear-thinning behaviour, with maximum viscosities of cell suspensions at 100×10^6 cells mL^{-1} being 3 fold greater at low shear than water. The impact of viscosity on the system hydrodynamics in very high cell density perfusion cultures was modelled using a low-concentration sodium alginate fluid mimic, and was found to have a negligible impact on the mixing time t_m at operational RPM. In addition to rheological considerations specific to perfusion culture processes, hydrodynamics of perfusion cultures are effected by the cell retention device, and specifically the positioning of the cell recirculation loop. It was found that recirculation configurations,

returning either from below the liquid level from a side port or above the liquid level from the headplate, has a negligible impact on t_m at $N = 250$ RPM, however minor deviations are observed at 400 RPM, the maximum process operational speed. This suggests at high RPM, where t_m in the bulk liquid is lower, t_m is limited by the recirculation flowrate. This is observed to a lesser extent for top recirculation configurations where return from above the liquid level induces turbulence at the surface.

Following analysis of the hydrodynamic environment, the novel 250mL BR was optimised for cell culture, initially in batch and fed-batch culture modes, which generated comparable μ_{Max} , metabolic profiles, and productivity to the 5L BR. Perfusion cultures were subsequently introduced with cell retention achieved via a tangential flow filter, achieving and maintaining VCDs 6 fold greater than fed-batch of 86×10^6 cells mL^{-1} , >96% viability at a perfusion rate of 1 VVD, exchanging with media blended with 15% Efficient Feed B. To maximise O_2 transfer at high cell density, operational RPM, initially set at 250, was incrementally increased to a maximum of 400, which enabled maintenance of the DO setpoint of 30%. Further experiments at 0.5 and 1.8 VVD generated maximum VCDs of 5 and 94×10^6 cells mL^{-1} respectively. Comparing performance in 250mL BR to that in the 5L BR at 1 VVD sees comparable performance, including μ_{Max} and q_{Ab} , and similar cell growth profiles until day 9 of culture. Deviations in VCD from day 9 are related to insufficient O_2 transfer in the 5L BR, $k_L a$ was increased incrementally in the 5L BR by increasing rotational speed and gas flowrate, similarly to in the 250mL BR, however maximum feasible RPM and gas flowrates were still unable to maintain DO setpoints at high cell density. Additionally, excessive foaming was induced which lead to the need for high concentrations of surfactant, increasing osmolality to levels detrimental to cell health. Process performance in the 5L BR, where geometries are fixed and were not designed specifically for perfusion culture, highlights the advantage of designing a novel device specific to the requirements. The 250mL BR

was designed on the basis of maximising mass transfer for support of very high cell density perfusion processes, since process parameters have limited ranges of operation and cannot necessarily improve an inefficient mass transfer or mixing environment within a vessel.

Comparing performance in the 250mL BR to quasi-perfusion culture in MWP demonstrates close comparability across a range of performance metrics including μ_{Max} and q_{Ab} , biomass and viability profiles. Notable deviations in MWP are a significantly lower q_{Lac} and reduced maximum VCDs compared to BRs, which can be attributed to discontinuous media exchange and reliance on diffusion for gas transfer in MWPs. In general, the quasi-perfusion at a range of perfusion rates in MWP is capable of accurate prediction a wide range of performance metrics in BRs under otherwise identical conditions, demonstrating good scalability from 1.2 mL to 250 mL at 0.5 – 1.8 VVD and further to 5 L scale at 1 VVD only, on the basis of constant power input per unit volume, and the maintenance of comparable k_{La} s.

Overall, two scale-down systems have been proposed that are capable of achieving the specific characteristics of perfusion culture, generating very high cell densities and elevated volumetric productivity by incorporating mechanisms of cell retention. In addition, both the MWP and 250mL BR mimics demonstrate comparability to bench-scale processes. Quasi-perfusion mimics in MWP demonstrates a powerful tool for high throughput early phase development, with the advantages of having a reduced volume and increased throughput compared to alternative quasi-perfusion scale-down methodologies. However, quasi-perfusion methodologies present a methodology for early high throughput screening only, since discontinuous media exchanges and inability to sparge O_2 to meet cell respiration demands limits culture performance. The novel 250mL BR provides an optimal environment, facilitating support of very high cell density cultures more comparable to large scale processes, and is therefore suitable for in-depth

investigation of a small number of process parameters. Providing optimal mass transfer was considered in all aspects of design, incorporating dual impeller configurations, an L-shaped sparger and baffles to maximise available capacity for O₂ delivery and CO₂ stripping compared to alternative reactors at comparable scales. Flexibility was incorporated into the design to ensure suitability to alternative expression systems with different mass transfer demands and shear tolerance, including variable baffle geometry and spacing, and removable baffles. It is however important to note that proof of concept across both developed systems has only been undertaken utilising one expression system, and performance of different cell hosts are expected to require some additional optimisation specific to the cell host.

6.2. Recommendations for future work

Chapter 3 describes the development of a quasi-perfusion approach in MWP at 1.2mL scale, achieving elevated cell densities compared to fed-batch by implementing sedimentation or centrifugation cell retention methodologies, and investigating a range of perfusion rates; constant VVD or constant CSPR, and a range of media compositions. Quasi-perfusion methodologies could be expanded by;

- Investigation of a range of cell lines, in combination with varying media compositions previously studied. Analysis of multiple cell lines and comparison of results at scale would further demonstrate the strength of the system as a high-throughput early screening device for perfusion culture.
- Improving the O₂ transfer in the system. It was predicted that the limiting factor to continued cell growth in MWP was DO concentration, since O₂ transfer was reliant on diffusion of atmospheric air enriched with CO₂ at 5% for pH control. Enriching the air with greater concentrations of O₂, either using specialised incubators capable of gas blending, or a chamber within the incubator enriched with O₂, would improve k_{La} and would support cell growth.

- Incorporation of instrumentation to monitor pH and DO throughout the culture. For example, utilising MWP's fitted pH and DO sensor spots (Presens) combined with external reading equipment. Consistent monitoring of pH and DO creates a system which can be more closely compared to BR systems, improving the data available for scale-up, and could be utilised to gain a deeper understanding of limitations to cell culture kinetics within the system.
- Automating MWP systems would allow for a greater number of plates to be manipulated at any one time, and is generally considered to reduce the risk of contamination. During the present study, feasibility of introducing automation was investigated, however there were several limiting factors including excess evaporation during long cell cultures. When introducing automation, a system with humidification would therefore be necessary, comparable to the protocol in manual systems, to limit evaporation.

Chapter 4 describes design, engineering characterisation and hydrodynamic analysis of 250mL BR, and compares values obtained experimentally to those determined in MWP and 5L BR using existing correlations. Characterisation could be furthered by;

- Implementing PIV or CFD analysis into the 250mL BR, to deepen understanding of bulk flow patterns within the vessel beyond that achieved with mixing maps. PIV could prove particularly useful for recirculation configurations, where mixing maps suggested turbulence induced at the point of return of the cell retention loop.
- Impeller power number and mixing time was determined in an un-gassed system, however impeller torque is reduced in gassed systems, and air bubbles from sparging result in differing hydrodynamics. The determination of impeller power number and mixing time in a gassed system would therefore give a

greater idea of power number and hydrodynamic behaviour during aerobic cell culture.

Chapter 5 develops cell culture techniques in the novel 250mL BR, in batch, fed-batch, and perfusion modes, and compares cell culture kinetics to MWP and 5L BR cultures. Perfusion culture in both novel 250mL and 5L was achieved with recirculation through a TFF. Expansion of cell culture experimentation in BRs could include;

- Investigate an increased range of conditions in the 250mL BR and the 5L BR. Quasi-perfusion cultures in MWPs were executed with a range of medium with varying nutritional depth, exchanged at VVD between 0.5-1.8 or at constant CSPR $0.02-0.06 \text{ nL cell}^{-1} \text{ day}^{-1}$, while cultures in the 250mL BR were conducted at 0.5-1.8 VVD and in the 5L BR at 1 VVD with a single media blend. Expansion to exchange with increased number of media compositions and to constant CSPR cultures will enable a greater depth of comparison to determine success of scale-up.
- Further increase mass transfer potential in 250mL BR by exchanging the L-shape sparger for a microsparger, which increases k_{La} by generating an increased number of small bubbles, increasing the surface area available for gas transfer.
- Perfusion cell culture in the 5L BR was limited by O_2 transfer, which can be elevated by improving the geometry. Mass transfer could be maximised by fitting of a dual impeller system comparable to the 250mL BR and/or improvements to the sparger. Mass transfer improvements will allow for greater assessment of scale-up between the 250mL and 5L BR.
- Investigation of filter types utilising the 250mL BR, including the impact of filter pore size, filter surface area, flux, or utilisation of alternative filter systems, for

example alternating tangential flow (ATF). In addition, alternative and emerging cell retention devices can be investigated, such as acoustic flow settlers.

- Incorporate empirical modelling or artificial intelligence algorithms to allow for performance prediction of particular media compositions or exchange rate based on previously determined data.
- Parallelisation of the 250mL BR system would enable in-depth analysis of a greater number of process variables by running a number of conditions simultaneously.

7. CHAPTER 7: RESEARCH IMPLEMENTATION

7.1. Validation and commercialisation

Quasi-perfusion methodologies were shown to be capable of achieving many of the specific characteristics of perfusion culture, and the 250mL BR has demonstrated capabilities in achieving and maintaining very high cell density perfusion cultures. Both small scale vessels demonstrated good comparability to cultures in bench scale vessels. While in this study a bench scale vessel was utilised as a comparison tool, there is a clear pathway to validation as a scale-down model when comparing to a commercially relevant manufacturing BR. The validation of scale-down models is typically carried out by running multiple cultures under a range of conditions and demonstrating comparability in terms of critical quality attributes (CQAs) and critical process parameters (CPPs) in the manufacturing scale vessel. CQAs can include product concentration, size, product glycosylation profiles and the % of aggregates or fragments present, while CPPs can include defining an acceptable temperature range, pH or DO concentration ranges. Having a validated scale-down model is incredibly beneficial when implementing process changes in a manufacturing process, or assessing the risk of changes, such as a small amount of time spent outside the range of a defined CPP.

Quasi-perfusion protocols demonstrate a robust, new methodology for the early phase development and screening of perfusion culture processes, however there is little scope for commercialisation since while the methodology is novel, materials and cell culture techniques are common. Whereas, the novel 250mL BR has the potential for subsequent commercialisation. Several BRs at the 100s of mL scale are commercially available, and are in frequent use in the industry for scale-down and process development of a range of cell culture processes. More recently, BRs have become available that are specific to perfusion cell culture development, by incorporating TFF and additional pumps for media exchange into pre-existing BR systems. In comparison to these systems which

retrofit perfusion systems into existing BRs previously used for batch and fed-batch culture, the 250mL BR has been specifically designed for use in cell culture processes. Key limitations of other small-scale BR systems that have been retrofitted for use in perfusion studies is limited mass transfer, over-crowding of the headplate and cell return from the headplate causing excessive foaming. Many of these limitations are specific to small scale vessels, where Reynolds number is often lower, space on the headplate is limited by reactor diameter and available headspace to accommodate excessive foam production is small. These limitations have been overcome in the 250mL BR with a design specific to maximising mass transfer, incorporating baffles and a dual impeller system, and purposely designed ports for cell retention connection, to minimise turbulence at the cell return causing foam production and to avoid headplate over-crowding. The 250mL BR has the additional benefit compared to several comparable systems to having a flexible design, with removable baffles, an adjustable impeller clearance and the ability to alter the impeller shaft for single impeller or alternative dual impeller configurations. The flexibility and power of the novel 250mL BR system to perform perfusion culture processes therefore means it is a strong candidate for future commercialisation.

7.2. Economic and environmental appraisal

High throughput scale down models are common in industry and academia to reduce costs associated with development, including reduction in timeline and a reduced consumable cost associated with culture including media volume. Quasi-perfusion techniques in MWP rely on relatively cheap, readily available equipment, in combination with shaken incubators, commonly found in cell culture labs. In comparison to alternative perfusion screening devices, which require the purchase or development specialised equipment, quasi-perfusion in MWPs requires little or no additional instrumentation which results in low capital outlay, and has a low cost of goods (CoGs), with a small number of inexpensive consumables associated with quasi-perfusion

methodologies. The investigation of up to 24 parameters on a single plate contributes to the reduction in CoGs with the implementation of DoE, and the 1.2mL culture volume represents a >10 fold decrease in culture volume compared to ambr™ and shake-tube based scale-down methodologies. An additional benefit is the reduction of plastic waste during investigations of multiple parameters and therefore a lower environmental impact compared to some alternative systems, where one plastic vessel is required per parameter investigated.

The 250mL BR is expected to be economically comparable to similar scale glass BR systems, such as the DASBOX®. Re-usable vessels typically are associated with higher capital costs but a reduced running costs, with a lower consumable demand. More generally, the economic benefits of a having a scale down mimic have been previously discussed, including shortening development timelines and reducing the media and consumable use. The environmental implications of a re-usable vessel compared to single use systems are complex, with re-usable systems consuming vastly less single-use plastic, but dependant on corrosive and energy-intensive methods for cleaning and sterilisation between cultures.

REFERENCES

- AGGARWAL, S. R. 2014. What's fueling the biotech engine - 2012 to 2013. *Nature Biotechnology*, 31, 32-39.
- ALOK, S. 2014. Effect of Different Impellers and Baffles on Aerobic Stirred Tank Fermenter using Computational Fluid Dynamics. *Journal of Bioprocessing & Biotechniques*, 04.
- APPLIKON. 2014. Integrating Acoustic Perfusion in Mammalian Cell Culture Scale up and Performance Characterization.
- ARJUNWADKAR, S. J., SARVANAN, A. B., KULKARNI, P. R. & PANDIT, A. B. 1998. Gas liquid mass transfer in dual impeller bioreactor. *Biochemical Engineering Journal*, 1, 99-106.
- ASCANIO, G., CASTRO, B. & GALINDO, E. 2004. Measurement of Power Consumption in Stirred Vessels—A Review. *Chemical Engineering Research and Design*, 82, 1282-1290.
- BAREITHER, R., BARGH, N., OAKESHOTT, R., WATTS, K. & POLLARD, D. 2013. Automated disposable small scale reactor for high throughput bioprocess development: A proof of concept study. *Biotechnology and Bioengineering*, 110, 3126-3138.
- BARRETT, T. A., WU, A., ZHANG, H., LEVY, M. S. & LYE, G. J. 2010. Microwell engineering characterization for mammalian cell culture process development. *Biotechnol Bioeng*, 105, 260-75.
- BETTS, J. I. & BAGANZ, F. 2006. Miniature bioreactors: current practices and future opportunities. *Microb Cell Fact*, 5, 21.
- BETTS, J. P. J., WARR, S. R. C., FINKA, G. B., UDEN, M., TOWN, M., JANDA, J. M., BAGANZ, F. & LYE, G. J. 2014. Impact of aeration strategies on fed-batch cell culture kinetics in a single-use 24-well miniature bioreactor. *Biochemical Engineering Journal*, 82, 105-116.
- BIELSER, J. M., DOMARADZKI, J., SOUQUET, J., BROLY, H. & MORBIDELLI, M. 2019. Semi-continuous scale-down models for clone and operating parameter screening in perfusion bioreactors. *Biotechnol Prog*, 35, e2790.
- BIOSANAPHARMA. Technology Highlights from the 2019 BioProcess International Conference. In: ROIS, M., ed. BioProcess International, 2019 Boston.
- BIRCH, J. R. & ARATHOON, R. 1990. Suspension culture of mammalian cells. *Bioprocess Technol*, 10, 251-270.
- BLUNT, W. G., M.; COLLET, C.; SPARLING, R.; GAPES, D.J.; LEVIN, D.B.; CICEK, N. 2019. Rheological Behavior of High Cell Density *Pseudomonas putida* LS46 Cultures during Production of Medium Chain Length Polyhydroxyalkanoate (PHA) Polymer. *Bioengineering*, 6.
- BONHAM-CARTER, J. & SHEVITZ, J. 2011. A Brief History of Perfusion Biomanufacturing. *BioProcess International*, 9, 24-30.
- BOWER, D. M., LEE, K. S., RAM, R. J. & PRATHER, K. L. 2012. Fed-batch microbioreactor platform for scale down and analysis of a plasmid DNA production process. *Biotechnol Bioeng*, 109, 1976-86.
- BROWN, D. E. 1997. The measurement of fermenter power input. *Chem Ind*, 16, 684-688.
- BUJALSKI, W., NIENOW, A. W., CHATWIN, S. & COOKE, M. 1987. The dependency on scale of power numbers of Rushton disc turbines. *Chem Eng Sci*, 42, 317-326.
- BUSCIGLIO, A., GRISAFI, F., SCARGIAI, F. & BRUCATO, A. Mixing time in unbaffled stirred tanks. In: BALDYGA, J., ed. 14th European Conference on Mixing 2012 Warsaw, Poland.
- CARSTENS, J. N. 2009. Perfusion! Jeopardy or the Ultimate Advantage? : CMC Biologics.

- CASTILHO, L. R. & MEDRONHO, R. A. 2002. Cell retention devices for suspended-cell perfusion cultures. In: SCHEPER, T. H. (ed.) *Advances in Biochemical Engineering/Biotechnology*. Berlin: Springer-Verlag.
- CHAPPLE, D., KRESTA, S. M., WALL, A. & AFACAN, A. 2002. The effect of impeller and tank geometry on power number for a pitched blade turbine. *Trans IChemE*, 80, 364-373.
- CHOO, C.-Y., TIAN, Y., KIM, W.-S., BLATTER, E., CONARY, J. & BRADY, C. P. 2007. High-Level Production of Monoclonal Antibody in Murine Myeloma Cells by Perfusion Culture using a gravity settler. *Biotechnol Prog*, 23, 225-231.
- CHOTTEAU, V. Process development in screening scale bioreactors and perspectives for very high cell density perfusion. In: FARID, S. S., GOUDAR, C., ALVES, P. & WARIKOO, V., eds. *Integrated Continuous Biomanufacturing III*, 2017 Cascais, Portugal.
- CHOTTEAU, V., ZHANG, Y. & CLINCKE, M. F. 2014. Very High Cell Density in Perfusion of CHO Cells by ATF, TFF, Wave Bioreactor, and/or CellTank Technologies – Impact of Cell Density and Applications. In: SUBRAMANIAN, G. (ed.) *Continuous Processing in Pharmaceutical Manufacturing*. Weinheim, Germany: Wiley-VCH Verlag GmbH & Co.
- CLAPP, K. P. C., A.; LINDSKOG, E.K. 2018. Chapter 24 - Upstream Processing Equipment. In: JAGSCHIES, G. L., E.; LACKI, K.; GALLIHER, P. (ed.) *Biopharmaceutical Processing*. Elsevier.
- CLINCKE, M. F., MOLLERYD, C., ZHANG, Y., LINDSKOG, E., WALSH, K. & CHOTTEAU, V. 2013. Very high density of CHO cells in perfusion by ATF or TFF in WAVE bioreactor. Part I. Effect of the cell density on the process. *Biotechnol Prog*, 29, 754-67.
- CROUGHAN, M. S., KONSTANTINOV, K. B. & COONEY, C. 2015. The future of industrial bioprocessing: Batch or continuous? *Biotechnology and Bioengineering*, 112, 648-651.
- DEO, Y. M., MAHANDEVAN, M. D. & FUCHS, R. 1996. Practical considerations in operation and scale-up of spin filter based bioreactors for monoclonal antibody production. *Biotechnol Prog*, 12, 57-64.
- DIAZ, A. & ACEVEDO, F. 1999. Scale-up strategy for bioreactors with Newtonian and non-Newtonian broths. *Bioprocess Engineering*, 21, 21-23.
- DOIG, S. D. 2006. High-throughput screening and process optimisation. In: RATLEDGE, C. & KRISTIANSEN, B. (eds.) *Basic Biotechnology*. Cambridge: Cambridge university press.
- DOIG, S. D., BAGANZ, F. & LYE, G. J. 2006. High-throughput screening and process optimisation. In: RATLEDGE, C. & KRISTIANSEN, B. (eds.) *Basic Biotechnology*. Cambridge: Cambridge University Press.
- DOIG, S. D., PICKERING, S., LYE, G. J. & BAGANZ, F. 2005. Modelling surface aeration rates in shaken microtitre plates using dimensionless groups. *Chem Eng Sci*, 60, 2741-2750.
- DORAN, P. M. 1995. *Bioprocess engineering principles*, San Diego, Academic Press.
- DUETZ, W. A. 2007. Microtiter plates as mini-bioreactors: miniaturization of fermentation methods. *Trends Microbiol*, 15, 469-75.
- DUETZ, W. A., RUEDI, L., HERMANN, R., O'CONNOR, K., BUCHS, L. & WITHOLT, B. 2000. Methods for intense aeration, growth, storage and replication of bacterial strains in microtiter plates. *Applied and Environmental Microbiology*, 66, 2641-2646.
- EIBL, D., EIBL, R. & PÖRTNER, R. 2008. Mammalian cell culture technology: An emerging field. In: EIBL, D. (ed.) *Cell and tissue reaction engineering: principles and practice*. Berlin: Springer.
- FARID, S. S. 2006. Established Bioprocesses for Producing Antibodies as a Basis for Future Planning. In: HU, W. S. (ed.) *Cell Culture Engineering*. Berlin: Springer.

- FITCHEN, J. M., M.; ROSSEBURG, A.; WUTZ, J.; WUCHERPFENNIG, T.; SCHLUTER, M 2019. Influence of Spacing of Multiple Impellers on Power Input in an Industrial-Scale Aerated Stirred Tank Reactor. *Chemie Ingenieur Technik*, 91, 1794-1801.
- FLICKINGER, M. C. N., A.W. 2010. Impeller Selection for Animal Cell Culture. In: FLICKINGER, M. C. (ed.) *Encyclopedia of Industrial Biotechnology*.
- FRENZEL, A. H., M.; SCHIRRMANN, T. 2013. Expression of recombinant antibodies. *Front. Immunol.*
- GAGLIARDI, T. M., CHELIKANI, R., YANG, Y., TUOZZOLO, G. & YUAN, H. 2019. Development of a novel, high-throughput screening tool for efficient perfusion-based cell culture process development. *Biotechnol Prog*, 35, e2811.
- GARCIA-OCHOA, F. & GOMEZ, E. 2005. Prediction of gas-liquid mass transfer coefficient in sparged stirred tank bioreactors. *Biotechnol Bioeng*, 92, 761-772.
- GETTS, D. R., GETTS, M. T., MCCARTHY, D. P., CHASTAIN, E. M. & MILLER, S. D. 2010. Have we overestimated the benefit of human(ized) antibodies? *MAbs*, 2, 682-94.
- GIBILARO, L. G., GALLUCCI, K., DI FELICE, R. & PAGLIAI, P. 2007. On the apparent viscosity of a fluidized bed. *Chemical Engineering Science*, 62, 294-300.
- GOMEZ, N., AMBHAIKAR, M., ZHANG, L., HUANG, C. J., BARKHORDARIAN, H., LULL, J. & GUTIERREZ, C. 2017. Analysis of Tubespins as a suitable scale-down model of bioreactors for high cell density CHO cell culture. *Biotechnol Prog*, 33, 490-499.
- GORENFLO, V. M., SMITH, L., DEDINSKY, B., PERSSON, B. & PIRET, J. M. 2002. Scale-up and optimization of an acoustic filter for 200 L/day perfusion of a CHO cell culture. *Biotechnol Bioeng*, 80, 438-44.
- GREIN, T. A., LEBER, J., BLUMENSTOCK, M., PETRY, F., WEIDNER, T., SALZIG, D. & CZERMAK, P. 2016. Multiphase mixing characteristics in a microcarrier-based stirred tank bioreactor suitable for human mesenchymal stem cell expansion. *Process Biochemistry*, 51, 1109-1119.
- HSU, W. T., AULAKH, R. P., TRAU, D. L. & YUK, I. H. 2012. Advanced microscale bioreactor system: a representative scale-down model for bench-top bioreactors. *Cytotechnology*, 64, 667-78.
- HU, W., BERDUGO, C. & CHALMERS, J. J. 2011. The potential of hydrodynamic damage to animal cells of industrial relevance: current understanding. *Cytotechnology*, 63, 445-60.
- HUANG, C., JR., LIN, H. & YANG, J. X. 2015. A robust method for increasing Fc glycan high mannose level of recombinant antibodies. *Biotechnology and Bioengineering*, 112, 1200-1209.
- HUTCHINSON, N. B., N.; MURRELL, N.; FARID, S.; HOARE, M. 2006. Shear stress analysis of mammalian cell suspensions for prediction of industrial centrifugation and its verification. *Biotechnology and Bioengineering*, 95, 483-491.
- JANEWAY, C. A., TRAVERS, P., WALPORT, M. & SHLOMCHIK, M. J. 2001. The structure of a typical antibody molecule. *Immunobiology: The Immune System in Health and Disease*. 5th edition ed. New York: Garland Science.
- JANOSCHEK, S., SCHULZE, M., ZIJLSTRA, G., GRELLER, G. & MATUSZCZYK, J. 2018. A protocol to transfer a fed-batch platform process into semi-perfusion mode: The benefit of automated small-scale bioreactors compared to shake flasks as scale-down model. *Biotechnology Progress*, 35.
- JARDON-PEREZ, L. E., AMARO-VILLEDA, A., GONZALEZ-RIVERA, C., TRAPAGA, G., CONEJO, A. N. & RAMIREZ-ARGAEZ, M. A. 2019. Introducing the Planar Laser-Induced Fluorescence technique (PLIF) to measure mixing time in gas-stirred ladles. *Metallurgical and Materials Transactions B*, 10, 2121-2133.
- JOSSEN, V., EIBL, R., PORTNER, R., KRAUME, M. & EIBL, D. 2017. Stirred Bioreactors: Current State and Developments, With Special Emphasis on Biopharmaceutical Production Processes. In: LARROCHE, C., SANROMAN, M. A., DU, G. & PANDEY, A. (eds.) *Current Developments in Biotechnology and Bioengineering: Bioprocesses, Bioreactors and Controls*. Amsterdam, NL: Elsevier.

- KADIC, E. & HEINDEL, T. J. Hydrodynamic considerations in bioreactor selection and design. Mechanical Engineering Conference Presentations, Papers and Proceedings, 2010 Montreal, Canada.
- KARIMI, A., GOLGABAEI, F., MEHRNIA, M. R., NEGHBAB, M., MOHAMMED, K., NIKPEY, A. & POURMAND, M. R. 2013. Oxygen mass transfer in a stirred tank bioreactor using different impeller configurations for environmental purposes. *Iranian journal of environmental health science & engineering*, 10.
- KARST, D. J., SERRA, E., VILLIGER, T. K., SOOS, M. & MORBIDELLI, M. 2016. Characterization and comparison of ATF and TFF in stirred bioreactors for continuous mammalian cell culture processes. *Biochemical Engineering Journal*, 110, 17-26.
- KARST, D. J., STEINEBACH, F. & MORBIDELLI, M. 2018. Continuous integrated manufacturing of therapeutic proteins. *Curr Opin Biotechnol*, 53, 76-84.
- KASAT, G. & PANDIT, A. B. 2004. Mixing time studies in multiple impeller agitated reactors. *The Canadian Journal of Chemical Engineering*, 82, 892-904.
- KELLEY, B. 2009. Industrialization of mAb production technology: The bioprocessing industry at a crossroads. *MAbs*, 1, 443-452.
- KELLY, W., VEIGNE, S., LI, X., SUBRAMANIAN, S. S., HUANG, Z. & SCHAEFER, E. 2018. Optimizing performance of semi-continuous cell culture in an ambr15 microbioreactor using dynamic flux balance modeling. *Biotechnol Prog*, 34, 420-431.
- KINGSTON, R. E. K., R.J.; BEBBINGTON, C.R.; ROLFE, M.R. 2002. Amplification using CHO cell expression vectors. *Current Protocols in Molecular Biology*, 60, 16231-162313.
- KLÖCKNER, W., TISSOT, S., WURM, F. & BÜCHS, J. 2012. Power input correlation to characterize the hydrodynamics of cylindrical orbitally shaken bioreactors. *Biochemical Engineering Journal*, 65, 63-69.
- KOMPALA, D. S. & OZTURK, S. S. 2006. Optimization of High Cell Density Perfusion Bioreactors. In: OZTURK, S. S. & HU, W.-S. (eds.) *Cell Culture Technology for Pharmaceutical and Cell-Based Therapies*. NW, US: Taylor & Francis
- KONSTANTINOV, K. C., C.L. 2015. White paper on continuous bioprocessing. *J Pharm Sci*, 104, 813-820.
- KORN, J. S., D; KIRMANN, T; BERTOGLIO, F; STEINKE, S.; HEISIG, J.; RUSCHIG, M.; ROJAS, G.; LANGREDER, N.; WENZEL, E.V.; ROTH, K.D.R.; BECKER, M.; MEIER, D.; VAN DEN HEUVEL, J.; HUST, M.; DÜBEL, S.; SCHUBERT, M. 2020. Baculovirus-free insect cell expression system for high yield antibody and antigen production. *Sci Rep*, 10, 213-293.
- KREYE, S., STAHN, R., NAWRATH, K., GORALCZYK, V., ZORO, B. & GOLETZ, S. 2019. A novel scale-down mimic of perfusion cell culture using sedimentation in an automated microbioreactor (SAM). *Biotechnol Prog*, 35, e2832.
- KREYE, S. & ZORO, B. 2016. ambr15 as a sedimentation-perfusion model for cultivation characteristics and product quality prediction. TAP Biosystems.
- LAMPING, S. R., ZHANG, H., ALLEN, B. & AYAZI SHAMLOU, P. 2003. Design of a prototype miniature bioreactor for high throughput automated bioprocessing. *Chem Eng Sci*, 58, 747-758.
- LANGHEINRICH, C. & NIENOW, A. W. 1999. Control of pH in large-scale, free suspension animal cell bioreactors: Alkali addition and pH excursions. *Biotechnology and Bioengineering*, 66, 171-179.
- LARA, A. R., GALINDO, E., RAMIREZ, O. T. & PALOMARES, L. A. 2006. Living with heterogeneities in bioreactors: understanding the effects of environmental gradients on cells. *Mol Biotechnol*, 34, 355-381.
- LIM, A. C., WASHBROOK, J., TITCHENER-HOOKER, N. J. & FARID, S. S. 2006. A computer-aided approach to compare the production economics of fed-batch and perfusion culture under uncertainty. *Biotechnol Bioeng*, 93, 687-97.

- LIU, J. K. 2014. The history of monoclonal antibody development - Progress, remaining challenges and future innovations. *Ann Med Surg (Lond)*, 3, 113-6.
- LU, S., SUN, X. & ZHANG, Y. 2005. Insight into metabolism of CHO cells at low glucose concentration on the basis of the determination of intracellular metabolites. *Process Biochemistry*, 40, 1917-1921.
- LYE, G., HUBBUCH, J., SCHROEDER, T. & WILLIAMANN, E. 2009. Shrinking the costs of bioprocess development. *Bioprocess International*, 18-22.
- MARTENS, D. E., VAN DEN END, E. J. & STREEFLAND, M. 2014. Configuration of Bioreactors. In: PÖRTNER, R. (ed.) *Animal Cell Biotechnology. Methods in Molecular Biology (Methods and Protocols)*. Totowa, NJ: Humana Press.
- MATTEAU, D., BABY, V., PELLETIER, S. & RODRIGUE, S. 2015. A Small-Volume, Low-Cost, and Versatile Continuous Culture Device. *PLoS One*, 10, e0133384.
- MELTON, L. A., LIPP, C. W., SPRADLING, R. W. & PAULSON, K. A. 2002. Dismt - Determination of mixing time through color changes. *Chemical Engineering Communications*, 189, 322-338.
- METZNER, A. B. & OTTO, R. E. 1957. Agitation of Non-Newtonian Fluids. *A.I.Ch.E Journal*, 3, 3-10.
- MICHELETTI, M., BARRETT, T., DOIG, S. D., BAGANZ, F., LEVY, M. S., WOODLEY, J. M. & LYE, G. J. 2006. Fluid mixing in shaken bioreactors: Implications for scale-up predictions from microlitre-scale microbial and mammalian cell cultures. *Chemical Engineering Science*, 61, 2939-2949.
- MICHELETTI, M. & LYE, G. J. 2006. Microscale bioprocess optimisation. *Curr Opin Biotechnol*, 17, 611-8.
- MIDDLETON, J. C. 1997. Gas-liquid dispersion and mixing. In: NIENOW, A. W., HARNBY, N. & EDWARDS, M. F. (eds.) *Mixing in the Process Industries*. 2nd Edition ed. Amsterdam, NL: Elsevier.
- MINOW, B., TSCHOEPE, S., REGNER, A., POPULIN, M., REISER, S., NOACK, C. & NEUBAUER, P. 2014. Biological performance of two different 1000 L single-use bioreactors applying a simple transfer approach. *Engineering in Life Sciences*, 14.
- MULLER, W. 1985. *Untersuchung von homogenisiervorgängen in nicht- Newtonschen flüssigkeiten mit einem neuen bildanalytischen verfahren*, Dortmund, VDI Forschungsber.
- MULUKUTLA, B. C. K., S.; LANGE, A.; HU, W-S 2010. Glucose metabolism in mammalian cell culture: new insights for tweaking vintage pathways. *Trends in Biotechnology*, 28, 476-484.
- NELSON, A. L., DHIMOLEA, E. & REICHERT, J. M. 2010. Development trends for human monoclonal antibody therapeutics. *Nat Rev Drug Discov*, 9, 767-74.
- NGIBUINI, M. 2014. Automated Mini Bioreactor Technology for Microbial and Mammalian Cell Culture. *BioProcess International*, 12, 3-8.
- NIENOW, A. W. 1997. On impeller circulation and mixing effectiveness in the turbulent flow regime. *Chem Eng Sci*, 52, 2557-2565.
- NIENOW, A. W. 2006. Reactor engineering in large scale animal cell culture. *Cytotechnology*, 50, 9-33.
- NIENOW, A. W. & MILES, D. 1971. Impeller Power Numbers in Closed Vessels. *Ind. Eng. Chem. Process Des. Dev.*, 10.
- NIENOW, A. W., RIELLY, C. D., BROSANAN, K., BARGH, N., LEE, K., COOPMAN, K. & HEWITT, C. J. 2013. The physical characterisation of a microscale parallel bioreactor platform with an industrial CHO cell line expressing an IgG4. *Biochemical Engineering Journal*, 76, 25-36.
- NIENOW, A. W. L., C.; STEVENSON, N.C.; EMERY, A.N.; CLAYTON, T.M.; SLATER, N.K.H 1996. Homogenisation and oxygen transfer rates in large agitated and sparged animal cell bioreactors: Some implications for growth and production. *Cytotechnology*, 22, 87-94.

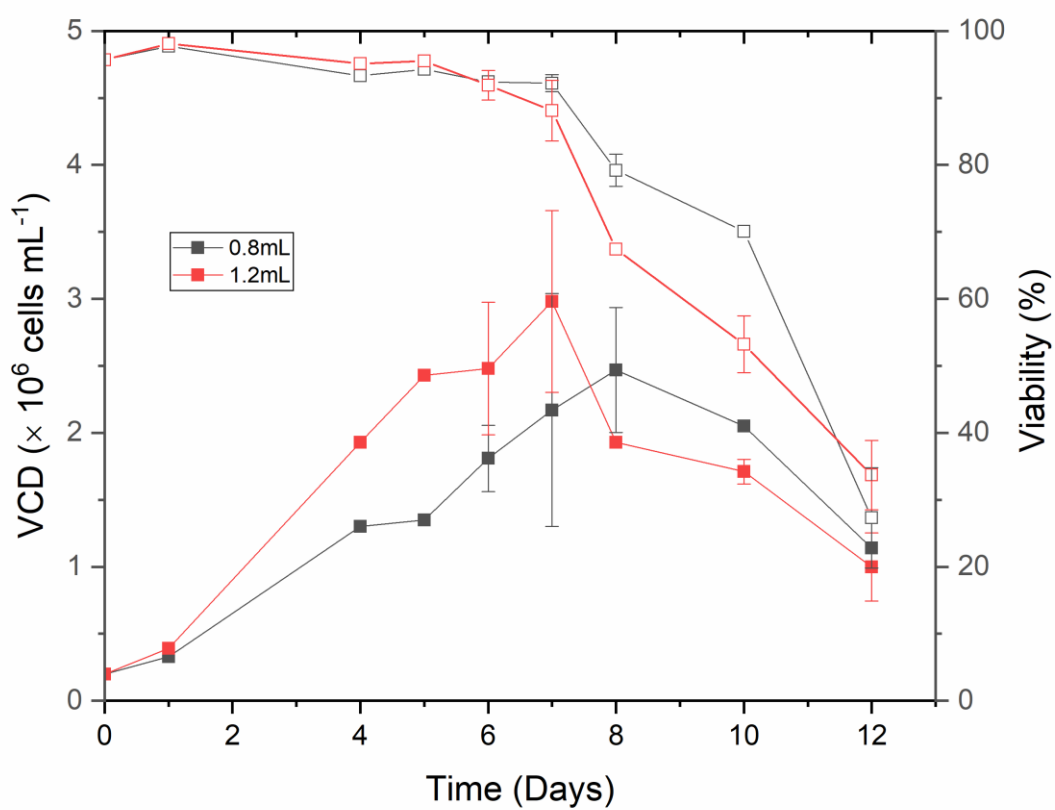
- OLDSHUE, J. Y. 1983. *Fluid mixing technology*, New York, NY, McGraw-Hill Publications Co.
- OOSTERHUIS, M. & KOSSEN, N. 1985. Modelling and Scale-up of bioreactors. *Biotechnology*. Berlin: Verlagsgesellschaft.
- OZTURK, S. S. 1996. Engineering challenges in high cell density cell culture systems. *Cytotechnology*, 22, 3-16.
- OZTURK, S. S. P., B.O. 1990. Effect of initial cell density on hybridoma growth, metabolism, and monoclonal antibody production. *J Biotechnol*, 16, 259-278.
- PALL 2014. Micro-24 MicroReactor System. In: PALL CORPORATION (ed.).
- PALMBERGER, D. R., D.; TAUBER, P.; KRAMMER, F.; WILSON, I.B.H; GRABHERR, R. 2011. Insect cells for antibody production: evaluation of an efficient alternative. *J Biotechnol*, 3, 160-166.
- POLLOCK, J., HO, S. V. & FARID, S. S. 2013. Fed-batch and perfusion culture processes: economic, environmental, and operational feasibility under uncertainty. *Biotechnol Bioeng*, 110, 206-19.
- POULSEN, B. R. Scale-down tools for the evaluation of perfusion processes. Cell Culture World, 2013 Munich.
- PUSKEILER, R., KAUFMANN, K. & WEUSTER-BOTZ, D. 2005. Development, parallelization, and automation of a gas-inducing milliliter-scale bioreactor for high-throughput bioprocess design (HTBD). *Biotechnol Bioeng*, 89, 512-23.
- RAVI, R. 2017. Reactor Design - General Principles. In: RAVI, R., GUMMADI, S. N. & COULSON, J. M. (eds.) *Coulson and Richardson's Chemical Engineering, Volume 3A - Chemical and Biochemical Reactors and Reaction Engineering (4th Edition)*. Kidlington, Oxford: Elsevier.
- RAZALI, F. 2007. Scale-up of stirred and aerated bioengineering bioreactor based on constant mass transfer coefficient. *Jurnal Teknologi*, 43.
- REINHART, D., DAMJANOVIC, L., KAISERMAYER, C. & KUNERT, R. 2015. Benchmarking of commercially available CHO cell culture media for antibody production. *Appl Microbiol Biotechnol*, 99, 4645-57.
- RODRIGUEZ, E. N. P., M.; CASANOVA, P.; MARTINEZ, L. Effect of Seed Cell Density on Specific Growth Rate Using CHO Cells as Model. In: LINDNER-OLSSON, E. C., N.; LÜLLAU, E., ed. 17th ESACT Meeting; Animal Cell Technology: From Target to Market, 2001 Tylösand, Sweden.
- RODRIGUEZ, G., WEHELIYE, W., ANDERLEI, T., MICHELETTI, M., YIANNESKIS, M. & DUCCI, A. 2013. Mixing time and kinetic energy measurements in a shaken cylindrical bioreactor. *Chemical Engineering Research and Design*, 91, 2084-2097.
- RUTHERFORD, K., LEE, K. C., MAHMOUDI, M. S. & YIANNESKIS, M. 1996. Hydrodynamic characteristics of dual Rushton impeller stirred vessels. *A.I.Ch.E Journal*, 42.
- SAMARAS, J. J., MICHELETTI, M. & DUCCI, A. 2020. Flow, suspension, and mixing dynamics in DASGIP bioreactors: Part 1. *AIChE Journal*, 66, e17014.
- SARDEING, R., AUBIN, J., POUX, M. & XUEREBO, C. 2004. Gas-Liquid Mass Transfer: Influence of Sparger Location. *Trans IChemE*, 82, 1161-1168.
- SEWELL, D. J., TURNER, R., FIELD, R., HOLMES, W., PRADHAN, R., SPENCER, C., OLIVER, S. G., SLATER, N. K. & DIKICIOGLU, D. 2019. Enhancing the functionality of a microscale bioreactor system as an industrial process development tool for mammalian perfusion culture. *Biotechnol Bioeng*, 116, 1315-1325.
- SHI, S., CONDON, R. G., DENG, L., SAUNDERS, J., HUNG, F., TSAO, Y. S. & LIU, Z. 2011. A high-throughput automated platform for the development of manufacturing cell lines for protein therapeutics. *J Vis Exp*.
- SHIMONI, Y., GOUDAR, C., JENNE, M. & SRINIVASAN, V. 2014. Qualification of Scale-Down Bioreactors: Validation of process changes in commercial production of animal-cell-derived products, Part 1 - Concept. *Bioprocess International*, 12, 38-45.

- SHUKLA, A. A., WOLFE, L. S., MOSTAFA, S. S. & NORMAN, C. 2017. Evolving trends in mAb production processes. *Bioeng Transl Med*, 2, 58-69.
- SIECK, J. B. 2017. Optimizing media for perfusion combining predictive scale-down models and multivariate approaches. In: FARID, S. S., GOUDAR, C., ALVES, P. & WARIKOO, V. (eds.) *Integrated continuous biomanufacturing III*. Cascais, Portugal.
- SIECK, J. B., SCHILD, C. & VON HAGEN, J. 2018. Perfusion Formats and Their Specific Medium Requirements. In: SUBRAMANIAN, G. (ed.) *Continuous Biomanufacturing: Innovative Technologies and Methods*, 1st ed. Germany: Wiley-VCH Verlag GmbH.
- SILK, N. J., DENBY, S., LEWIS, G., KUIPER, M., HATTON, D., FIELD, R., BAGANZ, F. & LYE, G. J. 2010. Fed-batch operation of an industrial cell culture process in shaken microwells. *Biotechnol Lett*, 32, 73-8.
- SIURKUS, J., PANULA-PERALA, J., HORN, U., KRAFT, M., RIMSELIENE, R. & NEUBAUER, P. 2010. Novel approach of high cell density recombinant bioprocess development: optimisation and scale-up from microliter to pilot scales while maintaining the fed-batch cultivation mode of E. coli cultures. *Microb Cell Fact*, 9, 35.
- SPADIUT, O. C., S.; KAINER, F.; GLIEDER, A.; HERWIG, C. 2014. Microbials for the production of monoclonal antibodies and antibody fragments. *Trends in Biotechnology*, 32, 54-60.
- STRESSMANN, M. & MORESOLI, C. 2008. Effect of Pore Size, Shear Rate, and Harvest Time During the Constant Permeate Flux Microfiltration of CHO Cell Culture Supernatant. *Biotechnol Prog*, 24, 890-897.
- TAKAGO, M. H., H.; YOSHIDA, T. 2000. The effect of osmolarity on metabolism and morphology in adhesion and suspension chinese hamster ovary cells producing tissue plasminogen activator. *Cytotechnology*, 32, 171-179.
- TESCIONE, L., LAMBROPOULOS, J., PARANANDI, M. R., MAKAGIANSAR, H. & RYLL, T. 2015. Application of bioreactor design principles and multivariate analysis for development of cell culture scale down models. *Biotechnol Bioeng*, 112, 84-97.
- TITCHENER-HOOKER, N. J., DUNNILL, P. & HOARE, M. 2008. Micro biochemical engineering to accelerate the design of industrial-scale downstream processes for biopharmaceutical proteins. *Biotechnol Bioeng*, 100, 473-87.
- VAN'T RIET, K. 1979. Review of Measuring Methods and Results in Nonviscous Gas-Liquid Mass Transfer in Stirred Vessels. *Ind. Eng. Chem. Process Des. Dev.*, 18, 357-364.
- VAN REIS, R., GADAM, S., FRAUTSCHY, L. N., ORLANDO, S., GOODRICH, E. M., SAKSENA, S., KURIYEL, R., SIMPSON, C. M., PEARL, S. & ZYDNEY, A. L. 1997. High performance tangential flow filtration. *Biotechnology and Bioengineering*, 56, 71-82.
- VAN REIS, R., LEONARD, L. C., HSU, C. C. & BUILDER, S. E. 1991. Industrial scale harvest of proteins from mammalian cell culture by tangential flow filtration. *Biotechnology and Bioengineering*, 38, 413-422.
- VASCONCELOS, J. M. T., ALVES, S. S., NIENOW, A. W. & BUJALSKI, W. 1998. Scale-up of mixing in gassed multi-turbine agitate vessels. *Can J Chem Eng*, 76, 398-403.
- VELEZ, D. M., L.; MACMILLAN, J.D. 1989. Use of tangential flow filtration in perfusion propagation of hybridoma cells for production of monoclonal antibodies. *Biotechnol Bioeng*, 33, 938-940.
- VÉLEZ SUBERBIE, M. D. L. 2013. *Characterisation of the Bioreactor Environment and its Effect on Mammalian Cell Performance in Suspension Culture during Antibody Production*. Doctor of Philosophy, UCL.
- VILLIGER-ÖBERBEK, A., YANG, Y., ZHOU, W. & YANG, J. 2015. Development and application of a high-throughput platform for perfusion-based cell culture processes. *J Biotechnol*, 212, 21-9.

- VOISARD, D., MEUWLY, F., RUFFIEUX, P. A., BAER, G. & KADOURI, A. 2003. Potential of cell retention techniques for large-scale high-density perfusion culture of suspended mammalian cells. *Biotechnol Bioeng*, 82, 751-65.
- WALLS, P. L. L., MCRAE, O., NATARAJAN, V., JOHNSON, C., ANTONIOU, C. & BIRD, J. C. 2017. Quantifying the potential for bursting bubbles to damage suspended cells. *Sci Rep*, 7, 15102.
- WALSH, G. 2018. Biopharmaceutical benchmarks 2018. *Nat Biotechnol*, 36, 1136-1145.
- WANG, S., GODFREY, S., RAVIKRISHNAN, J., LIN, H., VOGEL, J. & COFFMAN, J. 2017. Shear contributions to cell culture performance and product recovery in ATF and TFF perfusion systems. *J Biotechnol*, 246, 52-60.
- WOLF, M. K. F., LORENZ, V., KARST, D. J., SOUQUET, J., BROLY, H. & MORBIDELLI, M. 2018. Development of a shake tube-based scale-down model for perfusion cultures. *Biotechnol Bioeng*, 115, 2703-2713.
- WOLF, M. K. F., MULLER, A., SOUQUET, J., BROLY, H. & MORBIDELLI, M. 2019. Process design and development of a mammalian cell perfusion culture in shake-tube and benchtop bioreactors. *Biotechnol Bioeng*, 116, 1973-1985.
- WUEST, D. M., HARCUM, S. W. & LEE, K. H. 2012. Genomics in mammalian cell culture bioprocessing. *Biotechnol Adv*, 30, 629-38.
- XING, Z., KENTY, B. M., LI, Z. J. & LEE, S. S. 2009. Scale-up analysis for a CHO cell culture process in large-scale bioreactors. *Biotechnol Bioeng*, 103, 733-46.
- XU, P., CLARK, C., RYDER, T., SPARKS, C., ZHOU, J., WANG, M., RUSSELL, R. & SCOTT, C. 2017. Characterization of TAP Ambr 250 disposable bioreactors, as a reliable scale-down model for biologics process development. *Biotechnol Prog*, 33, 478-489.
- XU, S., GUPTA, B., HOSHAN, L. & CHEN, H. 2015. Rapid Early Process Development Enabled by Commercial Chemically Defined Media and Microbioreactors. *BioPharm International*, 28, 28-33.
- ZAGARI, F., JORDAN, M., STETTLER, M., BROLY, H. & WURM, F. M. 2013. Lactate metabolism shift in CHO cell culture: the role of mitochondrial oxidative activity. *N Biotechnol*, 30, 238-45.
- ZHA, D. 2012. Glycoengineered Yeast as an Alternative Monoclonal Antibody Discovery and Production Platform. In: PETRESCU, S. (ed.) *Glycosylation*. IntechOpen.
- ZHANG, J. 2010. Mammalian Cell Culture for Biopharmaceutical Production. In: BALTZ, R. H., DEMAINE, A. L. & DAVIES, J. E. (eds.) *Manual of Industrial Microbiology and Biotechnology*. 3rd ed. Washington DC: ASM Press.
- ZHANG, Y., STOBBE, P., SILVANDER, C. O. & CHOTTEAU, V. 2015. Very high cell density perfusion of CHO cells anchored in a non-woven matrix-based bioreactor. *J Biotechnol*, 213, 28-41.
- ZHU, L. S., B.; WANG, Z.; MONTEIL, D.T; SHEN, X; HACKER, D; WURM, F.M. 2017. Studies on fluid dynamics of flow field and gas transfer in orbitally shaken tubes. *Biotechnology Progress*, 33, 192-200.
- ZHU, M. M. G., A.; RANK, D.L.; GUPTA, S.K.; BOOM, T.V.; LEE, S.S. 2005. Effects of elevated pCO₂ and osmolality on growth of CHO cells and production of antibody-fusion protein B1: A case study. *Biotechnol Prog*, 21, 70-77.
- ZORO, B. & TAIT, A. Development of a novel automated perfusion mini bioreactor 'ambr® 250 perfusion. In: FARID, S. S., GOUDAR, C., ALVES, P. & WARIKOO, V., eds. *Integrated continuous biomanufacturing III*, 2017 Cascais, Portugal.

8. CHAPTER 8: APPENDIX

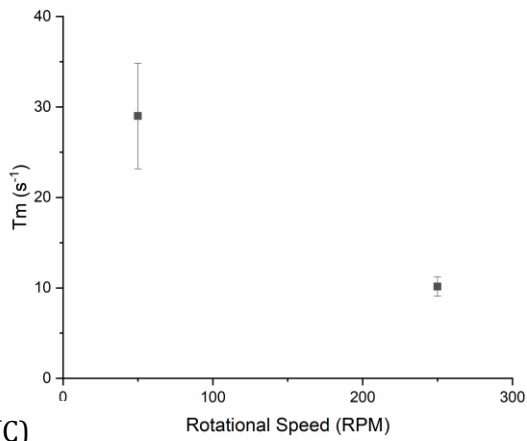
8.1. VCD in MWP with fill volumes of 0.8 and 1.2mL



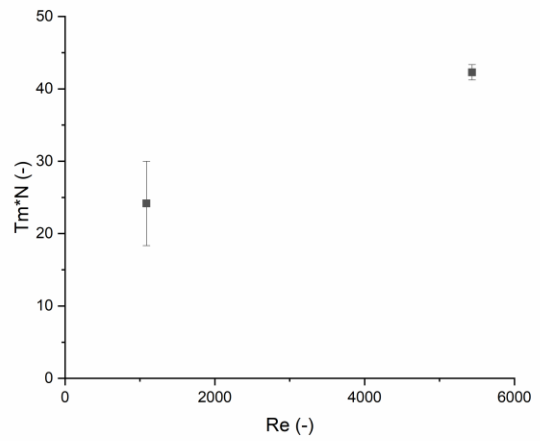
Comparison of cell growth kinetics in MWP at fill volumes of 0.8 or 1.2mL. Cell cultures were incubated at 37°C at an initial seeding density of $0.2 \times 10^6 \text{ cells mL}^{-1}$, N=220 RPM. Graph shows VCD (filled symbols) and viability (empty symbols) with time. Data represents 2 cultures \pm s.d.

8.2. T_m in 250mL BR fitted with single Rushton-style turbine $H_i = 2.5\text{cm}$

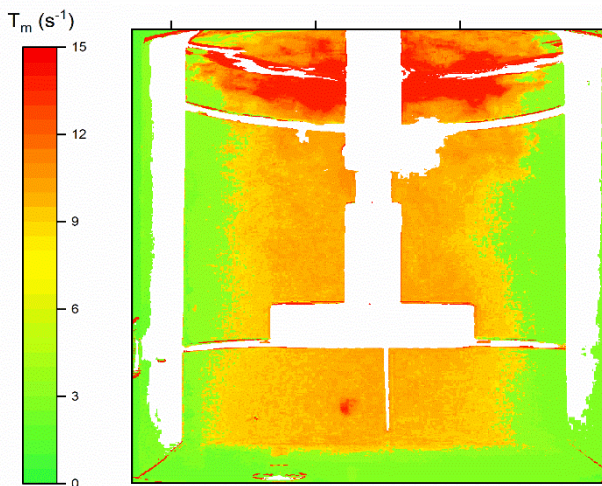
(A)



(B)

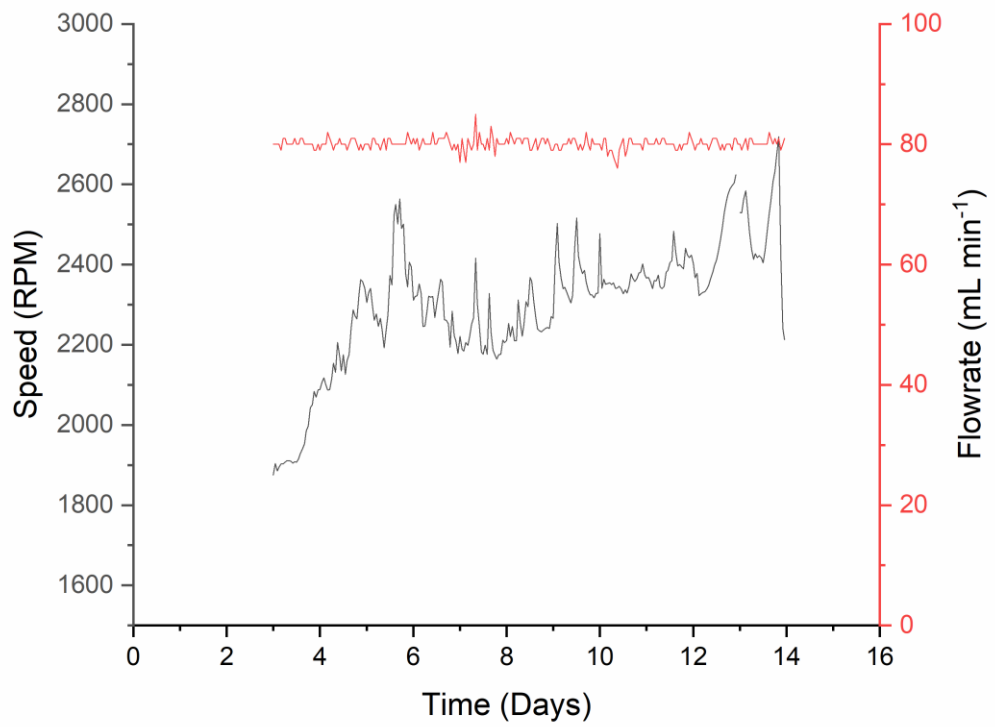


(C)



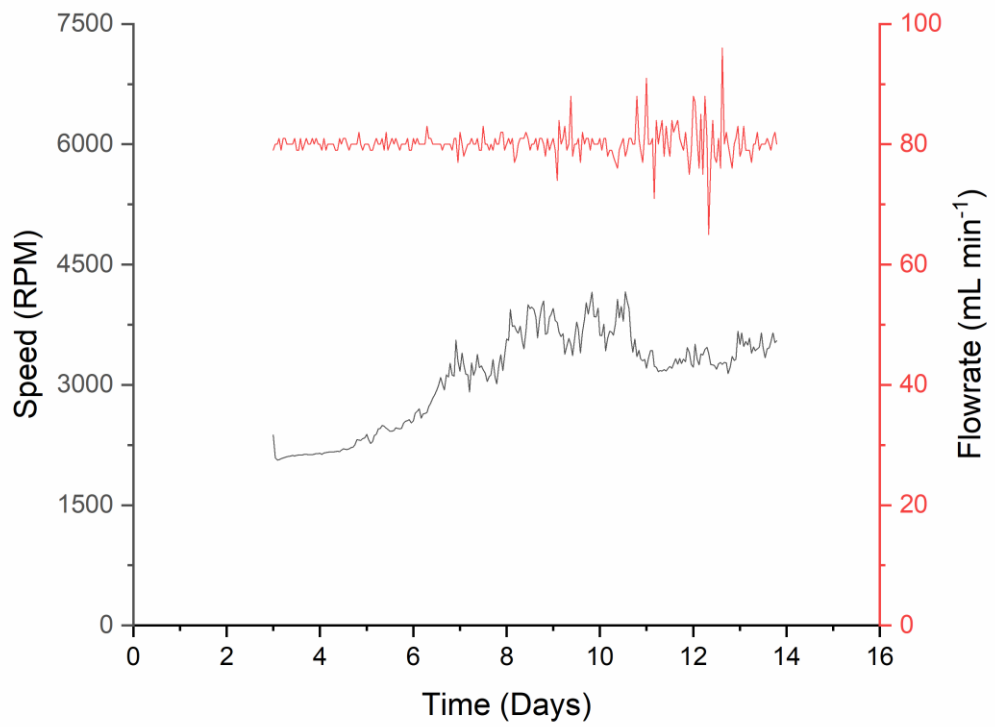
Mixing in 250mL BR fitted with Rushton-type impellers at $H_i = 2.5\text{cm}$, measured using DISMT method. (A) T_m at $N = 50$ and 250 RPM (B) $T_m \cdot N$ vs Re cm (C) Mixing map generated at $H_i = 2.5\text{cm}$, $N = 250\text{RPM}$

8.3. Rotational speed of centrifugal pump in 250mL BR at 0.5 VVD



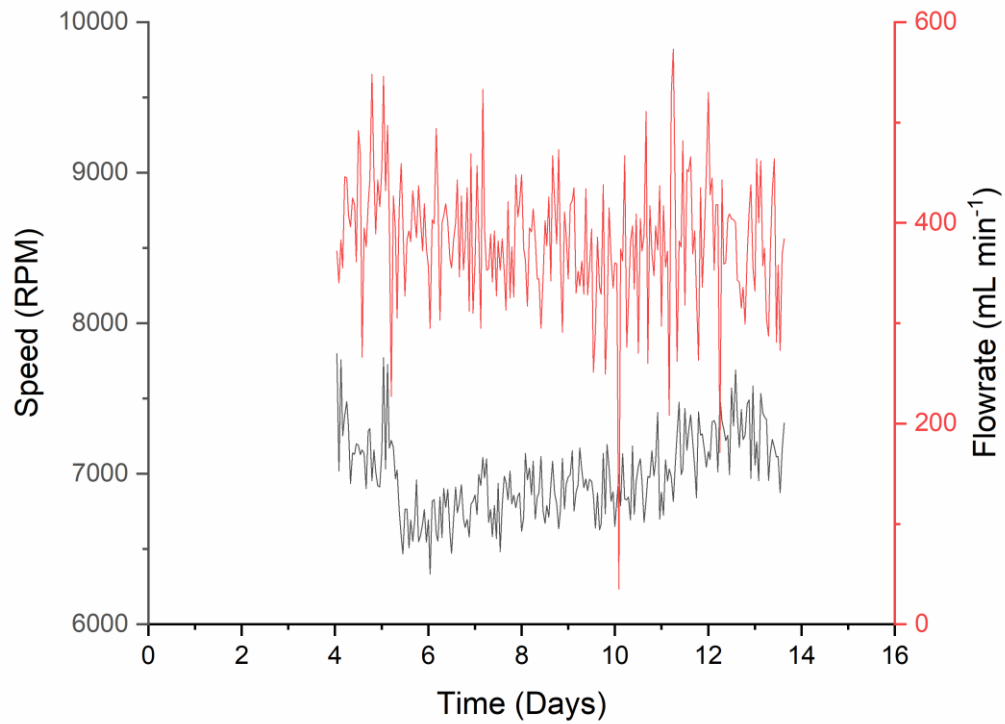
Rotational speed of centrifugal pump to maintain a recirculation flowrate of 80 mL min⁻¹ (black) and flowrate (red) in 250 mL BR in perfusion culture mode operated at 0.5 VVD.

8.4. Rotational speed of centrifugal pump in 250mL BR at 1.8 VVD



Rotational speed of centrifugal pump to maintain a recirculation flowrate of 80 mL min⁻¹ (black) and flowrate (red) in 250 mL BR in perfusion culture mode operated at 1.8 VVD.

8.5. Rotational speed of centrifugal pump in 5L BR



Rotational speed of centrifugal pump to maintain a recirculation flowrate of 400 mL min⁻¹ (black) and flowrate (red) in 5L BR in perfusion culture mode operated at 1 VVD.